

THE EFFECT OF HUMIC SUBSTANCES ON THE CRYSTALLISATION OF GYPSUM

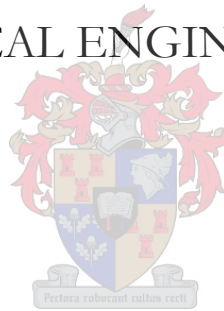
by

Heinrich Bock

Thesis presented in partial fulfilment
of the requirements for the Degree

of

MASTER OF ENGINEERING
CHEMICAL ENGINEERING



in the Faculty of Engineering
at Stellenbosch University

Supervisor

Prof A.J. Burger

March 2017

Declaration

By submitting this thesis electronically, I declare that the entirety of the work contained therein is my own, original work, that I am the sole author thereof (save to the extent explicitly otherwise stated), that reproduction and publication thereof by Stellenbosch University will not infringe any third party rights and that I have not previously in its entirety or in part submitted it for obtaining any qualification.

March 2017

Date:

ABSTRACT

High recovery mine water treatment plants generate brine streams that are highly supersaturated with inorganic salts. Intermediate crystallisation of gypsum is required for further treatment of these brine streams. The crystallisation of gypsum is influenced by various factors such as temperature, supersaturation, additives or impurities, pH and seeding.

The presence of natural organic matter (NOM), consisting of humic substances (HS), can prevent the onset of crystallisation. These substances, mainly composed of humic (HA) and fulvic acids (FA), are considered to be weak polyelectrolytes due to their carboxylic and phenolic functional groups. The aim of this study is to investigate the effect of HS on the crystallisation of gypsum to understand the mechanisms (nucleation and crystal growth) of crystallisation better. This knowledge can be used to improve the sizing and operation of crystallisers. The effect of HS was investigated at supersaturation (SS) of 2-4, pH of 4.5 – 9.5 and seed loading of 200, 1000 and 2000 mg/l through a batch crystallisation process.

An increase in HS concentration resulted in an increase in induction times due to the increased inhibitory effects of HA and FA through their functional groups. Induction times increased from 25 to 295 minutes with an increase in HA concentration from 0 to 15 mg/l at SS3 (0.0419 mol/l). At a HA concentration of 15 mg/l, an increase to SS4 (0.0566 mol/l) resulted in a decrease of induction times from 295 to 15 minutes, indicating the driving force of supersaturation. Increase in initial pH enhanced the inhibitory abilities of both HA and FA. Induction time increased from 115 to 415 min with an initial pH increase from 4.5 to 9.5 in the presence of 15 mg/l HA at SS3 (0.0419 mol/l). The effect of FA was far greater than HA, with crystallisation completely inhibited for a period of 2 days at a FA concentration of 5 and 15 mg/l in the absence of any seed crystals. At FA concentrations of 1.0 and 2.5 mg/l, induction times were 185 and 480 minutes, respectively. The greater effect of FA is attributed to an increase in the number of functional groups with a decrease in molecular weight.

Seeding the crystallisation process successfully overcame the inhibitory effects of HS (both HA and FA) at concentrations of 1000 and 2000 mg/l gypsum seed crystals. With a

seed concentration of 200 mg/l, an induction period of 50 min was observed in the presence of HA at 15 mg/l. With FA at 10 mg/l and a gypsum seeding of 200 mg/l, no crystallisation was induced. This again illustrated the enhanced effect of FA to block active growth sites successfully. In the presence of seed crystals pH has no effect, suggesting that only surface interaction is taking place. With HA, an increase in seed crystals resulted in an increased growth rate (from 0.50 to 4.91 litre.mol⁻¹.min⁻¹) due to an increase in available growth sites.

The inhibiting and retarding effect of HS on crystallisation is significant. Increasing supersaturation can override the inhibitory abilities of HS, while the presence of sufficient seed material will completely override the inhibitory abilities of HS and minimise the effects of these substances on crystallisation.

OPSOMMING

Hoë herwinning mynwater behandelingsaanlegte genereer pekelstrome wat hoogs oorversadig is met anorganiese soute. Intermediêre kristallasie van gips word vereis vir verdere behandeling van hierdie pekelstrome. Die kristallasie van gips word beïnvloed deur verskeie faktore soos temperatuur, oorversadigheid, bymiddels of onsuiverhede, pH en saad kristalle.

Die teenwoordigheid van natuurlike organiese materiaal (NOM), wat bestaan uit humus stowwe (HS), kan die aanvang van kristallasie voorkom. Humiese stowwe, hoofsaaklik humussuur (HA) en fulviensuur (FA), word beskou as swak poli-elektroliete as gevolg van hulle karboksiel en fenoliese funksionele groepe. Hierdie studie se doel is om die effek van HS op die kristallasie van gips te ondersoek en die meganismes (kernvorming en kristal groeitempo) van kristallasie beter te verstaan. Die kennis wat hier voorgelê word kan gebruik word om die ontwerp en werking van kristalliseerders te verbeter. Die effek van HS was ondersoek by 'n oorversadigingsvlak (SS) van 2-4, pH van 4.5 – 9.5 en saad konsentrasie van 200, 1000 en 2000 mg/l deur middel van 'n lot ("batch") kristallasie proses.

'n Toename in HS konsentrasie het tot 'n toename in induksie tyd gelei as gevolg van 'n toename in die vermoë van HA en FA om kristallasie te onderdruk deur middel van hul funksionele groepe. Induksie tye het toegeneem vanaf 25 tot 295 minute met 'n toename in HS konsentrasie vanaf 0 tot 15 mg/l by SS3 (0.0419 mol/l). 'n Verhoging van die oorversadigingskonsentrasie tot SS4 (0.0566 mol/l), in die teenwoordigheid van 15 mg/l HA, het gelei tot 'n afname in induksie tye, vanaf 295 tot 15 minutes. Dit dui dat oorversadiging 'n groot dryfkrag vir kristallasie is. Verhoogde aanvanklike pH, van 4.5 tot 9.5, het die kristallasieonderdrukkingsvermoë van beide HA en FA verbeter, met induksie tye wat toegeneem het vanaf 115 tot 415 minute, in die teenwoordigheid van 15 mg/l HA by SS3 (0.0419 mol/l). Die effek van FA was veel groter as HA, met kristallasie wat vir 'n tydperk van 2 dae ten volle onderdruk is by 'n FA konsentrasie van 5 en 15 mg/l, in die afwesigheid van enige saad kristalle. Die induksie tye by 'n FA konsentrasie van 1.0 en

2.5 mg/l was onderskeidelik, 185 en 480 minute. Die groter effek van FA is toegeskryf aan die toename in funksionele groepe met 'n afname in molekulêre massa.

Die vermoë van HS (beide HA en FA) om kristallasie te onderdruk is oorkom deur die kristallasie proses met gips saad kristalle te voed by konsentrasies van 1000 en 2000 mg/l. 'n Induksie periode van 50 min was waargeneem in die teenwoordigheid van 15 mg/l HS en by 'n saad konsentrasie van 200 mg/l. Met 'n FA konsentrasie van 10 mg/l en gips kristalle van 200 mg/l, het geen kristallasie plaasgevind nie. Dit het weereens die hoër vermoë van FA om aktiewe groeipunte suksesvol te blok, beklemtoon. pH het geen effek in die teenwoordigheid van saad kristalle nie, wat daarop dui dat slegs oppervlak interaksie plaasvind. In die teenwoordigheid van HA het 'n toename in saad kristalle gelei tot 'n toename in groeitempo (van 0.50 tot 4.91 liter.mol⁻¹.min⁻¹), as gevolg van 'n toename in beskikbare groeipunte.

Die vermoë van HS om kristallasie te onderdruk en vertraag was beduidend gevind. Deur die vlak van oorversadiging te verhoog, kan die vermoë van HS om kristallasie te onderdruk oorkom word, terwyl die teenwoordigheid van genoeg saad kristalle die onderdrukkende vermoë van HS heeltemal sal oorkom en sodoende die effekte van hierdie stowwe op kristallasie te minimiseer.

ACKNOWLEDGEMENTS

There are just too many people to mention that had a hand in the success and completion of this project. I wish that I could mention you all. I will attempt to mention some of the best.

First of all, many thanks to Prof. A.J. Burger for giving me the opportunity to come back and complete my master's degree. Thanks also for having lots of confidence in and patience with me, always giving a helping hand and sharing your extensive knowledge and understanding.

Dr. L.J. du Preez, thank you for all the advice and support with the writing of this thesis.

To my analytical family, where this journey started: Hanlie Botha for all the help with ICP analysis, analytical knowledge and support throughout. To Jaco van Rooyen, for all the help and support. Levine Simmers, for always being friendly, making my day better and always being willing to help.

To Tannie Lynette Bresler, who in all sadness retired before I could complete this thesis: you are dearly missed. Thank you for the hours of chats, listening and support. Thank you for believing in me.

To Tannie Juliana Steyl and Francis Layman: for all the help around placing orders and financial support.

To all the workshop and technical staff: thank you for all the tea sessions with the workshop, all the insight in the mechanical aspect of things that you shared and for teaching me so much. Thank you so much!

To my office and SepTech family: thank you for putting up with my craziness, loudness and always having a laugh on my account. You all made every single day worthwhile and without any of you, life would undoubtedly be boring. All the coffee and sun sessions will be profoundly missed.

To my family: my mom, for all your undying support and believing in me and to my dad, for giving me the opportunities to study and fulfill my dreams. My sister, for being who you are and always being there when I need a day off!

Every single one of you is **awesome!** Thank you!

Laastens, aan Liewe Jesus vir U genade, krag en liefde. Dankie vir die talente en verstand wat U my gegee het om sukses te behaal.

NOMENCLATURE & ABBREVIATIONS

Symbol	Description	Unit
A	Pre-exponential factor	-
A_c	Surface area of crystal	m^2
γ	Activity coefficient	-
B_0	Nucleation rate (equation 2.5)	nuclei/time
C	Solute concentration in the supersaturated solution	mol/l
c^*	Equilibrium concentration	mol/l
$[Ca^{2+}]_i$	Initial calcium concentration in the supersaturated solution (equation 3.1)	mol/l
$[Ca^{2+}]^1$	Initial calcium concentration (equation 4.2)	mol/l
$[Ca^{2+}]_{eq}$	Calcium concentration at equilibrium	mol/l
$[Ca^{2+}]_S$	Calcium solubility concentration of gypsum at 25°C = 0.0157 mol/l	mol/l
c_i	Solute concentration in solution at the crystal-solution interface	mol/l
D	Impeller Diameter	m
d	Normal particle size	m
Da	Daltons (Atomic Mass)	-
E	Activation energy	J/mol
g	Gravitational acceleration	$m.s^{-2}$
ΔG	Gibbs free energy	J
ΔG_{crit}	Maximum excess free energy at a critical particle radius	J
ΔG_v	Volume excess free energy (equation 2.3)	J
H	Dimensionless constant (equation 2.21)	-
σ	Interfacial tension (equation 2.3)	J/m
α	Ionic activity	-
IP	Product of free calcium and sulphate ions (equation 2.14)	-
k	Growth rate constant (equation 2.18)	$l.mol^{-2}.min^{-1}$
K_a	Activity solubility product	-
k_B	Boltzmann constant	$m^2kg.s^{-2}K^{-1}$
k_c	Mass-transfer coefficient	$l.mol.m^{-2}.min^{-1}$

Symbol	Description	Unit
k_d	Diffusion mass transfer coefficient	$\text{l.mol.m}^{-2}.\text{min}^{-1}$
k'	Overall growth rate constant (equation 4.1) $= k_G s_g$	$\text{l mol}^{-1}.\text{min}^{-1}$
K_G	Overall growth rate constant	$\text{l mol}^{-1}.\text{min}^{-1}$
k_G	Overall crystal growth coefficient	$\text{l.mol.m}^{-2}.\text{min}^{-1}$
k_r	Coefficient of surface reaction	$\text{l.mol.m}^{-2}.\text{min}^{-1}$
K_{sp}	Solubility product	-
L	Vessel diameter	m
m	Mass solute concentration	mg/l
M	Molar concentration	mol/l
m_s	Mass solute concentration at equilibrium	mg/l
n	Overall order of growth exponent (equation 2.11)	-
N	Impeller speed	rev.s^{-1}
ρ	Solid density	kg.m^{-3}
ρ_l	Liquid density	kg.m^{-3}
R	Universal gas constant	J/mol.K
r	Particle radius	mm
R_G	Growth rate	min^{-1}
S	Supersaturation ratio (equation 2.16)	-
s_g	Number of growth sites	-
$[SO_4^{2-}]_{eq}$	Sulphate concentration at equilibrium	mol/l
T	Temperature	K
t	Time of sample (equation 4.2)	min
t_{10}	Time at 10% above saturation	min
t_g	Growth time	min
t_{ind}	Induction time	min
t_n	Critical nuclei time	min
t_r	Relaxation time	min
t_s	Time at saturation	min
\mathcal{U}	Kinematic viscosity	$\text{m}^2.\text{s}^{-1}$
ν	Number of moles ions in one mole of electrolyte	-
v_s	Molar volume	m^3/mol
χ	Fraction of solids in the system	-

Abbreviation	Description
BL	Baseline
Eq	Equilibrium
CAPEX	Capital Expenditure
FA	Fulvic Acid
HA	Humic Acid
HS	Humic Substances
ICP	Inductively coupled plasma
IHSS	International Humic Standard Society
NF	Nanofiltration
NOM	Natural Organic Matter
OPEX	Operating Expenditure
QC	Quality Control
RO	Reverse osmosis
RSD	Relative standard deviation
SE	Standard Error
Smt	Smoothed data trend line
SS	Supersaturation
SS2	Supersaturation Level 2
SS3	Supersaturation Level 3
SS4	Supersaturation Level 4
STD	Standard deviation
TDS	Total Dissolved Solids
UF	Ultrafiltration

TABLE OF CONTENTS

Abstract	i
Opsomming	iii
Acknowledgements	v
Nomenclature & Abbreviations	vi
Chapter 1: Introduction	1
1.1. Background.....	1
1.2. Calcium sulphate crystallisation.....	3
1.3. Motivation of study	4
1.4. Problem statement and key questions	4
1.5. Objectives	5
Chapter 2: Literature review	6
2.1. Crystallisation	6
2.1.1. Mechanism of crystal growth	6
2.1.1.1. Nucleation	6
2.1.1.2. Crystal growth.....	10
2.2. Calcium sulphate-water system.....	13
2.2.1. Solubility of calcium sulphate	13
2.2.2. Thermodynamics of gypsum	15
2.3. Factors influencing crystallisation	16
2.3.1. Supersaturation	16
2.3.2. Temperature.....	17
2.3.3. Ionic strength.....	18
2.3.4. Additives and impurities.....	19
2.3.5. pH.....	22

2.3.6. Seeding	23
2.3.7. Agitation	25
2.4. Natural organic matter (NOM)	26
2.4.1. Humic substances (HS)	26
2.4.1.1. Humic acid (HA).....	27
2.4.1.2. Fulvic acid (FA).....	28
2.4.1.3. pH dependence and cation interactions	28
2.5. Literature summary.....	31
Chapter 3: Materials, methodology and research design	34
3.1. Materials	34
3.2. Experimental methodology.....	35
3.2.1. Experimental setup	35
3.2.2. Solution preparation.....	37
3.2.3. Experimental procedure summary.....	38
3.2.3.1. Equipment preparation	38
3.2.3.2. Experimental run	39
3.2.3.3. Analytical equipment	40
3.3. Theoretical methodology.....	41
3.3.1. Supersaturation concentrations	41
3.3.2. Processing of data	46
3.4. Experimental design.....	46
3.4.1. Preliminary runs unseeded and seeded	46
3.4.2. Experimental study	50
3.5. Error analysis.....	55
3.5.1. Experimental error	55
3.5.2. Analytical error	57
Chapter 4: Experimental Results and Discussion	59

4.1. Baseline conditions.....	59
4.1.1. The effect of supersaturation.....	62
4.1.2. Evaluation of crystallisation times	63
4.2. The effect of humic acid (HA)	65
4.2.1. Effect on induction times	65
4.2.2. Supersaturation effect	68
4.2.3. Effect of pH.....	70
4.2.4. Crystallisation times	81
4.3. Effect of fulvic acid (FA).....	85
4.3.1. Induction times.....	86
4.3.2. Effect of pH.....	89
4.4. Fulvic acid (FA) vs. humic acid (HA).....	92
4.5. Crystal growth kinetics in the absence of seeding	96
4.6. Seeded crystallisation.....	105
4.6.1. In the presence of humic acid (HA)	106
4.6.2. In the presence of fulvic acid (FA)	115
Chapter 5: Conclusions	121
Chapter 6: Recommendations	123
Chapter 7: References.....	124
Appendix A: Detailed Methodology	133
A.1. Solution preparation.....	133
A.1.1. Sodium sulphate	133
A.1.2. Calcium chloride.....	134
A.1.3. Ethylenediaminetetracetic acid (EDTA).....	134
A.1.4. Hydrochloric acid.....	134
A.1.5. Humic acid	134
A.1.6. Fulvic acid.....	135

A.2. Experimental procedure	136
A.3. Cleaning of equipment.....	139
A.4. pH calibration.....	140
A.5. ICP calibration	141
A.6. Reactor modifications	141
Appendix B: Experimental results	144
B.1. Preliminary results.....	144
B.2. Baseline data	154
B.3. Humic acid unseeded experimental data	156
B.4. Humic acid seeded experimental data.....	172
B.5. Fulvic acid experimental data	180
B.6. Fulvic acid seeded experimental runs.....	185
B.7. pH control.....	188
Appendix C: PHREEQC® output data	190
Appendix D: Error analysis and deviations	194
Appendix E: Analysis reports	201
Appendix F: Sample calculations	204
F.1. Supersaturation concentration.....	204
F.2. Concentration error with pH adjustment	205
F.3. Standard deviations, relative standard deviations and standard error	206

Chapter 1: INTRODUCTION

In recent years the purification of water has become one of the major discussion topics around the world alongside topics such as green technology, global warming and sustainability. Desalinating sea water is still an expensive technology and the recovery of water is low due to high energy input requirements and scaling limitations in desalination technologies.

To keep the fresh water intake around chemical industries to a minimum, process water used in such plants has to be recovered and reused. The recovery of these water streams is achieved by the implementation of various water treatment technologies such as: biological treatment; ion exchange; adsorption; filtration; reverse osmosis (RO). Advanced treatment methods, such as crystallisation, have to be implemented between stages in multistage treatment plants in order to achieve the highest possible recoveries, by reducing scaling potential of the brine streams between filtration steps.

1.1. Background

RO is normally one of the final treatment steps of water recovery. Multistage RO plants are used for the purification of water streams around mines, where a high recovery is desired. Brine streams, which are highly supersaturated with semi-soluble and insoluble salts, have to be treated as well to achieve high recoveries. These streams can become concentrated up to 4 times above saturation levels. In this supersaturated state certain salts become insoluble and can spontaneously precipitate out of solution which can result in the fouling of membranes.

The removal of these semi-soluble and insoluble inorganic salts becomes vital to prevent damage to membranes and improve the recovery of water. One such example is calcium sulphate dihydrate (gypsum), that is formed by the supersaturated calcium (Ca^{2+}) and sulphate (SO_4^{2-}) ions that are present. Removal of these scaling salts through crystallisation for further treatment of brine streams is one of the most commonly used processes [1]. Their

Chapter 1: Introduction

removal can become tricky and various factors can influence the onset of crystallisation, which can increase retention time in crystallisers and have a negative impact on water recovery, plant performance and capital expenditure (CAPEX) as well as operating expenditure (OPEX).

Natural organic matter (NOM) is one of the major fouling agents present in these streams and it has a significant effect on the crystallisation process [2]. NOM consists mainly of humic substances (HS), that are made up of humic (HA) and fulvic acid (FA). HS have been a point of discussion in various fields and are complicated to understand and completely formulate.

Although HS can be removed to a large degree through various pre-treatment processes, these substances can have major effects on water treatment plants [3]. So for example, the smaller molecules forming part of HS, such as FA, are small enough to pass through the membrane or clog membrane pores [4]. This also serve as feed material for microbial growth. This can lead to problems in downstream processes such as crystallisation.

Figure 1.1 presents a simplified drawing of an example of a multistage RO system. The focus of this study is on the enhanced recovery steps as outlined by the dashed line. The removal of supersaturated salts is achieved by means of crystallisation in order to enable further recovery of water in the brine stream by means of secondary RO.

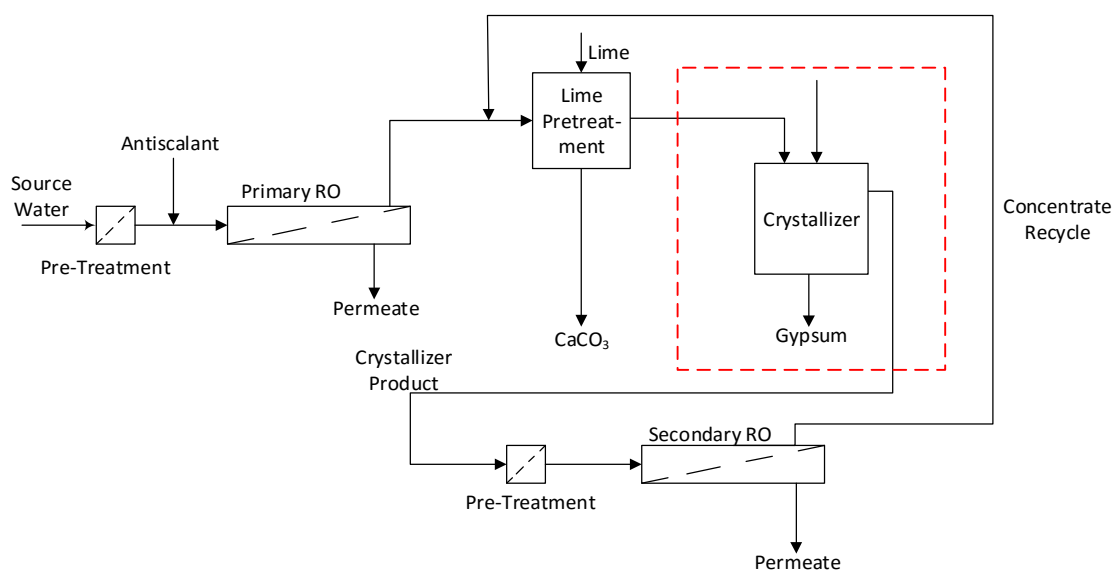


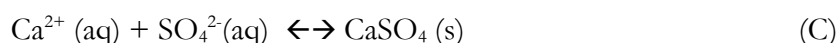
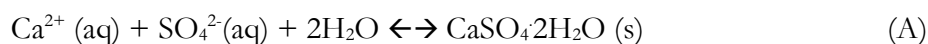
Figure 1.1: Illustration of a multistage RO system (Adapted from [1]).

1.2. Calcium sulphate crystallisation

Crystallisation is one of the oldest and most basic processes in the final treatment of products [5, 6]. The process of crystallisation is utilised in industry for the manufacturing of products, the purification of process or utility streams and the recovery of valuable by-products. The focus of crystallisation here will be on the purification of process water streams.

It is important to understand the different variables that can affect the process of crystallisation and why the process is affected by them. The study of crystallisation plays an important role in facilitating the design and optimisation of crystallisers for application in industry in the treatment of supersaturated brine streams.

The main focus of this study is on one variable (HS) that affects the crystallisation process of calcium sulphate under various conditions. Calcium sulphate crystallisation is especially important in the industry of petroleum drilling operations, in evaporative seawater desalination plants and in heat transfer units [5]. The formation of calcium sulphate is described by the following reactions:



In an artificial system containing only pure water, calcium (Ca^{2+}) and sulphate (SO_4^{2-}) ions, there are three primary crystalline salts that can form: calcium sulphate dihydrate, $\text{CaSO}_4 \cdot 2\text{H}_2\text{O}$ (gypsum) [reaction A]; calcium sulphate hemihydrate, $\text{CaSO}_4 \cdot 1/2\text{H}_2\text{O}$ (plaster of Paris) [reaction B] and calcium sulphate anhydrite, CaSO_4 [reaction C]. Gypsum is the most commonly formed salt of the three salts, while hemihydrate and anhydrite formation primarily occur in systems at elevated temperatures.

The removal of calcium and sulphate ions from brine streams for further treatment is achieved through gypsum crystallisation. This is mainly achieved by secondary crystallisation through the addition of gypsum seed crystals [1]. Unfortunately, the process can be retarded

Chapter 1: Introduction

by the presence of HS that can behave like an antiscalant in water. It is therefore important to understand the effect of HS on the crystallisation of gypsum.

1.3. Motivation of study

The removal of semi-soluble and insoluble salt ions (calcium and sulphate) is required for the treatment of supersaturated brine streams around multistage RO plants to enable high overall recoveries of water. HS are also present in these concentrated streams and can cause various problems in downstream processes. The motivation for this study is the need for a better understanding of the effect of HS on gypsum crystallisation, which takes place in intermediate precipitation processes. Improved understanding will assist with the efficient sizing and operation of relevant crystallisation reactors.

1.4. Problem statement and key questions

The crystallisation of gypsum from an artificial supersaturated solution can be affected by additives and impurities such as HS. These HS consist mainly of humic (HA) and fulvic acid (FA) that can behave like weak polyelectrolytes in water. Their behaviour as weak polyelectrolytes gives HS the ability to inhibit the crystal growth of gypsum or the onset thereof.

The key questions are:

- To what degree will the crystallisation of gypsum be inhibited by HS and how will the induction time and reaction kinetics of crystallisation be influenced?
- Will the addition of seed crystals completely override the inhibitory effect of HS and what seed concentrations are required?
- How will initial pH adjustment change the behaviour of HS and how will the crystallisation process be influenced?
- How does the effect of FA compare to that of HA?

1.5. Objectives

Considering the motivation for this study, as well as the key question posed, the following research objectives are evident.

- Experimentally generate desupersaturation curves for the crystallisation of gypsum from equimolar solutions of calcium chloride and sodium sulphate.
 - Study the effect of various concentrations of HA.
 - Study the effect of various concentrations of FA.
- Interpret experimental data by evaluating induction times, crystal growth times and the kinetics of gypsum crystallisation.
- Determine the effect of supersaturation level in the presence of HS.
- Determine the effect of initial pH change on gypsum crystallisation in the presence of HS.
- Determine the effect of seeding on the crystallisation of gypsum in the presence of HS.

Chapter 2: LITERATURE REVIEW

The literature review chapter gives a brief introduction to the basic concepts of crystallisation, what it entails and the mechanisms behind it. This is followed by an in-depth review on the factors influencing the crystallisation process. The second half of this chapter focuses on humic substances (HS) and the factors that influence their behaviour in solutions as well as the shortcomings in knowledge regarding this subject as identified in literature. Lastly, a summary of the conclusions from literature is given in support of the planning and execution of the experimental work.

2.1. Crystallisation

Crystallisation is the arrangement of atoms and molecules into a solid, stable structure known as a crystal. This can either occur naturally or artificially. The study of crystallisation processes has become of increasing interest over the last few decades. Many authors around the world have investigated crystallisation and published reliable data in their quest to understand the mechanism behind it [6, 7, 8].

2.1.1. Mechanism of crystal growth

To fully understand crystallisation one must comprehend the different mechanisms of crystallisation. The mechanisms of crystallisation can be separated into two parts, namely nucleation and crystal growth. These two mechanisms are the focus of the subsequent sections.

2.1.1.1. Nucleation

A prerequisite for crystallisation to take place is that the solution should be in the supersaturated state. This means that the associating salt ions (i.e. calcium, sulphates, etc.) are above their solubility limit. However, supersaturation alone cannot enforce crystallisation. For crystallisation to take effect a finite amount of stable solid particles needs to be present in the system [5]. This can either come to pass spontaneously or be brought on artificially known as primary and secondary nucleation, respectively.

2.1. Crystallisation

Figure 2.1 illustrates the different mechanisms of nucleation. Primary nucleation can either take place homogeneously or heterogeneously. Homogeneous nucleation is the spontaneous formation of nuclei over a period of time until a stable crystalline lattice is formed. Pure homogeneous crystallisation is difficult to achieve, even in pure water. The presence of some form of finite particles in the form of dust or working chemicals suspended in the atmosphere can influence the crystallisation process [5].

Heterogeneous nucleation is the growth of crystals induced by the addition of any crystals or foreign particles [5]. Secondary nucleation is nucleation that takes place in the presence of crystals of the same substance. Addition of these crystals to the solution is known as seeding of the process. The presence of seed crystals has the ability to reduce or override the induction period by removing the requirement for the formation of any new nuclei through the addition of active growth sites, as have been illustrated by numerous previous studies [9, 10, 11, 12, 13]. The addition of seed crystals does not necessarily always eliminate the induction period completely. The method of seeded crystal growth is discussed in depth in section 2.3.7.

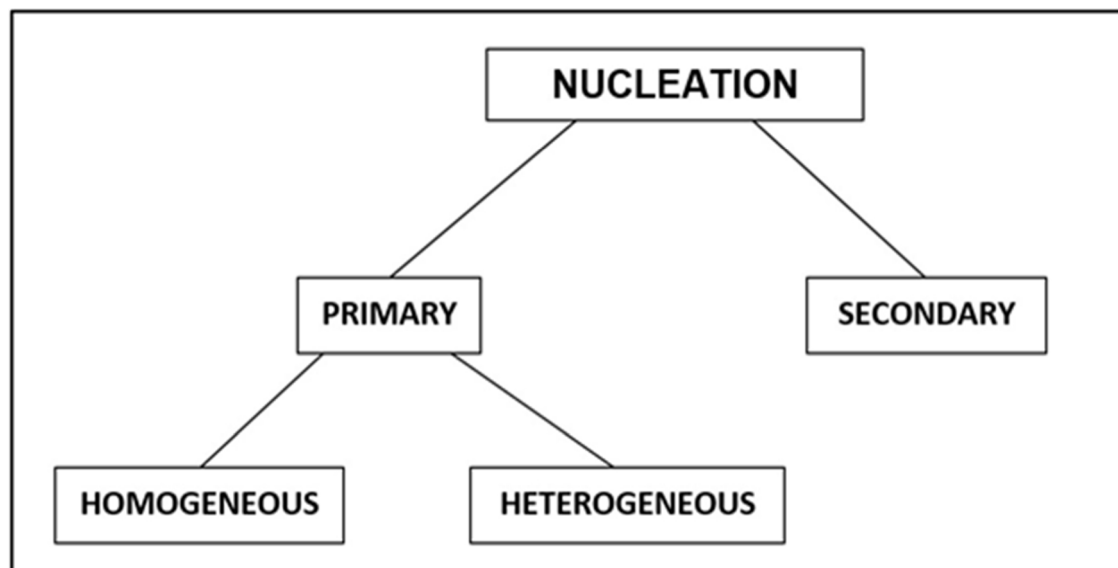


Figure 2.1: Mechanisms of Nucleation [5].

Chapter 2: Literature review

The rate of homogeneous primary nucleation, B_0 , can be represented by the Arrhenius reaction rate generally used for a thermally activated process [5, 14]:

$$B_0 = A \exp(-\Delta G / k_B T) \quad (2.1)$$

where A is a frequency factor, k_B is the Boltzmann constant, T is the temperature in Kelvin and ΔG is the overall excess free energy. The Gibbs-Thomson relationship for a solid-liquid system can be written as:

$$\ln \frac{c}{c^*} = \ln S = \frac{2\sigma v_s}{\nu k_B T r} \quad (2.2)$$

where v_s is the molar volume (m^3/mol), σ is the interfacial tension, r is the radius of a particle, ν is the number of moles of ions of one mole of electrolyte and S is the supersaturation ratio (equation 2.16). The volume excess free energy, ΔG_v , is given as

$$-\Delta G_v = \frac{2\sigma}{r} = \frac{RT\nu \ln S}{v_s} \quad (2.3)$$

The maximum value, ΔG_{crit} , required for a newly crystalline structure to form is defined as

$$\Delta G_{crit} = \frac{16\pi\sigma^3}{3(\Delta G_v)^2} \quad (2.4)$$

Substituting equation 2.4 in 2.3 and using equation 2.2, equation 2.1 is simplified to give a nucleation rate that is described as

$$B_o = A \exp \left[-\frac{16\pi\sigma^3 v_s^2}{3\nu^2 k^3 T^3 (\ln S)^2} \right] \quad (2.5)$$

Equation 2.5 indicate that nucleation is controlled by three important variables, the temperature, T , degree of supersaturation, S , and the interfacial tension, σ [5].

2.1. Crystallisation

Figure 2.2 illustrates the desupersaturation curve for a crystallisation reaction [9].

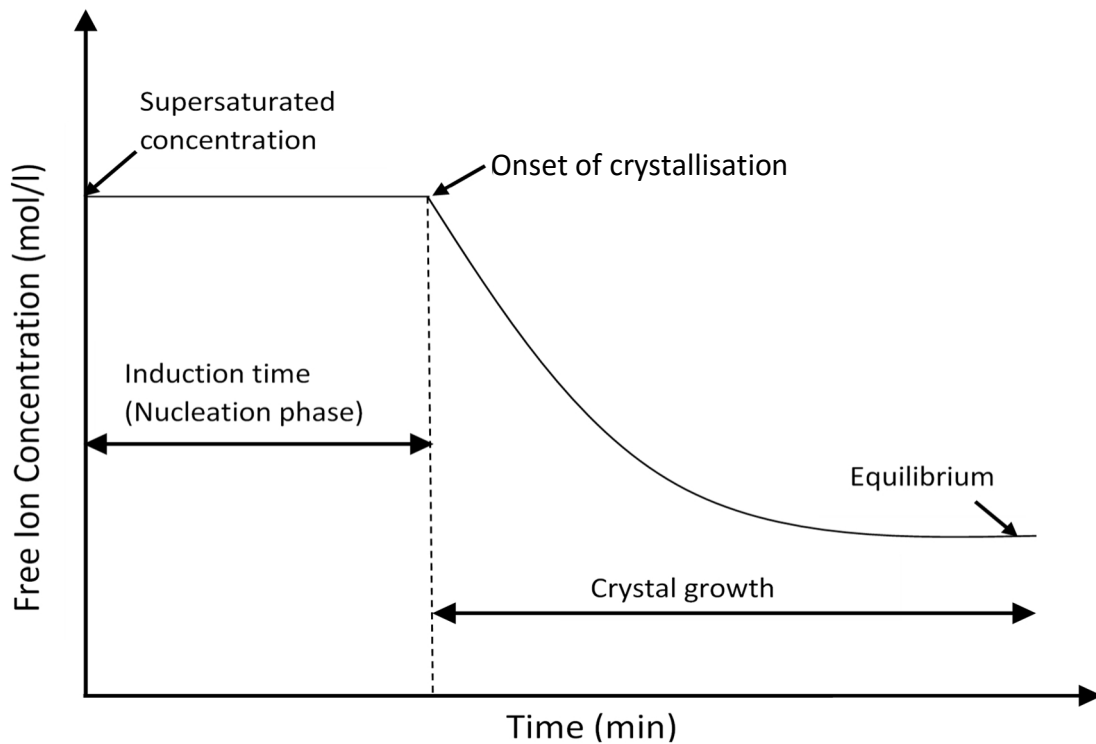


Figure 2.2: Illustration of a crystallisation desupersaturation curve (Redrawn from [9]).

The period of time until the appearance of stable crystals is known as the induction period. This period can be significantly influenced by the level of supersaturation, the degree of agitation, the presence of impurities, viscosity, etc.

Induction time can be described by t_{ind} as

$$t_{ind} = t_r + t_n + t_g \quad (2.6)$$

t_r is some 'relaxation time' required for the distribution of molecular groups to achieve a quasi-steady-state in the system, t_n is the time for the critical nuclei to form and t_g is the time for the nucleus to grow to a detectable size. Quantification of these individual terms is difficult to achieve, if not impossible. Induction times are generally measured visually, but more sensitive means can be used for more accuracy, e.g. turbidity measurements [5].

Chapter 2: Literature review

The induction/nucleation period is completed when the concentrations of the free ions of the insoluble salts start to decrease. The growth curve is the period from where the induction period terminated until equilibrium is reached. Equilibrium concentration is reached when the free ion concentration remains constant. It can take hours or days to achieve equilibrium conditions depending on the system conditions and its influence on the crystallisation process.

2.1.1.2. Crystal growth

Figure 2.2 indicates that crystal growth is the period after induction, when the onset of crystallisation occurs, until equilibrium is reached. Crystal growth based on equilibrium at the crystal-solution interface can be described by the following relationship [14]:

$$\frac{dm}{dt} = k_c A_c (m - m_s) \quad (2.7)$$

where, dm/dt is the rate of mass deposited on the crystal surface, A_c is the surface area of the crystal, k_c is the mass transfer coefficient, m is the mass solute concentration in the supersaturated solution and m_s is the mass solute concentration at equilibrium.

Equation 2.7 is not easy to apply in practice, due to the fact that the measurement of interfacial concentration is required [5]. The measurement of the interfacial concentration is difficult. It is usually more convenient to make use of an overall concentration driving force, $(c - c^*)$, that is easier to measure. A general equation for crystallisation is then described by [15]:

$$\frac{dm}{dt} = k_G A_c (c - c^*)^n \quad (2.8)$$

where k_G is the overall crystal growth coefficient and n is the exponent that refers to the order of the overall crystal growth process. Inorganic salt that crystallises from aqueous solution follow an overall growth rate order of between 1 and 2. Crystal growth can be divided into two different steps [15].

2.1. Crystallisation

Chapter 2: Literature review

Equation 2.8 is then divided into two separate steps:

$$R_G = \frac{1}{A_c} \cdot \frac{dm}{dt} = k_d(c - c_i) \quad (\text{diffusion}) \quad (2.9)$$

$$= k_r(c_i - c^*)^n \quad (\text{reaction}) \quad (2.10)$$

Equation 2.9 describes the diffusion process where the solute molecules move from the bulk of the fluid phase to the surface of the solid. This is followed by a reaction process (equation 2.10), where the formation of the stable crystal lattice occurs. k_d is the coefficient of mass transfer by diffusion, k_r is the coefficient of surface reaction (integration), c is the solute concentration in the supersaturated solution, c_i is the solute concentration in the solution at the crystal-solution interface and c^* is the equilibrium concentration at a specific temperature and ionic strength. It is difficult to measure the concentration at crystal-solution interface and, therefore, it is more convenient to make use of an overall driving force ($c - c^*$). Equation 2.9 and 2.10 can then be written for an overall rate:

$$R_G = K_G(c - c^*)^n \quad (\text{overall}) \quad (2.11)$$

where K_G is the overall growth rate constant normally in $\text{l mol}^{-1}\text{min}^{-1}$.

From work carried out by Nancollas [8], it was found that crystallisation reactions largely follow a second order rate equation. In numerous previous studies [12, 16, 17] it was concluded that crystal growth based on calcium concentration follows a second order rate. Equation 2.8 can be further simplified based on calcium concentration to:

$$-\frac{d[Ca^{2+}]}{dt} = k_G s_g ([Ca^{2+}]_i - [Ca^{2+}]_{eq})^2 \quad (2.12)$$

where s_g is the number of growth sites, $[Ca^{2+}]_i$ is the calcium concentration (mol/l) in the supersaturated solution and $[Ca^{2+}]_{eq}$ is the calcium equilibrium concentration (mol/l) at a specific temperature and ionic strength.

2.2. Calcium sulphate-water system

Equation 2.12 mostly holds true in cases where no induction times are observed, the process is seeded with crystals or a sufficient number of growth sites are available. Nucleation must occur first in cases where the stable crystal lattice has to form first before the onset of crystallisation can be achieved. After completion of nucleation and the first phase of crystallisation, the rate would be more diffusion limited up to a point where a sufficient amount of growth sites have formed, at which stage it will become more of an integration and surface reaction [8]. In previous studies [12, 17, 18], equation 2.12 was successfully applied to predict growth rates and growth rate constants in the presence of seed crystals for crystallisation reactions where induction periods were observed.

2.2. Calcium sulphate-water system

As discussed in Chapter 1, calcium sulphate primarily consists of three different crystal phases. These are the anhydrite, hemihydrate and dihydrate (gypsum) phases. Calcium sulphate dihydrate is the most likely crystalline to form at lower temperatures whereas the other two phases primarily only occur at elevated temperatures [19].

2.2.1. Solubility of calcium sulphate

Figure 2.3 illustrates the solubility of calcium sulphate hydrates in water over a range of temperatures. The solubility of the dihydrate phase increases from 0 to 25°C and then slightly decreases with a further increase in temperature. Gypsum's solubility at 25°C is approximately 0.015 mol/l. The hemihydrate is unstable from 0 to 200°C, whereas the solubility of the anhydrite decreases with an increase in the temperature. Anhydrite is more stable at higher temperature than gypsum, and the conversion point between the two phases is around 42°C [20].

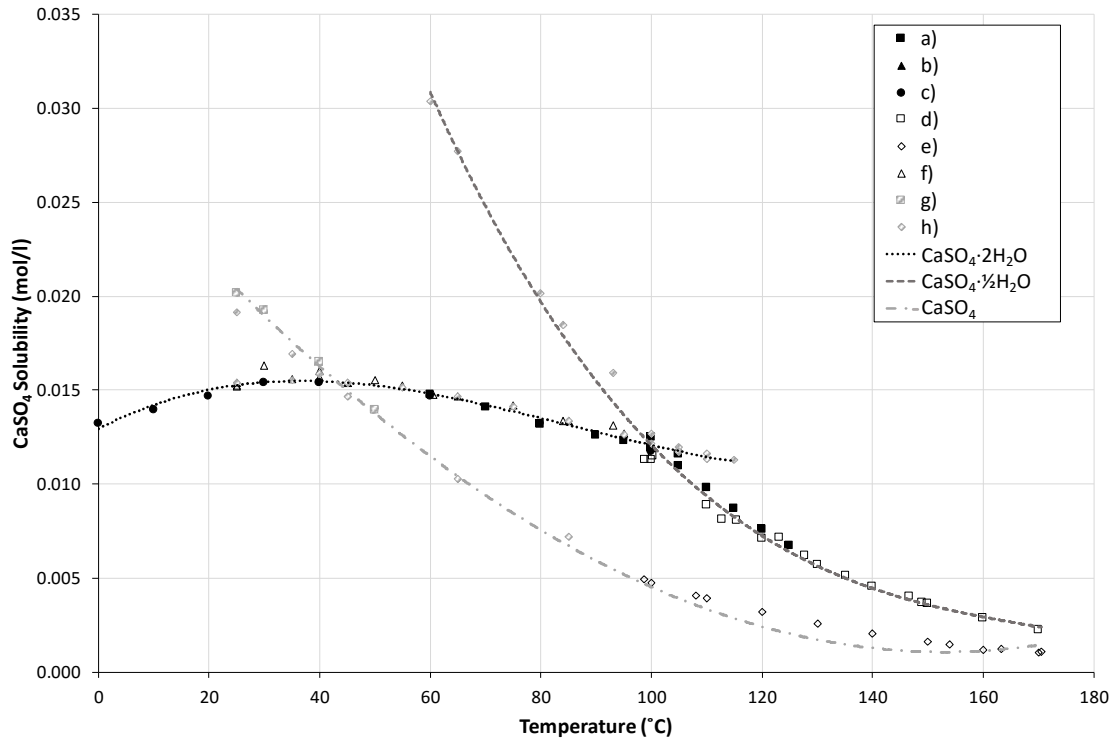
Chapter 2: Literature review

Figure 2.3: Solubility of calcium sulphate hydrates in water over a range of temperatures { \blacksquare a) [18]; \blacktriangle b) [21]; \bullet c) [5]; \square d) [22]; \diamond e) [23]; \triangle f) [24]; \blacksquare g) [25]; \diamond h) [26]}.

A variety of extensive studies [21, 22; 24-27] have been carried out over the years on the solubility of calcium sulphate in the presence of sodium chloride (NaCl) at different temperatures. It was observed that with an increase in NaCl, there is a dramatic increase in the solubility of calcium sulphate dihydrate. Figure 2.4 is a presentation of the increase in calcium sulphate dihydrate solubility with an increase in NaCl concentration at a temperature of 25°C. With a slight increase from 0 to 0.25 mol/l NaCl, the solubility of calcium sulphate dihydrate doubles from approximately 0.015 mol/l to ~0.03 mol/l as indicated in the highlighted section of Figure 2.4.

2.2. Calcium sulphate-water system

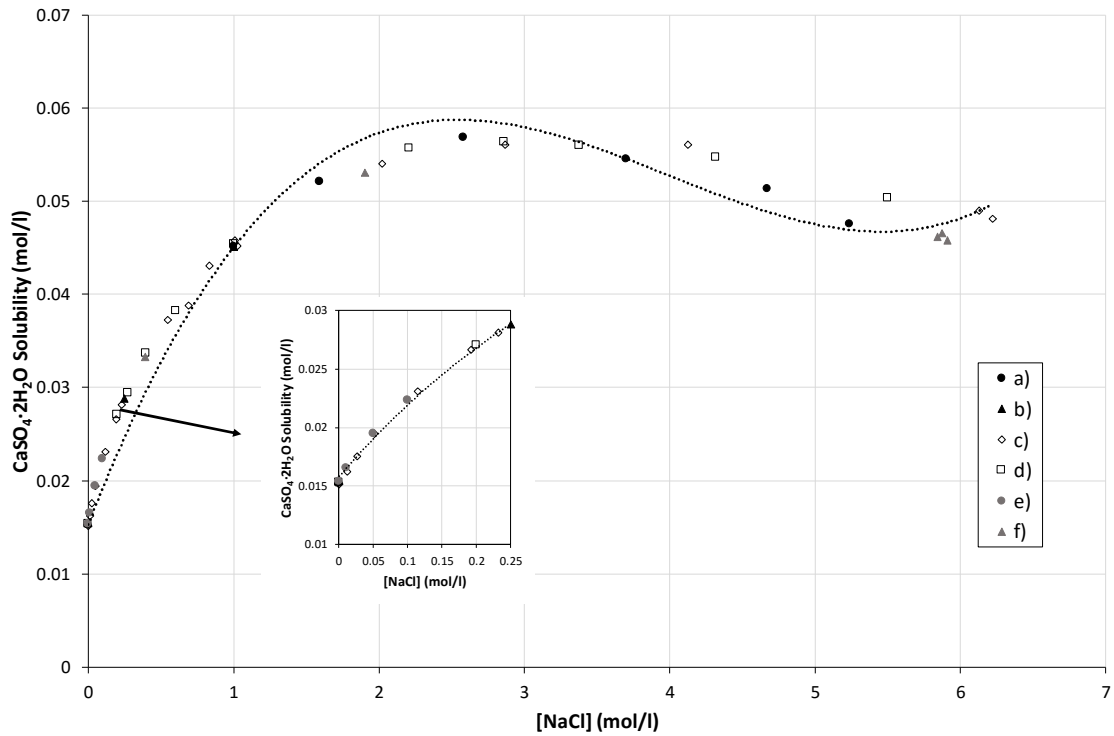


Figure 2.4: Solubility of gypsum in the NaCl-H₂O system (• a) [24]; ▲ b) [26]; ◇ c) [27]; □ d) [23]; • e) [28]; ▲ f) [29]).

2.2.2. Thermodynamics of gypsum

The driving force for gypsum formation can be expressed by the Gibbs free energy of transfer [30].

$$\Delta G = -\frac{RT}{2} \ln \left(\frac{IP}{K_{sp}} \right) \quad (2.13)$$

where R is the universal gas constant (8.314 J/mol.K), T is the absolute temperature in Kelvin, IP is the product of free calcium and sulphate ion activity at time, t , described in equation 2.14 and K_{sp} is the solubility product based on equation 2.15.

$$IP = (\alpha_{Ca^{2+}})(\alpha_{SO_4^{2-}}) \quad (2.14)$$

$$K_{sp} = \gamma_{Ca^{2+}}[Ca^{2+}]_{eq} \cdot \gamma_{SO_4^{2-}}[SO_4^{2-}]_{eq} \quad (2.15)$$

Chapter 2: Literature review

where α is the ionic activity and γ is the activity coefficient of species i in the solution. The equilibrium concentration, $[i]_{eq}$, is the concentration of the free calcium or sulphate ions in solution at the point where crystal growth has ceased. K_{sp} is dependent on temperature, which in effect will mean that the equilibrium concentrations will also be dependent on temperature.

In a solution that only contains pure water, calcium and sulphate ions, K_{sp} is the saturation concentration of calcium sulphate at a specific temperature. With background ions present in the solution, the saturation concentration will shift depending on the amount of ions present in solution as shown in Figure 2.4.

2.3. Factors influencing crystallisation

Numerous studies have investigated several different factors that influence the crystallisation of calcium sulphate [9, 13, 16, 17, 30]. The following factors have been shown by previous studies to have an impact on the crystallisation of calcium sulphate and these will be discussed in the subsequent sections:

- Level of supersaturation.
- Temperature.
- Ionic strength.
- Additives and impurities.
- pH.
- Seed crystals, seed size and seed area.
- Agitation

2.3.1. Supersaturation

At a specific temperature a saturated solution is in thermodynamic equilibrium with the solid phase. The solution is in the supersaturated state when that solution contains more dissolved solid than that which is represented by the saturation condition [5].

Figure 2.5 shows a solubility-supersolubility diagram. Three different solubility regions exist. These are firstly the unsaturated region (stable), where crystallisation is impossible. Secondly there is the metastable region which lies between the solubility and supersolubility curves.

Chapter 2: Literature review

Spontaneous crystallisation is not likely to take place in the metastable region, unless the process is seeded for growth to take place. Thirdly there is the supersaturated (unstable/liable) region, above the supersolubility curve, which is the last region where spontaneous crystallisation is most probable but not definite [5, 14]. Even if the system is in the supersaturated state, crystallisation can be inhibited by various factors such as impurities and additives. These are discussed in the following sections.

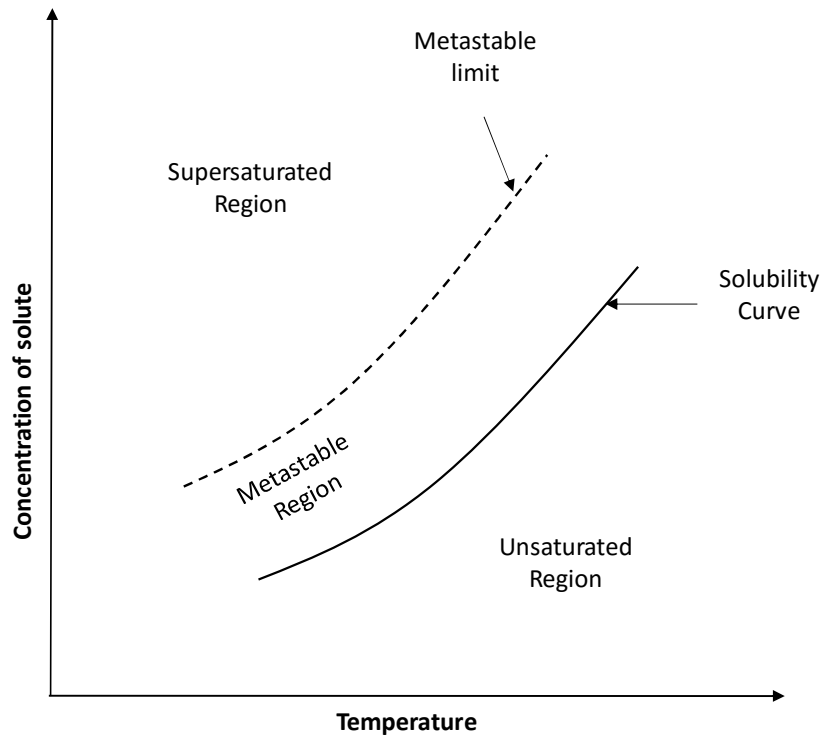


Figure 2.5: Solubility-super solubility diagram (Redrawn from [14]).

The supersaturation ratio, S , is defined very broadly [31, 32, 17, 33]. It is most commonly described by the following relationship [5].

$$S = \frac{c}{c^*} \quad (2.16)$$

where c is the supersaturated solution concentration and c^* is the equilibrium concentration at a specific temperature and ionic strength.

2.3. Factors influencing crystallisation

For sparingly soluble electrolytes in aqueous media, the supersaturation ratio can be described by the following relationship

$$S = \left(\frac{IP}{K_a} \right)^{1/v} \quad (2.17)$$

where IP is the ion activity product of the lattice ions in solution (equation 2.14), K_a is the activity solubility product of the salt and v is the number of moles of ions per one mole of salt.

Various authors [34, 35, 36] have shown that the level of supersaturation greatly enhances crystallisation. Where induction times are observed in the absence of seeded crystals, the nucleation rate is highly dependent on the level of supersaturation (equation 2.5), which in turn affects the induction time. The level of supersaturation is one of the main factors impacting spontaneous crystallisation and the driving force thereof.

2.3.2. Temperature

Temperature does not only influence the solubility of solute but it has a representative effect on the crystal growth. The effect of temperature on the crystal growth rate constant, k , can be described by the Arrhenius equation [5].

$$k = A \cdot \exp\left(\frac{-E}{RT}\right) \quad (2.18)$$

where E is the activation energy for the specific reaction, R is the universal gas constant and T is the absolute temperature in Kelvin. Taking the log of equation 2.18 gives:

$$\ln k = \ln A - \frac{E}{RT} \quad (2.19)$$

Findings from literature is summarised in Table 2.1. It was found that the growth rate can significantly increase with an increase of only 10°C. According to Mullin [5], crystal growth rate becomes diffusion controlled at elevated temperatures and integration controlled at lower temperatures. However, both these processes can be influential over a significant

Chapter 2: Literature review

intermediate temperature range, and according to an Arrhenius plot of crystal growth data, the result can be a curve that is non-linear rather than linear. This indicates that the activation energy for the overall growth process is dependent on temperature.

Table 2.1: Effect of temperature on the growth rate of crystallisation.

Temperature (°C)	Growth rate constant (l mol ⁻¹ min ⁻¹)	Reference
20	-0.380	
30	0.130	
40	0.320	[5]
50	0.730	
60	1.130	
70	1.480	
30	-0.660	
50	0.500	[17]
70	1.300	
90	1.520	
25	0.298	
35	0.580	[10]
45	1.600	
25	0.400	
35	0.740	[13]
45	1.030	
55	1.310	
60	8.300	
70	12.70	
80	25.70	[18]
90	32.30	
95	39.20	
100	68.50	

2.3.3. Ionic strength

As mentioned in section 2.2.1, the solubility of calcium sulphate is highly dependent on the ionic strength of the media. As described by Ahmed et al. [37], the effect of calcium sulphate solubility on crystal growth can be significant. With an increase in the solubility of the crystallite there will be a decrease in the driving force, $(C-C^*)$, and therefore a decrease in nucleation rate.

2.3. Factors influencing crystallisation

Ahmed et al. [37] also observed an increase in induction times and a decrease in growth rates when there was an increase in ion (such as Mg^{2+}) concentration. In their investigation Mg^{2+} had a dual effect by being an inhibitor and by increasing the ionic strength. Ahmed et al. [37] further suggested that the effect on gypsum crystallisation could be attributed to a reduction in ionic activities and a variation in solubility as well as the formation of the MgSO_4 ion pair.

An increase in growth rates was observed in the presence of background ions (such as Na^+ , Cl^- or NO_3^-) in the work carried out by Witkamp et al. [38] and Brandse et al. [39]. Again this was attributed to the change in solubility with the increase in ionic strength. It was further suggested that the background ions could have influenced the surface charge of the crystals and promoted the transfer of ions (Ca^{2+} and SO_4^{2-}) towards the surface. Thus, the growth rate of crystallisation can be influenced by increased ionic strength, depending on the medium used to increase the ionic strength. However, keeping the ionic strength constant throughout would not affect crystallisation.

2.3.4. Additives and impurities

Additives and impurities can have an extreme effect on the growth of a crystal. In the case of membrane systems and heat exchange surfaces, additives are added to the process to prevent crystallisation from occurring. Various studies [10, 11, 19, 30, 40, 41] show that additives can have a significant impact on the crystal growth of certain salts and the inhibition thereof. The most common additive investigated is polyelectrolytes.

Polyelectrolytes have been shown to be very effective inhibitors of crystal growth due to the nature of their polyelectrolyte architecture, their molecular weight and ionic charge. They contain functional groups such as carboxylic acid ($-\text{COOH}$), sulfonic acid ($-\text{SO}_3\text{H}$), esters ($-\text{COOR}$) and phenolic groups ($-\text{OH}$) [30]. Amjad [30] and Amjad et al. [10] observed a decrease in the crystal growth inhibitory effect and an increase in precipitation rate with an increase in polyelectrolyte molecular weight.

*Chapter 2: Literature review***Table 2.2: Summarised polyelectrolytes and their effect on gypsum crystallisation.**

Polyelectrolyte	Polyelectrolyte Concentration (ppm)	Mass of calcium sulphate dihydrate deposited (g)	Reference
None	0.000	1.570	[30]
	0.000	1.620	
Tannic Acid (TA)	1.000	1.310	
	2.500	0.940	
	5.000	0.770	
	15.000	0.440	
Fulvic Acid (FA)	1.000	1.200	
	2.500	0.850	
	5.000	0.637	
Poly-AA	0.100	1.020	
	0.100	0.860	
	0.300	0.480	
	0.500	0.200	
	1.000	0.050	
P-AA:SA	0.200	0.790	
P-AA:SA:SS	0.200	0.880	
None	0.000	1.170	
PAA (A)	0.100	0.780	
	0.050	0.740	
	0.100	0.580	
	0.200	0.360	
	0.500	0.100	
PAA (B)	2.000	0.000	
	0.025	0.970	
	0.050	0.880	
	0.100	0.680	
	0.200	0.420	
PAA (C)	0.500	0.150	
	2.000	<0.100	
	0.100	0.810	
	0.100	1.060	
	0.100	1.210	
PAA (D)	0.000	1.670	
	0.000	1.580	
Poly(acrylic acid)	0.075	1.250	
	0.150	0.890	
	0.200	0.710	
	0.300	0.510	
	0.300	0.480	
	0.500	0.250	
	1.000	0.080	
	0.300	0.520	
	1.000	0.120	
Poly(maleic acid)	0.300	1.190	
	1.000	0.340	
Poly-AA:MSA	0.300	1.550	
	1.000	1.500	
Poly(vinylpyrrolidone)	0.300	1.6400	
	1.000	0.169	
Poly-AA:AMSA	0.300	0.650	
Poly-AMSA:SS	0.300	0.880	

2.3. Factors influencing crystallisation

Table 2.2 summarises information on the different polyelectrolytes studied in literature and their effect on the crystal growth of gypsum. It has been observed that poly acrylic acid (PAA), which mostly consists of carboxylic functional groups, has the largest effect on the crystal growth of gypsum. All of the studies have shown that an increase in polyelectrolyte concentration has an effect on the induction period and crystal growth during gypsum crystallisation. In the work of Amjad [11, 40], the effect of different molecular weights together with an increase in polyelectrolyte concentration is discussed.

Amjad [30] investigated a natural organic additive, namely fulvic acid (FA), together with tannic acid (TA), PAA and poly acrylic acid: 2-acrylamido-2-methyl propane sulfonic acid (PSA). It was found that the behaviour of FA is similar to that of a polyelectrolyte and that it can have an inhibitory effect on the crystal growth of gypsum. Figure 2.6 illustrates the effect of FA together with various other polyelectrolytes on the crystallisation of gypsum.

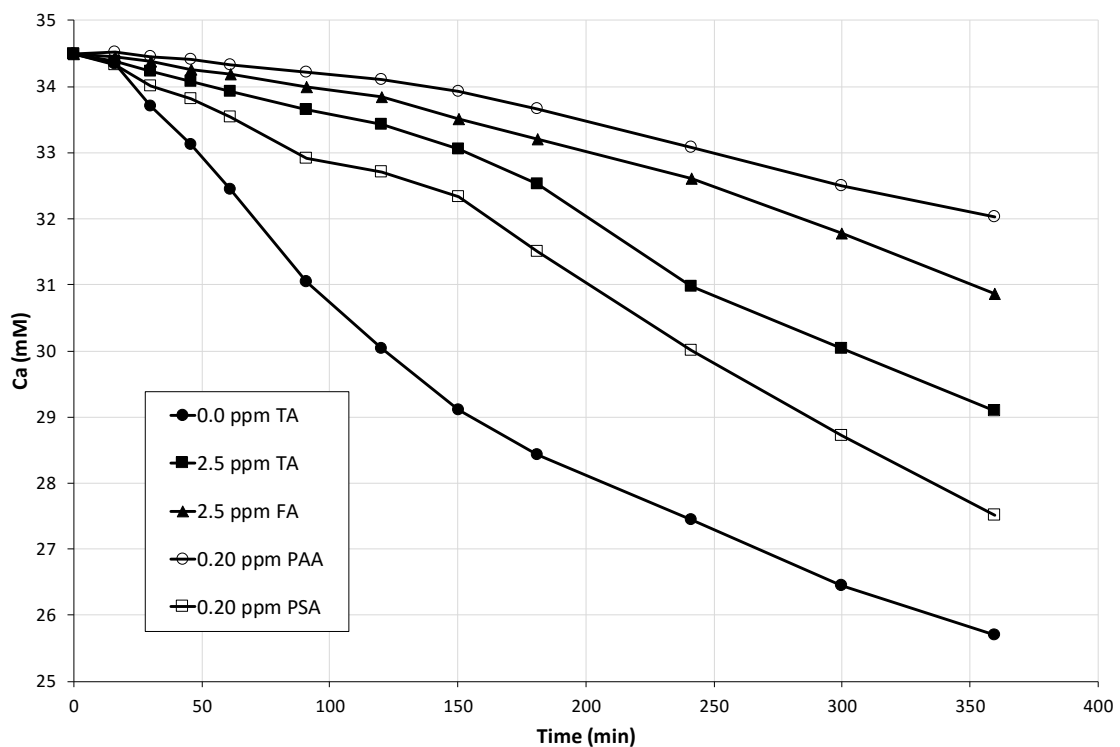


Figure 2.6: Gypsum growth in the presence of tannic acid (TA), fulvic acid (FA), poly acrylic acid (PAA) and PSA (Data extracted from [30]).

Chapter 2: Literature review

From Figure 2.6 it is evident that FA can inhibit the crystal growth of gypsum to some degree at fairly low concentrations. Although the initial concentration of calcium is at a very low supersaturation, the impact of FA is still an important finding compared to other polyelectrolytes. FA is discussed in section 2.4.1.2 of this document.

To the best of the author's knowledge, the work of Amjad [30] is the only findings in literature that describe an investigation into the influence of HS on the crystallisation of calcium sulphate, specifically gypsum. Klepetsanis et al. [42] investigated the inhibition of calcium carbonate (calcite) crystallisation in the presence of HA, FA and PAA. They concluded that HA expresses a larger degree of inhibition than FA at rather low concentrations (0.1 – 0.5 ppm), due to HA having a higher tendency to adsorb onto calcium carbonate than FA.

The supersaturated Ca^{2+} ion concentration relative to gypsum is much higher than Ca^{2+} relative to calcium carbonate. FA can then have an increased effect in this case (gypsum crystallisation) due to the combination of the higher content of functional groups and the ability to adsorb onto active growth sites. From the work of McCool et.al [1, 43], antiscalent removal from RO brine streams via calcium carbonate (calcite) crystallisation is investigated. They concluded that antiscalent scavenging occurs via surface adsorption onto the available crystal surface area. This can suggest that, in the case of calcite crystallisation, higher molecular weight substances can have a greater effect through adsorption onto active growth sites.

The effect of HS on the crystallisation of aluminium hydroxide ($\text{Al}(\text{OH})_3$) and Fe(III) oxides were investigated by Singer et.al [44] and Kodama et.al [45, 46]. They concluded that crystallisation was inhibited with an increase in HS concentration. They also noted that the crystalline structure was influenced by the pH and the prevailing concentration of HS.

2.3.5. pH

It has been observed that pH affects the crystallisation process of certain soluble salts in the presence of polyelectrolytes that contain carboxylic and phenolic functional groups [11]. Change in pH affects the neutrality of the substance. A negatively charged

2.3. Factors influencing crystallisation

particle can become positively charged and vice versa. The inhibitory effect increases due to an increase in the deprotonation degree of an additive [47, 48].

Studies have found that a change in pH level, without addition of any additives or inhibitors, have no significant impact on the rate of crystal growth [11, 12]. A change in pH will have no effect on crystallisation in a system where no additives are present. The driving force for crystallisation will then be purely based on the initial concentration and degree of supersaturation.

Amjad [47] has shown that a change in pH can have a significant impact on crystallisation induction time in the presence of an inhibitor - even if seed crystals are present as well. Table 2.3 summarises the effect of pH on the induction time in the presence of an inhibitor.

Table 2.3: The effect of pH on the induction time with 0.22 mg/1 of polyacrylate [47].

pH	2.8	3.4	5.2	7	8.6
Induction Time (min)	0	150	180	195	190

2.3.6. Seeding

As previously stated, the addition of seed crystals can completely override the need for a nucleation period. The onset of crystal growth can be induced immediately by the addition of active growth sites. Addition of seed crystals negates the need for nuclei formation and crystal growth can occur mainly through surface reaction/integration onto the active growth sites of the crystal surfaces. Nucleation can be made unnecessary in most cases, depending on the amount of seed added, the initial concentration of the solution and other external factors such as temperature and additives [10, 12].

Experimental work is found to be more reproducible in experiments with seed crystal addition than in unseeded experiments, depending on the other conditions of the system [5, 10]. Table 2.4 summarises some findings from literature that show that the induction period for the crystallisation of gypsum is eliminated in the presence of seed crystals.

*Chapter 2: Literature review***Table 2.4: Effect of seeding on induction time in gypsum crystallisation experiments.**

Temperature (°C)	Seed (mg/l)	Induction Time (min)	Reference
25	2000	0	
25	3200	0	
25	1970	0	
25	2020	0	[11]
35	1990	0	
50	1970	0	
50	1960	0	
25	1980	0	
35	2000	0	[10]
35	1970	0	
45	1990	0	
25	1930	0	
35	1930	0	[13]
45	1930	0	
55	1930	0	
15	2000	0	
20	2000	0	[9]
25	1000	0	

It is evident from Table 2.4 that seeded experiments in literature are mostly conducted at a seed loading of about 2000 mg/l. At this level of seeding and at a lower seed level of 1000 mg/l, the induction period is completely eliminated as is evident from the findings.

The nucleation period is not always completely eliminated by the addition of seed crystals. The presence of additives can influence the task of seed crystals to some degree as observed in the work of Amjad [11]. It is important to investigate the effect of seeding in the presence of additives to determine the degree of seeding required to override the effect of inhibitors or inhibitor-like impurities and to optimise the design of industrial crystallisers.

2.3. Factors influencing crystallisation

2.3.7. Agitation

In a crystallising system, agitation is introduced to keep the crystals in suspension. This promotes the interphase mass transfer between particles through turbulence in the liquid phase [49]. In this manner the rate of crystallisation can be promoted or demoted.

Mixing energy introduced into a system is consumed by the collision of particles. This leads to the development of secondary nucleation. Low energy inputs and low blade tip velocities are then preferred. Mixing promotes the dispersion of solid particles in the solution. Mixing improves particle collision frequency at supersaturation levels leading to higher agglomeration, and can result in the dispersion of particles at increased mixing rates [49].

Predicting a critical minimum mixing rate and particle distribution throughout a vessel for optimum crystallisation is difficult. Zweitering [50] described a widely used relationship to determine minimum impeller speed, N , for optimal particle suspension [5]. The relationship is described as:

$$N = H[\nu^{0.1} d^{0.2} x^{0.13} D^{-0.85} (g\Delta\rho / \rho_l)^{0.45}] \quad (2.20)$$

where ν is the kinematic viscosity of the liquid in m^2s^{-1} ; d is the normal particle size in meter (m), x is the fraction of solids in the system, D is the impeller diameter in meter (m); g is the gravitational acceleration in $\text{m}\cdot\text{s}^{-2}$, ρ is the liquid density, ρ_l is the solid density and N the impeller speed in $\text{rev}\cdot\text{s}^{-1}$.

H is defined as:

$$H = (L / D)^a \quad (2.21)$$

where $a = 0.82$ for propeller agitators and 1.3 for radial flow impellers and L is the vessel diameter in meter (m).

From the above relationship it is clear that the impeller geometry and speed, the vessel dimensions and the physical properties of the solid system are important factors to consider

Chapter 2: Literature review

in the crystallisation system. The aim would be to increase the surface contact area of particles and not over promote collision that could lead to dispersion of particles.

2.4. Natural organic matter (NOM)

Natural organic matter (NOM) is one of the major factors involved in fouling problems at water treatment facilities [2, 51]. Studies of NOM fouling have drastically increased over the last decades. In aquatic environments, 30-50% of NOM consists of humic substances (HS), that can range from small to large macromolecules (500-10 000 Da) [52].

In the subsequent subsections the behaviour of HS in aqueous media, their interactions with metals (especially calcium) and their pH dependence are discussed.

2.4.1. Humic substances (HS)

HS are complex macromolecules that are still a major problem to characterise due to variations in the sizes and structures of these compounds, which are found throughout the world. HS can cause a significant amount of problems due to their electronegativity in neutral to basic media, their attraction to metal ions in solution and the formation of metal complexes or colloids.

HS molecules are yellow to black in colour and are usually heterogeneous. They are generally considered to consist of three distinct material classes [53].

- 1) Humic Acid (soluble in alkaline media, partially soluble in water and insoluble in acidic media, $\text{pH} \leq 2$).
- 2) Fulvic Acid (soluble in both basic and acidic solutions).
- 3) Humin (insoluble at all pH levels)

HS contain a large amount of carboxylic (-COOH) and phenolic (-OH) functional groups and behave as negatively charged particles at the pH range of natural waters. About 60 – 90% of all the functional groups in HS are carboxylic groups [52]. Due to the large presence of carboxylic and phenolic functional groups around these HS, it is believed that this organic matter can act like polyelectrolytes in natural waters.

2.4. Natural organic matter (NOM)

2.4.1.1. Humic acid (HA)

HA is the predominant organic matter found in NOM and one of the major fouling agents in water filtration systems. Humic acids are large macromolecules that can vary in molecular weight from 5000 – 10 000 Da [51, 54]. Figure 2.7 depicts a hypothetical macromolecular structure of HA, illustrating that a large portion of the structure contains the functional groups -COOH and -OH which give HA its inhibitory ability.

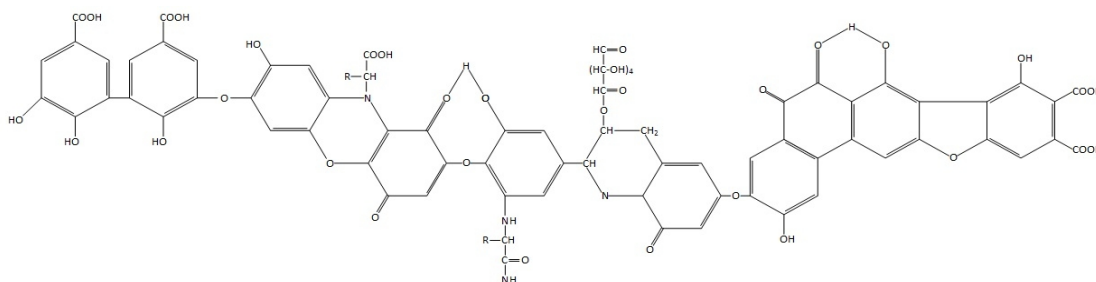


Figure 2.7: Hypothetical macromolecular structure of HA (Redrawn from [55]).

Due to their electro-negative and -hydrophobic nature, HAs are able to form aggregates in aqueous media or in the solid state. These aggregates can be stabilised in the presence of metal ions such as Ca^{2+} [56]. Aggregation strongly depends on conditions such as pH, ionic strength and the presence of multivalent metal ions.

In the presence of cations, such as Ca^{2+} , aggregation is promoted in the form of charge neutralisation which can lead to the bridging of different HA molecules [56, 53]. The bridging of these molecules can lead to the formation of colloids that can keep the metal ions suspended in solution and so inhibit the onset of crystallisation.

To the knowledge of the author, scientific literature does not contain any studies that focus on the effect of HA on the crystallisation of gypsum. Studies have been carried out on other salt solutions (i.e. aluminum hydroxides and calcium carbonate) in the presence HA [42, 44, 57]. The effect of HA on filtration has also been studied extensively over the years and is still a notable topic of discussion [2, 58, 59].

Chapter 2: Literature review

2.4.1.2. Fulvic acid (FA)

FA is essentially HA that is smaller in size and weight. The molecular weight of FA ranges from 500 to 2000 Da [54]. HA can be removed to a large degree by pre-filtration (UF/NF) methods. However, FA can be small enough to pass through some pre-filtration steps and can even be small enough to cause irreversible fouling of advanced filtration methods downstream in a treatment process [60].

As previously stated, not much information can be found in scientific literature on the study of the effect of FA on crystallisation processes or membrane systems. Amjad [19] showed that FA can behave like a polyelectrolyte and inhibit crystallisation to some degree. FA at relatively low concentrations (< 5 ppm) can even inhibit crystallisation more than some of the commercially used inhibitors.

The hypothesis that FA can inhibit the onset of crystallisation, specifically for gypsum, more than HA, is based on the observation described in scientific literature that there is an increase in the relative carboxylic and phenolic functional group content in the smaller macromolecules [53]. FA is also completely soluble in water compared to the semi-solubility of HA. This means that its degree of dissociation is larger, which can result in a larger degree of functional group deprotonation. Charge neutralisation will in effect increase with an increase in functional groups and an increase in deprotonation.

2.4.1.3. pH dependence and cation interactions

The behaviour of HS, i.e. HA and FA, is highly dependent on pH as well as cation interaction. As pH is increased, the carboxylic and phenolic groups are deprotonated. These groups become negatively charged and the electrostatic repulsion of the groups causes the molecules to assume a more stretched configuration [Figure 2.8 a)] [53]. Mechanism A in Figure 2.8 depicts the deprotonation of the functional groups. A decrease in pH (Mechanism B), i.e. increase in H⁺ ions, will lead to the protonation of the functional groups and the HA molecules will adopt a coiled and compact structure [Figure 2.8 b)]. As the pH is decreased, intermolecular aggregation increases and a further decrease in pH to below 2 can result in the precipitation of the HA particles [61].

2.4. Natural organic matter (NOM)

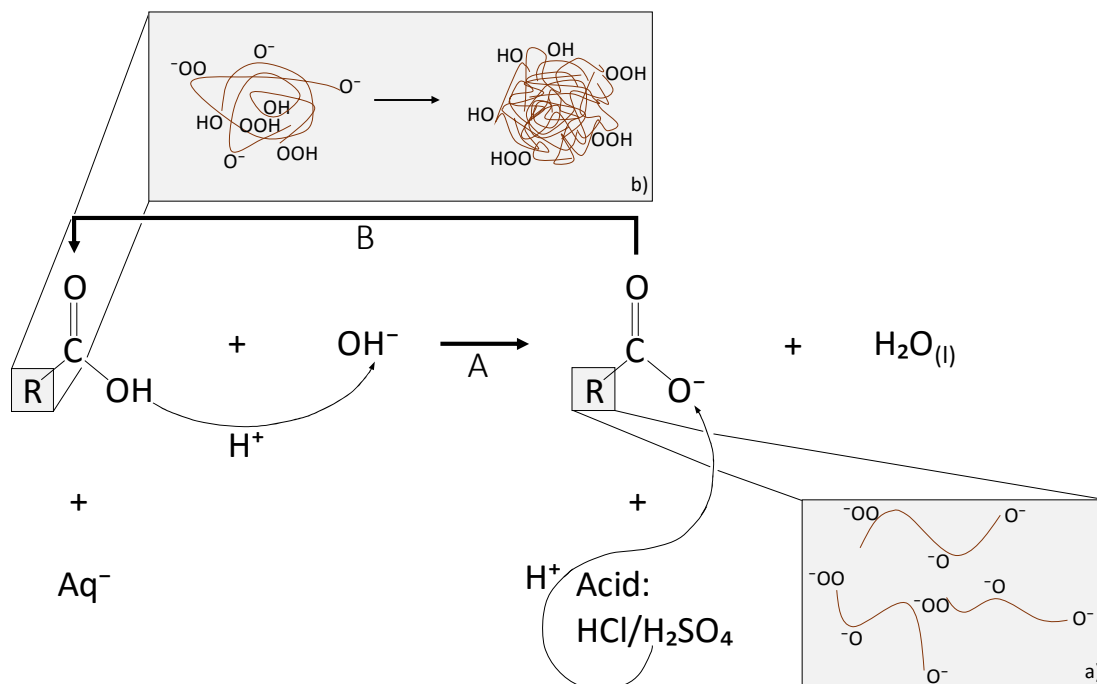


Figure 2.8: Behaviour of HA molecules A: deprotonation of carboxylic and phenolic functional groups with increase in pH; B: decrease in pH and the protonation of functional groups. a) Neutral and basic media stretched configuration of HA molecules; b) Decrease in pH results in intermolecular aggregation and precipitation of HA molecules.

At low pH levels, where HA is insoluble to semi-soluble, an increase in pH increases the dissolution rate of HA particles. This is attributed to surface reactions that take place. According to Brigante et al. [62], molecules at the surface of HA are interacting with molecules located within the particle. In water the surface molecules are in contact with water molecules and dissolved ions and this results in sorption-desorption reactions at the surface of the molecules. Increase in pH increases the deprotonation of functional groups, which in turn promotes the development and ongoing increase in the negative charge of the molecules. This trend continues with a rise in pH until around 10 and 11 where most of the functional groups are deprotonated [63].

The inorganic cation neutralises the charge of HA particles at higher pH levels the same way as hydrogen ions at low pH values do. According to Brigante et al. [61, 62], the carboxylic and phenolic functional groups have a strong affinity for divalent inorganic cations that can bind to the HA molecules in solution or at the surface of solid HA particles.

Chapter 2: Literature review

Divalent metal cations can interact with more than one HA molecule. This can result in the bridging of functional groups of adjacent HA molecules, which increases the attractive forces between them. Bridging between molecules can lead to metal complex formation through the metal ions. Figure 2.9 mechanism B illustrates the cation interaction where the charge is neutralised. Figure 2.9 a) illustrates the interaction between HA molecules through the functional groups and Figure 2.9 b) illustrates the bridging by divalent cations that can lead to the formation of metal complexes.

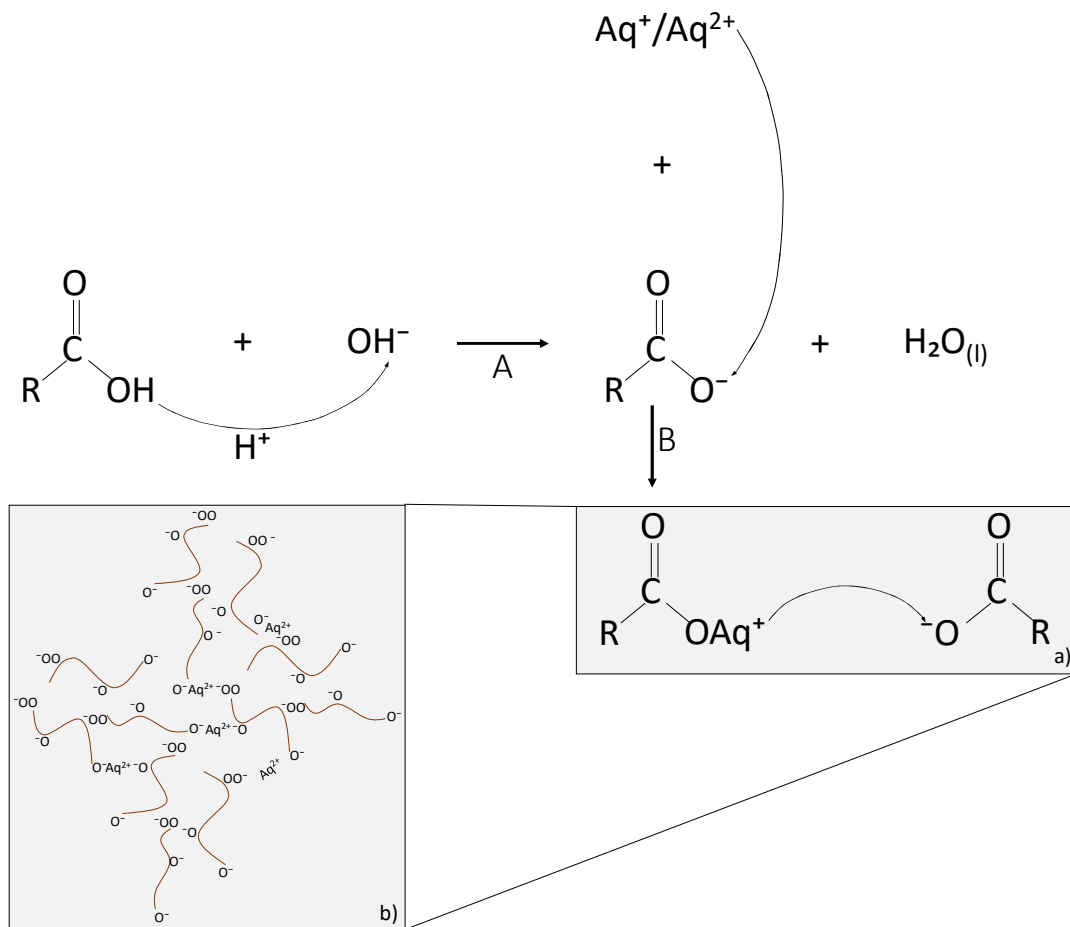


Figure 2.9: Behaviour of HA molecules A: Deprotonation of functional groups with increase in pH; B: Cation ($\text{Aq}^+/\text{Aq}^{2+}$) interaction charge neutralisation. a) bridging of molecules and b) the formation of complexes.

There is an increase in the interaction of HA molecules with divalent cations in neutral to alkaline solution due to the affinity of the HA functional groups for cations. This can interfere or completely inhibit crystal growth during crystallisation in neutral to alkaline solution. The interaction of the crystallite cation with the HA molecules is dependent on the

2.5. Literature summary

amount of active sites that are available, the electron charge and the affinity of the HS functional groups for the metal ions in solution [53].

The binding capacity of HS molecules is associated with the molecular weight of the substances. HS fractions that are smaller in molecular weight have the highest phenolic and carboxylic group content. With an increase in functional groups the binding to metal ions will be more efficient [64]. The small fractions of HS can be related to FA, which again highlights the fact that FA can have a greater effect on crystallisation than HA.

The metal binding effect of HS can shift the degree of supersaturation and so prevent crystallisation from taking place. A decrease in the “supersaturation” leads to a decrease in the overall primary driving force of crystallisation. This in turn can lead to an increase in induction time and a decrease in nucleation rate in a spontaneous crystalline environment where no seed material is present.

2.5. Literature summary

From this literature review it is clear that crystallisation plays an important role in the water treatment industry. The crystallisation of gypsum has been studied extensively during the last decades, but there are still shortcomings in the understanding of this mechanism. Very few, if any, studies that focus on the effect of HS on calcium sulphate crystallisation can be found in scientific literature. However, some work has been carried out on the crystallisation of calcium carbonate and aluminium hydroxides in the presence of HS.

Some of the major scaling problems affecting water treatment systems dealing with supersaturation brine streams are caused by gypsum and NOM. The crystallisation of gypsum is still an important study today and there are numerous effects, which prohibit the crystal growth of gypsum, that require further investigation. Impurities such as HS found in NOM can affect the crystallisation process of gypsum.

Although HS are still, at present, difficult to completely characterise and investigate, sufficient sources have implied that HS can behave like weak polyelectrolytes in aqueous media. HS, in the form of HA and FA, have been shown to have a high content of carboxylic and phenolic functional groups which gives them their inhibitory ability. FA is smaller in size

Chapter 2: Literature review

and molecular weight with an increased functional group content that can result in it having a greater inhibitory effect than HA.

Other factors that influence the process of crystallisation were found to be supersaturation, temperature, ionic strength, pH in the presence of additives, addition of seed crystals and the rate of mixing.

The growth rate is independent of solution pH in the absence of any additives. In the presence of additives, the pH can enhance or reduce the inhibitory ability. HA and FA become highly negatively charged with an increase in pH. In the presence of multivalent cations, such as Ca^{2+} , they can become aggregated and start to bridge with adjacent HS molecules. This can lead to the formation of metal complexes and colloids in suspension. These metal complexes can decrease the supersaturation and so decrease the driving force ($c-c^*$) of crystallisation.

Supersaturation plays a vital role in the crystallisation process. Without the supersaturated state, crystallisation cannot occur. It is one of the main driving forces of crystallisation and is extensively used to evaluate the kinetics of crystal growth. With highly supersaturated solutions, the induction period is decreased and the driving force for crystallisation is significantly increased.

With the addition of seed crystals, the surface area for growth is increased by the increased amount of active growth sites. The onset of crystallisation can be induced with immediate effect at high seed loading. Seeding plays an important role in reducing or eliminating the induction and nucleation period and increasing the growth rate in the presence of additives such as HS.

The crystallisation of gypsum can be affected greatly by various conditions. The main aim of this study was to study the effect of HS on the crystallisation process. It was expected that these HS would have an effect on the crystallisation process and the study determined to what degree this is true. The ability of HS to affect gypsum crystallisation can be enhanced or reduced through the manipulation of pH, level of supersaturation, seeding, temperature and agitation. Mechanical inputs can have an effect on crystallisation. However, for the

2.5. Literature summary

purpose of this study, the focus was primarily on the chemical manipulations of systems conditions. The effects of ionic strength, temperature and agitation were not part of the scope of this study.

Chapter 3: MATERIALS, METHODOLOGY AND RESEARCH DESIGN

The materials, methodology and research design chapter describes the materials that were used and the experimental setup. It also briefly describes the theoretical and experimental methodology approach that was followed in order to meet the aims of this project. The second part of this chapter is an error analysis and it discusses experimental and analytical errors observed during the experimental work.

3.1. Materials

Table 3.1 lists the chemicals that were used in this study along with their purity and supplier.

Table 3.1: List of chemicals utilised in this study.

Component	Assay	Supplier
Calcium Chloride dihydrate	98%	Merck
Sodium Sulphate anhydrous	98%	Merck
Calcium sulphate dihydrate	98%	Kimix
Calcium Standard	1000 mg/l	Sigma-Aldrich
Sodium Hydroxide Solution	50%	Kimix
Hydrochloric Acid	32%	Merck
Humic Acid	-	Sigma-Aldrich
Fulvic Acid	-	IHSS**
Ethylenediaminetetraacetic acid (EDTA)	98%	Sigma-Aldrich
pH 4.00 Buffer Solution	-	Merck
pH 7.00 Buffer Solution	-	Merck
pH 10.00 Buffer Solution	-	Merck
Potassium Hydroxide	98%	Merck

***International Humic Substance Society.*

Argon baseline 5.0 (Afrox) was used for the determination of metal ion content by inductively coupled plasma (ICP) analysis.

3.2. Experimental methodology

The particle size of HA was determined by means of a Micromeritics® Particle size analyser at Stellenbosch University – Process Engineering Analytical laboratory. The mean size was determined to be 218.5 μm (see appendix E for the report).

The surface area of the seed crystals (gypsum) used in this study was determined by Brunauer–Emmett–Teller (BET) analysis on a Micromeritics® BET analyser. The nitrogen adsorption method was used. A surface area of 15.3378 m^2/g was determined. The particle size was determined in the same manner as described above. The mean particle size of gypsum crystals were determined to be 13.95 μm .

3.2. Experimental methodology

3.2.1. Experimental setup

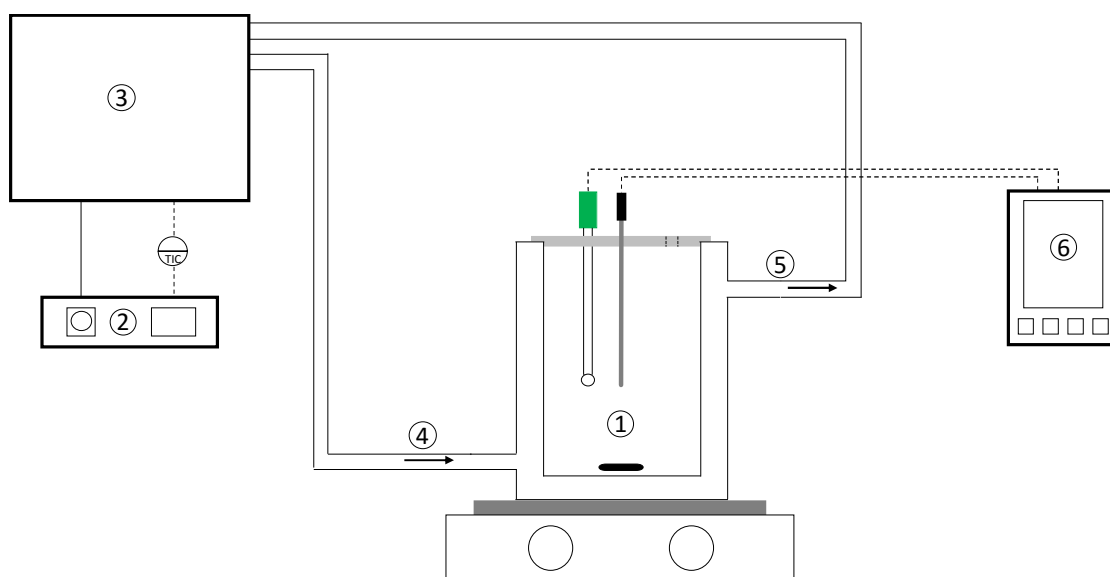


Figure 3.1: Simplified schematic of the experimental setup. 1) Jacketed glass vessel; 2) Control unit for water heating bath; 3) Heating bath; 4) Heating fluid in; 5) Heating fluid out; 6) pH and Temperature meter.

The process of batch crystallisation has been fully developed in previous work [30, 10, 9]. The experimental work in this study was carried out in the same manner as previously developed [9]. The process was straight forward and generated accurate and reliable results.

Chapter 3: Materials, methodology and research design

Figure 3.1 shows a simplified schematic of the experimental setup. Experiments were carried out in jacketed glass vessels of approximately 500 ml in volume. Reactor one has an inside diameter of 80 mm and a height of 115 mm while reactor two has an inside diameter of 72 mm and a height of 130 mm. Due to the difference in reactor sizes, one supersaturated concentration was used per reactor. The mechanical differences and inputs of these reactors fall outside the scope of this study. Water was used as the heating fluid and was circulated through the jacketed vessel using a heating bath. The temperature was controlled with an accuracy of ± 0.1 °C with a Delta[®] temperature controller. Temperature and pH were measured using a Hanna[®] HI4222 pH/ISE/mV meter.

Figure 3.2 shows a photograph of the experimental setup in the laboratory. Two reactors (jacketed vessels) were used in parallel to achieve the experimental outcomes of this study.

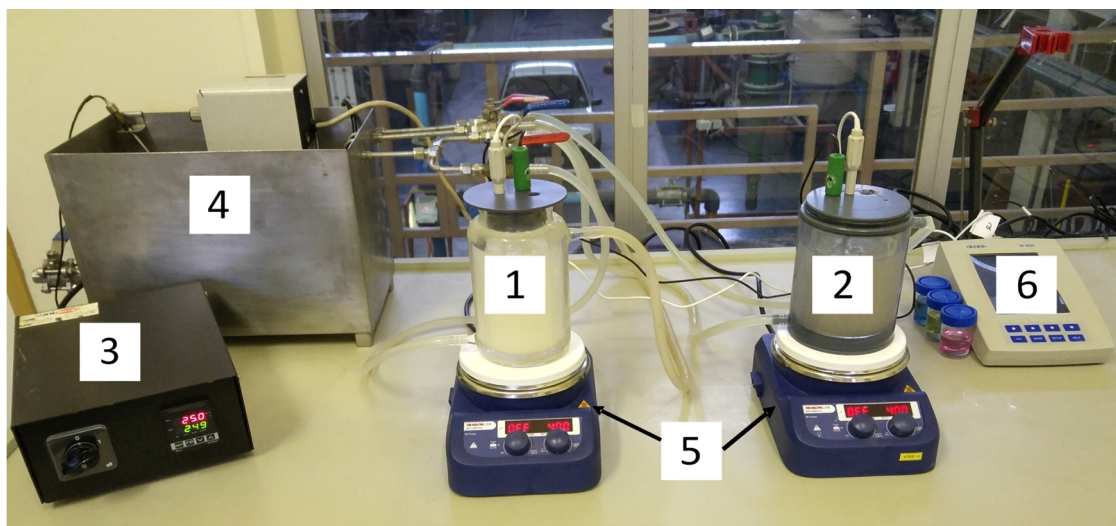


Figure 3.2: Photograph of the actual experimental setup in the lab. 1) Reactor 1; 2) Reactor 2; 3) Control unit for heating bath; 4) Heating bath; 5) Magnetic stirrers 6) pH and Temperature meter.

Figure 3.3 shows a detailed diagram of the structure of reactor vessel one. A magnetic stirrer was used to agitate the working fluid at a constant stirring rate. The magnetic stirrer bar is made of Teflon with dimensions of 28.6×7 mm (length \times height). A PVC lid with holes for the temperature probe, the pH probe and for sampling covered each of the reactor vessels. Temperature and pH were measured with a Hanna[®] Pt100 and HI 1053 pH probe during the experiments. Temperature and pH were recorded using the Hanna[®] meter's

3.2. Experimental methodology

continuous logging capabilities. Sampling was carried out through the sampling port at certain time intervals using a 5 ml grade A glass pipette.

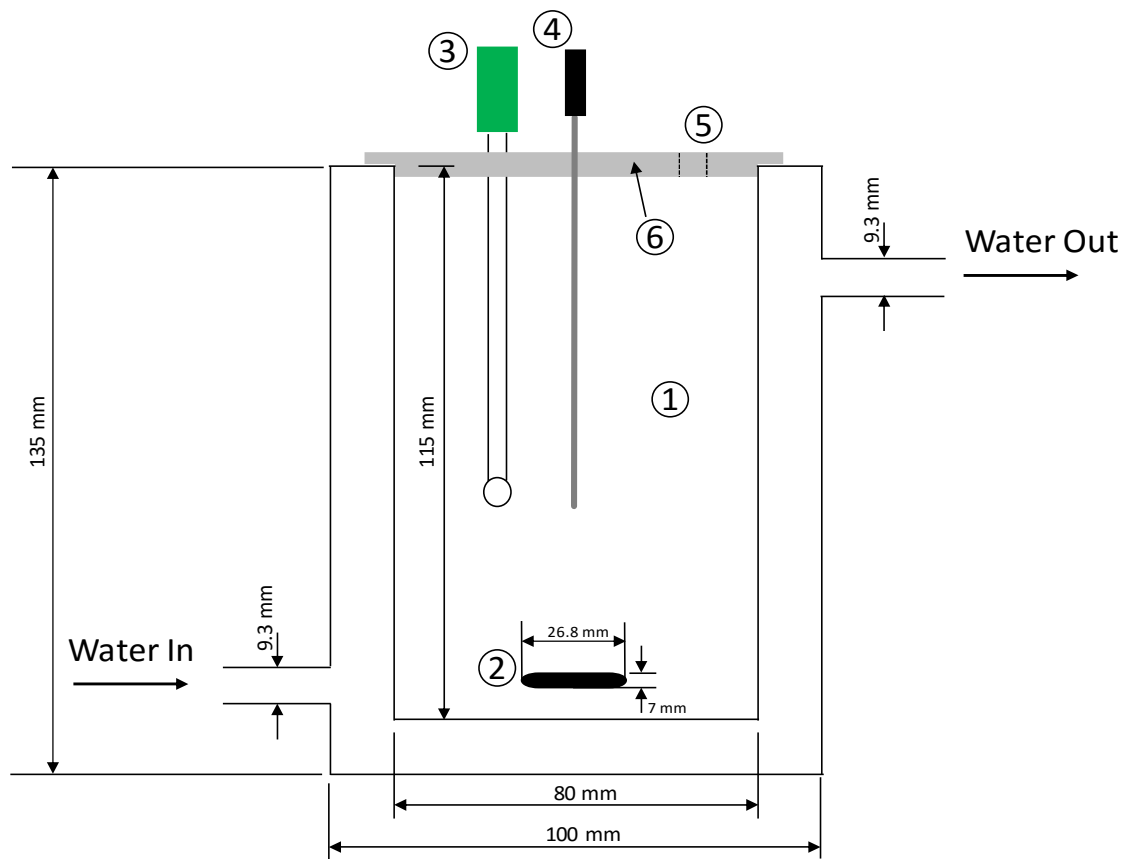


Figure 3.3: Schematic of jacketed vessel used in the experimental setup. 1) ± 500 ml Jacketed vessel; 2) Teflon magnetic stirrer bar; 3) pH probe; 4) Temperature probe; 5) Sample port; 6) PVC lid.

3.2.2. Solution preparation

All glassware utilised for the preparation of solutions were grade A and were thoroughly cleaned and dried before use. All solids were weighed with an analytical scale with an accuracy of ± 0.001 grams. MilliQ[®] water with a resistivity of 18 megohm was used in the preparation of all the experimental solutions.

Anhydrous sodium sulphate salt was dried overnight in a vacuum oven at 60-80°C to ensure that it was completely dry. The dried salt was placed in a desiccator to cool down to ambient temperature (depending on the season, ambient temperature ranged from 16-25°C). The desired amount of sodium sulphate was then weighed and dissolved in water. Although

Chapter 3: Materials, methodology and research design

sodium sulphate is very soluble in water, its reaction with water is endothermic and the addition of heat will assist in the process.

Calcium chloride has an extremely hygroscopic nature, which makes it possible for the calcium chloride to absorb water. This can result in lower calcium concentration than calculated. The calcium salt was therefore carefully weighed as rapidly as possible and dissolved in water. Both solutions were stored in a cupboard and left overnight before use for complete dissolution to take effect.

Commercial HA obtained from Sigma-Aldrich was used without further purification of the powder. Three HA stock solutions were prepared (see Appendix A.1). The required amount was weighed and dissolved in water. The stock solution had to be mixed thoroughly due to the semi-soluble nature of HA. Ten millilitres of the bulk solution was used in each experimental run.

FA obtained from the International Humic Substance Society (IHSS) was used with no further purification of the powder. Due to the expensive nature of this chemical, a single solution of 615 mg/l was prepared. A volume of 250 ml of the solution was prepared by dissolving ± 154 mg of FA in water. The prepared solution was stored in a fridge at a temperature of $\pm 4^\circ\text{C}$. The stock solution was diluted to 12 ml of the required concentration and 10 ml thereof was used in each experimental run. Refer to Appendix A.1 for a detailed description of preparation and the concentrations of diluted solutions.

3.2.3. Experimental procedure summary

3.2.3.1. Equipment preparation

At the start of each experimental run it was ensured that the inside of the reactor was completely dry to minimise any contamination. The magnetic stirrer bar was carefully placed inside the reactor. The inlet and outlet pipes of the heating fluid to the jacketed vessels were checked to make sure that they were secure and the valves from the heating bath were opened. The heating bath, circulator and control unit were switched on and set to the correct temperature. The ambient temperature inside the laboratory was controlled between 18 and 22°C.

3.2. Experimental methodology

Each of the supersaturated solutions, calcium chloride and sodium sulphate, was then poured into a 200 ml grade A volumetric flask from the respective stock solutions. All glassware utilised during the experimental study was thoroughly cleaned and dried before each experimental run (see Appendix B for a detailed cleaning procedure).

3.2.3.2. Experimental run

Each experimental run was carried out by mixing 200 ml of equimolar solutions of calcium chloride (CaCl_2) [solution 1] and Sodium sulphate (Na_2SO_4) [solution 2]. Solution 1 was carefully poured into the reactor and left for 30 – 40 minutes until a temperature of 25°C was reached. Solution 2 was placed in the heating bath and only added to solution 1 when the set temperature was reached.

The pH meter was calibrated before every experimental run to ensure that the pH reading recorder was accurate and reliable. HA or FA was added as soon as the pH reading stabilised, in the first minute after solution 2 was added. Thereafter, the pH was adjusted to the desired point. Two to three minutes were given for the adjustment of pH. The first sample was taken at 5 minutes. With seeded experiments, seed crystals were added at 6 minutes after the manipulation of conditions and a minute after the first sample was taken.

Five minutes may seem like a long time in the crystallisation process. However, observation of induction times in preliminary and baseline experiments showed that sampling of the first sample at five minutes gave ample time for the manipulation of conditions. The first sample was taken at time 0 for each experiment and the subsequent time intervals were normalised to time 0. Sampling was done using a grade A 5 ml pipette.

The time interval for each experiment was dependent on the duration of induction observed. As soon as crystallisation was observed sampling was carried out every 10 minutes for the first hour, every 20 minutes for the second hour and every half hour to an hour until equilibrium was achieved. Equilibrium was evaluated through analytical results and if it was not achieved, the experimental run was repeated with the addition of an extra hour or two. Crystallisation was observed visually when the solution became milky or when fairly large crystals were seen in the solution.

Chapter 3: Materials, methodology and research design

The sample was filtered through a 0.22 µm Nylon syringe filter. The filtered sample was diluted 20 times with 0.1 M hydrochloric acid (HCl) solution in a grade A 100 ml volumetric flask. From the 100 ml flask the diluted sample was poured into two 15 ml centrifugal tubes for analysis. One tube was sent for analysis and the other was kept as a replicate sample.

3.2.3.3. Analytical equipment

Various analytical techniques can be utilised for the measurement of free metal ion (e.g. calcium ion) concentration in solution. A continuous measurement of calcium can be done by using an Ion Selective Electrode (ISE) [30, 10]. ISE is a simple method to measure free calcium ions in solution, but calibration has to be performed regularly and accurately. This technique is not suitable for measurements in the presence of any organic material and the concentration range it is able to measure is limited. It was therefore decided not to make use of this method due to the potential interference by the organic material that was used in the experiments and due to the fact that the concentration range of this study falls outside the ISE range.

A more accurate means of measurement can be achieved through EDTA titrations, but this process is very tedious and expensive. Simpler and less expensive techniques such as Inductively Coupled Plasma Optical Emission Spectrometry (ICP-OES) and Atomic Adsorption (AA) analyses can also be used for the measurement of metal ions.

In order to utilise the AA for analysis, more dilution of the samples would have been necessary due to the AA's limited detection range. ICP-OES was chosen as the analytical technique that was most appropriate for the planned analytical work based on the above reasoning and the following advantages of using this technique: an ICP-OES analytical instrument was readily available, no further dilution of samples was necessary after sampling and initial dilution, it is less time consuming and it is an accurate and reliable analytical technique.

The samples were analysed with a Thermo-Fischer ICAP 6000 Series ICP-OES at Stellenbosch University – Process Engineering analytical laboratory. No further sample preparation was required after sampling and dilution. Calcium was analysed through the

3.3. Theoretical methodology

radial (side-on view) configuration at a wavelength of 396.847, 317.933 and 422.673 nm. Quality control samples were inserted between samples in order to check the accuracy of ICP-OES analysis. Yttrium was used as an internal standard and all results were calculated relative to the internal standard. The calcium peak at a wavelength of 422.673 nm gave the most reliable results and was, therefore, used throughout. Deviations and standard errors are discussed in section 3.5. The sample preparation and the standards used for the calibration of the ICP-OES are described in Appendix B.

3.3. Theoretical methodology

This section on theoretical methodology will describe the theoretical work carried out in preparation for the experimental work, the data processing of experimental results and the software tools that were used for data processing.

3.3.1. Supersaturation concentrations

The PHREEQC[®] (Version 2) software package was used to determine the supersaturation concentrations of each of the two solutions. This was achieved by determining the saturation concentration of pure calcium sulphate with respect to calcium and sulphate ions in pure water at a temperature of 25°C. The scaling index of gypsum was set to 0 as well as to the anhydrite form and the pH was taken as 7.0. Output of the PHREEQC[®] simulations can be found in Appendix C. The normal phreeqc.dat built-in database was utilised for the determination of the solubility of gypsum in this study. Figure 3.4 shows the PHREEQC[®] calculated (using the phreeqc.dat and pitzer.dat databases) solubility of gypsum with an increase in sodium chloride concentration, compared to data found in scientific literature.

Chapter 3: Materials, methodology and research design

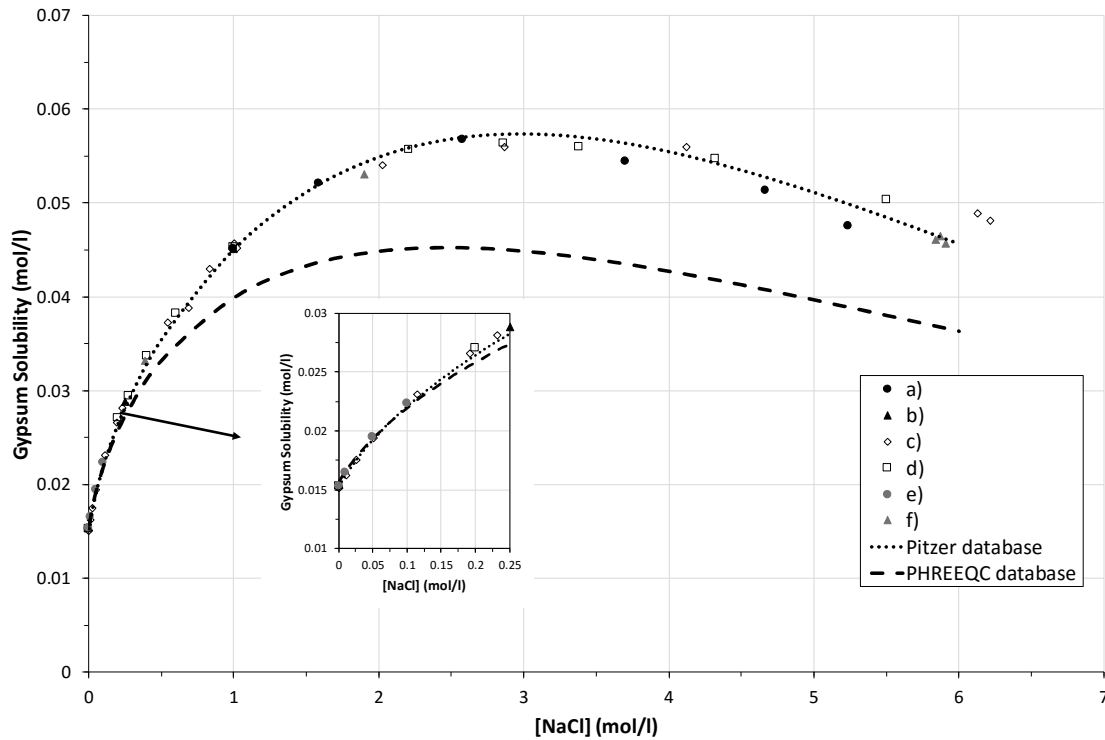


Figure 3.4: Solubility of gypsum determined by PHREEQC[®] models compared to literature described solubility in NaCl at 25°C (• a) [24]; ▲ b) [26]; ◇ c) [27]; □ d) [23]; • e) [28]; ▲ f) [29]).

From Figure 3.4 it is clear that gypsum solubility increases with an increase in NaCl concentration up to a maximum for all presented data. With the PHREEQC[®] database, the predictions become inaccurate at NaCl concentrations above 0.2 mol/l, whereas the predictions compare well with the literature data when using the Pitzer database. In this study, the maximum theoretical concentration of NaCl that could be present was 0.125 mol/l. In the NaCl concentration range applied in this study, the two models generated by the PHREEQC[®] and Pitzer databases compare well. The use of the PHREEQC[®] built-in model was therefore accurate in the concentration range used in this study.

3.3. Theoretical methodology

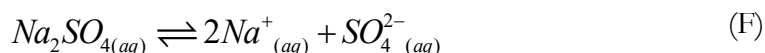
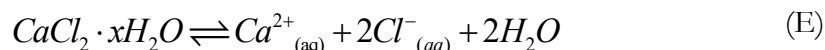
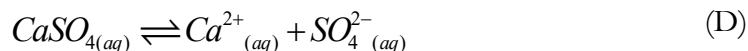
The supersaturation ratio is then defined by the following relationship (from equation 2.16):

$$S = \frac{[Ca^{2+}]_i}{[Ca^{2+}]_s} \quad (3.1)$$

S (2, 3 or 4) is the supersaturation ratio and $[Ca^{2+}]_i$ is the concentration of the initial free calcium ions in solution. $[Ca^{2+}]_s$ is the saturation concentration of calcium with respect to calcium sulphate saturation at 25°C, taken as 0.0157 mol/l as determined by PHREEQC[®]. For the purpose of this study, this saturation concentration in the absence of NaCl was used for all initial supersaturation concentration calculations. The supersaturation is therefore relative to the solubility of pure gypsum at a temperature of 25°C. Equation 3.1 can be rewritten as:

$$[Ca^{2+}]_i = S \times [Ca^{2+}]_s \quad (3.2)$$

Solution species concentrations were then determined by performing a species balance using the following relationships:



The molecular weight of the dihydrate was used for the calculation of the calcium chloride concentration. Due to the hygroscopic nature of calcium chloride and its affinity for water molecules, the actual concentration of calcium can differ slightly. For this reason, stock solution concentration was thoroughly analysed and this analytically determined concentration was then taken as the initial concentration.

The calculated calcium chloride and sodium sulphate concentrations were then multiplied by a factor of 2.05 to obtain the concentration of each of the solutions. This was necessary since the stock solution was diluted by a factor of 2 to obtain the required working

Chapter 3: Materials, methodology and research design

fluid concentration. This dilution factor was further increased by 0.05 to account for the 10 ml of concentrated organic solution that was added to the 400 ml of supersaturated solution. A summary of the different stock solutions used is given in Table 3.2 and a species balance for each supersaturation level of the working fluid is given in Table 3.3.

It is important to note that the supersaturation level is related to the pure gypsum saturation. The saturation of gypsum in the working fluid will shift depending on the temperature, the total dissolved solids (TDS) and the initial calcium concentration. This calculation of supersaturation level is used in order to assure that there is sufficient time to adjust system conditions and measure reliable and reproducible kinetic data for the crystallisation of gypsum. For more information on the calculation of the level of supersaturation refer to the sample calculations in Appendix F.

3.3. Theoretical methodology

Table 3.2: Theoretical concentrations of saturated and supersaturated stock solutions and the working fluid.

Chemical	Molecular Weight (g/mol)	Stock solution		Working fluid	
		Concentration $\times 10^3$ (mol/l)	Concentration (ppm)	Concentration $\times 10^3$ (mol/l)	Concentration (ppm)
<i>Saturation</i>					
Sodium sulphate (Na ₂ SO ₄)	142.04	32.08	4557.00	15.65	2222.93
Calcium chloride (CaCl ₂ \cdot xH ₂ O)	147.02	32.08	4716.77	15.65	2300.86
<i>2 \times Saturation (SS2)</i>					
Sodium sulphate (Na ₂ SO ₄)	142.04	76.14	10814.50	37.14	5275.37
Calcium chloride (CaCl ₂ \cdot xH ₂ O)	147.02	76.14	11193.66	37.14	5460.32
<i>3 \times Saturation (SS3)</i>					
Sodium sulphate (Na ₂ SO ₄)	142.04	96.25	13671.00	46.95	6668.778
Calcium chloride (CaCl ₂ \cdot xH ₂ O)	147.02	96.25	14150.31	46.95	6902.589
<i>4 \times Saturation (SS4)</i>					
Sodium sulphate (Na ₂ SO ₄)	142.04	128.30	18228.00	62.60	8891.70
Calcium chloride (CaCl ₂ \cdot xH ₂ O)	147.02	128.30	18867.08	62.60	9203.45

Table 3.3: Theoretical species concentrations for saturation and supersaturation of the working fluid.

Cations	Ionic Charge	Molar Mass (g/mol)	Concentration $\times 10^3$ (mol/l)	Concentration (mg/l)	Equivalent Weight (g/mol)	meq/litre ions	Anions	Ionic Charge	Molar Mass (g/mol)	Concentration $\times 10^3$ (mol/l)	Concentration (mg/l)	Equivalent Weight (g/mol)	meq/litre ions
<i>Saturation</i>													
Na	1	22.99	31.30	719.59	22.99	31.30	Cl	1	35.45	31.30	1109.59	35.45	31.30
Ca	2	40.08	15.65	627.25	20.04	31.30	SO ₄	2	96.07	15.65	1503.50	48.04	31.30
<i>2 \times Saturation (SS2)</i>													
Na	1	22.99	74.28	1707.70	22.99	74.28	Cl	1	35.45	74.28	2633.23	35.45	74.28
Ca	2	40.08	37.14	1488.57	20.04	74.28	SO ₄	2	96.07	37.14	3568.04	48.04	74.28
<i>3 \times Saturation (SS3)</i>													
Na	1	22.99	96.90	2158.76	22.99	93.90	Cl	1	35.45	93.90	3328.76	35.45	93.90
Ca	2	40.08	46.95	1881.76	20.04	93.90	SO ₄	2	96.07	46.95	4510.49	48.04	93.90
<i>4 \times Saturation (SS4)</i>													
Na	1	22.99	125.20	2878.35	22.99	125.2	Cl	1	35.45	125.20	4438.34	35.45	125.20
Ca	2	40.08	62.60	2509.01	20.04	125.2	SO ₄	2	96.07	62.60	6013.99	48.035	125.20

Chapter 3: Materials, methodology and research design

3.3.2. Processing of data

Microsoft Excel 2016

Experimental results obtained from the ICP-OES were processed using Microsoft Excel 2016. Results taken from the ICP-OES already had the necessary dilution factor taken into account. Desupersaturation curves were generated by plotting the free calcium ion concentration on the y-axis vs. the time interval of each sample on the x-axis. These plots were used to represent, evaluate and compare all results.

Matlab® 2015b

In order to represent results better, Matlab® 2015b was used to smooth the data and illustrate the realistic trend that the experimental data follows. The data were smoothed with a built-in smoothing function by using methods of regression and moving averages.

Growth rate constants were solved utilising the ODE45 built-in function of Matlab®. This was done by using experimental values to minimise the sum of squared errors.

PHREEQC® (Version 2)

PHREEQC® (Version 2) was only used for the generation of saturation concentrations as well as for the generation of the scaling indexes of salts that could precipitate.

3.4. Experimental design

3.4.1. Preliminary runs unseeded and seeded

Through preliminary experiments the procedure for the batch crystallisation method was familiarised, validated and finalised. An average concentration of 0.05 M Ca²⁺ was chosen for the preliminary experiments. The effect of pH was not investigated during the preliminary experiments. However, the effect of HA was tested during the preliminary experimental runs in order to establish if and to what degree HA affects the crystallisation of gypsum. HA concentrations of 5, 10 and 15 mg/l were applied in this investigation. It was also vital to determine repeatability of the process and the experimental equipment. All relevant preliminary experimental data can be found in Appendix B.1.

3.4. Experimental design

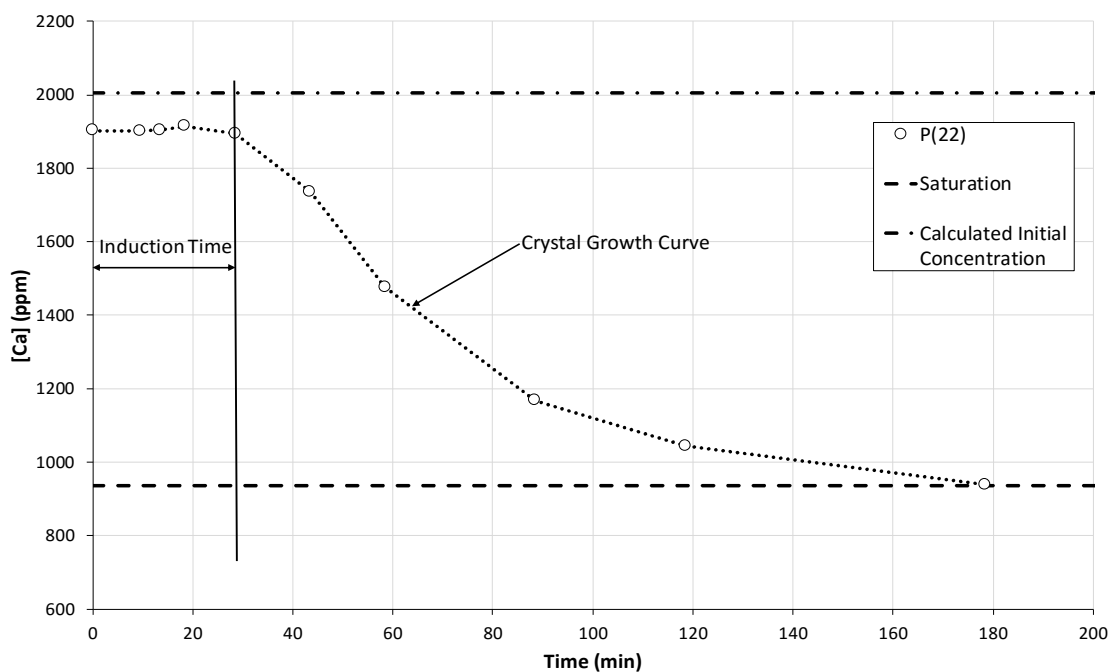


Figure 3.5: Desupersaturation curve example from preliminary run in the absence of seed crystals at $[Ca] = 0.05 \text{ mol/l}$ and Temperature 25°C .

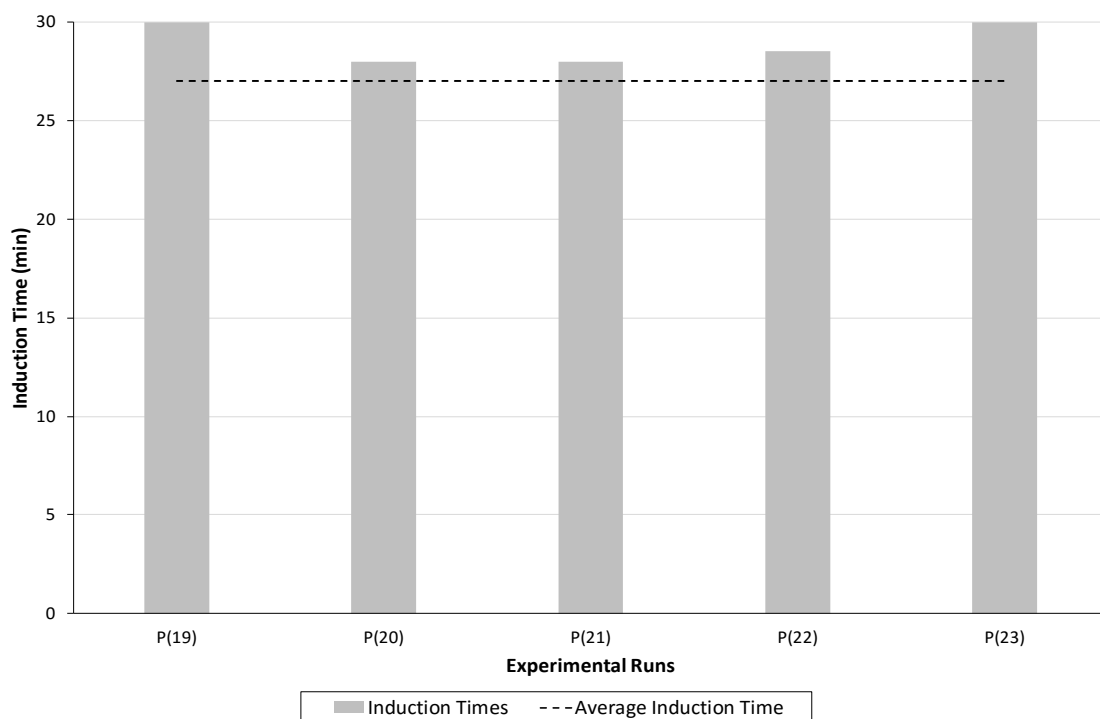


Figure 3.6: Evaluation of induction times for repeat preliminary runs with no seeding at $[Ca] = 0.05 \text{ mol/l}$ and Temperature 25°C .

Chapter 3: Materials, methodology and research design

Figure 3.5 gives an example of a desupersaturation curve. It indicates the induction period, the crystal growth/desupersaturation period and the equilibrium. From this work the batch process was successfully validated and familiarised.

Figure 3.6 represents the evaluation of repeat preliminary runs with a calcium concentration of ~ 0.05 mol/l at a constant temperature and stirring rate of 25°C and 400 rpm, respectively. An average induction period of 29 minutes was observed with a standard deviation of 1 minute and an RSD of 3.55%. The repeatability of results was therefore deemed acceptable and all deviations could be explained. All deviations and possible errors are outlined in section 3.5.

Figure 3.7 presents the results of preliminary runs in the presence of HA in the concentration range of 0 to 15 mg/l. It is evident that HA strongly inhibits crystallisation, in the absence of other manipulation. The large effect of HA observed in the preliminary experiments motivated further investigation of the effect of HA at the concentrations of 5, 10 and 15 mg/l.

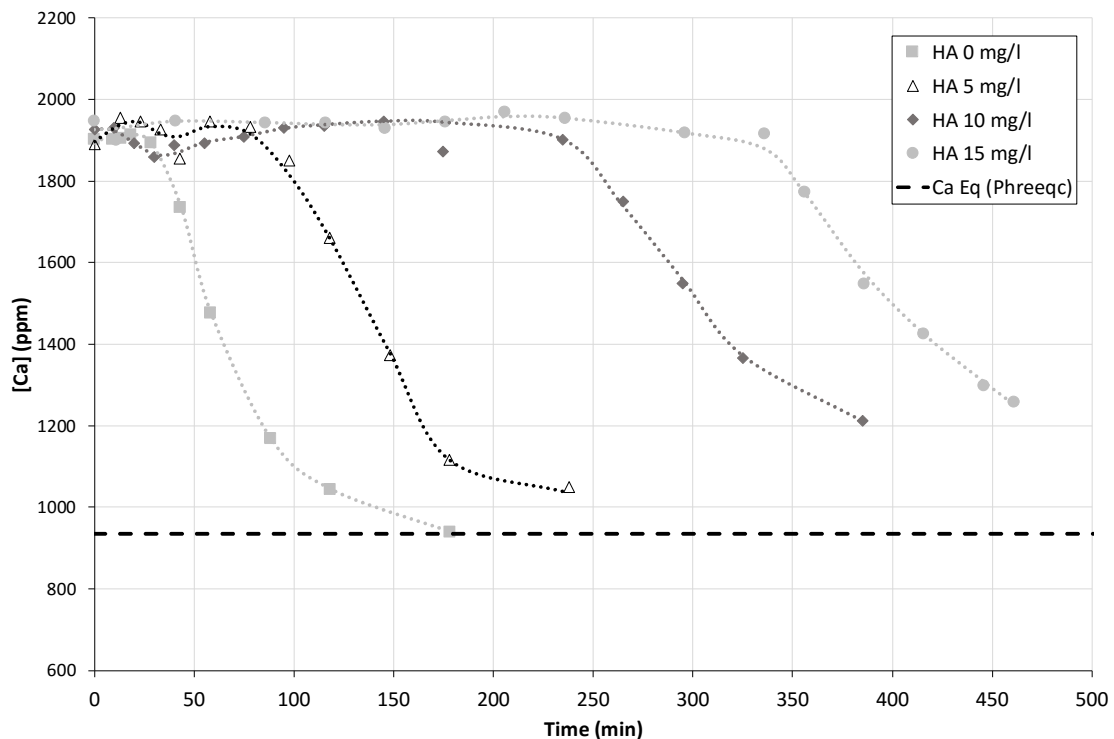


Figure 3.7: Desupersaturation curve for preliminary run on the effect of humic acid. $[\text{Ca}] = 0.05$ mol/l; Temperature 25°C .

3.4. Experimental design

Seeded experimental runs were conducted in order to determine the amount of seeding required for the experimental study part of the project. Figure 3.8 presents the results of the preliminary experimental runs in the presence of seed crystals (50 – 2000 mg/l) with 15 mg/l of HA.

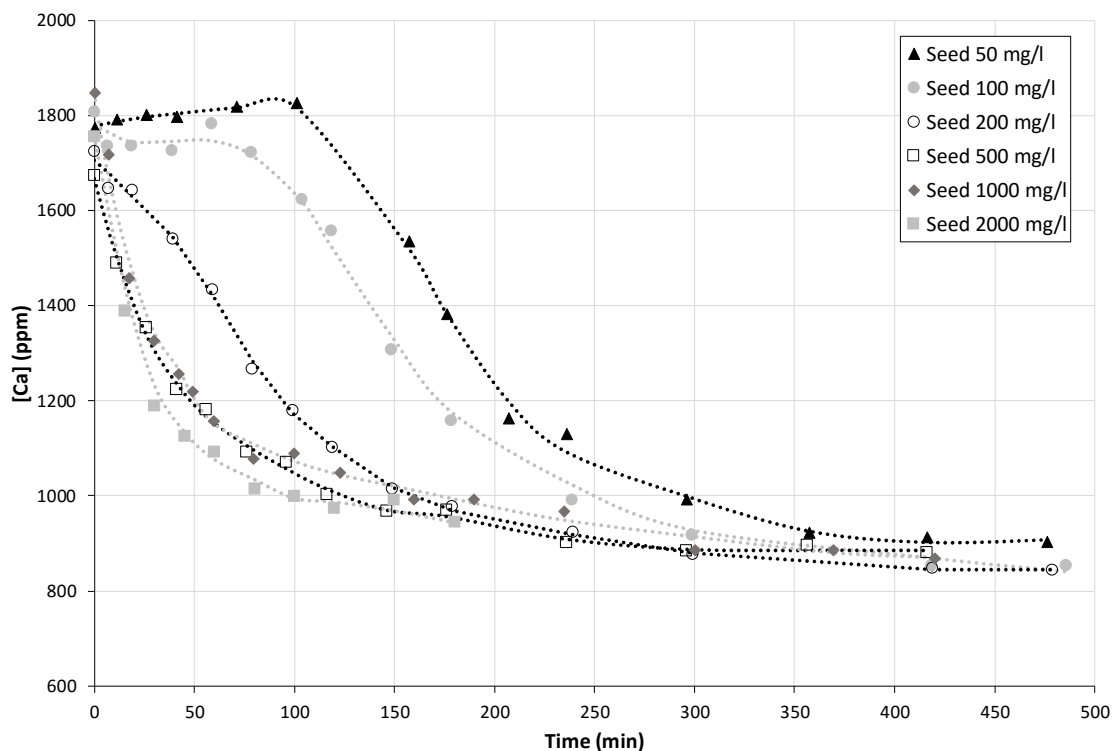


Figure 3.8: Desupersaturation curves at various levels of seeding at [Ca] = 0.05 mol/l, HA 15 mg/l and Temperature 25°C.

From Figure 3.8 it is clear that the amount of seeding plays an important role during crystallisation in the presence of HA. From the results of these preliminary experimental runs three levels of seeding were chosen for further investigation.

It is evident from Figure 3.8 that the two lowest seeding levels (50 and 100 mg/l) still show a significant period of inhibition. The aim with the addition of seed crystals is to override the induction period. Thus, in order to significantly decrease the induction period or completely eliminate it, seeding of neither 50 mg/l nor 100 mg/l was considered. With an increase in seed crystal concentration, the induction period is significantly minimised or completely overwritten. No real difference was observed between a 500 and 1000 mg/l level of seeding. For these reasons, seeding levels of 200, 1000 and 2000 mg/l were chosen for further investigation.

Chapter 3: Materials, methodology and research design

3.4.2. Experimental study

A design of experiments was used to determine the required amount of experiments. Due to the unpredictable nature of crystallisation, all experimental runs were repeated at least once at first. After repeatability was successfully achieved, the repeat of experimental runs was minimised due to the cost of chemicals and supplies, sample storage and analysis time.

From literature findings and preliminary experiments, certain factors were shown to be important for a full investigation of the effect of HS on the crystallisation process of gypsum. These factors are listed in Table 3.4 along with the levels in which they were varied during the study. Neither the effect of temperature nor that of stirring rate was investigated, because the aim was to investigate only the chemical aspects of the process and not the effect of mechanical inputs. It is known that agitation and temperature can affect the crystallisation process (see section 2.3). Additional investigation on the effects of temperature and agitation rate would have added too many variables to the system and would have overcomplicated the study. Temperature and stirring rate were therefore kept constant at 25°C and 400 rpm, respectively.

Table 3.4: Experimental variables for investigation of the effect of HA.

Supersaturation Level	pH	Humic Substance Concentration (mg/l)	Seeding (mg/l)
2	4.5	0	0
3	7.0	5	200
4	9.5	10	1000
		15	2000

In the first part of this study, baseline conditions were determined for the crystallisation of gypsum in the absence of any physical or chemical manipulation of conditions.

Table 3.5: Experiments for the determination of baseline conditions without HS.

Experiment Name	Repeat	Supersaturation level	Humic Substance Concentration (mg/l)	Seeding (mg/l)
BL-SS2	1	2	-	-
BL-SS2	2	2	-	-
BL-SS3	1	3	-	-
BL-SS3	2	3	-	-
BL-SS4	1	4	-	-
BL-SS4	2	4	-	-

3.4. Experimental design**Table 3.6: Experiments to test the effect of HA at various conditions in the absence of seed crystals.**

Experimental Order	Experiment Name	Replicate	Supersaturation Ratio	Humic Substance Concentration (mg/l)	pH
1	HA-03_A	1	2 [#]	5	9.5
2	HA-02_A	1	2 [#]	5	7
3	HA-01_A	1	2 [#]	5	4.5
4	HA-09_B	2	4	5	9.5
5	HA-25_A	1	4	15	4.5
6	HA-05_A	1	3	5	7
7	HA-15_A	1	3	10	9.5
8	HA-27_B	2	4	15	9.5
9	HA-07_B	2	4	5	4.5
10	HA-16_B	2	4	10	4.5
11	HA-13_A	1	3	10	4.5
12	HA-09_A	1	4	5	9.5
13	HA-14_B	2	3	10	7
14	HA-17_A	1	4	10	7
15	HA-08_B	2	4	5	7
16	HA-05_B	2	3	5	7
17	HA-26_A	1	4	15	7
18	HA-23_A	1	3	15	7
19	HA-26_B	2	4	15	7
20	HA-27_A	1	4	15	9.5
21	HA-06_A	1	3	5	9.5
22	HA-15_B	2	3	10	9.5
23	HA-23_B	2	3	15	7
24	HA-18_B	2	4	10	9.5
25	HA-17_B	2	4	10	7
26	HA-22_B	2	3	15	4.5
27	HA-22_A	1	3	15	4.5
28	HA-25_B	2	4	15	4.5
29	HA-08_A	1	4	5	7
30	HA-24_A	1	3	15	9.5
31	HA-06_B	2	3	5	9.5
32	HA-04_B	2	3	5	4.5
33	HA-18_A	1	4	10	9.5
34	HA-14_A	1	3	10	7
35	HA-24_B	2	3	15	9.5
36	HA-04_A	1	3	5	4.5
37	HA-07_A	1	4	5	4.5
38	HA-16_A	1	4	10	4.5
39	HA-13_B	2	3	10	4.5

#SS2 did not yield any crystallisation and was removed from the experimental design.

Chapter 3: Materials, methodology and research design

Table 3.5 lists the experiments that were done to obtain this baseline data along with the conditions that were applied during these experiments. The second part of the study was performed in the presence of HA. Table 3.6 lists the experiments that were carried out and the conditions that were applied at various levels. Experiments in this part of the study were carried out in random order to test the reproducibility of the process.

After the completion of the study on the effect of HA in the absence of seed crystals, another experimental set was carried out with the addition of seed crystals. For this experimental set only one supersaturation was used to study the effect of seeding. For this purpose SS3 was chosen, due to the fact that it gave reliable data and ample time to manipulate experimental conditions. Table 3.7 lists the experiments carried out in the presence of seed crystals. Tests to determine the effect of pH was not repeated again, since it had been shown to have a minimal effect in the presence of seed crystals (section 2.3.5). The repeatability of the data was found to be acceptable based on the results of the first set of experiments and the results obtained were found to be more accurate and reliable in the presence of seed crystals (see section 2.3.6). The set was designed for a single run of experiments and some of the experiments were repeated at random.

Table 3.7: Experiments to test for the effect of seeding in the presence of HA.

Experimental Order	Experiment Name	Supersaturation level	Humic Substance Concentration (mg/l)	Seeding (mg/l)
1	HS-03	3	10	1000
2	HS-08	3	10	200
3	HS-09	3	15	200
4	HS-10	3	15	1000
5	HS-11	3	5	1000
6	HS-12	3	5	200
7	HS-14	3	5	2000
8	HS-15	3	15	2000
9	HS-16	3	10	2000

After the completion of the study on the effect of HA on the crystallisation process, the study was further expanded to include investigation on the effect of FA on the crystallisation process. With FA it was difficult to set up a full experimental design, due to the expensive nature of this chemical. The aim was to repeat the first set that was carried out in the presence of HA, but the effect of FA was far greater than that of HA. The design had to be adjusted accordingly and the concentration of FA was lowered. Table 3.8 lists the

3.4. Experimental design

experiments that were done and the conditions that were applied to study the effect of FA on spontaneous crystallisation without seed crystal addition.

Table 3.8: Experiments to test for the effect of FA at various conditions in the absence of seed crystals.

Experimental Order	Experiment Name	Supersaturation level	Humic Substance Concentration (mg/l)	pH
1	FA-01	3	15	7.0
2	FA-02	3	5.0	7.0
3	FA-03	3	5.0	4.5
4	FA-04	3	2.5	4.5
5	FA-05	3	2.5	7.0
6	FA-06	3	1.0	7.0
7	FA-07	3	1.0	4.5
8	FA-08	3	1.0	9.5
9	FA-09	3	2.5	9.5

The last set of experiments that were carried out, was the effect of FA with the addition of seed crystals. A partial study on this effect was performed with only two FA concentrations investigated. The experiments are listed in Table 3.9.

Table 3.9: Experiments to determine the effect of seeding in the presence of FA.

Experimental Order	Experiment Name	Supersaturation level	Humic Substance Concentration (mg/l)	Seeding (mg/l)
1	FS-01	3	10	200
2	FS-02	3	5	200
3	FS-03	3	5	1000
4	FS-04	3	5	2000
5	FS-05	3	10	2000
6	FS-06	3	10	1000

Figure 3.9 gives a simplified schematic diagram summarising the experiments carried out in the preliminary stage and the experimental stage of this study.

Chapter 3: Materials, methodology and research design

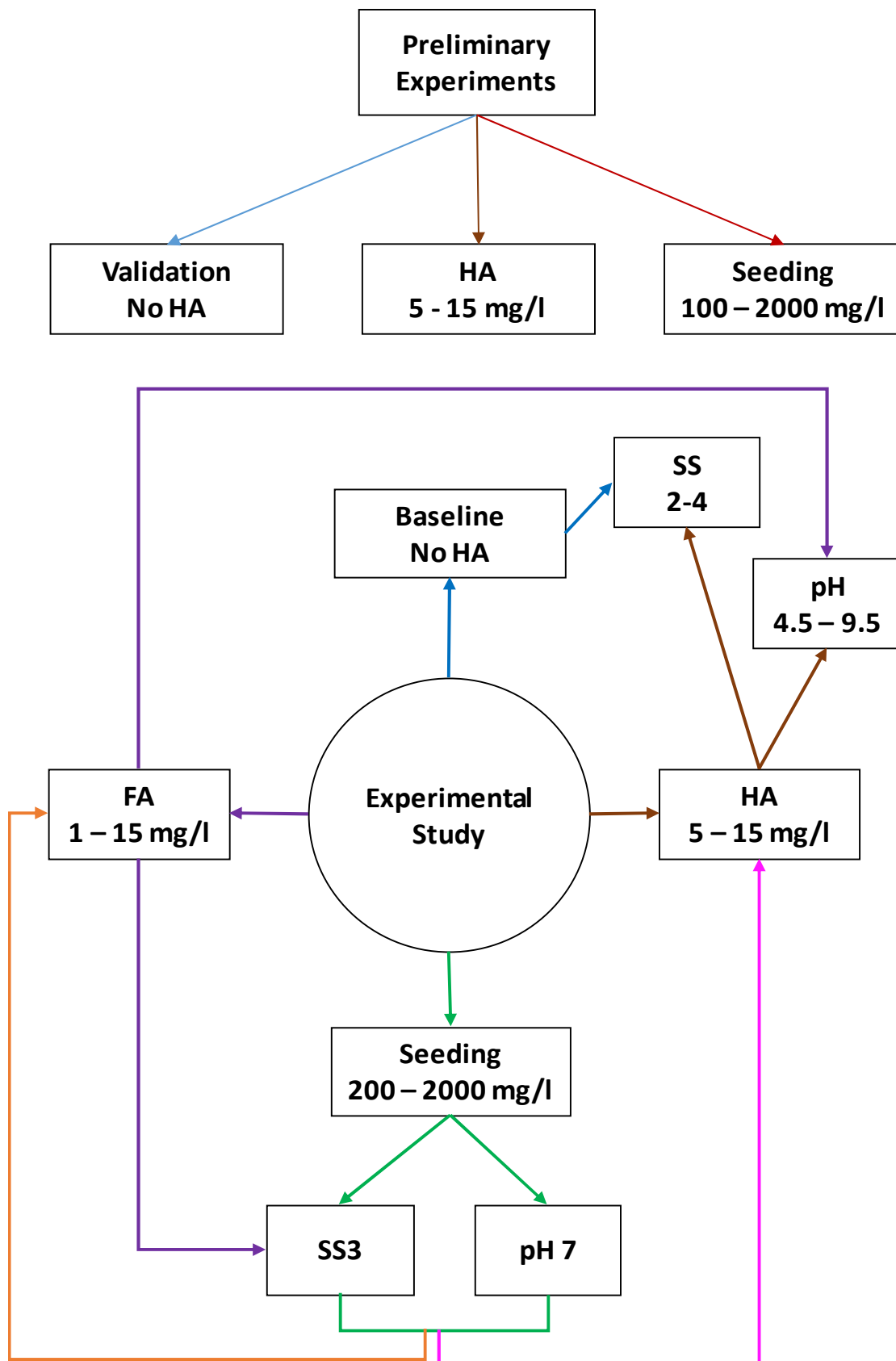


Figure 3.9: Schematic diagram of experiments carried out in this study.

3.5. Error analysis

During the experimental part of this project, various errors that could potentially occur were identified and, as far as possible, quantified. For this purpose, this section is divided into two separate parts, namely the experimental and analytical parts. All relevant calculations have been outlined in the sample calculations found in Appendix F. All relevant deviation results are given in Appendix D.

3.5.1. Experimental error

As outlined in the experimental procedure of this chapter, various steps were followed to complete an experimental run. The main errors that were identified were that of sampling and dilution.

Sampling takes about half a minute to a minute to complete. The time was recorded at the point of sampling when the glass pipette was inserted into the solution. Drawing up the required amount of solution took at least 10 to 20 seconds. For the sample time, the error was deemed to be negligible and there could be a maximum error of about ± 1 min. In all experiments the initial times were normalised to time zero.

The adjustment of pH required the addition of buffer solution to the working fluid. Depending on the pH that was required, a maximum of about 1 ml buffer solution was added to the working fluid. This could lead to an error of 0.243% which is approximately a further dilution of about 5 ppm. This was very small and together with other errors could be negligible.

The main deviations were attributed to the dilution of samples and the sampling itself. With sampling, errors may arise due to wall effects on the inside surface of the pipette. The pipette was rinsed thoroughly. Therefore the wall effects should be negligible, but some cross contamination may occur and affect the concentration of the sample slightly. When crystallisation is in full effect the amount of crystals in the sample can have an effect on the volume uptake. An average error of 1.11% could be possible. This was quantified by weighing samples and taking into account the temperature of the environment in the

Chapter 3: Materials, methodology and research design

calculations of densities and volume. The overall STD, RSD and SE for sampling were determined to be 0.054 ml, 1.10% and 0.013 ml, respectively.

With dilution the same method of weighing and calculating the volume was used. The average error was determined to be 1.14%. The STD, RSD and SE for dilution were 0.222 ml, 1.10% and 0.052 ml, respectively. With sampling and dilution an overall error of 1.59% was possible.

Due to the hydration effect of CaCl_2 , the actual concentration of the solution was lower than the calculated concentration. For this reason a stock solution was prepared and a number of samples from the stock solution were analysed to determine their calcium and sodium concentrations. Figure 3.10 presents these analytical results obtained for the stock solution.

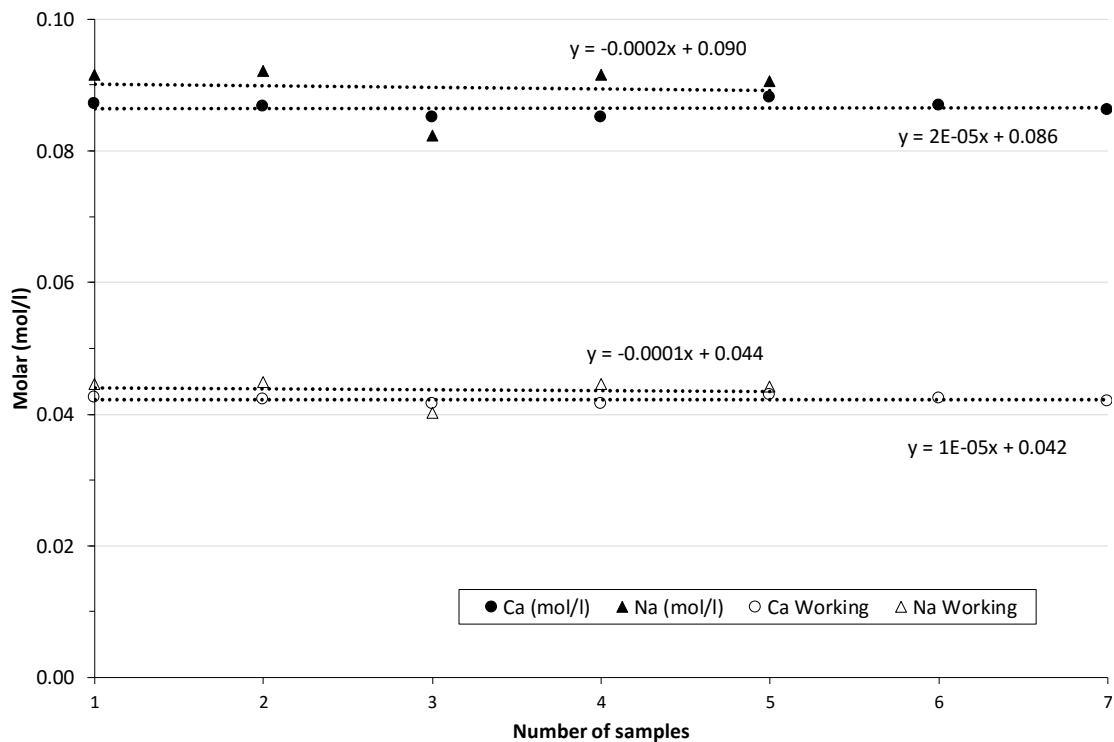


Figure 3.10: Analytical results for stock solution concentration of calcium and sodium.

3.5. Error analysis

A slight variation in sodium and calcium concentrations was observed. An average standard deviation between calcium and sodium of 0.002 mol/l was determined with an RSD of 2.26% and a SE of 0.0014 mol /l.

It was difficult to present error bars on the graph since in the working range these errors were very small. The standard deviations, RSD and SE for calcium were determined to be 0.000484 mol/l, 1.15% and 0.00016 mol/l, respectively. For sodium the standard deviation, RSD and SE were 0.00167 mol/l, 3.78% and 0.00056 mol/l, respectively. The analytically determined concentrations for sodium and calcium were hence forth used as the actual concentrations of the stock solution.

3.5.2. Analytical error

All metal analysis results gathered during this study were obtained by ICP-OES analysis at Stellenbosch University – Process Engineering analytical laboratory. In order to determine the amount of analytical deviation, a number of initial concentration samples were repeated for both SS3 and SS4. Figure 3.11 presents the repeat analysis results for SS3.

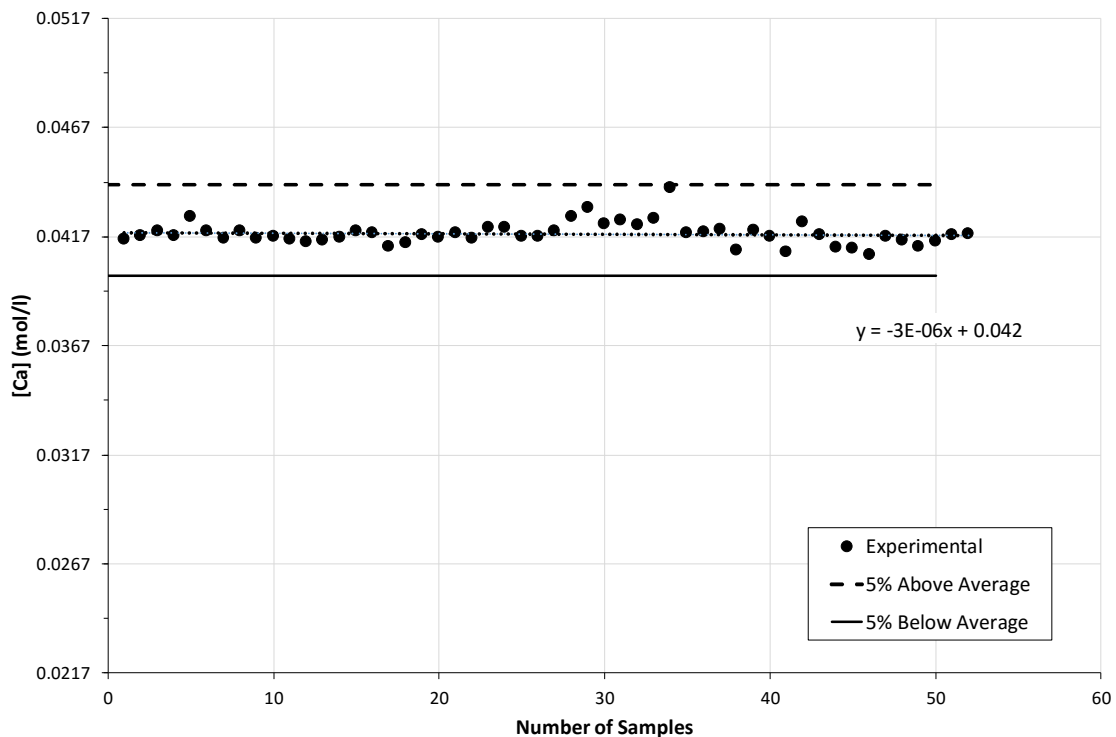


Figure 3.11: Analytical results for initial concentration at SS3.

Chapter 3: Materials, methodology and research design

It is clear from Figure 3.11 that the average initial calcium concentration at SS3 was 0.042 mol/l during this study. The average standard deviation between results was found to be 1.8×10^{-5} mol/l with an RSD of 0.424%. The standard error was determined to be 7.171×10^{-5} mol/l.

Figure 3.12 presents the analytical results for the initial concentration at SS4. The average initial calcium concentration during this study was 0.056 mol/l. A standard error of 1.210×10^{-4} mol/l was determined with an average standard deviation of 2.333×10^{-5} mol/l and an RSD of 0.41%.

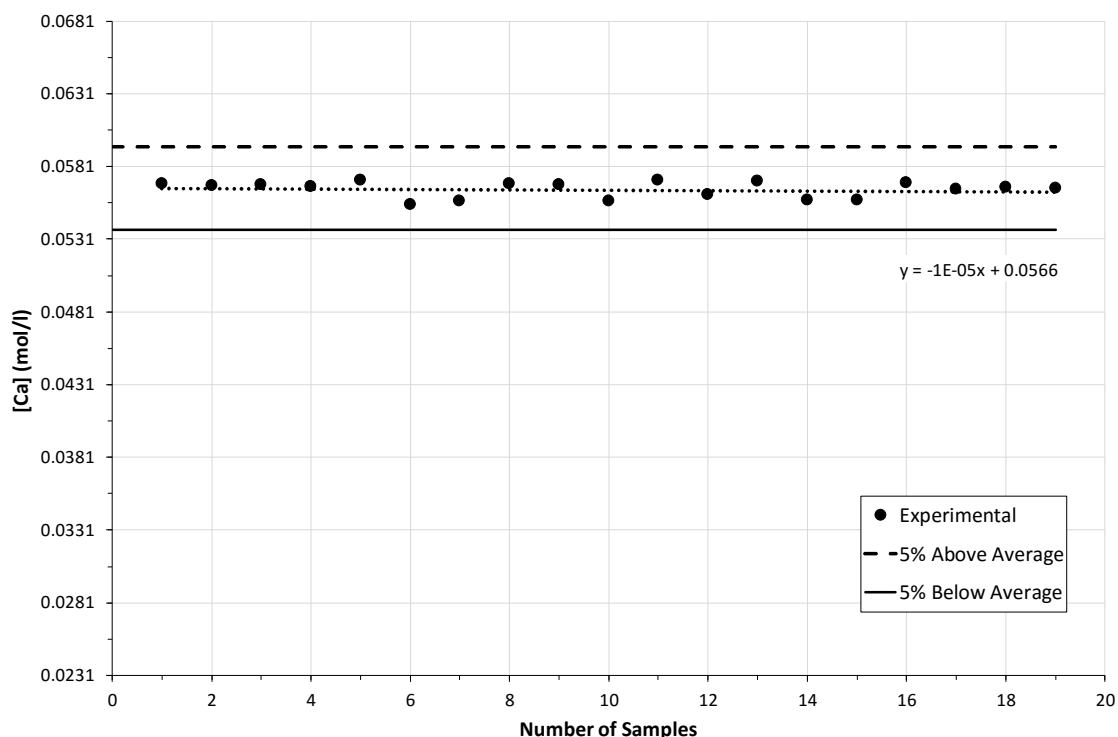


Figure 3.12: Analytical result for initial concentration at SS4.

With the deviations reported above, all experimental data was in a 10% band of the average. Any analytical results outside this band were either reanalysed or determined to be an error and were not included in further data analysis. Therefore, the amount of analytical deviation, repeatability and error in the analytical data was known and the results could be evaluated with confidence.

Chapter 4: EXPERIMENTAL RESULTS AND DISCUSSION

With the methods detailed in the previous chapter, focus now shifts to the results of the experimental study and the discussion thereof. This chapter describes the effect of HA and FA in the absence of seed crystals and in the context of pH and supersaturation variation. The effect of FA is then compared to that of HA. Crystal growth kinetics in the absence of seed crystals are then outlined before the results of seeded crystallisation are discussed. In order to understand the effect of HS better, baseline conditions were determined first in the absence of any HS and are presented first.

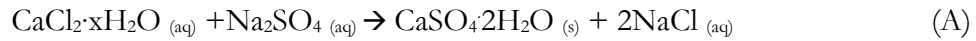
4.1. Baseline conditions

As outlined in the experimental design section (section 3.4), three levels of supersaturation were chosen for investigation in this study. Baseline conditions were determined before the addition of any additive or the physical or chemical manipulation of any other factors. These conditions are seen as the ‘desired case’ of crystallisation with no manipulation of system conditions or the presence of foreign particles. Induction periods, crystallisation times and saturation concentrations were extracted from the determined baseline conditions. This data were used for the comparison and evaluation of results generated in the presence of HS and under various experimental conditions (pH and SS variation).

Baseline data were generated by the spontaneous crystallisation of gypsum at SS2, SS3 and SS4 without doing any other physical or chemical manipulations. Saturation concentrations were predicted by PHREEQC[®] and are presented in Figure 4.1. Concentrations generated by PHREEQC[®] compared well with the experimental saturation results (Figure 4.1). An average STD and RSD (between the predicted and experimental results) of 3.33 ppm (mg/l) and 0.37%, respectively were observed.

Chapter 4: Experimental Results and Discussion

As is evident from Figure 4.1, a slight increase in the saturation concentrations is seen with an increase in the supersaturation. This is expected, since an increase in supersaturation will result in an increase of total dissolved solids (TDS). An increase in background ions (primarily from NaCl) will result in a change in solubility of the ions in solution. The crystallisation of gypsum in this setup is expected to follow the chemical reaction (A).



Calcium and sulphate ion concentration are assumed to be in equimolar quantities. From reaction (A) it is evident that when the initial calcium concentration is increased, an increase in sodium sulphate concentration will also be required. This in total will result in an increase in the TDS levels and an increase in background ions. The background ions, such as sodium chloride, have an effect on the solubility (see section 2.2.1) and crystallisation of calcium sulphate, as is evident from the work carried out by Ahmed [37] and Brandse et al [39].

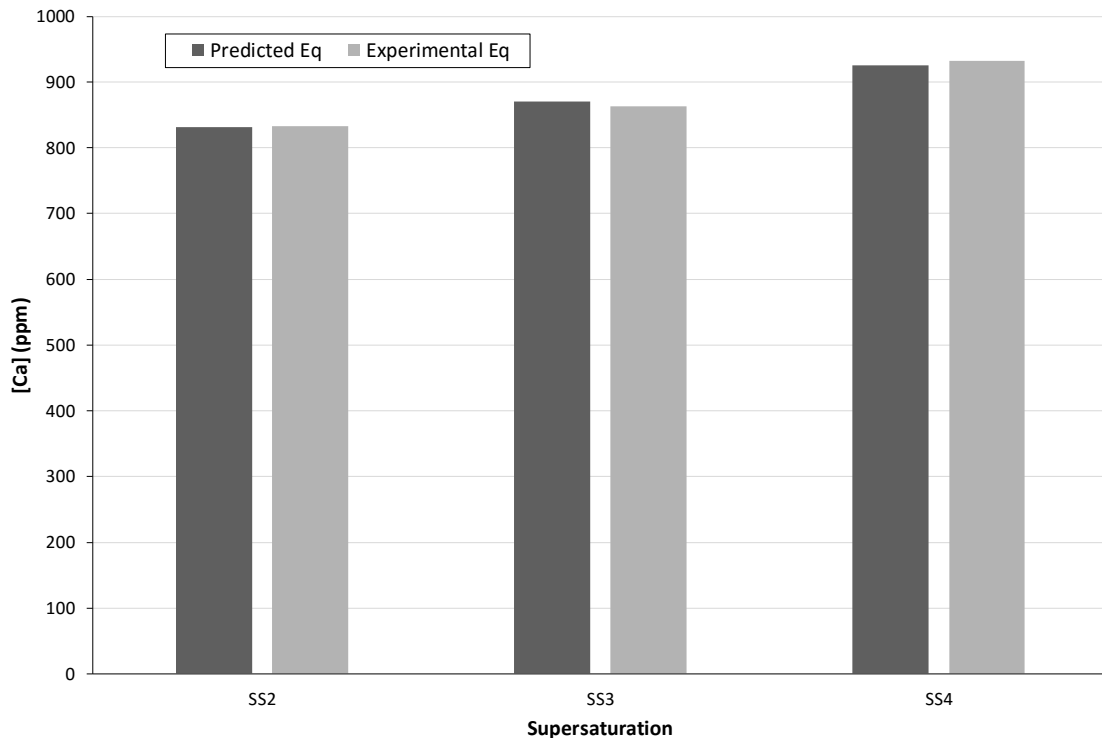


Figure 4.1: Saturation concentrations predicted by PHREEQC[®] (Version 2) and average experimental saturation concentrations for SS2, SS3 and SS4.

4.1. Baseline conditions

Figure 4.1 presents the desupersaturation curves for the baseline experiments as well as the saturation concentration predicted by PHREEQC®. This indicates that the experimental saturation concentrations compare reasonably well with the predicted saturation concentrations. Slight deviations are observed and are assumed to be contributed by small experimental and analytical errors which can occur, as described in section 3.5.

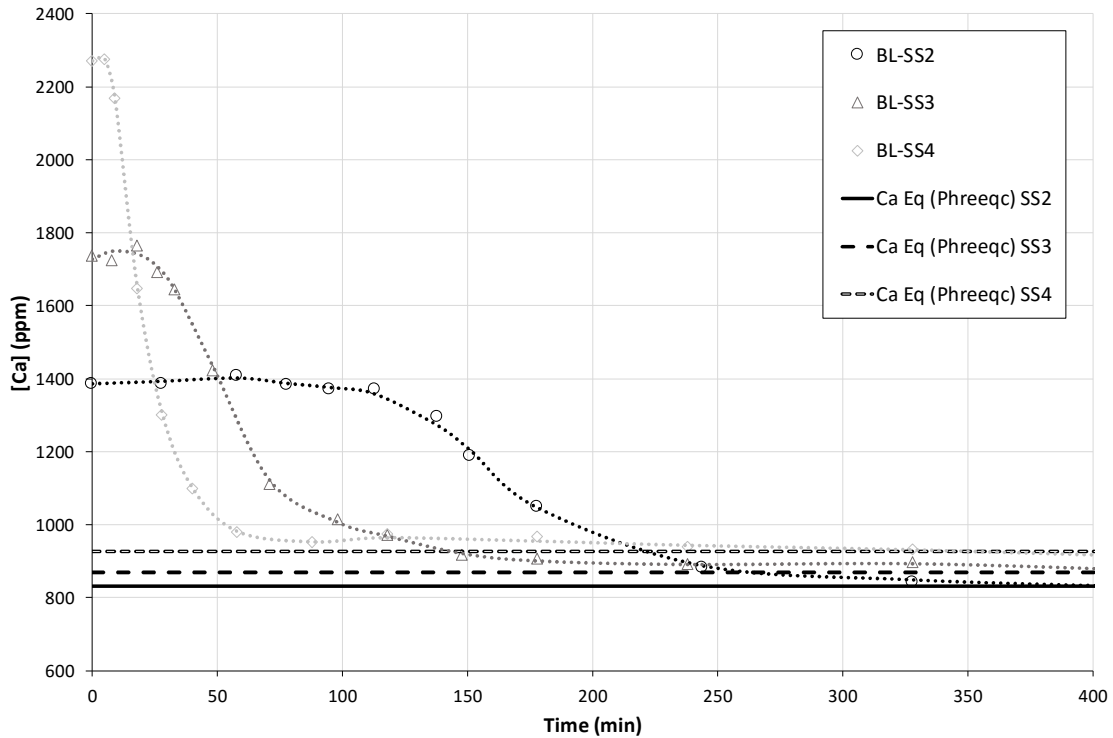


Figure 4.2: Desupersaturation curve for baseline experiments with predicted saturation concentrations from PHREEQC®.

Error! Reference source not found. presents the calculated initial concentrations of the individual baseline experiments. The average induction times observed from the desupersaturation curves are also presented.

Table 4.1: Supersaturation concentrations and induction times for baseline experiments.

Experiment Name	Initial Concentration C		Supersaturation Ratio	Induction time (min)
	(ppm)	$\times 10^3$ (mol /l)		
BL-SS2	1486.97	37.1	2	106
BL-SS3	1679.35	41.9	3	25
BL-SS4	2268.53	56.6	4	7

Chapter 4: Experimental Results and Discussion

4.1.1. The effect of supersaturation

The effect of supersaturation on crystallisation can be observed in Figure 4.3. With a decrease in supersaturation from SS4 to SS2, induction times increase from 7 to 106 minutes. The spontaneous formation of a stable crystal lattice or critical nuclei takes place rapidly high above the solubility limit of gypsum. Moving closer to saturation concentrations the nucleation rate is slowed considerably and the time that it takes for the first stable crystal to form is increased. Equation 2.5 shows that the nucleation rate is dependent on supersaturation. Thus, as observed, there will be an increase in nucleation rate with an increase in supersaturation, which will result in a decrease in the induction period.

Figure 4.3 shows the dramatic decline in induction times with an increase in supersaturation concentration. The effect of supersaturation is further interpreted by evaluating the time of crystallisation.

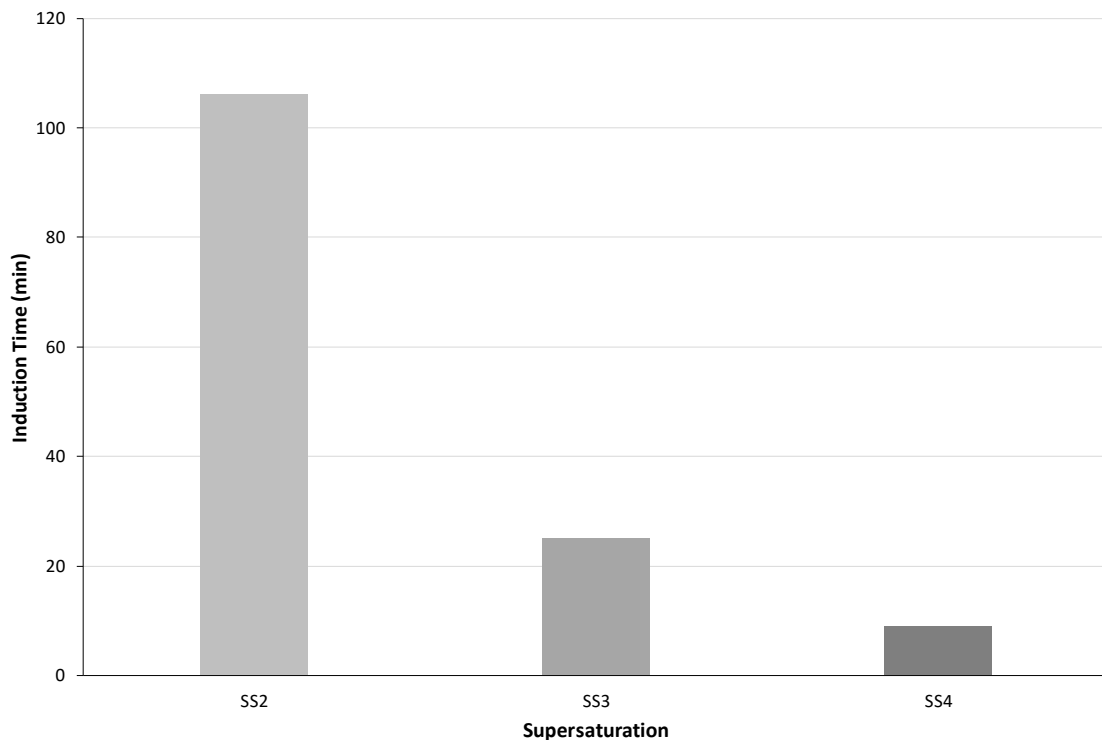


Figure 4.3: Inductions times observed in baseline experiments.

4.1.2. Evaluation of crystallisation times

It is important to eliminate induction periods completely in order to reduce retention times in reactors. However, induction periods give us insight into methods of inhibiting crystallisation. Inhibition of crystallisation is important in protecting membranes, heat exchanger surfaces and in prevention of fouling. Evaluation of the crystallisation times plays a critical role in understanding the kinetics of crystallisation and how these kinetics can be influenced. Figure 4.4 illustrates the crystallisation times for baseline experimental runs carried out at the respective supersaturation concentrations.

For the purposes of evaluating crystallisation times, t_{10} is defined as the time from the point when crystal growth starts, until a concentration that is 10% above the saturation concentration is reached. The total crystallisation time, t_s , is the time from the point where crystal growth starts until saturation is reached. Figure 4.4 presents the crystallisation times (t_{10} and t_s) for the baseline experiments. Table 4.2 indicates the concentrations that are 10% above the respective supersaturation levels' saturation concentrations.

Table 4.2: t_{10} Concentrations.

Supersaturation level	t_{10} concentration $\times 10^3$ (mol/l)*	t_{10} concentration (ppm)
3	23.87	956.71
4	25.41	1018.43

*Calculated by PHREEQC[®] (Version 2).

Note that absolute complete crystallisation times are difficult to interpret due to deviations that may arise from experimental and analytical errors. Interpreting trends in this case is more than adequate to understand the effects on crystallisation from an engineering perspective. For this purpose, t_{10} is compared to t_s . Most crystallisation runs studied occurs up to the time point t_{10} . All times that are quoted should not be taken as absolute values, but as representative of the interpretation of the results generated in this study.

Figure 4.4 shows that an increase in supersaturation resulted in a decrease in all crystallisation times. When considering only t_{10} , the fastest crystallisation time observed was

Chapter 4: Experimental Results and Discussion

around 50 minutes at SS4. For SS2 and SS3, the times observed were 115 and 75 minutes respectively.

Crystallisation is induced from the formation of the first stable crystal particle. Crystal growth is then rapid up to a certain point. According to Mullin [5], two separate stages of crystal growth can exist. The first stage of growth is known as agglomeration and takes place very rapidly. The second stage of growth that exists is known as ‘ageing’ in which crystallisation gradually approaches its saturation level and this can take up to hours or days.

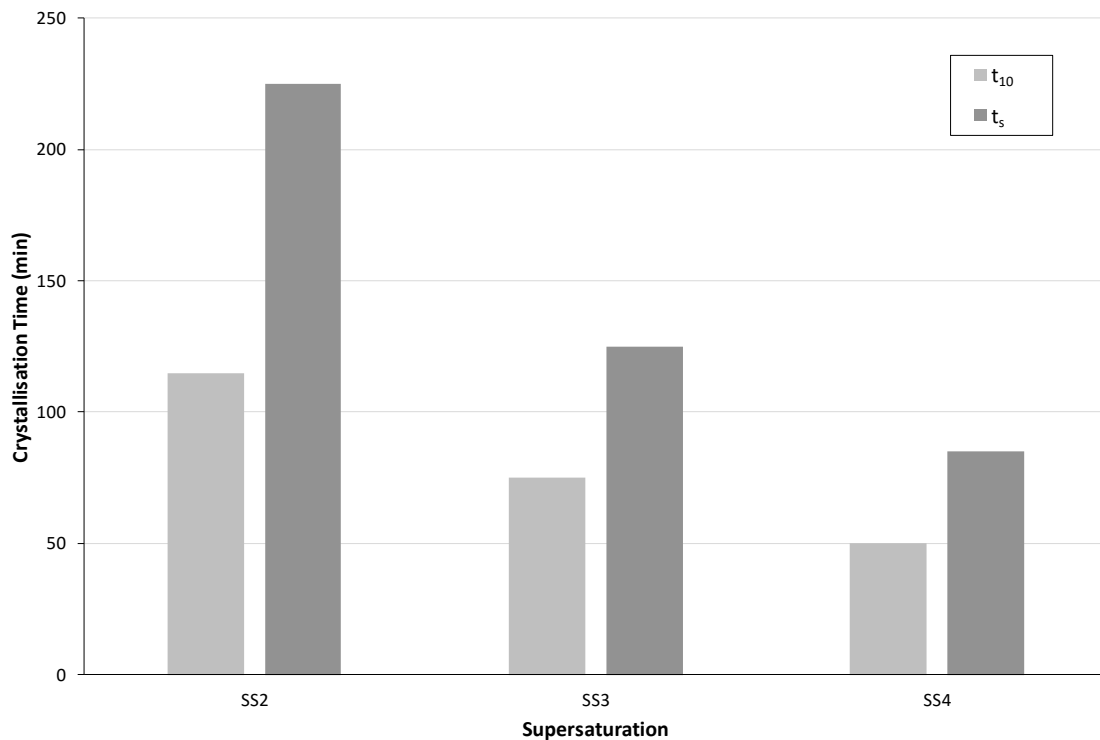


Figure 4.4: Evaluation of crystallisation times at baseline conditions and at SS2, SS3 and SS4 without seeding.

It is evident that for all the supersaturation levels, crystallisation to t_{10} , is achieved in 50-110 minutes. Total crystallisation times, t_s , of SS2, SS3 and SS4 are approximately 225, 125, and 108 minutes respectively. It therefore takes up to 110 minutes more to reach complete crystallisation after completion of the first crystallisation stage up to time t_{10} . This almost doubles the time that it takes to reach complete crystallisation after the first rapid stage.

4.2. The effect of humic acid (HA)

From evaluation of the crystallisation times above, it is evident that supersaturation is clearly the driving force of crystallisation. With a decrease in supersaturation, the overall driving force ($c-c^*$) is decreased and this is one of the major factors that can affect the crystallisation of gypsum.

Retention times can be optimised and improved through the evaluation and understanding of crystallisation times and how they can be affected. The best scenario would be to achieve complete crystallisation in the shortest amount of time. All times interpreted from baseline results will be used as the 'desired case' in evaluating and discussing the results of this chapter. This will only be the case for experimental runs in the absence of seed crystals.

4.2. The effect of humic acid (HA)

The following subjects are discussed separately under individual headings in this section: the effect of HA on induction times; the effect of supersaturation; the effect of pH on humic acid behaviour and evaluation of crystallisation times in the presence of HAs and the absence of seed crystals. Relevant experimental data are provided in Appendix B.

4.2.1. Effect on induction times

Figure 4.5 to Figure 4.7 present the results separately for each of the initial supersaturation conditions (SS2, SS3 and SS4) in the presence of various HA concentrations.

It is evident from Figure 4.5 that at SS2, the onset of crystallisation is completely inhibited for a period of at least 8 hours at a HA concentration of only 5 mg/l. This result clearly indicates the polyelectrolyte ability of HA at lower concentrations and low supersaturation. Higher HA concentrations at SS2 were not investigated. The strong inhibitory effect of HA at this level of supersaturation indicates that this effect will be even greater with an increase in HA concentration.

Chapter 4: Experimental Results and Discussion

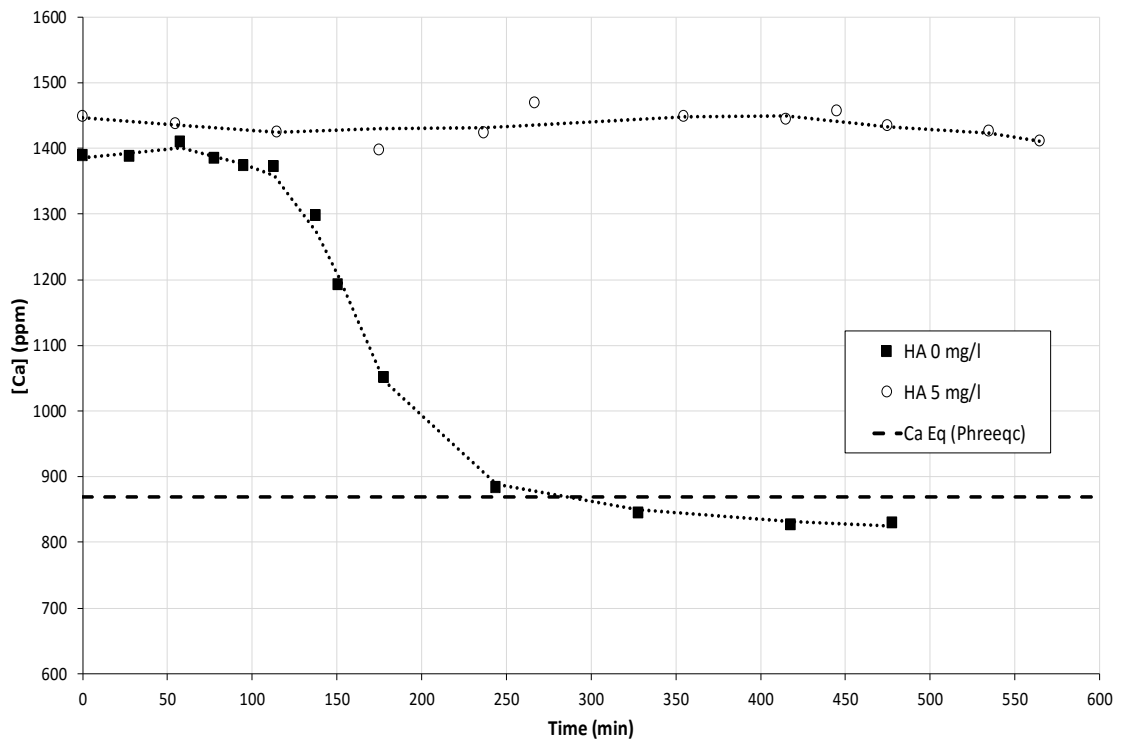


Figure 4.5: Desupersaturation curve in the presence of 0 and 5 mg/l HA at SS2. Initial adjusted pH of 7.0 and Temperature of 25 °C without seeding.

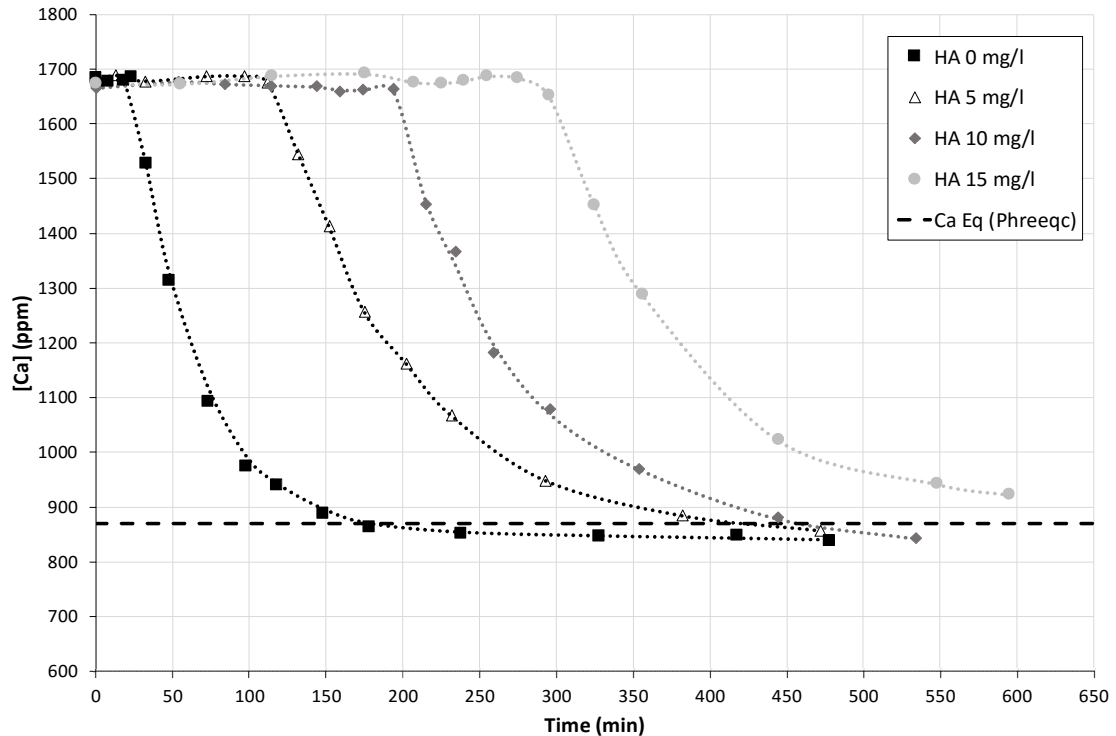


Figure 4.6: Desupersaturation curves in the presence of HA at 0, 5, 10 & 15 mg/l and at SS3. Initial adjusted pH of 7.0 and Temperature of 25 °C without seeding.

4.2. The effect of humic acid (HA)

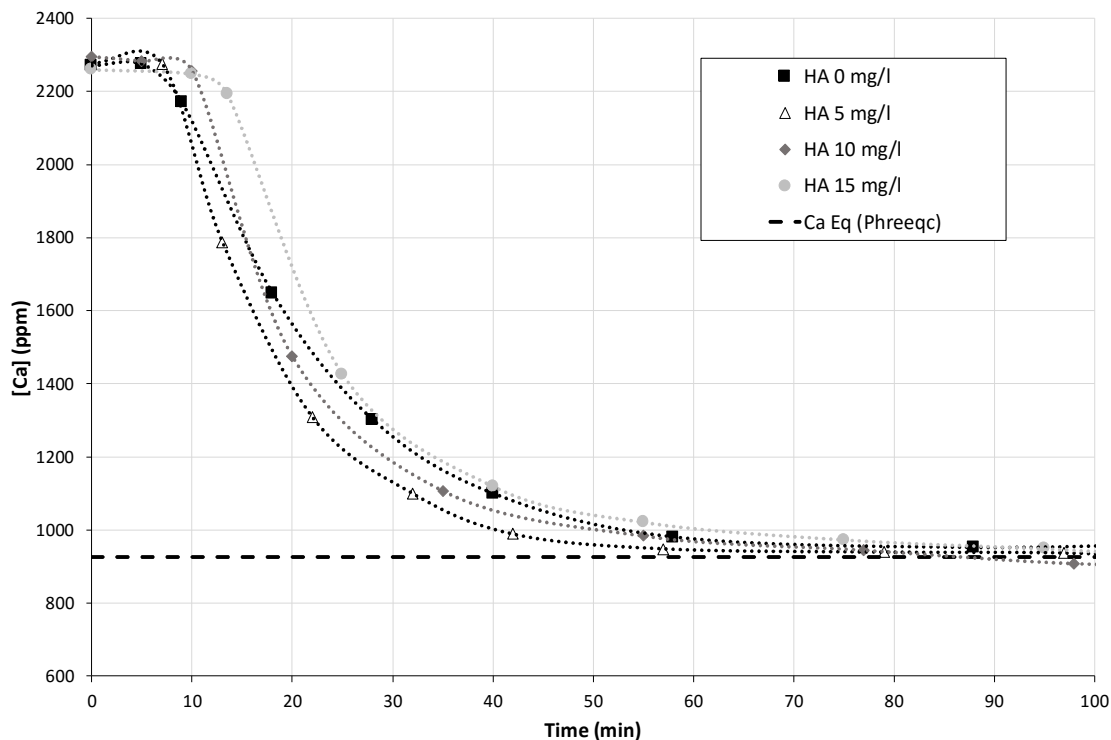


Figure 4.7: Desupersaturation curves in the presence of HA at 0, 5, 10 & 15 mg/l and at SS4. Initial adjusted pH of 7.0 and Temperature of 25 °C without seeding.

Figure 4.6 shows that an increase in HA concentration resulted in an increase in induction times at SS3. Induction time increased from 98 to 295 minutes with a HA increase from 5 to 15 mg/l. At SS4, induction time only increased slightly from 7 to 15 minutes. Compared to baseline conditions, the increase in induction time was small. This increase in induction period is notably small and clearly illustrates the driving force of higher supersaturation levels (see section 4.2.2).

An increase of 100 minutes is observed with a HA increase from 5 to 10 mg/l and from 10 to 15 mg/l at an initial calcium concentration of 0.0419 mol/l (SS3). Under the same conditions with a higher initial calcium concentration of 0.0566 mol/l (SS4) only a 5 min increase is observed. At a higher HA concentration, a higher functional group concentration (-OH and -COOH) is expected. It is the functional groups forming part of their structure which give HAs their inhibitory abilities [10, 30]. Therefore, this increase in functional group concentration at higher HA concentration will result in an increase in inhibitory effect and in the excellent polyelectrolyte ability of HA at lower supersaturation conditions. It is also evident from the literature review that HS, in the form of HA, have a strong inhibitory effect on gypsum crystallisation.

Chapter 4: Experimental Results and Discussion

Table 4.3 presents the induction times of each of the experiments along with the initial calcium concentration and HA concentration of each.

Table 4.3: Induction times and experimental conditions at pH 7.0 and T = 25°C.

Experiment Name	Initial Concentration C		Supersaturation Ratio	Humic Acid Concentration (mg/l)	Induction time (min)
	(ppm)	$\times 10^3$ (mol/l)			
HA-02_B	1488.57	37.1	2	5	>8 hours
HA-05_A	1679.35	41.9	3	5	98
HA-14_B	1679.35	41.9	3	10	195
HA-23_B	1679.35	41.9	3	15	295
HA-08	2268.53	56.6	4	5	7
HA-17	2268.53	56.6	4	10	11
HA-26	2268.53	56.6	4	15	15

4.2.2. Supersaturation effect

Figure 4.8 presents the induction times for an increase in supersaturation with an increase in HA concentration. All times were given in Table 4.3 in the previous section.

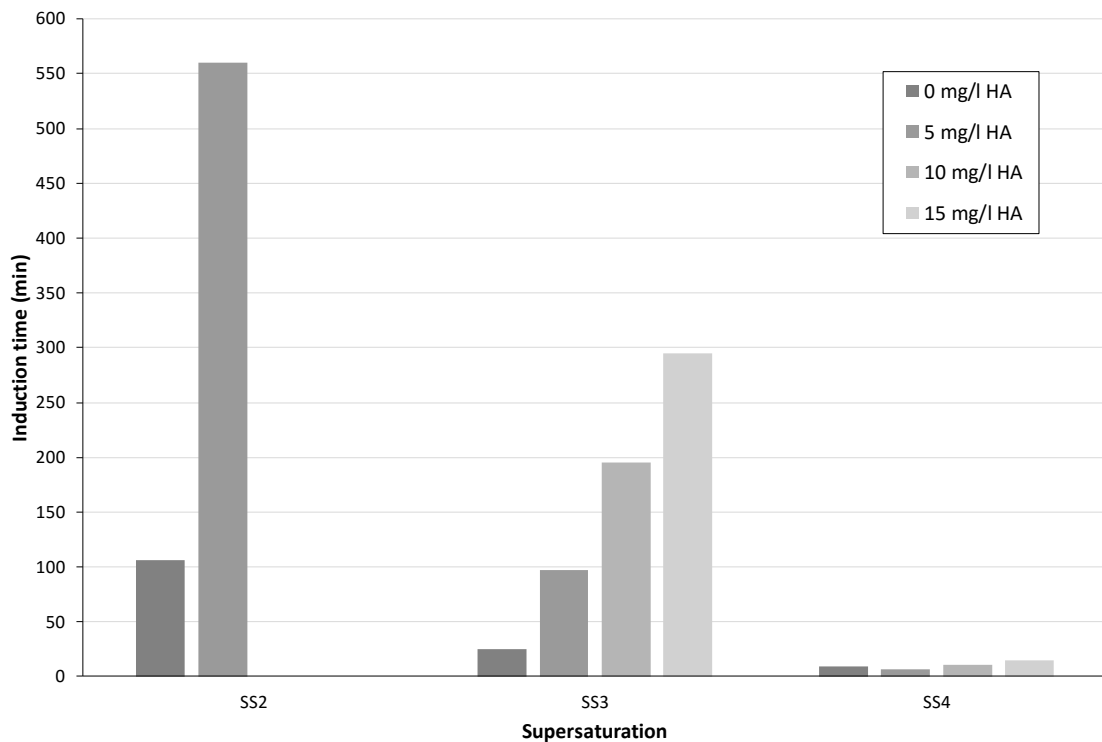


Figure 4.8: Induction times in the presence of HA (0, 5, 10 & 15 mg/l) at SS2, SS3 & SS4. Initial adjusted pH of 7.0 and Temperature of 25°C without seeding.

4.2. The effect of humic acid (HA)

Figure 4.8 shows that with an increase in supersaturation a decrease in overall induction times is observed, while an increase in HA resulted in a strong increase in induction times. At SS2, 5 mg/l HA was able to inhibit crystallisation completely for a period of 565 minutes (~9.4 hours). This is attributed to the ability of HA to effectively block the active growth sites, not only through interaction with calcium, but also through adsorption. The larger molecular weight and linear configuration of the HA molecules promotes the adsorption of calcium [65].

The predominant effect of supersaturation can be clearly seen at higher supersaturation. The driving force for crystallisation is greater and the activation energy required is decreased. The work of Alimi et al. [66] shows that with an increase in supersaturation there is a decrease in the activation energy for crystallisation. At these higher concentrations it can be difficult to manipulate chemical and physical conditions before the onset of crystallisation. With the increase in nucleation, variation in sampling speed could have had an effect on the times that were observed. However, repeat runs yielded the same results.

With an increase in supersaturation from SS3 to SS4 in the presence of 15 mg/l HA, induction time is decreased from 295 to 15 minutes. This is a decrease in induction times of ~20 times. At these supersaturations, there are approximately 1012 and 1584 ppm calcium ions available (i.e. ions above respective saturation concentrations) for crystallisation at SS3 and SS4, respectively. The increase in calcium and sulphate particles with a transition from SS3 to SS4 is ~1.6 times. The presence of more particles results in an increase in surface area. More HA will then be required to block the increased number of particles. This also means that particles will be more closely packed to each other and will reduce the ability of the HA to block all active growth sites successfully, as it is able to do at the lower supersaturation of SS2.

With an increase in supersaturation there will be an increase in nucleation rate, as described by equation 2.5. This means that the maximum excess free energy required will be decreased, thereby reducing the required critical nucleus radius necessary to form a stable crystal lattice.

Chapter 4: Experimental Results and Discussion

The increase in particles also means that the collision of particles is promoted due to the fact that the solution is being agitated. Through this agglomeration is increased, which in turn will also promote nucleation and the onset of crystallisation.

4.2.3. Effect of pH

In this section of the chapter the effect of pH in the presence of HA is discussed. The effect of pH was investigated by doing an initial adjustment of pH to the desired level. Only one experiment was carried out at a controlled pH of 9.5 in order to determine if this would have a significant influence.

Figure 4.9 presents the results over a pH range of 4.5 to 9.5 for SS2 and a HA concentration of 5 mg/l.

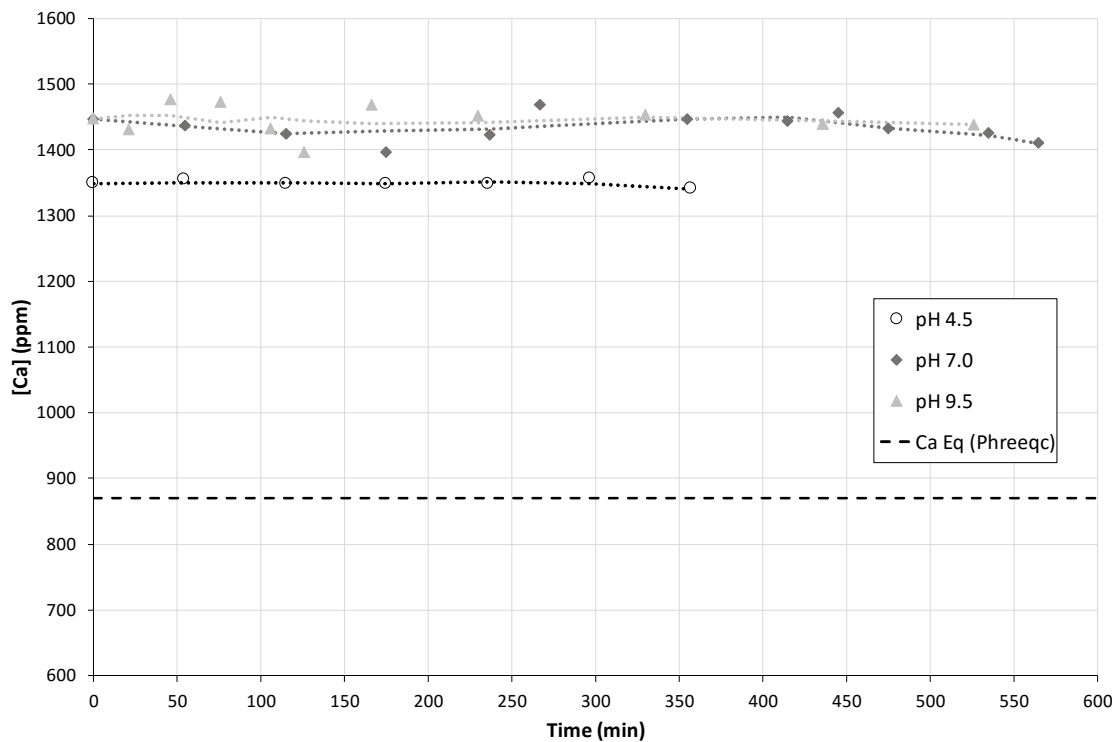


Figure 4.9: Desupersaturation curves in the presence of HA (5 mg/l) at SS2. Initial adjusted pH of 4.5, 7.0 and 9.5 and Temperature of 25°C with no seeding.

4.2. The effect of humic acid (HA)

No crystallisation could be induced over the entire pH range investigated (Figure 4.9). Induction times were monitored for a period of at least 8 hours. At SS2, the ability of HA to inhibit crystallisation was clearly highlighted. The inhibitory ability of HA over the investigated pH range was illustrated at the higher supersaturation conditions as well.

In Figure 4.10 to Figure 4.12 results are presented for each individual HA concentration (5, 10 and 15 mg/l) at an initial calcium concentration of 0.0419 mol/l (SS3).

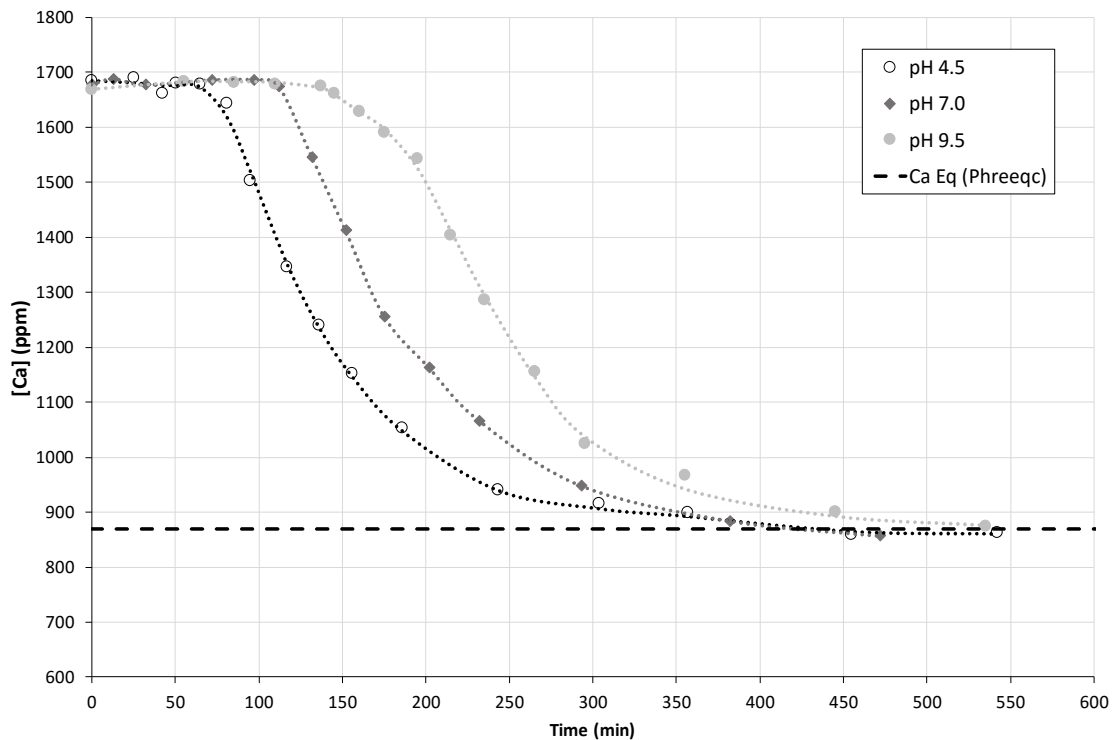


Figure 4.10: Desupersaturation curves in the presence of HA (5 mg/l) at SS3, initial adjusted pH 4.5, 7.0 & 9.5 and Temperature 25°C with no seeding.

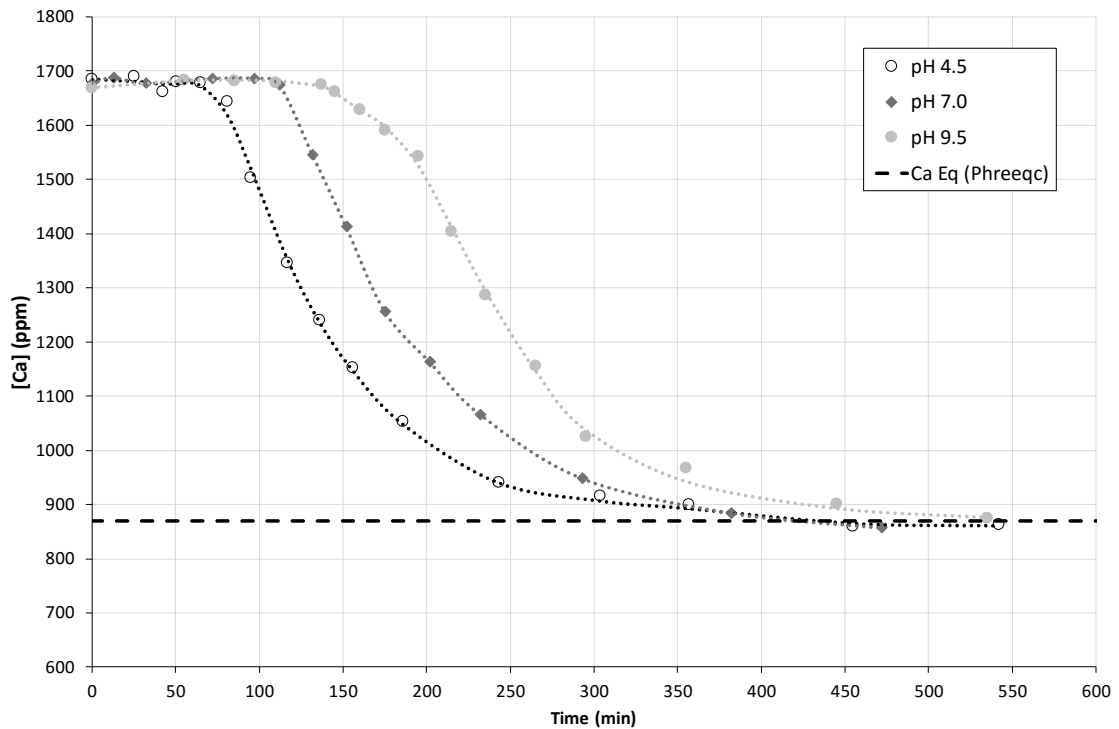
Chapter 4: Experimental Results and Discussion

Figure 4.11: Desupersaturation curves in the presence of HA (10 mg/l) at SS3, initial adjusted pH 4.5, 7.0 & 9.5 and Temperature 25 °C with no seeding.

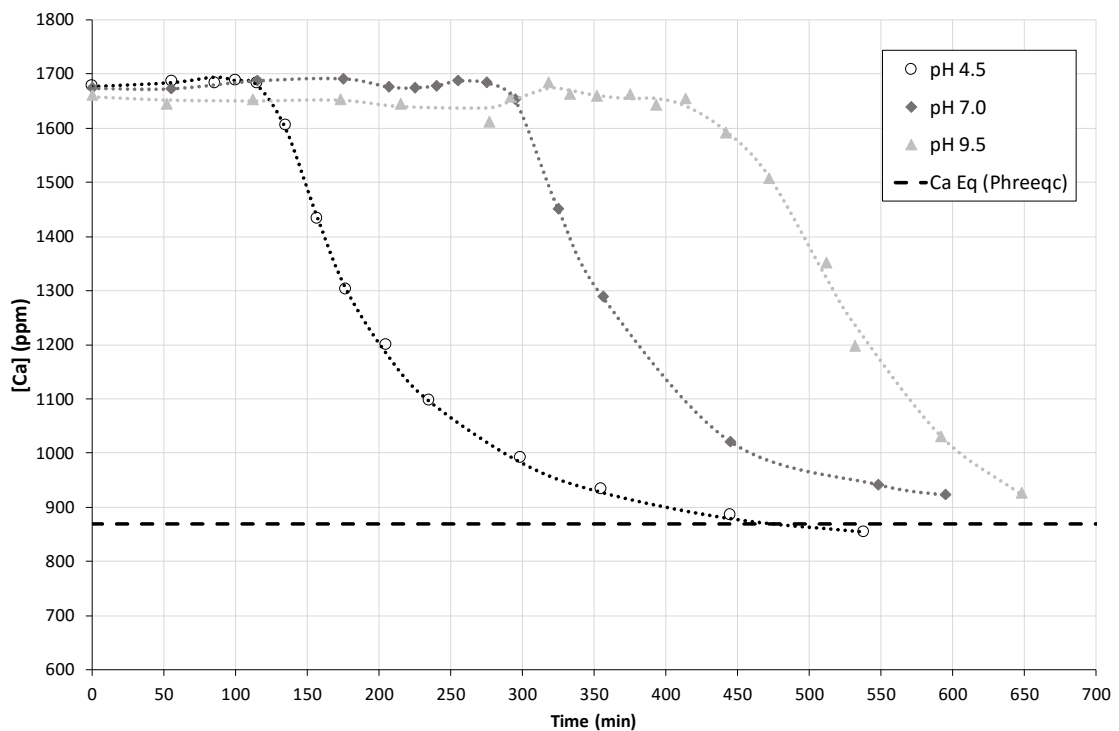


Figure 4.12: Desupersaturation curves in the presence of HA (15 mg/l) at SS3, initial adjusted pH 4.5, 7.0 & 9.5 and Temperature 25 °C with no seeding.

4.2. The effect of humic acid (HA)

With an increase in pH, an increase in induction times are clearly observed at all investigated HA concentrations. At SS3, crystallisation is not completely inhibited. The inhibitory effect of HA increased with an increase in pH. At an initial pH adjustment of 9.5, induction times of 180, 240 and 415 min were observed at HA concentrations of 5, 10 and 15 mg/l, respectively.

In industry, pH levels may typically be raised to above 9 by the addition of lime. The addition of lime will seed the crystallisation process as well as increase the supersaturation through the addition of calcium ions. Thus, the increase in pH through the addition of lime will increase the inhibitory effect of HA, but will also increase the driving force of crystallisation, which will help in decreasing induction times and increasing nucleation rate. The addition of lime will also seed the crystallisation process which can help to override any inhibitory abilities (see section 4.6).

As surmised from literature, the increased inhibitory effect of HA at higher pH is attributed to an increased deprotonation of its functional groups. With an increase in pH, the functional groups of HA macromolecules become more negatively charged. The result is that the multivalent cations (i.e. calcium ions in the solution) interact with these negatively charged functional groups on and between HA molecules. This leads to the bridging of molecules and the formation of metal complexes/colloids in solution. The Ca^{2+} ions then act as charge neutralisers in the same manner as H^+ ions do at lower pH levels.

The phenomenon of charge neutralisation by the Ca^{2+} ions is evident from the change in pH illustrated in Figure 4.13. A greater change in pH is observed at a pH of 9.5, where the inhibitory effect of HA is the largest, compared to a pH of 7.0 or 4.5. A large degree of charge neutralisation takes place, which leads to increases in induction times. No significant change in pH was observed at a pH of 4.5. This pH level was achieved by the addition of H^+ ions which act as charge neutralisers. Thus, at a pH of 4.5, the inhibitory effect of HA is decreased, due to a decreased requirement for charge neutralisation.

Calcium ions are shielded from the sulphate ions through their interaction with HA molecules and they can therefore no longer participate in the crystallisation reaction. The result is that supersaturation is in effect “lowered”. Therefore, the nucleation rate is

Chapter 4: Experimental Results and Discussion

decreased, which results in an increased induction period. When and if the onset of crystallisation is eventually achieved, crystals will have to grow large enough to fully induce crystallisation. Crystal growth will proceed by surface integration when the surface area of the crystals becomes large enough. At this point the supersaturation will be higher at the surface of the crystals than in the bulk of the solution. The adsorption of the HA molecules onto the calcium sulphate crystals will then also take effect.

Figure 4.13 illustrates the monitoring of pH change from three initial pH levels for the duration of an experimental run. At higher pH levels, the pH tended to decrease and converge to a more neutral level. Crystallisation also tends to affect pH behaviour through the removal of positive and negative ions from solutions.

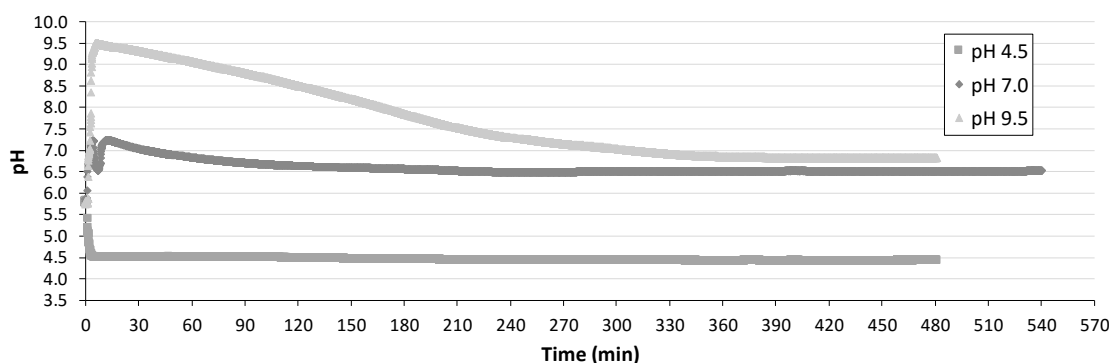


Figure 4.13: Recorded pH from initial adjusted pH of 4.5, 7.0 and 9.5 in the presence of HA.

Due to the fact that only the free calcium ions were measured, it is difficult to say whether the decrease in calcium can be purely attributed to crystallisation. The reduction in calcium concentration may result not only from crystallisation, but may also be due to adsorption onto HA molecules. The HA molecules interact with the free calcium ions in solution to form complexes that adsorb onto the crystal surfaces. Experimentally determined calcium saturation concentrations compare well with the theoretically predicted saturation concentrations. Unidentified substances in the samples interfered with the measurement of sulphate ion concentrations by ion chromatography and these measurements were therefore inconclusive. Therefore, it was not possible to verify if saturation sulphate concentrations had been achieved. The influence of HA on the growth rate of gypsum is discussed in sections 4.2.4 and 4.5.

4.2. The effect of humic acid (HA)

Changing from a more acidic and neutral to a basic medium increases the dissolution of HA. This leads to a continuous increase in the deprotonation of functional groups as HA becomes more soluble at higher pH levels [62]. This increase in HA dissolution results in an increase in its inhibitory effect as is evident from Figure 4.10 to Figure 4.12. At acidic pH levels, HA becomes less soluble and can even precipitate from solution. This could lead to the seeding of the crystallisation process, which in effect can increase crystallisation and reduce induction times.

Figure 4.14 gives a comparison of the induction times over the chosen pH range for each of the investigated HA concentrations.

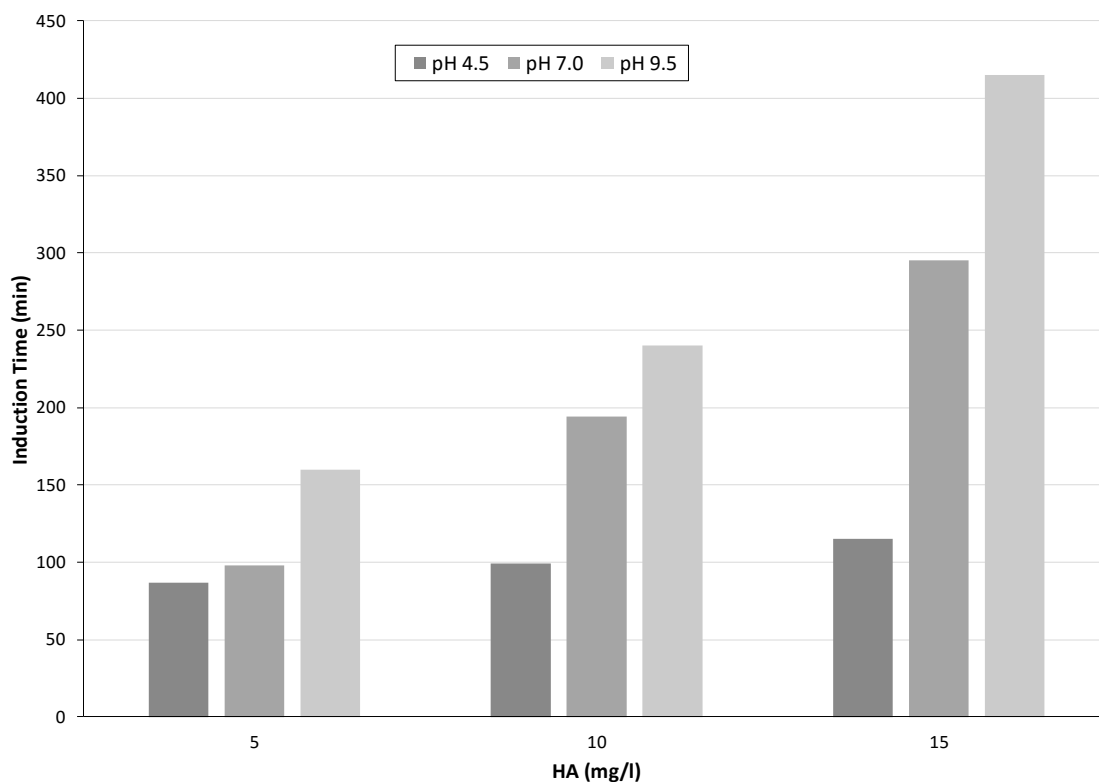


Figure 4.14: Effect of pH on induction times in the presence of HA (5, 10 & 15 mg/l) at SS3 and Temperature 25°C with no seeding.

At a pH of 4.5 and a HA concentration of 5 mg/l, an induction time of 81 minutes was observed. At the other extreme (pH 9.5 and HA concentration of 15 mg/l), induction time was increased to 415 minutes. This is an increase of about 5 times.

Chapter 4: Experimental Results and Discussion**Table 4.4: Induction times in the presence of HA (5, 10 & 15 mg/l) at SS3, pH 4.5, 7.0 & 9.5 and Temperature 25°C with no seeding.**

Experiment Name	Initial Concentration C		Supersaturation Ratio	Humic Acid Concentration (mg/l)	pH	Induction time (min)
	(ppm)	$\times 10^3$ (mol/l)				
HA-04_B					4.5	81
HA-05_A	1679.35	41.9	3	5	7.0	98
HA-06_B					9.5	180
HA-13_A					4.5	99
HA-14_B	1679.35	41.9	3	10	7.0	194
HA-15_B					9.5	240
HA-22_B					4.5	115
HA-23_B	1697.35	41.9	3	15	7.0	295
HA-24_A					9.5	415

Table 4.4 gives the induction times and experimental conditions over the investigated pH range at a supersaturation of 0.0419 mol/l calcium (SS3).

Experiment HA-15, where the pH was controlled at 9.5 and not adjusted, was repeated. Figure 4.15 presents the desupersaturation curves for the control and adjustment of pH at 9.5.

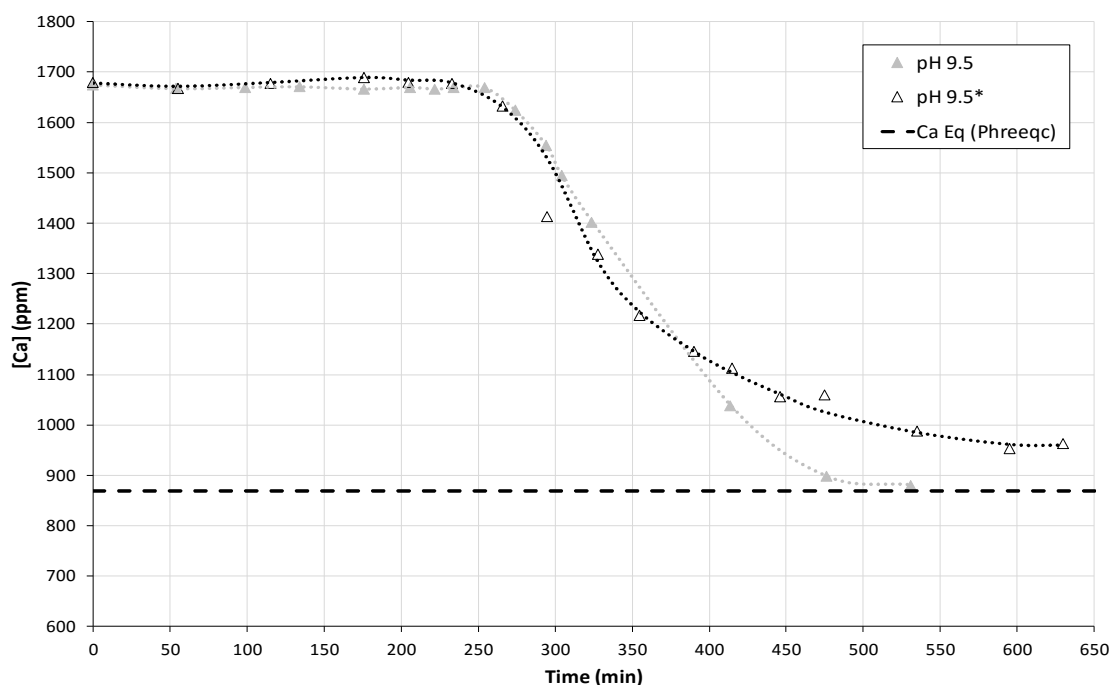


Figure 4.15: Desupersaturation curves for the effect of controlled and initial adjusted pH 9.5 at SS3, HA 10 mg/l and Temperature 25°C with no seeding.

**pH controlled at 9.5 and not adjusted.*

4.2. The effect of humic acid (HA)

Figure 4.15 illustrates that controlling the pH at 9.5 did not enhance the inhibitory ability of HA and there was no change in the induction time. The first stage of the crystallisation growth curve with pH control agrees with the first stage of the curve obtained without pH control. With pH controlled at 9.5 the crystallisation period seems to start its gradual approach to equilibrium much earlier. This suggests that HA might have more of an effect on the growth of gypsum at a constant pH level. When keeping the pH at 9.5, the deprotonation of the HA functional groups is ongoing and the HA molecules are kept in their stretched configurations. This ongoing deprotonation could also increase surface integration through adsorption of the HA molecules.

The continuous addition of Na^+ and OH^- during pH control has an effect on the solubility of gypsum as well as the crystallisation process itself. Shukla et al. [67] studied the effect of pH with an increase in ionic strength and found that there was no significant change in gypsum solubility at higher pH levels. The effect of sodium hydroxide on the solubility of gypsum was investigated by Hanaa et al. [68], who reported that gypsum solubility is promoted by a low sodium hydroxide concentration. Further in-depth investigation into this phenomenon is necessary.

Figure 4.16 to Figure 4.18 present the desupersaturation curves obtained at the investigated pH levels (4.5, 7.0 and 9.5) for each of the HA concentrations at an initial supersaturation of 0.056 mol/l (SS4). The same trend is observed in all of these figures: increase in pH resulted in an increase in the induction period. The increase in induction period is significantly small compared to SS2 and SS3, where changes in induction periods of up to 80 times larger were observed. These results once again highlight the strong driving force of supersaturation.

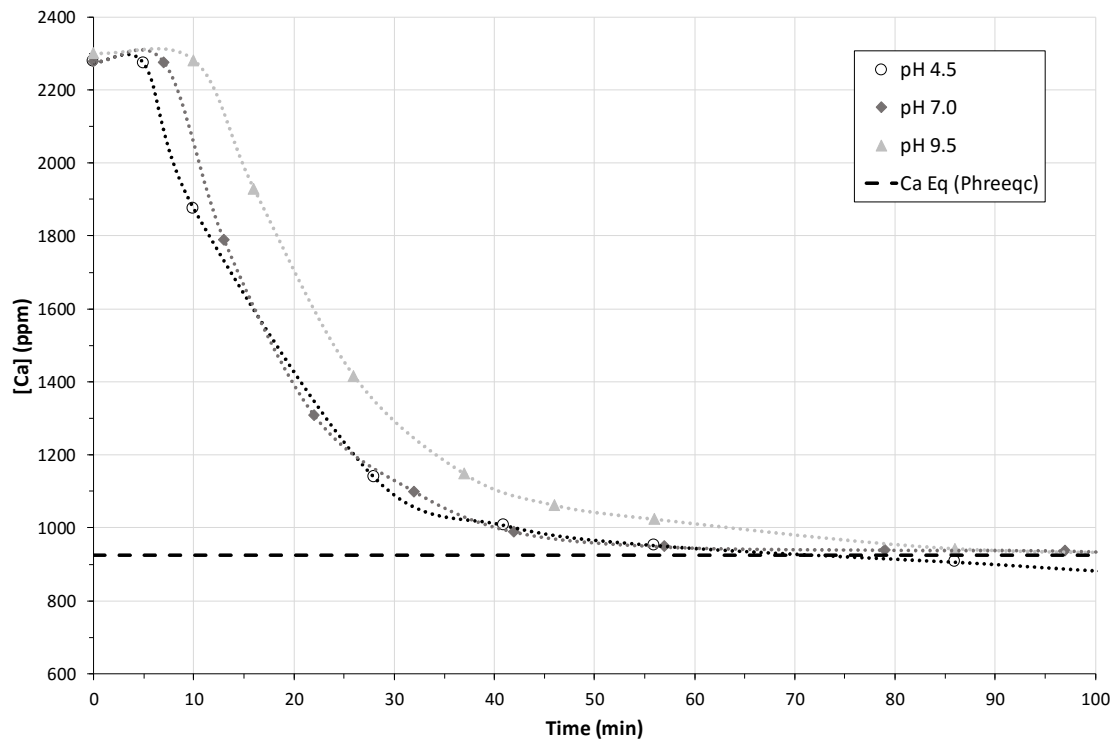
Chapter 4: Experimental Results and Discussion

Figure 4.16: Desupersaturation curves in the presence of HA (5 mg/l) at SS4, initial adjusted pH 4.5, 7.0 & 9.5 and Temperature 25 °C with no seeding.

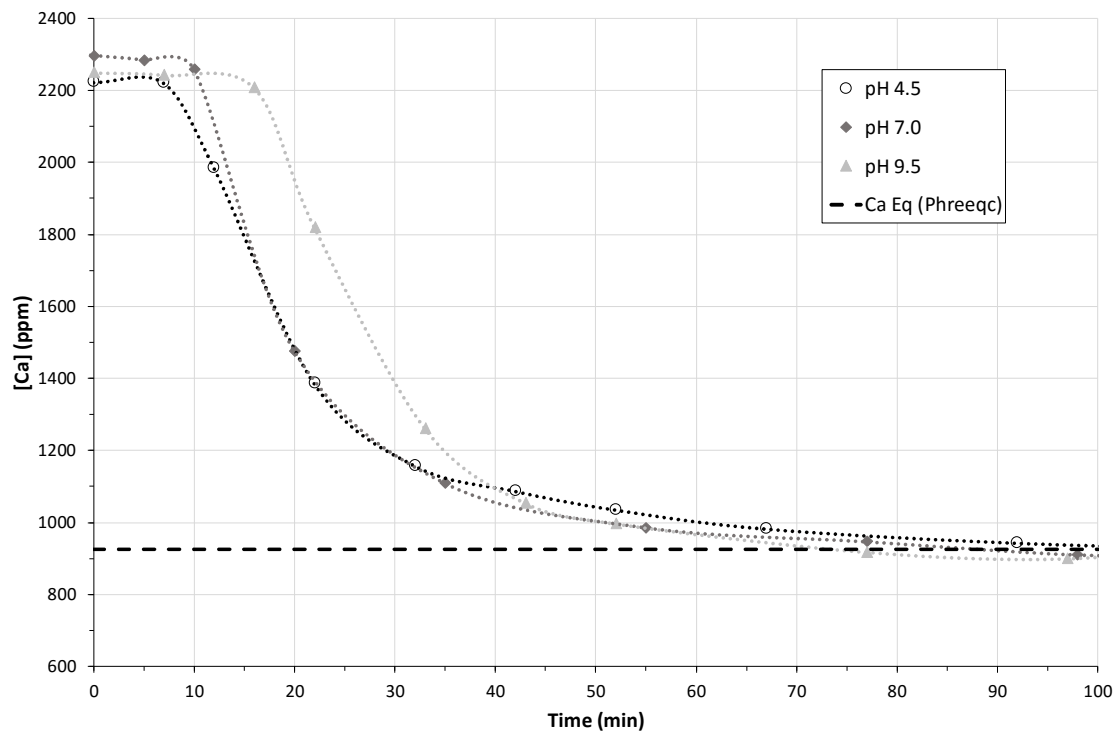


Figure 4.17: Desupersaturation curves in the presence of HA (10 mg/l) at SS4, initial adjusted pH 4.5, 7.0 & 9.5 and Temperature 25 °C with no seeding.

4.2. The effect of humic acid (HA)

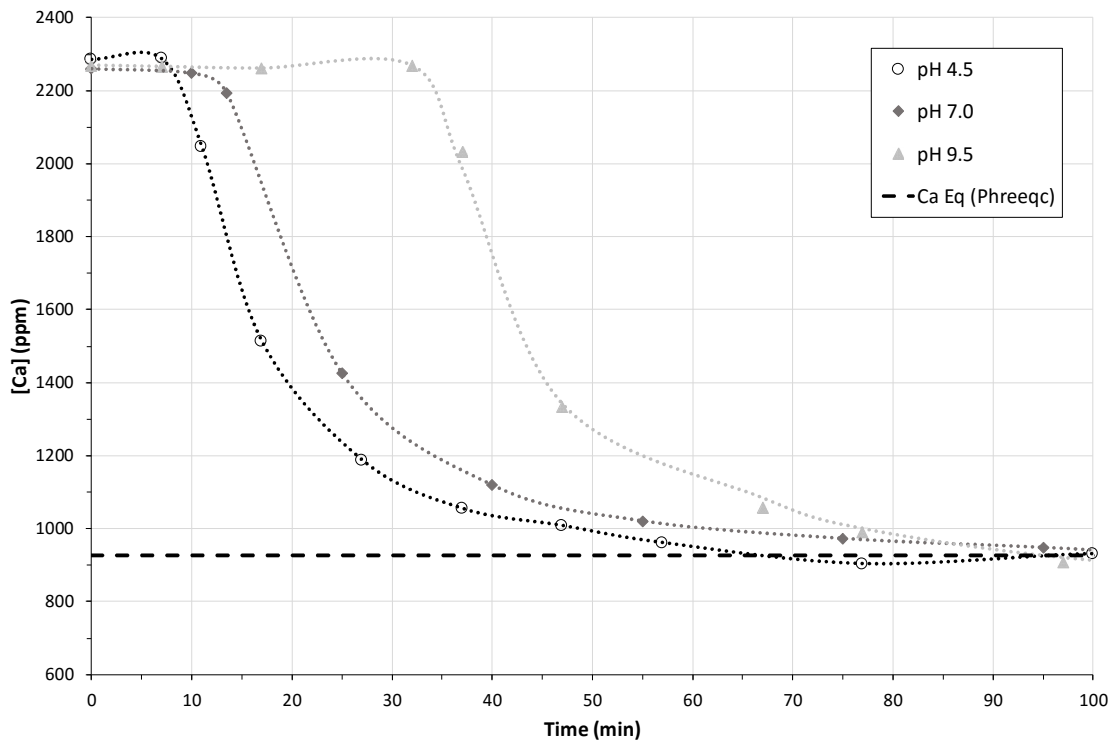


Figure 4.18: Desupersaturation curves in the presence of HA (15 mg/l) at SS4, initial adjusted pH 4.5, 7.0 & 9.5 and Temperature 25°C with no seeding.

Table 4.5 presents the induction times observed and the experimental conditions that were used over the investigated pH range at a supersaturation of 0.056 mol/l calcium (SS4).

Table 4.5: Induction times at SS4 with no seeding.

Experiment Name	Initial Concentration C		Supersaturation Ratio	Humic Acid Concentration (mg/l)	pH	Induction time (min)
	ppm	$\times 10^3$ (mol/l)				
HA-07_B					4.5	5
HA-08_A	2268.53	56.6	4	5	7.0	8
HA-09_A					9.5	10
HA-16_A					4.5	7
HA-17_A	2268.53	56.6	4	10	7.0	11
HA-18_A					9.5	16
HA-25_B					4.5	7
HA-26_A	2268.53	56.6	4	15	7.0	15
HA-27_C					9.5	30

At a HA concentration of 5 mg/l, a maximum induction period of 10 min was observed (Figure 4.16). This is in the same range as the baseline results, where a maximum induction period of around 7 min was observed. The change in induction time is from 5 to 10 minutes with a pH change from 4.5 to 9.5. This is a rather small change in induction

Chapter 4: Experimental Results and Discussion

period and can even be attributed to experimental errors as explained in Chapter 3, since manipulation of system conditions at SS4 can be difficult.

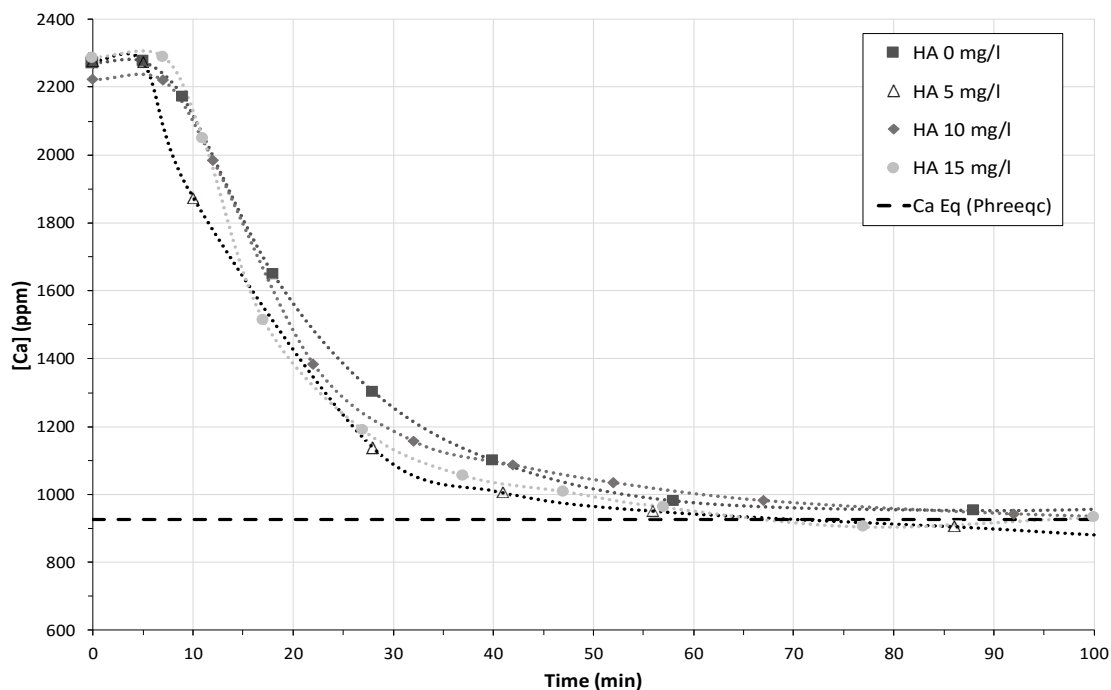


Figure 4.19: Desupersaturation curves in the presence of HA (0, 5, 10 & 15 mg/l) at SS4, initial adjusted pH 4.5 and Temperature 25°C with no seeding.

There is no significant change in induction period with an increase in HA at a pH of 4.5 and at SS4 (Figure 4.19). Compared to the baseline results, no significant change is evident either. If there is any change, it would be difficult to accurately measure it at this condition of high supersaturation. The effect of HA may be restricted at this low pH level and high supersaturation. At more acidic pH levels, the solubility of HA decreases. The increase in H^+ through adjustment of pH, results in an increased degree of protonation of the HA functional groups. Therefore, at SS4 the driving force for crystallisation is solely the degree of supersaturation and the nucleation rate will be dependent on supersaturation. The inhibitory effect of HA is eliminated at this pH and supersaturation level.

At a HA concentration of 15 mg/l the effect of pH on the induction period becomes more apparent (Figure 4.18). A maximum induction period of 30 minutes was observed. This is still approximately 14 times smaller than observed at the same conditions at an initial calcium concentration of 0.0419 mol/l (SS3). Figure 4.20 presents a comparison of the two

4.2. The effect of humic acid (HA)

supersaturation conditions (SS3 and SS4) for all the investigated HA concentrations and pH levels.

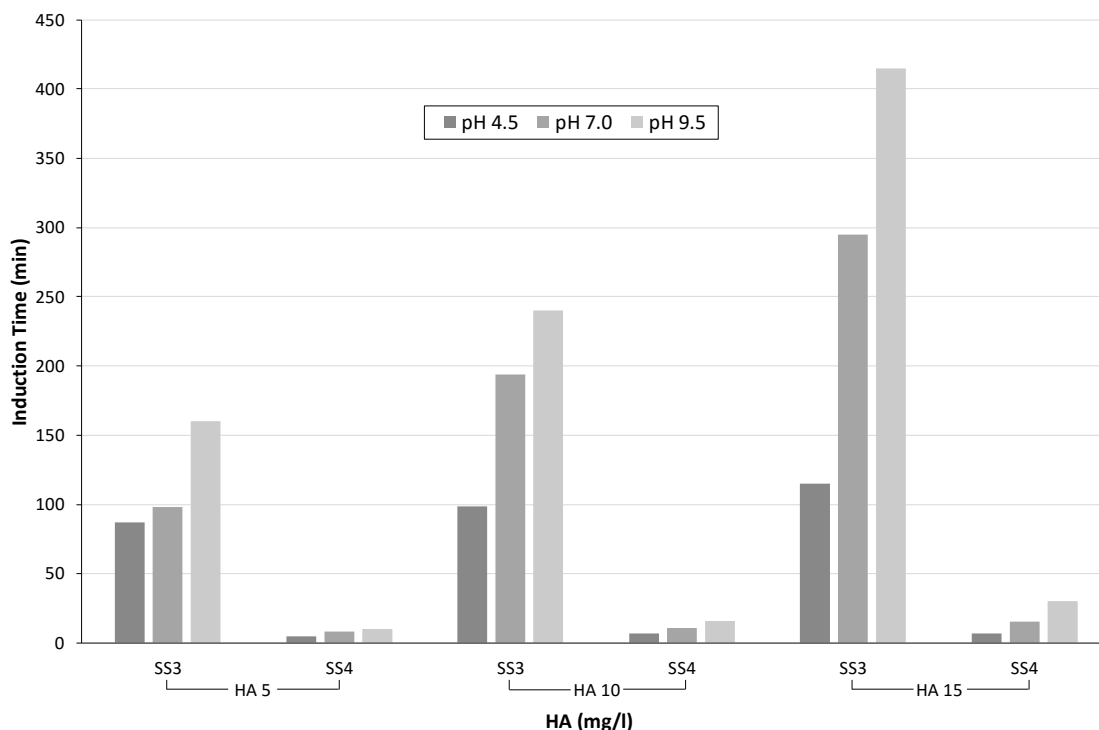


Figure 4.20: Effect of pH on induction times at SS3 & SS4, HA at 5, 10 and 15 mg/l and Temperature 25 °C with no seeding.

The general trend that was observed was that an increase in supersaturation resulted in an overall decrease in induction times through an increase in the driving force, active growth sites and a decrease in activation energy. With an increase in HA and pH, induction times were increased. It can be clearly seen that induction times were much smaller at a higher supersaturation level compared to those at a lower supersaturation level.

4.2.4. Crystallisation times

Crystallisation times were observed in the same manner as for the baseline results previously reported. Induction times were removed, time was normalised relative to the point where crystallisation started and the concentration measured over the induction period was averaged. Figure 4.21 gives an example of the growth curves for experiments BL-SS3_B, HA-05_A, HA-14_B and HA-23_B at an initial adjusted pH of 7.0. For all relevant experimental data and growth curves, see Appendix B.

Chapter 4: Experimental Results and Discussion

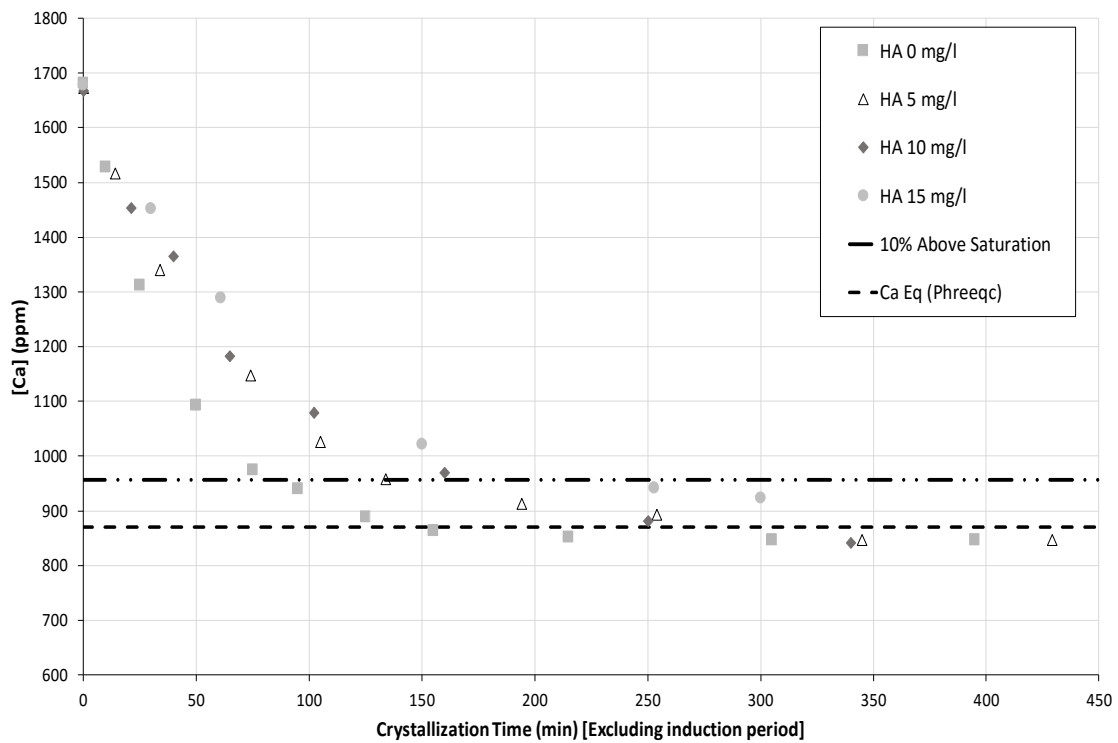


Figure 4.21: Desupersaturation curve for the effect of HA (0-15 mg/l) without induction periods at SS 3 and pH 7.00 with no seeding.

An overall shift is seen in the growth curve in the presence of HA compared to the baseline curve in the absence of HA. With the increase in HA no significant change in the curve trend is observed. Slight shifts in crystallisation times can be extrapolated. The absolute significance of this becomes more apparent on evaluation of the crystal growth kinetics (see section 4.5).

Figure 4.22 presents the average crystallisation times t_s and t_{10} , for both SS3 and SS4, with an increase in pH level. Figure 4.23 presents the average crystallisation times t_s and t_{10} , for both SS3 and SS4, with an increase in HA concentration.

4.2. The effect of humic acid (HA)

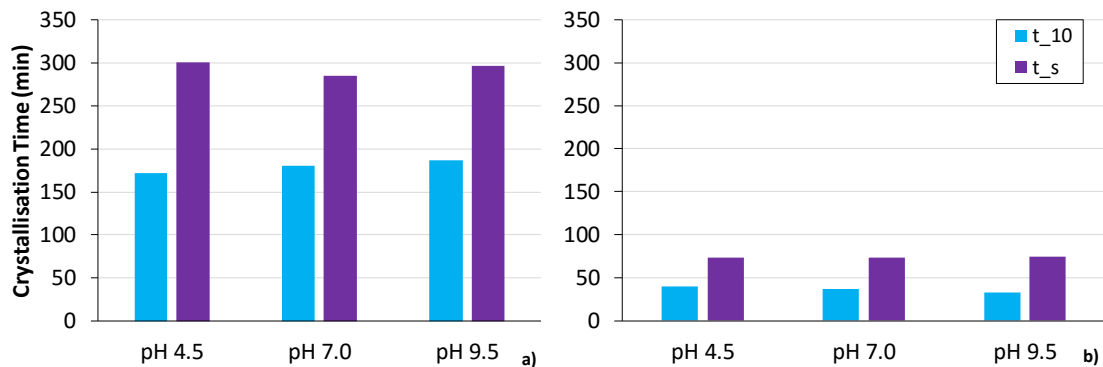


Figure 4.22: Crystallisation times (t_{10} & t_s) for a) SS3 and b) SS4 at pH 4.5 to 9.5 with no seeding.

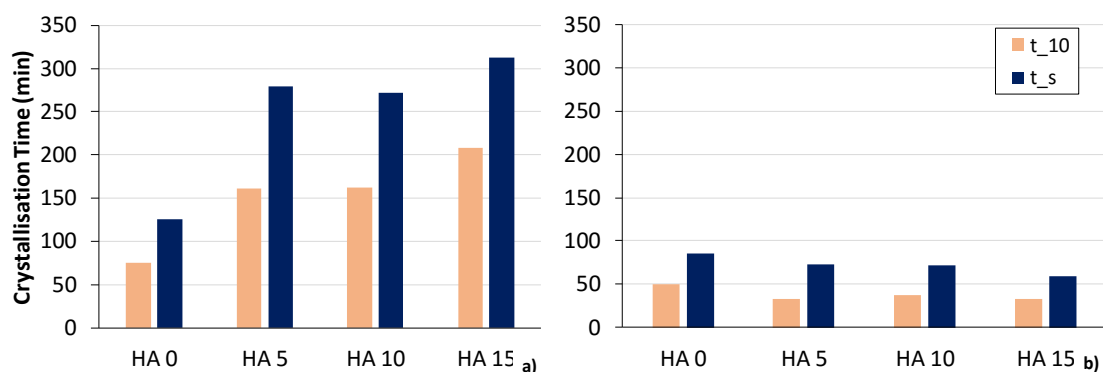


Figure 4.23: Crystallisation times (t_{10} & t_s) for a) SS3 and b) SS4 in the presence of HA (0, 5, 10 & 15 mg/l) with no seeding.

Crystal growth for both supersaturation levels seems to be independent of pH. An increase in pH yielded no significant increase in crystal growth times. For SS3 and SS4 the respective total crystallisation times are 295 and 80 minutes. This suggests that the pH level enhanced the inhibitory ability of HA only up to the point where the onset of crystallisation was achieved. This suggests that after complete crystallisation takes effect, the formation of new nuclei is minimised and crystal growth proceeds through secondary crystallisation at a slightly slower rate compared to the rate at baseline conditions.

In the presence of HA there is a definite increase in crystallisation times. An increase in HA concentration from 0 to 15 mg/l resulted in an increase in total crystallisation time from 125 to 313 minutes at SS3. This increase from baseline conditions would suggest that some form of surface interaction with HA molecules is taking place. An increase in HA concentration from 5 to 10 mg/l did not result in a significant change in crystallisation times

Chapter 4: Experimental Results and Discussion

(t_s stayed relatively constant at ~ 275 min). With a further increase to 15 mg/l HA, an increase of approximately 40-50 minutes in t_s was observed. The effect of HA on crystal growth seems to be more evident at higher HA concentrations and at a higher pH level (15 mg/l and 9.5 respectively).

With an increase in HA concentration at SS3, there is likely to be interference in crystal growth by the adsorption of HA onto the active growth sites of the crystals. In these conditions there are enough HA particles to slow down growth and to keep some free ions in solution occupied. In this manner the growth is slowed down by both active shielding of growth sites and adsorption on HA molecules. This effect on crystal growth would most likely have been even more evident if the concentration of HA was increased even further.

At SS4 there was no significant change in crystallisation times with an increase in HA concentration. A small difference between baseline crystallisation times and crystallisation times in the presence of HA was observed, but this falls within the experimental error. A definite decrease in crystallisation times (from ~ 300 to ~ 70 min) was observed from SS3 to SS4, again illustrating the driving force of increased supersaturation.

Due to the high level of supersaturation, an increase in nucleation rate leads to rapid crystal growth. The increased formation of crystals leads to an increase in surface areas and active growth sites. With an increase in HA and a higher pH level, crystallisation can be increased by the binding of HA to the divalent cations in solution and the adsorption of this complex onto the active growth sites. The question then arises if pure gypsum crystal growth does indeed take place.

It can be suggested that desupersaturation could take place through complex formation with HA molecules and then the adsorption of these complexes onto the already formed crystals in solution. Therefore, more study of crystal formation and how it is affected by the presence of HA is needed.

Table 4.6 presents the results for t_{10} and t_s at SS3 and SS4 in the presence of HA with no seeding.

4.3. Effect of fulvic acid (FA)**Table 4.6: Crystallisation times (t_{10} & t_s) for SS3 and SS4 with no seeding.**

Experiment Name	Supersaturation Ratio	Crystallisation Times (min)	
		t_{10}	t_s
SS3		75	125
HA-04		145	245
HA-05		157	264
HA-06		175	300
HA-13	3	179	314
HA-14		163	276
HA-15		176	238
HA-22		185	310
HA-23		226	311
HA-24		211	316
Bl-SS4			50
HA-07		40	70
HA-08		40	85
HA-09		38	61
HA-16	4	36	73
HA-17		37	69
HA-18		37	76
HA-25		23	76
HA-26		34	61
HA-27		22	39

4.3. Effect of fulvic acid (FA)

Attention now shifts to crystallisation in the presence of fulvic acid (FA). The effect of FA was investigated under the same conditions as those that were used for HA. The effect of supersaturation on crystallisation inhibition was not repeated for FA due to the difficulty of manipulating conditions at higher supersaturation, the expensive nature of this chemical and the fact that the results obtained in the presence of HA gave more than adequate information on the effect of supersaturation. All FA experimental runs were carried out at a supersaturation concentration of 0.0419 mol/l (SS3). The effect of FA was evaluated in the same manner as for HA. The results that were obtained on the effect of FA are reported in this section and thoroughly discussed in the next section (section 4.4), where the FA effect is compared to that of HA. All relevant experimental data is provided in Appendix B.

Chapter 4: Experimental Results and Discussion

4.3.1. Induction times

Figure 4.24 illustrates the effect of FA concentrations of 5 and 15 mg/l on crystallisation at initial adjusted pH of 7.0.

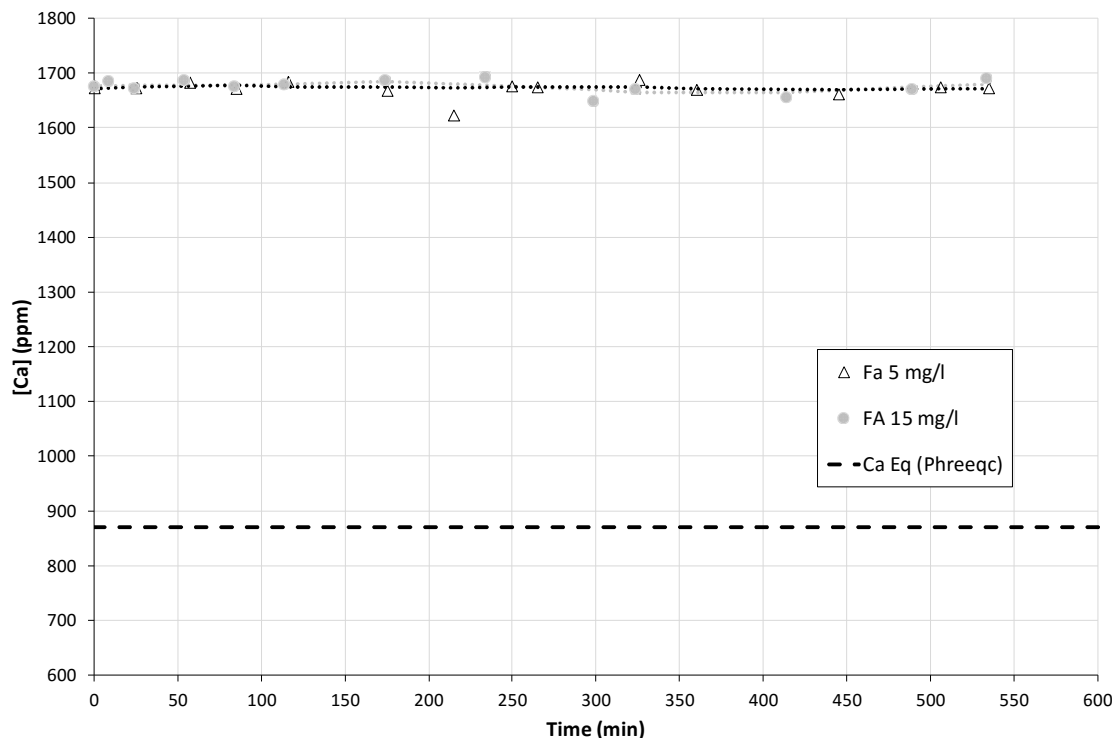


Figure 4.24: The effect of FA (5 & 15 mg/l) at SS3, initial adjusted pH 7.0 and Temperature 25°C with no seeding.

The effect of FA was greatly underestimated and at the above concentrations of FA (5 and 15 mg/l) no crystallisation took place for a period of at least 9 hours. Both experimental runs were left to run further for a total of 2 days. After 2 days, still no crystallisation was achieved in the presence of 15 mg/l FA. At a FA concentration of 5 mg/l, some crystal formation was observed after 36 hours but no definite crystallisation took place. The temperature stability of the system was questionable and the crystal formation could have been the result of an increase in temperature. The effect of temperature falls outside the scope of this study and is a condition that could require further study.

Crystallisation is inhibited to a large degree in the presence of FA. It is evident from Figure 4.24 that FA can completely inhibit gypsum crystallisation at a high concentration of 15 mg/l and even at a low concentration of 5 mg/l. As a result of the large inhibitory effect

4.3. Effect of fulvic acid (FA)

of FA, lower concentrations of FA (1.0 and 2.5 mg/l) were also investigated in the absence of seed crystals.

Figure 4.25 illustrates the inhibitory effect of FA at 1.0, 2.5 and 5.0 mg/l at an initial adjusted pH of 7.0.

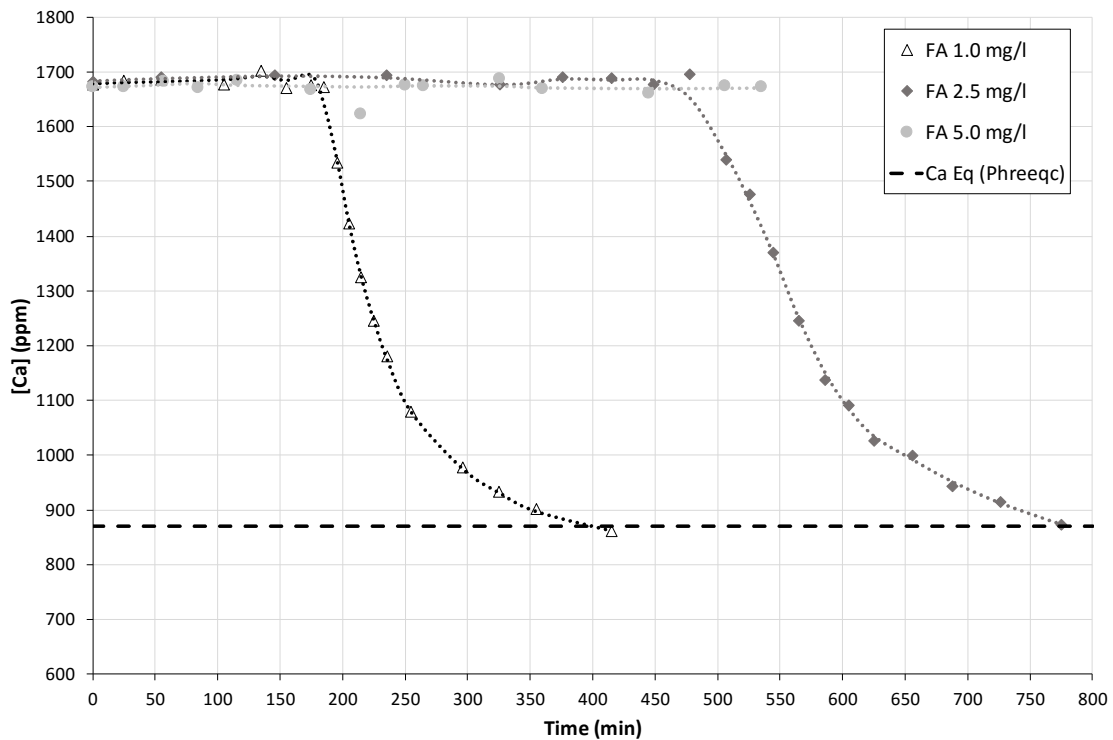


Figure 4.25: Desupersaturation curves in the presence of FA (1.0, 2.5 & 5.0 mg/l) at SS3, initial adjusted pH 7.0 and Temperature 25°C with no seeding.

Table 4.7 presents the induction times obtained for each of the experimental runs along with the FA concentrations and the initial calcium concentrations.

Table 4.7: Induction times and initial concentrations in the presence of FA without seeding.

Experiment Name	Initial Concentration C		Supersaturation Ratio	Fulvic Acid Concentration (mg/l)	Induction time (min)
	(ppm)	$\times 10^3$ (mol/l)			
FA-06_A	1679.35	41.9	3	1.0	185
FA-05_B	1679.35	41.9	3	2.5	480
FA-02_A	1679.35	41.9	3	5.0	>24 hours
FA-01_A	1679.35	41.9	3	15.0	>48 hours

Chapter 4: Experimental Results and Discussion

It is clear from Figure 4.25 that the effect of FA is large even at much lower concentrations of FA. At a concentration of 5 mg/l FA, no crystallisation was achieved. On decreasing the concentration of FA to 2.5 mg/l, an induction period of 480 minutes was observed. Lowering the concentration even further to 1.0 mg/l FA, an induction time of 185 minutes was observed. This is a decrease by a factor of 2.6, which is about the same order of magnitude by which the FA concentration was decreased (2.5 times). Although there still remained a significant degree of FA inhibition even at the lowest investigated FA concentration (1.0 mg/l), these results give valuable insight into FA and its ability as a polyelectrolyte to inhibit crystallisation.

The results indicate that FA can act as an excellent natural inhibitor. The polyelectrolyte ability of FA is clearly evident from the results obtained in the concentration range from 1 to 15 mg/l. This is in good agreement with the understanding in scientific literature that FA possesses increased inhibitory power on gypsum crystallisation due to an increased content of functional groups (-COOH and -OH) in FA molecules [30, 69].

Figure 4.26 illustrates the inhibitory effect on crystallisation of FA at 1.0, 2.5 and 5.0 mg/l at an initial adjusted pH of 4.5. The effect of pH is presented in the following section.

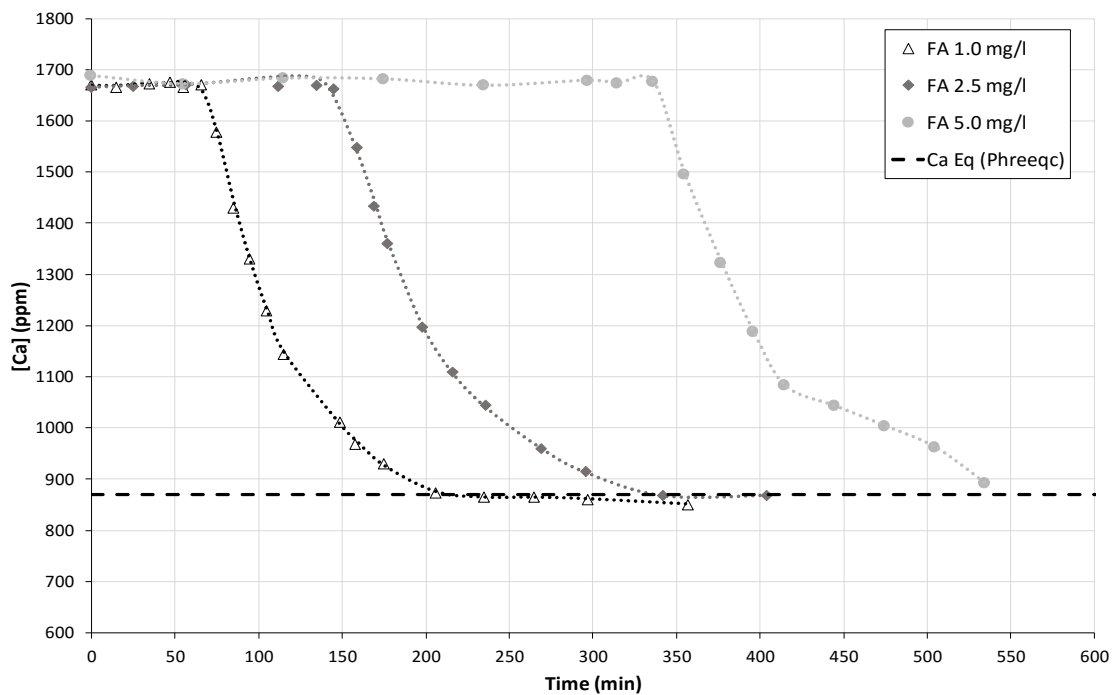


Figure 4.26: Desupersaturation curves in the presences of FA (1.0, 2.5 and 5.0 mg/l) at SS3, initial adjusted pH 4.5 and Temperature 25°C with no seeding.

4.3. Effect of fulvic acid (FA)

4.3.2. Effect of pH

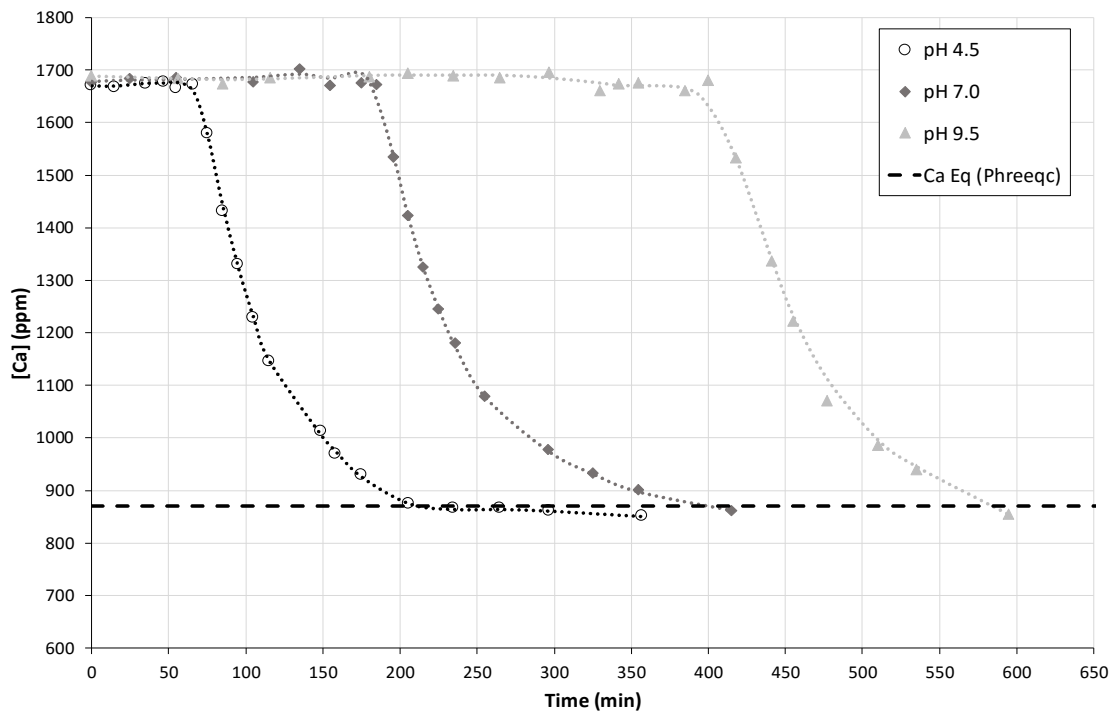


Figure 4.27: Desupersaturation curves in the presence of FA 1.0 mg/l at SS3, initial adjusted pH 4.5 to 9.5 and Temperature 25°C with no seeding.

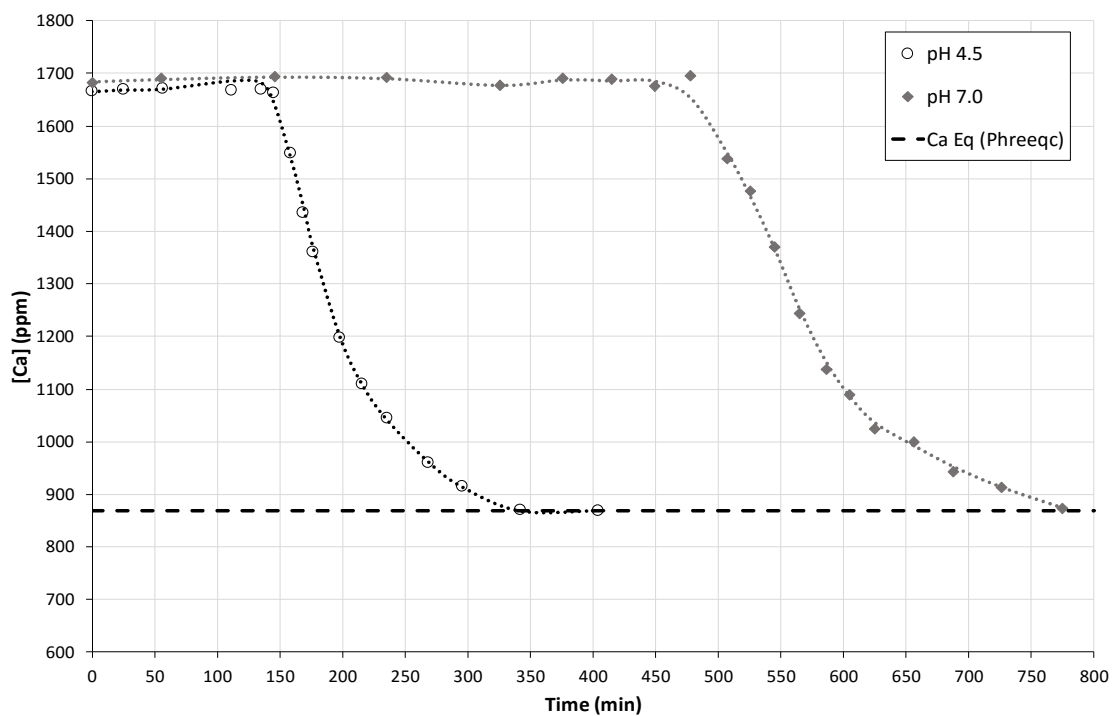


Figure 4.28: Desupersaturation curves in the presence of FA 2.5 mg/l at SS3, initial adjusted pH 4.5 & 7.0 and Temperature 25°C with no seeding.

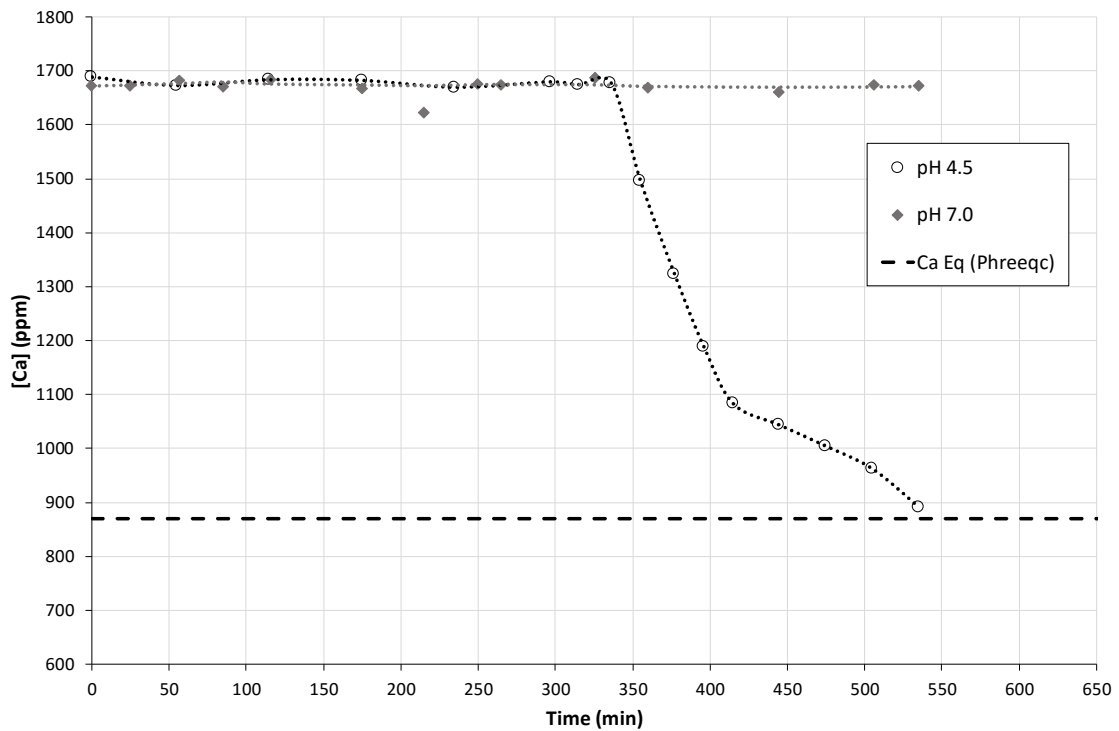
Chapter 4: Experimental Results and Discussion

Figure 4.29: Desupersaturation curves in the presence of FA 5.0 mg/l at SS3, initial adjusted pH 4.5 & 7.0 and Temperature 25 °C with no seeding.

Figure 4.27 to Figure 4.29 illustrate the inhibitory effect on crystallisation resulting from each individual FA concentration (1.0, 2.5 and 5 mg/l) over the investigated pH range. Table 4.8 gives the induction times and experimental conditions over the investigated pH range at the SS3 calcium concentration in the presence of FA.

Table 4.8: Induction times in the presence of FA at SS3 with no seeding.

Experiment Name	Initial Concentration C		Supersaturation Ratio	Fulvic Acid Concentration (mg/l)	pH	Induction time (min)
	(ppm)	$\times 10^3$ (mol/l)				
FA-07_A					4.5	66
FA-06_A	1679.35	41.9	3	1.0	7.0	185
FA-08_A					9.5	400
FA-04_A	1679.35	41.9	3	2.5	4.5	145
FA-05_B	1679.35	41.9	3	2.5	7.0	480
FA-03_A	1679.35	41.9	3	5.0	4.5	335
FA-02_A	1679.35	41.9	3	5.0	7.0	>24 hours

4.3. Effect of fulvic acid (FA)

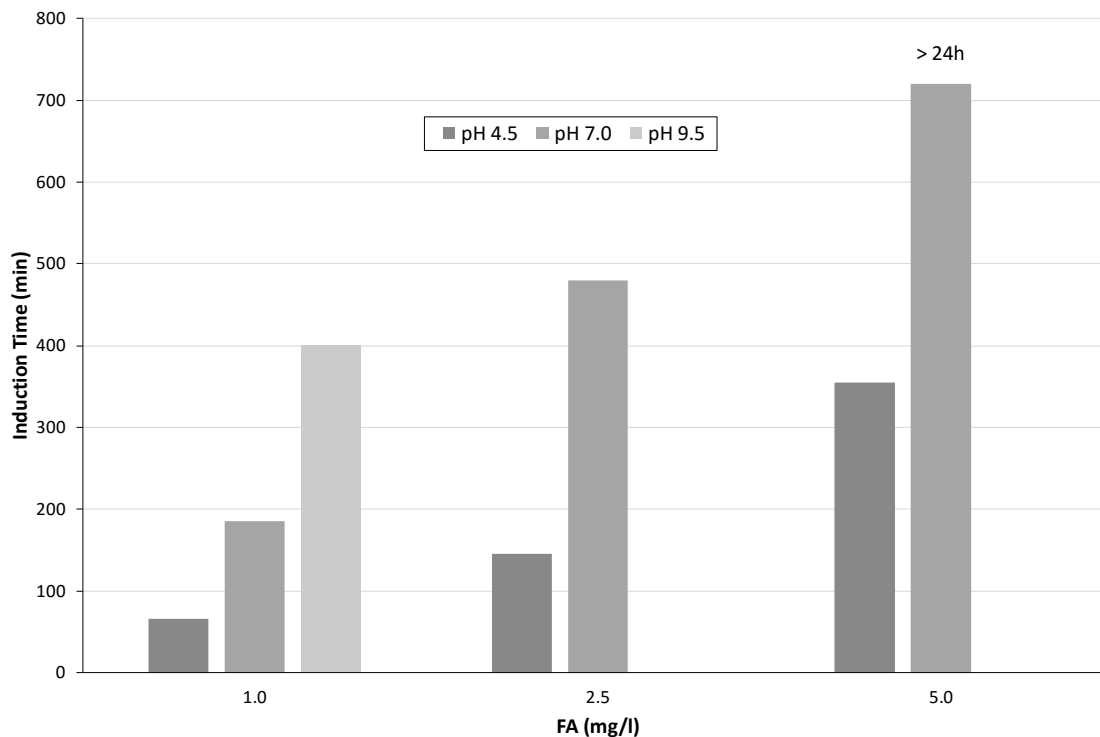


Figure 4.30: Induction times in the presence of FA (1.0, 2.5 & 5.0 mg/l) at SS3, initial adjusted pH 4.5, 7.0 & 9.5 and Temperature 25 °C with no seeding.

The increases in induction times are illustrated in Figure 4.30. With an increase in pH, a significant increase in induction times was observed. At a concentration of 1.0 mg/l FA, the induction period is increased 6 times by an initial pH adjustment from 4.5 to 9.5. The inhibitory ability of FA was enhanced by the increase in pH. The fact that FA has an increased equivalent of functional groups is again illustrated here. An increase in functional groups will lead to an increase in deprotonation with the increase in pH. FA is also soluble over the whole pH range investigated and this on its own will enhance the inhibitory ability of FA as well.

From Figure 4.30 it is evident that an increase in pH in the presence of FA resulted in an increase in induction period. Figure 4.31 illustrates how the recorded pH changed over time from the three initial adjusted pH levels, in the presence of FA. The same trends, that had previously been observed in the presence of HA, were observed here as well. However, at an initial adjusted pH of 9.5, the decrease in pH was much slower than was the case in the presence of HA. Although the pH stayed constant in the case of the initial pH of 4.5, it needs to be taken into account that there still was a significant FA inhibitory effect on crystallisation and the inhibitory ability of FA was only decreased and not suppressed. This may be due to

Chapter 4: Experimental Results and Discussion

the complete solubility of FA and the ability of FA to bind with calcium ions and adsorb actively onto the crystal surfaces.

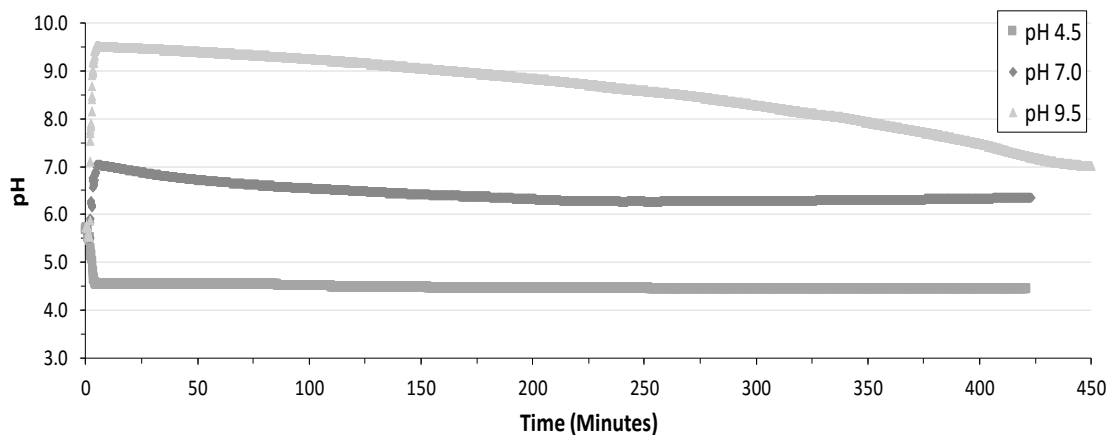


Figure 4.31: Recorded pH from initial adjusted pH of 4.5, 7.0 and 9.5 in the presence of FA.

4.4. Fulvic acid (FA) vs. humic acid (HA)

From the results reported in the previous section it is clear that the inhibitory effect of FA is far greater than that of HA. Even at lower concentrations of FA the effect was still greater. Figure 4.32 presents the comparison between FA (5 and 15 mg/l) and HA (5 and 15 mg/l) at the same conditions of initial adjusted pH of 7.0 and initial calcium concentration of 0.0419 mol/l (SS3).

No crystallisation was observed in the presence of FA at these conditions in comparison to the experimental runs done in the presence of HA, where crystallisation did take place. The result would indeed suggest that FA has an increased content of carboxylic and phenolic functional groups, which give HS their polyelectrolyte and inhibitory abilities.

4.4. Fulvic acid (FA) vs. humic acid (HA)

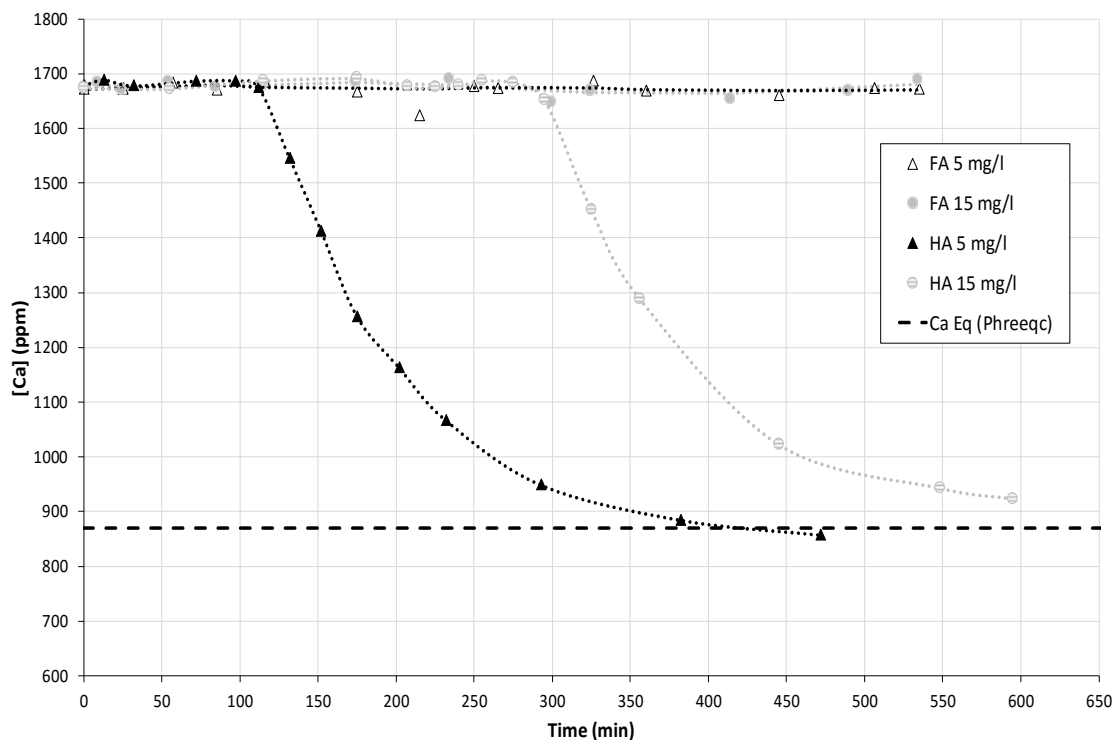


Figure 4.32: Desupersaturation curves in the presence of HS (FA and HA) at concentrations of 5 & 15 mg/l at SS3, initial adjusted pH 7.0 and Temperature 25° C with no seeding.

Table 4.9 presents some literature data on the total acidity and functional groups that are present in these HS. Although the HA and FA, mentioned in the table, are different from those that were used in this study, the information provides insight into the nature of HS. The table shows that FA has an overall higher total acidity and carboxylic content compared to HA. Although reports vary on the composition of HS, the overall observation is that FA has an overall increased content of functional groups, especially carboxylic groups.

Table 4.9: Total acidity and functional group content of HS (all values in meq/g).

	Total Acidity	Carboxylic	Phenolic (OH)	Alcoholic OH	C=O	OCH ₃	Source
HA	6.7	3.6	3.9	2.6	2.9	0.6	[69]
FA	10.3	8.2	3.0	6.1	2.7	0.8	[69]
HA	6.0	-	-	-	-	-	[53]
FA	-	11.17	2.84	-	-	-	[70]

Figure 4.33 compares the induction times in the presence of FA with those that were observed in the presence of HA. The increase in the induction period in the presence of FA is greater than that observed in the presence of HA. With FA, crystallisation was inhibited completely for more than 2 days, whereas with HA, crystallisation was achieved within

Chapter 4: Experimental Results and Discussion

8 hours. FA is completely soluble in water at these conditions at all pH levels, whereas HA is only partially soluble, with the solubility and diffusion increasing as the pH increases. This further emphasises the enhanced ability of FA to inhibit crystallisation and the higher functional group content of FA.

The molecular weight of FA is lower than that of HA (section 2.4.1). The work of de Melo [53] showed that a decrease in the molecular weight of HS resulted in an increase in their relative functional group content. The results reported here is in good agreement with the observation that FA has an increased functional group content.

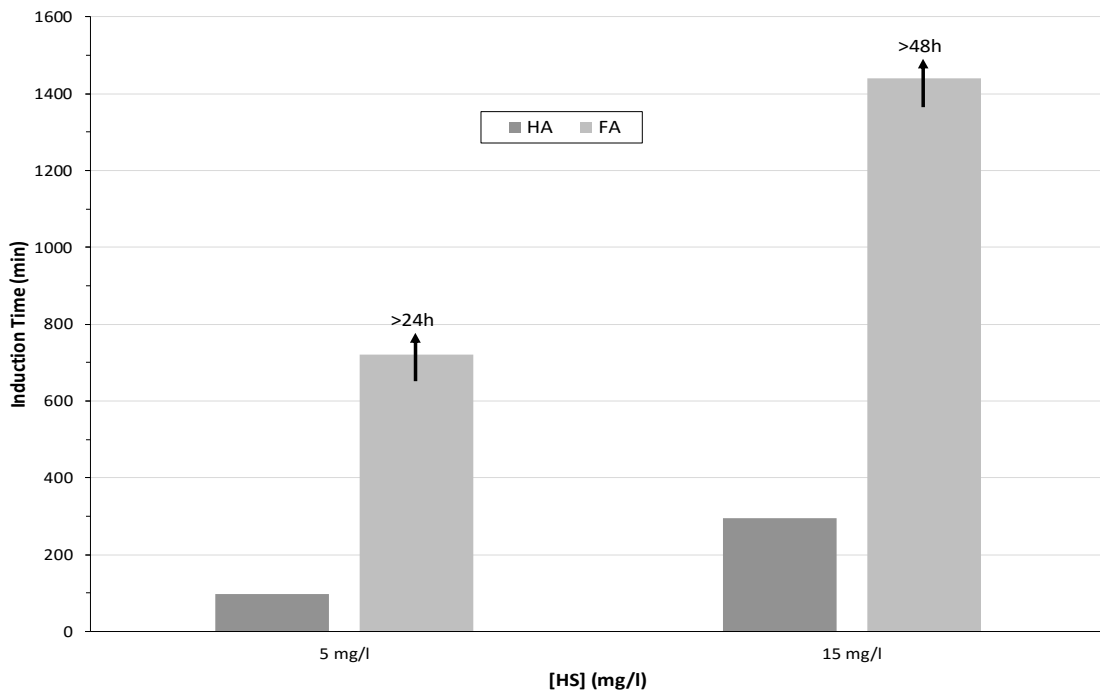


Figure 4.33: Induction times in the presence of HS (5 & 15 mg/l) at SS3, initial adjusted pH of 7.0 and Temperature 25°C with no seeding.

In order to further compare FA with HA, the FA concentration was lowered to 1.0, 2.5 and 5.0 mg/l. Figure 4.34 presents the comparison of HA (5, 10 and 15 mg/l) with lower FA concentrations (1.0, 2.5 and 5.0 mg/l) at an initial adjusted pH of 7.0. Figure 4.35 presents a comparison of the induction times found in the presence of these two HS.

4.4. Fulvic acid (FA) vs. humic acid (HA)

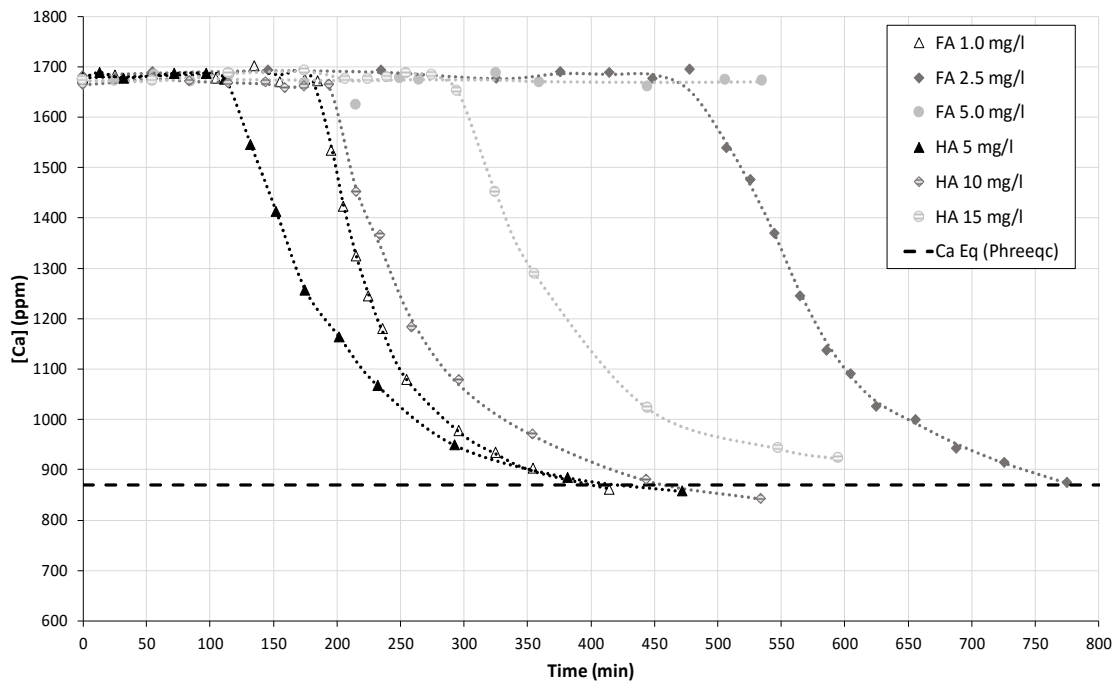


Figure 4.34: Desupersaturation curves in the presence of HA (5, 10 and 15 mg/l) and FA (1, 2.5 and 5 mg/l) at SS3, initial adjusted pH of 7.0 and Temperature 25°C with no seeding.

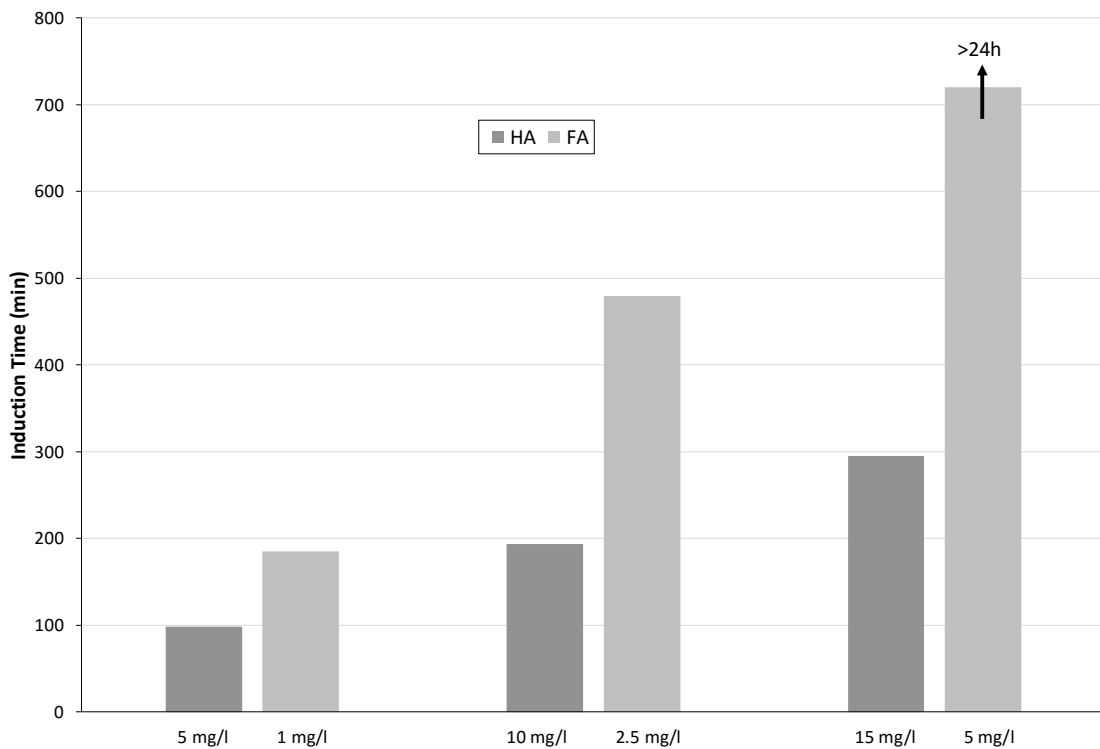


Figure 4.35: Induction times in the presence of HA (5, 10 and 15 mg/l) and FA (1.0, 2.5 and 5.0 mg/l) at SS3, initial adjusted pH of 7.0 and Temperature 25°C.

Chapter 4: Experimental Results and Discussion

Figure 4.35 compares the inhibitory effect of 1 mg/l FA with that of 5 mg/l HA, the inhibitory effect of 2.5 mg/l FA with that of 5 mg/l HA and the inhibitory effect of 5 mg/l FA with that of 15 mg/l HA. At the lowest concentrations of FA, the effect is still far greater than that of HA. At 1 mg/l FA and 5 mg/l HA, induction times of 185 and 98 minutes were observed, respectively. This is a difference of 61% with a concentration difference of 133%. At 2.5 mg/l FA and 10 mg/l HA, the induction periods were 480 and 195 minutes, respectively. This is a difference in induction period of 84% with a 120% difference in HS concentration. In the presence of 5 mg/l FA, crystallisation was not achieved compared to an induction period of 295 minutes in the presence of 15 mg/l HA.

The work of Oner et al. [65] showed that with a decrease in polyelectrolyte molecular weight, there is an increase in induction period. FAs have an increased ability to adsorb onto active growth sites, due to their smaller molecular weight compared to those of HAs. The larger molecular weight of HAs can result in these substances having more steric hindrance than FAs, resulting in a decreased adsorption ability which decreases their effect on the crystallisation of gypsum.

4.5. Crystal growth kinetics in the absence of seeding

Now that the full effect of HA and FA has been reported and discussed in the previous sections, focus shifts to the kinetics of crystal growth in the absence of seed crystals. The 2nd order rate equation (equation 2.12) is examined to determine if crystallisation under these conditions, in the absence of seeding, can be explained to some degree. It is understood that the proposed rate predicts seeded growth well. In the case of spontaneous crystallisation reactions, there is still much uncertainty around the proposed rate and if first order growth is followed or second order growth is more predominant, especially in the presence of additives such as HS.

Note that in this section the overall rate constant, k' , is evaluated for the purpose of determining if crystal growth is influenced by the presence of HS. Comparing k' values to literature was difficult due to the dependence on saturation levels and initial concentrations, and due to the fact that finding reliable data for spontaneous crystallisation was unsuccessful.

4.5. Crystal growth kinetics in the absence of seeding

A second order rate equation from literature [12, 17] on gypsum crystallisation was applied to the experimental data (equation 4.1) and k' was calculated. For the purpose of this study, $k' = k_g s_g$, where s_g is the number of active growth sites. From first principles the rate coefficient k_g is independent of concentration. The number of active growth sites (s_g) is a variable of concentrations. Thus, k' is dependent on active growth sites which is dependent on concentration. In the batch experiments carried out, there were no active growth sites at the start and while primary nucleation was taking place. The presence of HS also influences the number of active growth sites in both unseeded and seeded experiments. The number of growth sites is a variable in crystallisation and not easy to determine. Equation 2.12 is simplified to give:

$$-\frac{d[Ca^{2+}]}{dt} = k'([Ca^{2+}] - [Ca^{2+}]_{eq})^2 \quad (4.1)$$

where k' is the overall growth rate constant in $\text{litre} \cdot \text{mol}^{-1} \cdot \text{min}^{-1}$. k' was determined by using Matlab[®] as outlined in Chapter 3. All deviations are reported in Appendix D. The integration of equation 4.1 gives:

$$([Ca^{2+}] - [Ca^{2+}]_{eq})^{-1} - ([Ca^{2+}]^i - [Ca^{2+}]_{eq})^{-1} = k't \quad (4.2)$$

where $[Ca^{2+}]^i$ is the initial calcium supersaturation concentration, $[Ca^{2+}]_{eq}$ is the saturation concentration of calcium at the specific supersaturation, taken as 0.0217 and 0.0231 mol/l for SS3 and SS4 respectively (calculated by PHREEQC[®]) and $[Ca^{2+}]$ is the concentration of calcium at time, t . The average SSE, standard deviations (STD) and relative standard deviations (RSD) of the calculated values and experimental values are summarised in Table 4.10 for both supersaturations.

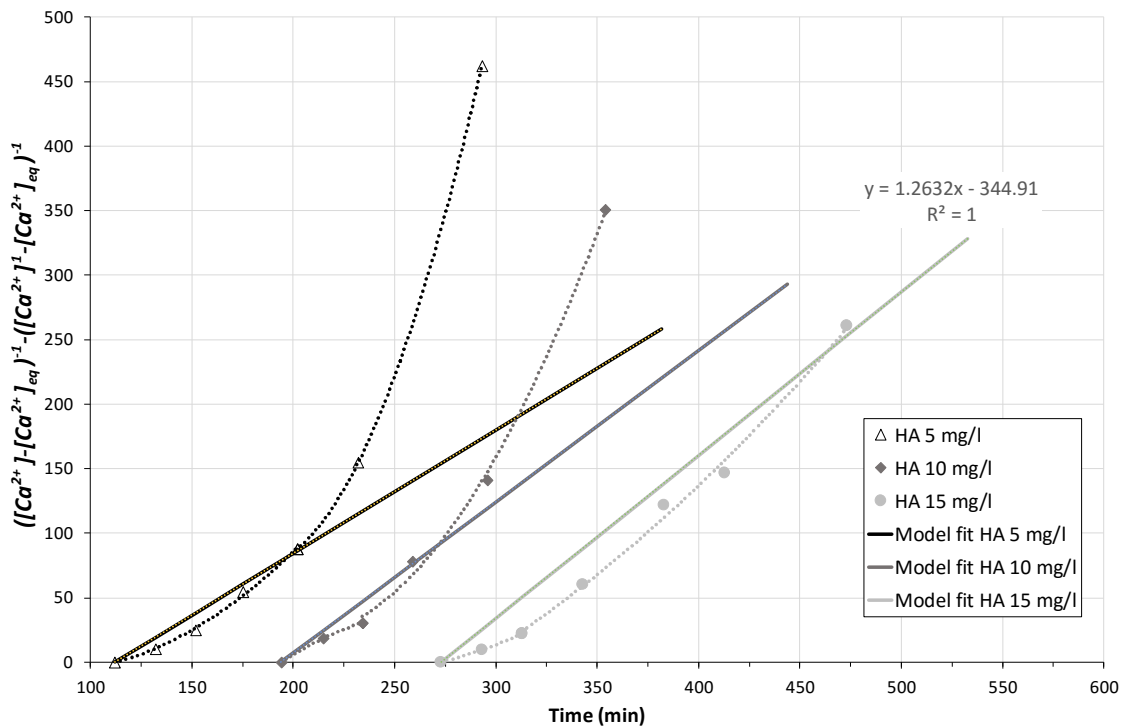
Table 4.10: SSE, STD and RSD values for growth rate constants.

Supersaturation level	SSE	STD	RSD
3	2.578×10^{-5}	1.015×10^{-3}	3.54%
4	4.633×10^{-5}	1.554×10^{-3}	5.07%

Chapter 4: Experimental Results and Discussion

Non-linear plots were obtained when $([Ca^{2+}] - [Ca^{2+}]_{eq})^{-1} - ([Ca^{2+}]^1 - [Ca^{2+}]_{eq})^{-1}$ was plotted against time for the spontaneous crystallisation of both supersaturations, SS3 and SS4, in the presence of HA. Figure 4.36 shows an example of such a plot for a spontaneous crystallisation in the presence of 5, 10 and 15 mg/l HA, at an initial adjusted pH of 7.0 and SS3. All other experimental runs yielded the same non-linear plots with different slopes. The deviation from this linearity is shown in Figure 4.36 by plotting equation 4.2 with the determined k' values from Table 4.11.

This non-linearity can explain various phenomena that are observed in the crystallisation of gypsum under these conditions. However, it could be that the 2nd order rate does not apply in the presence of HA and that various other variables should be taken into account. Due to the lack of sufficient experimental data and variation in experimental data, it is difficult to ascertain exactly what the order of growth should be or if in fact it is actually a second order rate. However, the aim here is only to consider the proposed rate and determine if the proposed rate can be used to describe the crystallisation of gypsum under these conditions.



4.5. Crystal growth kinetics in the absence of seeding

Figure 4.36: Kinetic plots in the presence of HA (5-15 mg/l) at SS3, initial adjusted pH 7.0 and Temperature 25°C without seeding (solid line is the model fit and dashed line is a trend).

In the absence of seed crystals, the onset of crystallisation has to take effect spontaneously. From the start of crystallisation and the first formation of crystal particles, the rate will be controlled by diffusion until a critical mass of particles is reached [39]. In this period of diffusion and secondary nucleation, the number of active growth sites, S_g , will increase until a point where the process will in effect be 'seeded' by the newly formed crystals. Crystal growth will then progress further through surface integration onto the newly formed active growth sites. Due to the fact that S_g is increasing through the growth of newly formed crystals via spontaneous crystallisation and that k' is dependent on S_g , an increase in S_g will result in an increase in k' .

An increase in the level of supersaturation leads to an increase in the driving force of crystallisation and an increase in calcium ions in solution. This leads to an increase in nucleation rate which can lead to an increase in the formation of active growth sites in the first stage of crystallisation. Thus, increasing the supersaturation will result in an increased number of active growth sites which will change the value of k' .

It should further be taken into account that it is assumed that initial $[Ca^{2+}] = [SO_4^{2-}]$. Due to preparation and experimental errors there may be slight differences where $[Ca^{2+}]/[SO_4^{2-}] \neq 1$, which will result in distinct deviations from the proposed rate. As previously mentioned, analysing for sulphate ions were unsuccessfully and determining this ratio was not possible. This in turn will have an effect on the calculated k' values.

All growth rate constants in the presence of HA without seeding are given in Table 4.11. An overall increase in rate constants was observed with an increase in supersaturation, as is presented in Figure 4.37.

At SS3, the overall rate constants are ~ 2 times smaller in the presence of HA compared to those in the absence of HA. At 5 mg/l HA, this change in rate constants is small. With an increase to 15 mg/l HA and an increase in pH to 9.5, there is a decrease in the rate constants

Chapter 4: Experimental Results and Discussion

from 1.036 to 0.610 $\text{l mol}^{-1} \text{min}^{-1}$. This is a reduction in rate of about ~ 1.7 times, emphasising that which was observed and stated in section 4.2.4. Crystallisation time, t_{10} , increased from 145 to 211 minutes, which agrees with a decrease in the rate constants. This decrease in the overall rate constant with the increase in HA and pH is mainly attributed to the decrease or blockage of newly formed active growth sites.

Table 4.11: Growth rate constants for all experiments (SS3 & SS4).

Experiment Name	Initial Concentration C		Humic Acid Concentration (mg/l)	pH	k' ($\text{l mol}^{-1} \text{min}^{-1}$)
	(ppm)	$\times 10^3$ (mol/l)			
BL-SS3			-	-	2.393
HA-04				4.5	1.240
HA-05			5	7.0	1.182
HA-06				9.5	1.036
HA-13	1679.35	41.9		4.5	1.115
HA-14			10	7.0	1.162
HA-15				9.5	0.765
HA-22				4.5	1.164
HA-23			15	7.0	0.960
HA-24				9.5	0.610
BL-SS4			-	-	4.194
HA-07				4.5	4.624
HA-08			5	7.0	4.540
HA-09				9.5	3.608
HA-16	2268.53	56.6		4.5	3.777
HA-17			10	7.0	5.731
HA-18				9.5	4.559
HA-25				4.5	4.523
HA-26			15	7.0	5.645
HA-27				9.5	4.529

There is a significant increase of ~ 4.5 times in rate constants with an increase in supersaturation. Figure 4.37 indicates the difference in rate constants of the two supersaturations.

Compared to the rate in the absence of HA, there is an overall slight increase in rate constants at SS4 in the presence of HA, which reiterates what has been previously observed at SS4. There seems to be an increase in rate constants approaching a more neutral pH level at SS4. It is unknown if this is truly the case or whether crystal growth is actually increased by the more neutral pH at SS4. More investigation and a more extensive study on the kinetic rate constants would be required to answer this question.

4.5. Crystal growth kinetics in the absence of seeding

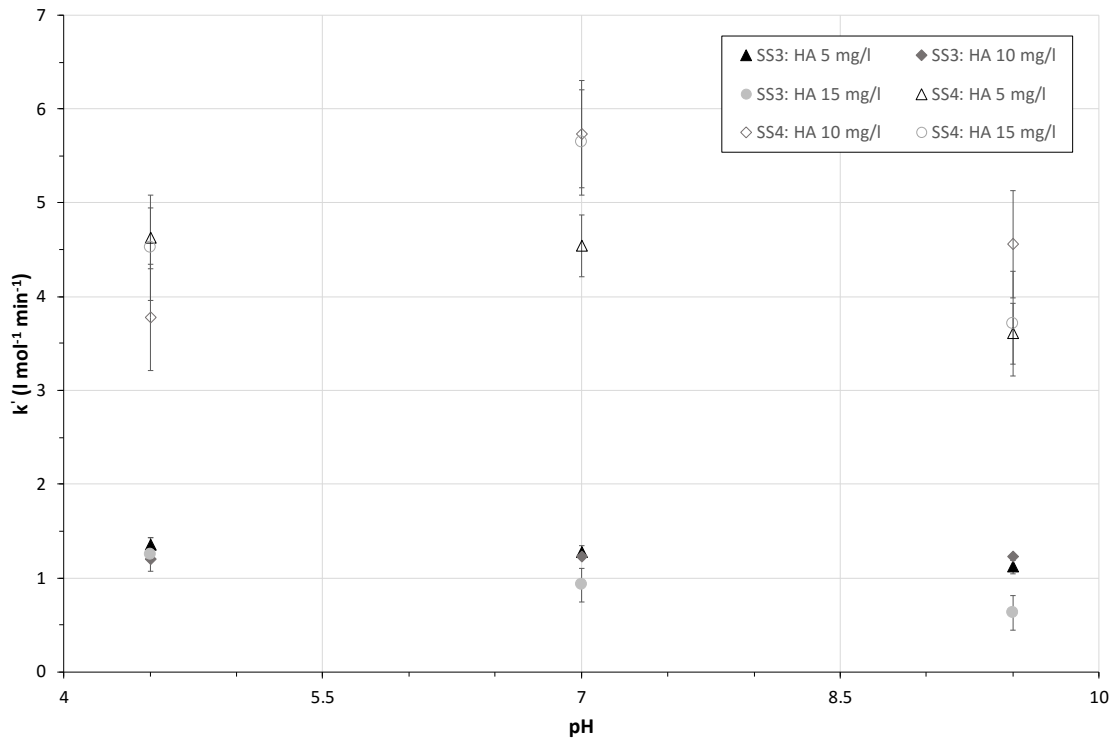
Chapter 4: Experimental Results and Discussion

Figure 4.37: Overall kinetic rate constants for SS3 and SS4 over the investigated pH range (4.5 – 9.5).

Liu et al. [12] studied the kinetics of gypsum crystallisation and determined a k' value of $2.97 \text{ litre}\cdot\text{mol}^{-1}\cdot\text{min}^{-1}$ at an initial calcium concentration of 0.0442 mol/l and temperature of 25°C in the presence of 1890 mg/l seed crystals without additives. Their k' values were compared to these experimental data, which were generated in the presence of 15 mg/l HA and at an initial calcium concentration of 0.0419 mol/l . Although Liu et al. used a different initial calcium concentration and added seed crystals, their study is the closest to the experimental conditions in this study that could be found in scientific literature. Figure 4.38 displays the fitted curves with the experimental data of experiment HA-23.

4.5. Crystal growth kinetics in the absence of seeding

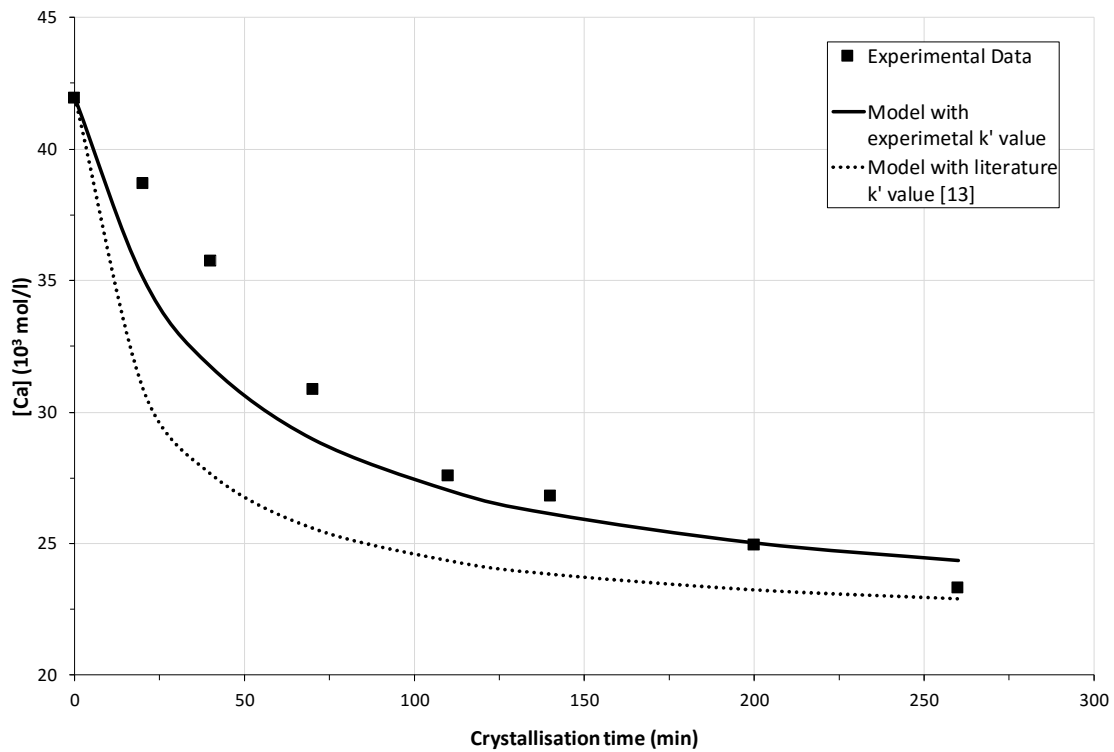


Figure 4.38: Experimental data fitted with determined and literature derived rates.

It is clear from Figure 4.38 that the literature fitted curve deviates fairly much from the fitted curve generated from the experimental data. This can be expected with the addition of HA. It can further be observed that the proposed rate struggle to account for the first linear stage of crystallisation. This further indicates that more variables have to be considered in order to properly account for all the factors that can influence the crystallisation.

Figure 4.39 shows a plot of $([Ca^{2+}] - [Ca^{2+}]_{eq})^{-1} - ([Ca^{2+}]^1 - [Ca^{2+}]_{eq})^{-1}$ against time in the presence of 1 mg/l FA at SS3 and in the investigated initial adjusted pH range. Table 4.12 presents the growth rate constants for the experiments that exhibited crystal growth in the presence of FA.

Chapter 4: Experimental Results and Discussion

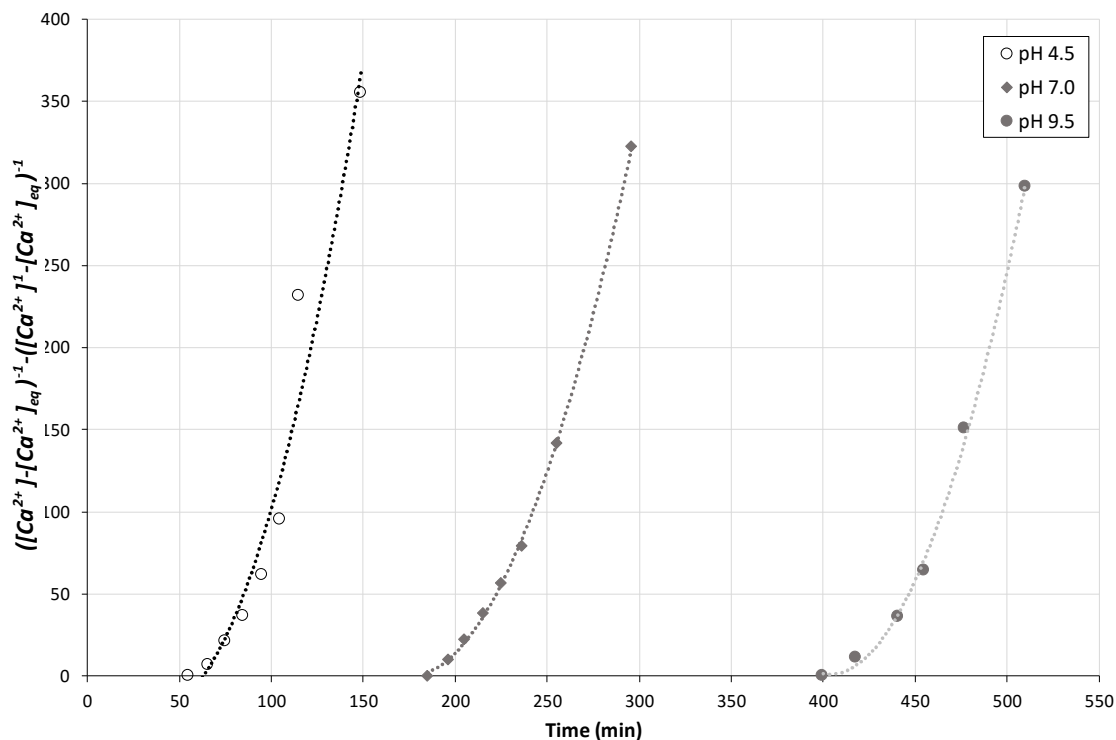


Figure 4.39: Kinetic plots in the presence of FA 1 mg/l at SS3, initial adjusted pH 4.5, 7.0 & 9.5 and Temperature 25 °C without seeding (dashed lines are illustrating trends).

Table 4.12: Kinetic growth rate constants in the presence of FA.

Experiment Name	Initial Concentration C		FA Concentration (mg/l)	pH	k' (l mol ⁻¹ min ⁻¹)
	(ppm)	$\times 10^3$ (mol/l)			
BL-SS3			-	-	2.393
FA-07				4.5	1.806
FA-06			1.0	7.0	1.587
FA-08				9.5	1.315
FA-04	1679.35	41.9	2.5	4.5	1.353
FA-05				7.0	0.744
FA-03				4.5	1.353
FA-02			5.0	7.0	-
FA-01			15.0	7.0	-

To summarise, there is much uncertainty regarding the proposed rate and the determination of k' values in the context of spontaneous crystallisation in the presence of HS without any seed material. Visual evaluation of the resulting growth curves and crystal growth times indicated that there was no significant change in the growth curves under these conditions. From these observations and the rate constants reported above it can be

4.6. Seeded crystallisation

concluded with sufficient confidence that the effect of HS on the growth rate itself was marginal and would fall within the error range that is reported in Chapter 3.

When crystallisation took effect, it proceeded at a fairly constant rate in the same order for each of the initial calcium concentrations. At SS3 a slight shift from the baseline results (absence of HA) was observed, which indicated that some form of surface interaction was taking place through the adsorption of HA (Figure 4.21). At SS4 there were no shift in the curves from the baseline (absence of HA), which again indicated the driving force of supersaturation (refer to Figure B.6 to Figure B.8 in Appendix B.3). The fact that the value of k' increased significantly with the increase in supersaturation, suggests a significant increase in active growth sites. It would be interesting to observe the outcome at higher concentrations of HA under the same supersaturation conditions. This approach could be considered for future investigation.

In the following section results are reported of experiments, where seed crystals were added in the presence of HS, and the proposed rate was evaluated under these conditions as well.

4.6. Seeded crystallisation

The effect of HA and FA on crystallisation in the absence of seed crystals was discussed in the preceding sections. Attention now shifts to the results generated with the addition of seed crystals. In this section crystallisation data are presented for crystallisations that were seeded with gypsum crystals in the presence of HA and FA. Chapter 3 describes the properties of gypsum crystals that were used as seed crystals. All experimental runs were carried out at the same constant conditions of temperature and agitation as was done previously and at an initial supersaturation of 0.0419 mol/l (SS3). Three levels of seeding were carried out in the presence of HS. Relevant experimental data are provided in Appendix B.

Seeding in the presence of either HA or FA is discussed separately in the following subsections. In the case of FA, a full study was not carried out and further investigation would be necessary to fully apprehend the effect of FA in the presence of seed crystals and

Chapter 4: Experimental Results and Discussion

to determine whether seeding the process would be able to override the inhibitory effect of FA successfully.

4.6.1. In the presence of humic acid (HA)

In order to conclude the investigation on the effect of pH, experiments were carried out in the presence of 1000 mg/l seed crystals and 10 mg/l HA over the pH range of 4.5 – 9.5. Figure 4.40 presents the results for experiments HS-01 to HS-05 over the investigated pH range.

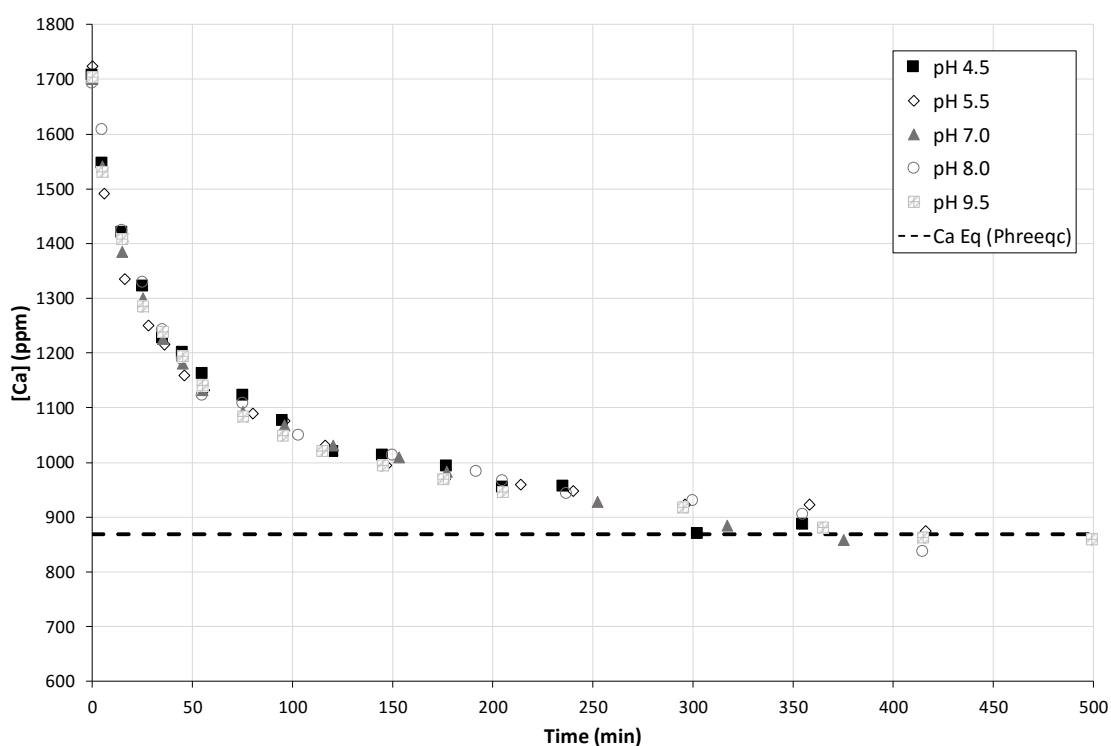


Figure 4.40: Desupersaturation curve for the effect of pH (Experiments HS-01 – HS-05) at SS3, Seed 1000 mg/l, HA 10 mg/l and Temperature 25°C.

From Figure 4.40 it is evident that an increase in pH yielded no change in crystal growth in the presence of the seed crystals. Furthermore, it can also be observed that the induction period is completely eliminated. Thus, in the presence of sufficiently high concentrations of seed crystals, the inhibitory effect of HA was completely overridden. Table 4.13 delineates the experiments over the investigated pH range and gives the overall kinetic growth rate constant (k') for each.

4.6. Seeded crystallisation

Table 4.13: Kinetic growth rate constants for experiments HS-01 to HS-05.

Experiment Name	Initial Concentration C		Humic Acid Concentration (mg/l)	Seed crystals (mg/l)	pH	k' ($\text{l mol}^{-1} \text{min}^{-1}$)
	(ppm)	$\times 10^3$ (mol/l)				
HS-01					4.5	1.726
HS-02					5.0	2.036
HS-03	1679.35	41.9	10	1000	7.0	1.883
HS-04					8.0	1.703
HS-05					9.5	1.905

The average standard deviation of the determined calcium concentrations were 18.42 ppm with an RSD of 1.55 %. The standard deviation of the growth rate constants were $0.138 \text{ l.mol}^{-1}\text{min}^{-1}$ with an average k' value of $1.851 \text{ l.mol}^{-1}\text{min}^{-1}$. These deviations are considered to be small and to fall within the errors reported in Chapter 3. This suggests that there is no significant difference between crystallisation rates with an increase in pH under these conditions. As have been concluded from literature (section 2.3.5), pH have no significant effect on crystallisation in the absence of additives. In the presence of additives and seed crystals, the effect of HA is overridden, the ability of pH to change or enhance the behaviour of HA is restricted and crystallisation will occur onto the active growth sites on the surface of the seed material.

From the results of the investigation on the effect of pH in the presence of HA and the absence of seed crystals it is clear that the inhibitory effect of HA is enhanced with an increase in pH. However, the presence of seed crystals induces crystallisation immediately and homogeneous nucleation is effectively eliminated. Secondary nucleation takes effect and the formation of new critical nuclei is not required. From the results it is evident that the inhibitory effect of HA seems to be non-existent in the presence of enough seed crystals. It is still debatable if crystal growth takes place solely through a surface reaction mechanism or through interaction of the free ions in the solution with HA molecules that have adsorbed onto the crystal surface. However, the small change, if any, in the overall growth rate constants with pH change, suggests that crystallisation is mostly occurring through surface integration.

The theory on crystallisation in the presence of HA is that the HA molecules, due to their large size ($\sim 218.5 \text{ nm}$), shield the free calcium ions to some degree from the active growth sites [65]. At the same time the HA molecules can and will interact with the free

Chapter 4: Experimental Results and Discussion

calcium ions in solution and desupersaturation occurs through adsorption of these molecules onto the seed crystals. This is dependent on the amount of seeding and the concentration of HA molecules present.

With a lower seed concentration of 200 mg/l and the same pH range (4.5 - 9.5), the same results were obtained. With an increase in pH no significant difference in the growth curve was observed (Figure 4.41). For the three experimental runs (HS-06, HS-08 and HS-07), the standard deviation and RSD were 36.145 ppm and 2.58%, respectively.

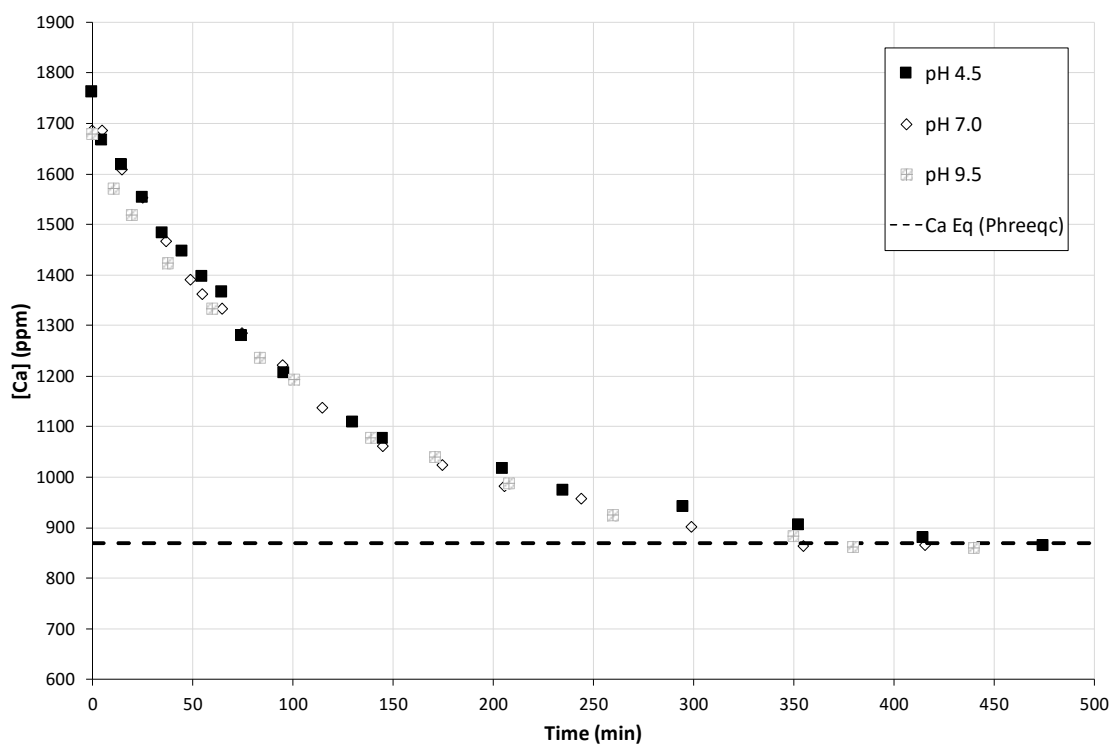


Figure 4.41: Desupersaturation curves illustrating the effect of pH (Experiments HS-06, HS-08 and HS-07) at SS3, Seed concentration: 1000 mg/l, HA concentration: 10 mg/l and Temperature: 25°C.

Experiments HS-07 and HS-05 were repeated with and without pH control at pH 9.5. Figure 4.42 presents the desupersaturation curves of experiments that were done with and without pH control at pH 9.5. It is evident that at a seeding level of 1000 mg/l there is no difference between the curve where pH was controlled and the curve where it wasn't. However, a shift in equilibrium was observed with pH control. This suggests that the ongoing addition of Na^+ and OH^- ions increased the solubility of gypsum and thereby shifted the saturation concentration.

4.6. Seeded crystallisation

Decreasing the seed concentration to 200 mg/l resulted in a slight shift in the crystal growth curve. The curve seems to follow the same trend in the beginning of the curve as was observed with a constant pH in the absence of seed crystals. Further along the curve the gradual approach to equilibrium is also slower. However, a shift in equilibrium was not observed again. These observations seem to suggest that at this lower seed loading concentration with continuous pH control, some degree of HA inhibition of crystal growth was taking place. This could be through the continuous deprotonation of the HA functional groups and the increased pH that keeps the HA molecules in a stretched configuration. This results in the shielding of active growth sites and the decrease of crystal growth. Further investigation is warranted to fully apprehend the effect under these conditions.

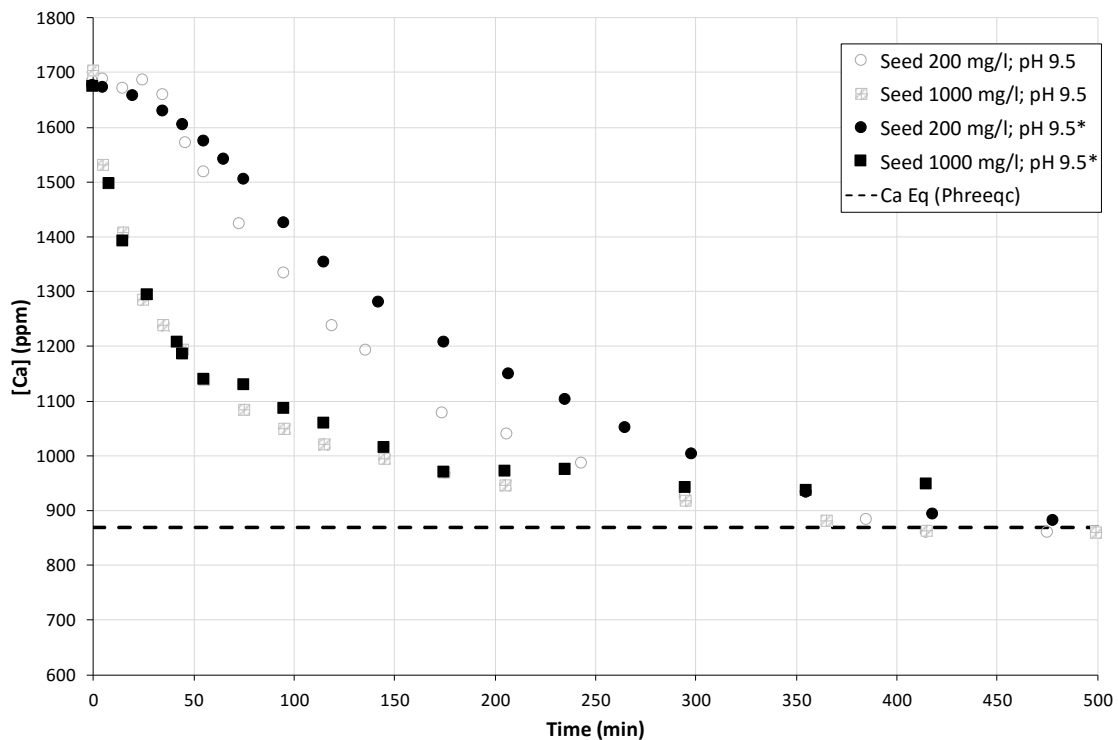


Figure 4.42: Desupersaturation curves illustrating the effect of pH controlled at 9.5 at SS3, Seeding of 200 & 1000 mg/l, 10 mg/l HA and Temperature of 25°C.

**pH controlled at 9.5 and not adjusted.*

All further experiments were carried out at an adjusted pH of 7.0, investigating the effect of the level of seeding in the presence of different concentrations of HA.

In Figure 4.43 to Figure 4.45 results are presented for three levels of seeding at HA concentrations of 5, 10 and 15 mg/l.

Chapter 4: Experimental Results and Discussion

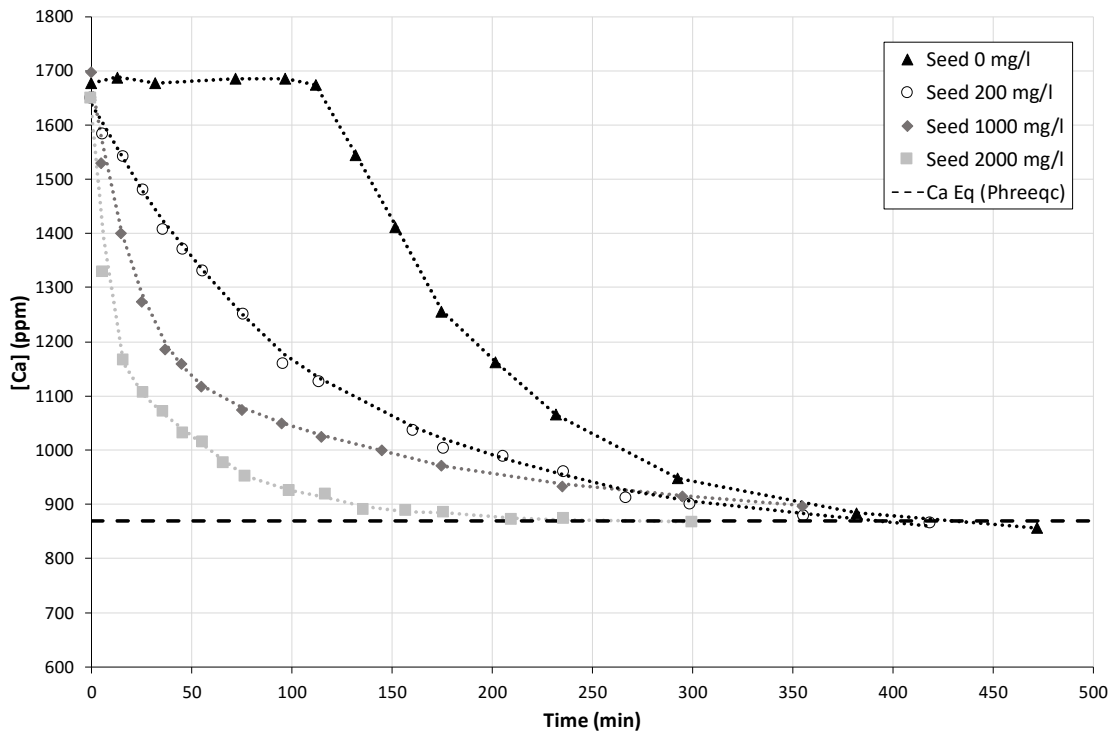


Figure 4.43: Desupersaturation curves illustrating the effect of seeding (0, 200, 1000 & 2000 mg/l) at SS3, 5 mg/l HA, initial adjusted pH 7.0 and Temperature 25°C.

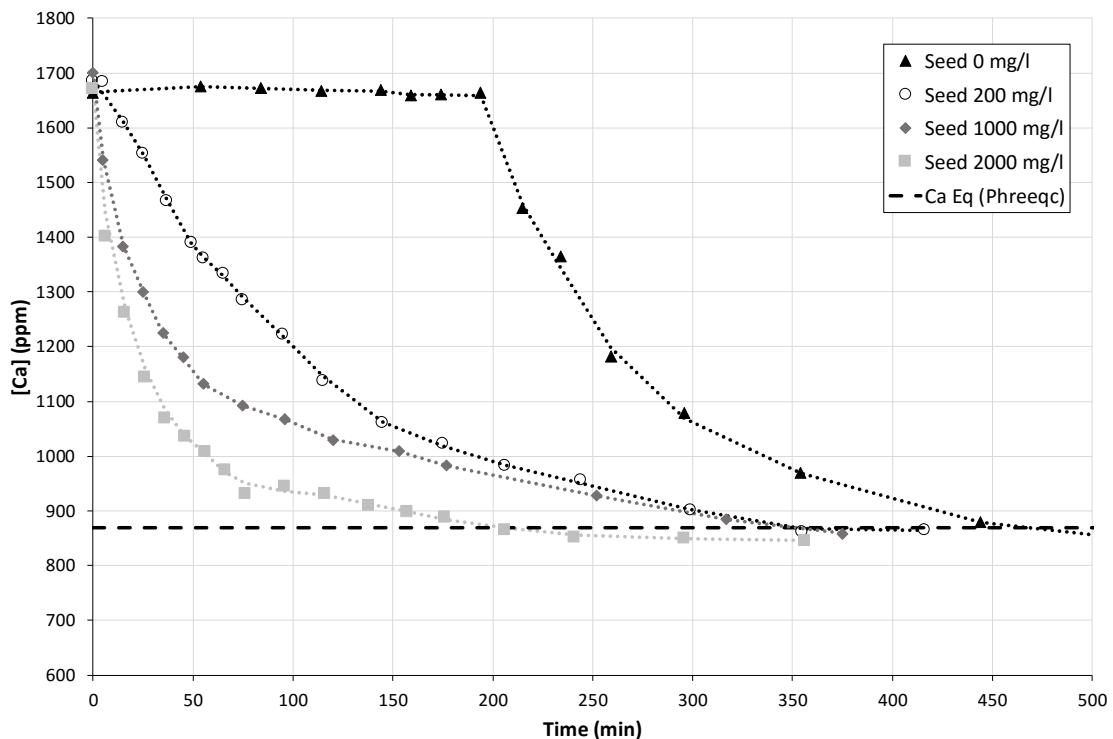


Figure 4.44: Desupersaturation curves illustrating the effect of seeding (0, 200, 1000 & 2000 mg/l) at SS3, 10 mg/l HA, initial adjusted pH 7.0 and Temperature 25°C.

4.6. Seeded crystallisation

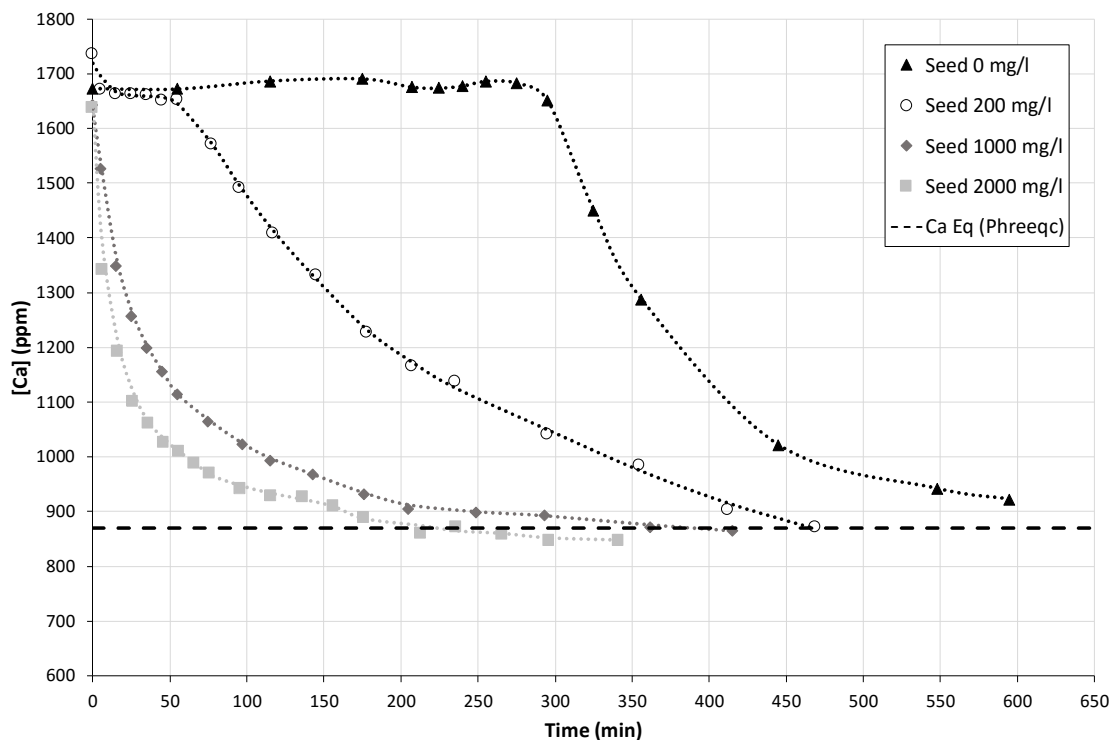


Figure 4.45: Desupersaturation curves illustrating the effect of seeding (0, 200, 1000 & 2000 mg/l) at SS3, 15 mg/l HA, initial adjusted pH 7.0 and Temperature 25°C.

It is evident from Figure 4.43 to Figure 4.45, that the inhibitory ability of HA was completely overridden in most cases. However, at a low seed addition and high HA concentration (200 mg/l and 15 mg/l respectively), an induction period of 55 minutes was observed. This suggests that some form of inhibition effect was taking place under these conditions, even with the addition of seed crystals. As previously stated, it could be that at a lower seed concentration, some form of shielding by HA molecules was taking place between the added crystals and the free ions in solution. When the onset of crystallisation was eventually achieved, a more linear growth curve was observed than the growth curve that was obtained in the absence of seed crystals or the growth curves that were obtained at any of the other investigated seed concentrations. This suggests a decrease in growth rate. The time that it took for crystallisation to achieve near saturation levels was also decreased. With all other seeding experiments in the presence of HA, no induction periods were observed.

It is further evident that with an increase in the level of seeding there is a shift in the growth curves. With an increase in the amount of seeding an increase in growth rate is observed. A plot of $([Ca^{2+}] - [Ca^{2+}]_{eq})^{-1} - ([Ca^{2+}]^1 - [Ca^{2+}]_{eq})^{-1}$ against time is presented

Chapter 4: Experimental Results and Discussion

in Figure 4.46 for an increase in seed concentration in the presence of 15 mg/l HA at a pH of 7.0. In the presence of seed crystals and at higher seed levels more linear curves were observed. With a decrease in the seed concentration to 200 mg/l, the curves displayed more non-linearity. It is evident from the kinetic plots that with an increase in the seed level there was an increase in the slope. This reveals the increase in the growth rate of crystallisation that was observed and emphasises that the crystallisation takes place mainly on the surface of the seed material.

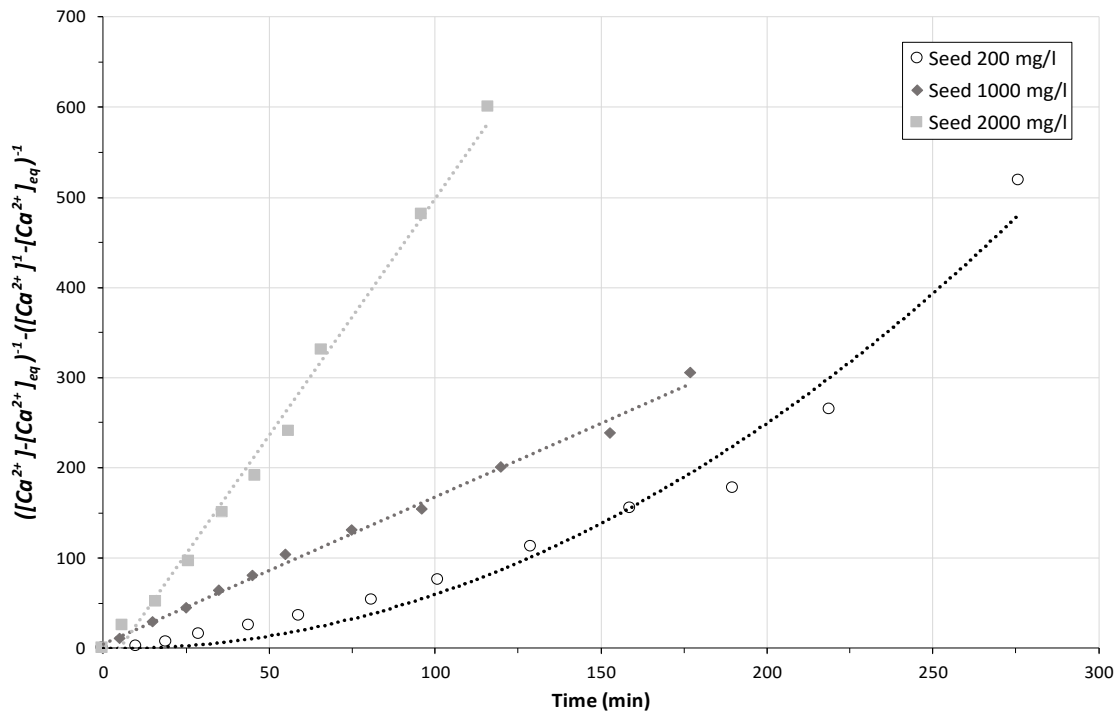


Figure 4.46: Kinetic plots in the presence of seed crystals at SS3, 10 mg/l HA, initial adjusted pH 7.0 and Temperature 25°C (dashed lines are illustrating trends).

Table 4.14 presents the results for the overall kinetic growth rate constants. From these results it is clear that there was an increase in the k' value with an increase in seed crystals. The reason for this observation is that k' is dependent on the number of active growth sites (S_g) and an increase in seed concentration resulted in an increase in the active growth sites, resulting in an increase in the k' values.

With an increase in seed crystals, growth is accelerated. Crystals will grow on the surface of the seed crystals and thereby the requirement for spontaneous nucleation is eliminated.

4.6. Seeded crystallisation

Table 4.14: Kinetic growth rate constants and seeded experimental conditions in the presence of HA.

Experiment Name	Initial Concentration C		Seed Concentration (mg/l)	Humic Acid Concentration (mg/l)	k' ($l\ mol^{-1}\ min^{-1}$)
	(ppm)	$\times 10^3$ (mol/l)			
HS-12			200		0.901
HS-11			1000	5	2.015
HS-14			2000		5.205
HS-08			200		0.834
HS-03	1679.35	41.9	1000	10	1.883
HS-16			2000		4.321
HS-09			200		0.500
HS-10			1000	15	2.190
HS-15			2000		4.910

Figure 4.47 presents a plot of the k' values against seed concentration for the experiments summarised in Table 4.14. An overall linear increase in the overall growth rate constants was observed with an increase in seed concentration. This suggested that k' is directly proportional to the amount of seed crystals. The same trend was observed from the work of Tadros et.al [71] where the crystallisation of calcium hydroxide was investigated.

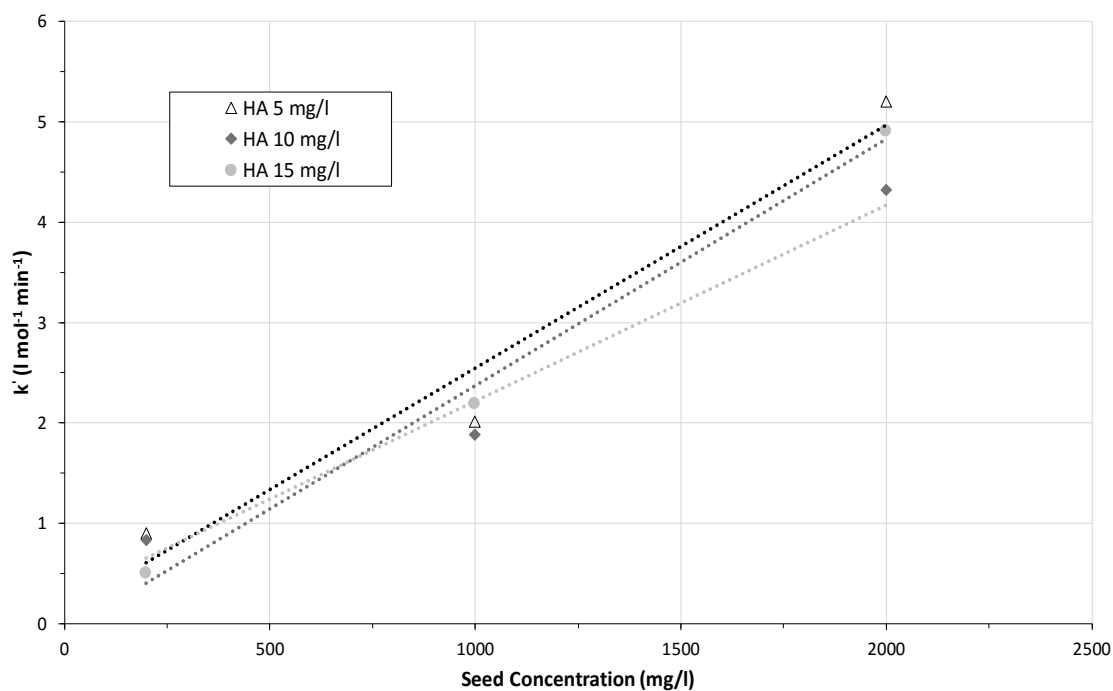


Figure 4.47: Overall kinetic growth rate constants in the presence of seed crystals (200, 1000 & 2000 mg/l) at SS3, HA at 5, 10 & 15 mg/l, initial adjusted pH 7.0 and Temperature 25°C.

Chapter 4: Experimental Results and Discussion

With seeding of 1000 and 2000 mg/l, no significant difference was observed with an increase in HA concentration (see Appendix B.4. for figures). A spread of k' values was observed at the higher seeding level. It is still questionable if crystallisation follows a second order growth rate under these conditions or if the suggested rate can accurately predict the experimental results. Slight deviations between experimental results can result in deviations in calculated k' values. Taking experimental and analytical errors into account these deviations are acceptable. All deviations are reported in Appendix D.

In the presence of HA, the differences in k' values can also be attributed to the fact that HA can interfere with the number of active growth sites. Thus, with the blockage of active growth sites, the value of k' can change. The dependence of k' on the active growth sites is discussed in section 4.5.

At a seeding level of 200 mg/l an increase in HA yielded significantly different results. Figure 4.48 presents the desupersaturation curves obtained in the presence of 200 mg/l seed crystals over an increase in HA concentrations.

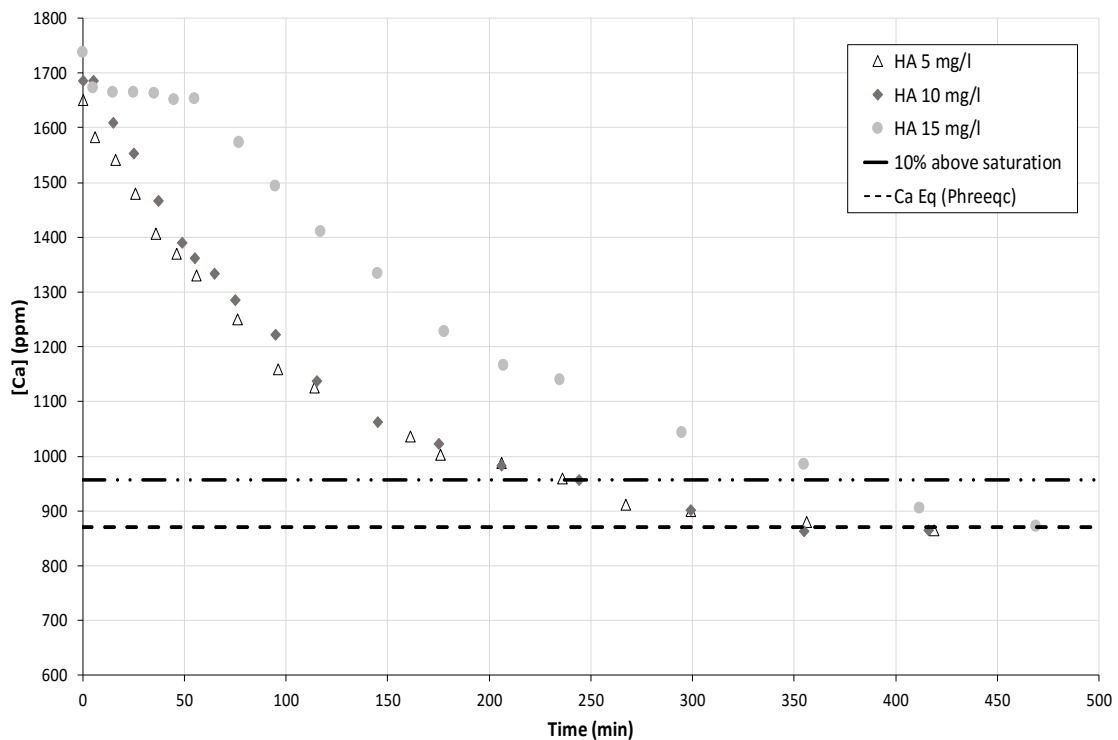


Figure 4.48: Desupersaturation curves illustrating the effect of HA (5, 10 & 15 mg/l) in the presence of seed crystals (200 mg/l) at SS3, initial adjusted pH 7.0 and Temperature 25°C.

4.6. Seeded crystallisation

No significant difference was evident between the curves that were obtained in the presence of 5 and 10 mg/l HA, at a seed crystal addition of 200 mg/l. With an increase in HA to 15 mg/l, an induction period of 55 minutes was observed, which shifted the growth curve. However, no significant change in the growth curve itself was observed when crystal growth took effect. On removing the induction period and considering the k' values, a slight decrease was observed with the increase of HA from 5 to 10 mg/l. A larger decline in k' was observed with an increase from 10 to 15 mg/l HA that yielded a k' value of $0.5 \text{ mol}^{-1} \text{ min}^{-1}$. This suggests that HA successfully blocked the number of active growth sites and inhibited the crystallisation of gypsum. Thus, the growth was not solely through surface integration but nucleation was also occurring.

4.6.2. In the presence of fulvic acid (FA)

Figure 4.49 presents the desupersaturation curve illustrating the effect of seeding in the presence of 5 mg/l FA.

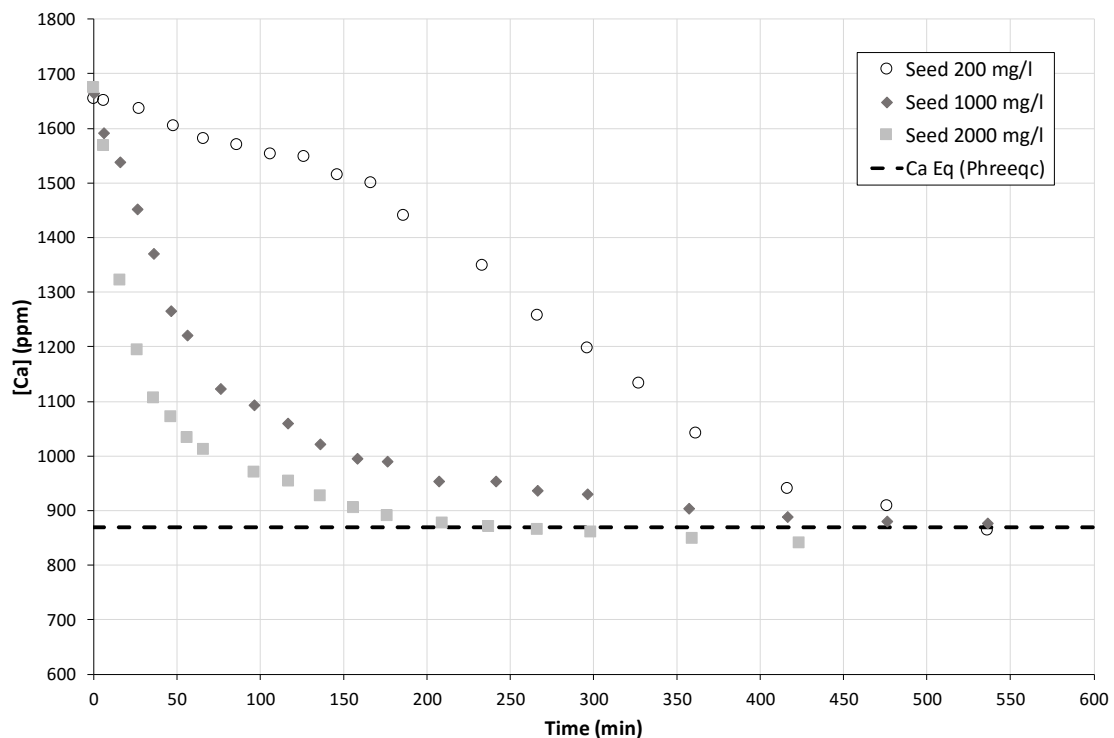


Figure 4.49: Desupersaturation curve illustrating the effect of seeding in the presence of FA (5 mg/l) at SS3, initial adjusted pH 7.0 and Temperature 25°C.

Chapter 4: Experimental Results and Discussion

Figure 4.49 shows that very different results were obtained in the presence of FA compared to those obtained in the presence of HA. However, the same trend was observed in that an increase in the amount of seeding resulted in an increase in the crystallisation rate. The induction period was also completely eliminated. The growth curve at a seed crystal addition level of 200 mg/l in the presence of 5 mg/l FA was significantly different from the growth curves obtained at higher seeding levels. The growth was slower compared to the higher seeding levels (1000 mg/l and 2000 mg/l), and a short induction period of 5 min was observed, followed by a slow linear decrease in the curve up to 160 min. Thereafter the growth increased linearly until saturation was achieved.

Figure 4.50 presents the desupersaturation curve illustrating the effect of seeding in the presence of 10 mg/l FA. At the lowest seeding level (200 mg/l), the addition of seed particles was unable to override the inhibitory effect of FA for a period of at least 8 hours. This once again proves the ability of FA to inhibit crystallisation at higher concentrations. Even in the presence of seed crystals, FA was still able to inhibit crystallisation. This could most likely be attributed to the fact that FA is completely soluble in water in contrast to HA, which is only partially soluble. The better solubility of FA will give these compounds the ability to interact more strongly with the free ions in the solution. The increase in functional group content of FA, as previously mentioned, will also largely contribute to the inhibitory ability of these molecules through the blockage of active growth sites on the added seed material.

Crystallisation took place without any induction period when the seed concentration was at 2000 mg/l, as shown in Figure 4.50. At this higher seed concentration, seeding was able to completely override the inhibitory effect of FA. However, crystallisation took more than 400 minutes to achieve near saturation levels, which is more than double the time it took for crystallisation to take place in the presence of HA under the same conditions. By decreasing FA to 5 mg/l in the presence of 2000 mg/l seed crystals, an increase in crystallisation was observed (see Figure 4.51).

4.6. Seeded crystallisation

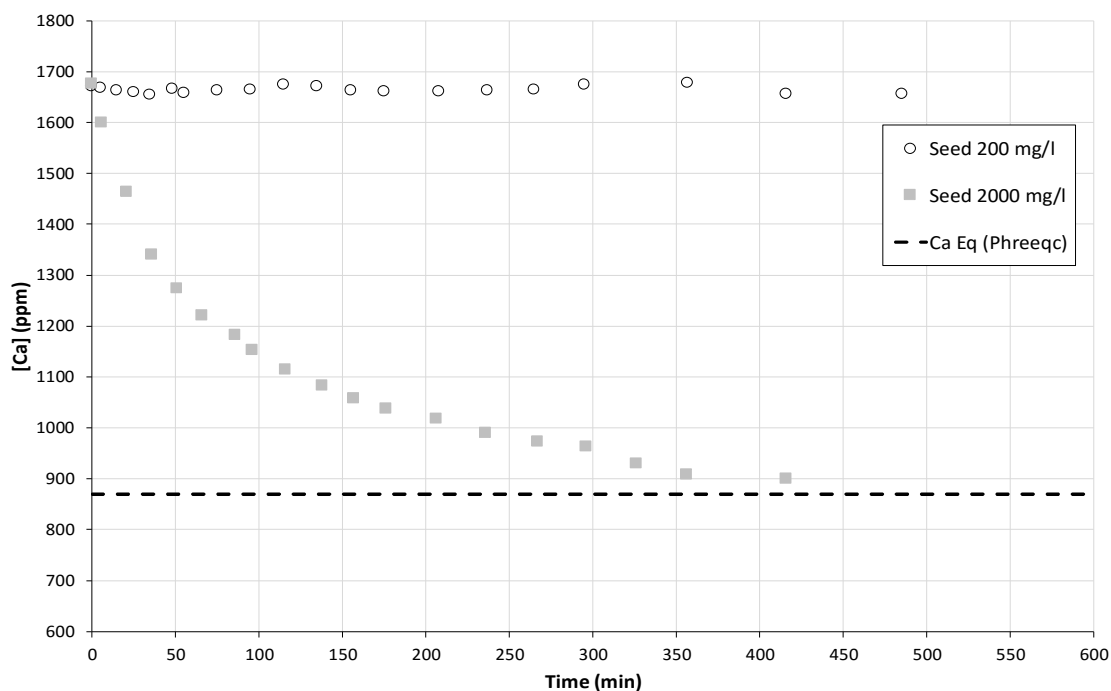


Figure 4.50: Desupersaturation curves in the presence of seed crystals (200 and 2000 mg/l) at SS 3, 10 mg/l FA, initial adjusted pH 7.0 and Temperature 25°C.

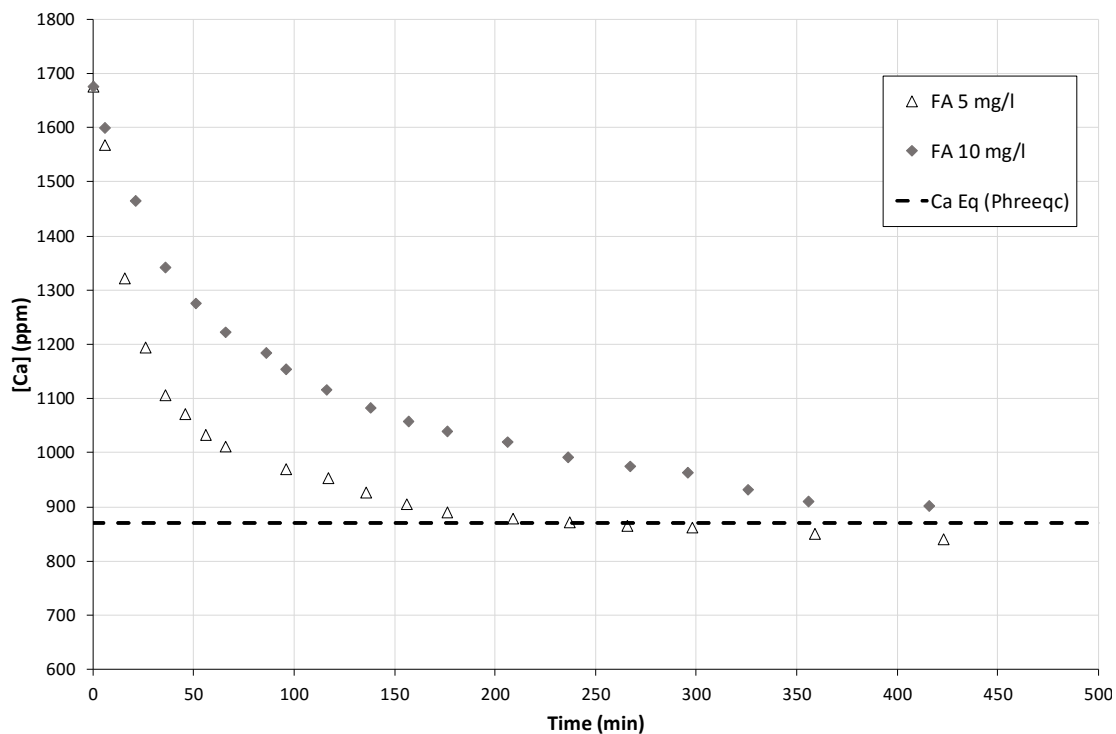


Figure 4.51: Desupersaturation curves in the presence of FA (5 & 10 mg/l) at SS3, 2000 mg/l seeding, initial adjusted pH 7.0 and Temperature 25°C.

Chapter 4: Experimental Results and Discussion

Table 4.15 presents the overall kinetic growth rate constants of seeded crystallisation experiments in the presence of FA.

Table 4.15: Kinetic growth rate constants and seeded experimental conditions in the presence of FA at SS3, initial adjusted pH 7.0 and Temperature 25°C.

Experiment Name	Initial Concentration C		Seed Concentration (mg/l)	Fulvic Acid Concentration (mg/l)	k' (l mol ⁻¹ min ⁻¹)
	(ppm)	× 10 ³ (mol/l)			
FS-02			200		-
FS-03			1000	5	1.214
FS-04	1679.35	41.9	2000		3.116
FS-01			200		0
FS-05			2000	10	1.027

Unfortunately it was difficult to predict the growth rate constants for seeded crystallisation in the presence of FA for the proposed rate equation (equation 4.1). Further questions need to be asked concerning the prediction of the kinetics of crystallisation reactions and their growth rate constants in the presence of additives and impurities with and without seeding. More variables need to be taken into account, especially regarding the behaviour of FA. Variables, such as the activity of the ions in solution and how it is influenced by additives and impurities in solution, should be considered in the determination of the value k' and the rate of crystallisation. Even considering catalytic reaction kinetics in the presence of seed material could be advantageous. Seed material can act as catalysts that promote crystallisation. This falls outside the scope of this study and is something that can be considered for further investigation in future.

An overall kinetic growth rate constant was not determined for the lowest seed concentration at a FA concentration of 5 and 10 mg/l. For the higher seed levels, growth rate constants were successfully calculated (see Table 4.15). With an increase in FA from 5 to 10 mg/l at 2000 mg/l seeding, k' was decreased by a factor of ~3. In this experiment the seed concentration remained constant and the value of k' was expected to stay more or less constant, which was not the case. This further highlights the uncertainty of the proposed rate.

Compared to the results obtained in the presence of HA under the same conditions (Figure 4.52), the overall growth rate constants were more than doubled in the presence of 10 mg/l FA. This again illustrates the increased effect of FA relative to that of HA. This also

4.6. Seeded crystallisation

suggests that FA has a higher affinity for adsorption at higher concentrations and similar levels of seeding. Higher affinity for adsorption will result in increased blockage of active growth sites and slower kinetics.

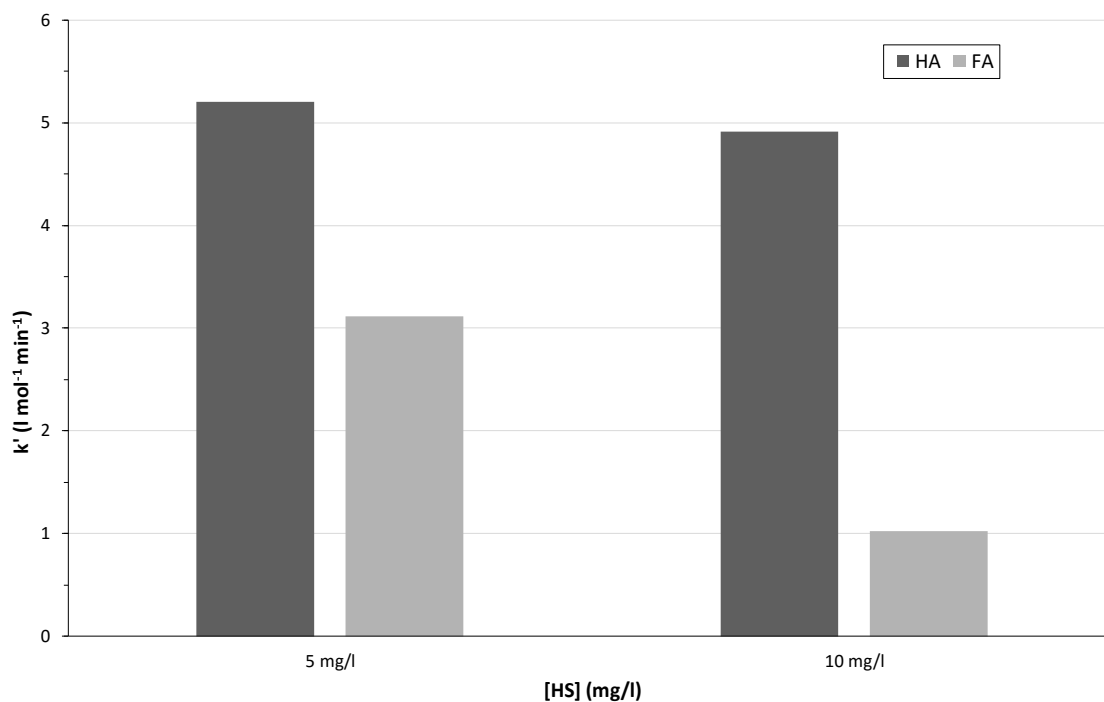


Figure 4.52: Kinetic growth rate constants (k') in the presence of HS (5 & 10 mg/l) at SS3, seed 200 mg/l, initial adjusted pH 7.0 and Temperature 25°C.

Adding seed material resulted in the successful crystallisation of gypsum in the presence of both HA and FA. However, in the presence of FA, crystallisation was slower. Thus, if enough seed material (more than 1000 mg/l) is added to the process, inhibitory effects can be overridden. In industry, crystallisation reactions are seeded through recycling of crystals and the addition of lime, as previously mentioned, to induce and accelerate crystallisation. Adding more seed material in crystallisers and thereby adding more active growth sites to the process will hopefully increase the growth rate and reduce any inhibitory effects.

The significant inhibitory effect of FA on the crystallisation process, even in the presence of seed crystals, suggests that this effect would be even greater if FA concentrations would be increased above 15 mg/l. In industry, FA concentrations can be even higher than

Chapter 4: Experimental Results and Discussion

those that were investigated in this study and therefore enough seed material would need to be added to override the effects of FA. As previously stated, lime is added in industry to increase the pH. However, as the pH is increased the inhibitory effect of FA will be increased. This would require further addition of seed material to override the effect or a different seed material is required that does not affect the pH to a large extent. It would be interesting to see whether the driving force of crystallisation, through an increase in calcium ions and supersaturation, would be able to override the inhibitory effect of FA as effectively as in the case of HA. Further study would be required to determine this.

It can therefore be concluded that the inhibitory effect of HA can be minimised through an increase in supersaturation. Furthermore, the addition of seed material can effectively override the inhibitory ability of both HA and FA, especially at a seed concentration of 2000 mg/l.

Chapter 5: CONCLUSIONS

From findings in the literature as well as the experimental results of this study, the following conclusions can be drawn:

Effect of Supersaturation.

HS significantly inhibited the onset of crystallisation in the absence of seed crystals, especially at lower gypsum supersaturation levels. At two times above gypsum saturation, crystallisation of gypsum was completely inhibited and no crystallisation was observed for a period of at least 8 hours at 5 mg/l HA. At SS3 and SS4, induction times increased from 25 to 295 min and 7 to 15 min, respectively with an increase in HA from 0 to 15 mg/l. Increasing the level of supersaturation resulted in a significant decrease in the inhibitory effect of HS, indicating the clear power of the driving force of supersaturation.

Effect of pH.

An increase in the initial pH of the system resulted in an increased inhibitory ability of HS. At a HA concentration of 15 mg/l and an initial pH adjustment from 4.5 to 9.5, induction times increased from 115 to 415 minutes. A rise in pH increases the deprotonation of the HA functional groups (-COOH and -OH), which results in more negatively charged HA molecules and an increased affinity of HA to bind to calcium and inhibit the crystallisation process. An evaluation of crystal growth times for supersaturation three and four times (SS3 & SS4) gypsum saturation revealed that crystal growth was independent of pH with crystallisation times that were 180 and 295 minutes, respectively.

FA vs. HA.

The inhibitory effect of FA was greatly underestimated at the start of experimentation. At SS3 with FA at 5 and 15 mg/l, crystallisation was completely inhibited for more than 2 days. The FA concentration was therefore lowered to 1.0 and 2.5 mg/l, where induction

Chapter 5: Conclusions

periods of 185 and 480 min, respectively were observed. In contrast, with HA at a concentration of 5 and 10 mg/l and using the same supersaturation level (SS3), induction times of 98 and 195 min, respectively were observed. This reveals a significant difference in inhibitory effect. Literature indicates that FA has a lower molecular weight and a higher relative functional group (-COOH and -OH) content, which gives these substances their inhibitory ability. Due to FA's lower molecular weight, these molecules will experience less steric hindrance, which should increase their ability to adsorb onto active growth sites.

Effect of Seeding.

At SS3, the addition of seed crystals (gypsum), at seed concentrations of 1000 and 2000 mg/l, effectively overrides the inhibitory effect of HS. In the presence of 15 mg/l HA, an increase in seed concentration resulted in an increase in the determined kinetic growth constants from 0.5 to 4.91 litre·mol⁻¹·min⁻¹. This confirms the effect of an increase in active growth sites with an increasing number of seed crystals. With a relatively low concentration of seed crystals (200 mg/l) and a HA concentration of 15 mg/l, an induction time of 50 min was observed, suggesting that a significant degree of adsorption of the inhibitor was still taking place and in so blocking the sites necessary for forming a stable crystal lattice. It was further determined that seeding was independent of pH and that any effect of HS was through surface interaction.

It can therefore be concluded that HS have a significant inhibiting and delaying effect on crystallisation in the absence of seed material. Supersaturation can be increased to override and minimise this inhibitory effect of HS. The addition of enough seed material, typically more than 1000 mg/l, will override these inhibitory abilities and thereby minimise the inhibitory effects of HS.

Chapter 6: RECOMMENDATIONS

From this study on the crystallisation of gypsum in the presence of HS, the following recommendations for future work are made:

- The study of the crystallisation process at higher HS concentrations in order to determine its effect on the crystal growth rate.
- Conduct an experimental study under conditions of controlled pH.
- Do experiments at higher temperatures, especially in the presence of FA. This would help to determine if elevated temperatures can induce the onset of crystallisation at higher concentrations of FA.
- A more in-depth study is required on the rate equation that is used to describe the crystallisation process. There is still uncertainty about the order of growth in the presence of these HS. It may be necessary to investigate the same rate equations at lower supersaturation levels. At higher supersaturation levels it may be necessary to take more variables into account, i.e. the activities of the ions as well as the actual solubility of the crystalline and not only the predicted values.
- A more in-depth study is required on crystallisation in the presence of FA and seed material to further explain the strong inhibitory ability of FA.
- A study on the crystal morphology will give insight of the adsorption mechanism of these HS and whether pure gypsum is crystallised.
- Study on the effect of FA at higher supersaturation levels. It would be interesting to observe the effect of supersaturation in the presence of FA and to determine the influence of higher supersaturation on the FA inhibitory effect.

Chapter 7: REFERENCES

- [1] A. Rahardianto, B. C. McCool and Y. Cohan, “Accelerated desupersaturation of reverse osmosis concentrate by chemically-enhanced seeded precipitation,” *Desalination*, vol. 264, pp. 256-267, 2010.
- [2] T. Lin, Z. Lu and W. Chen, “Interaction mechanisms of humic acid combined with calcium ions on membrane fouling at different conditions in an ultrafiltration system,” *Desalination*, vol. 357, pp. 26-35, 2015.
- [3] H. Odegaard, S. Osterhus, E. Melin and B. Eikebrokk, “NOM removal technologies - Norwegian experiences,” *Drinking Water Engineering and Science*, vol. 3, pp. 1-9, 2010.
- [4] C. Tang, Z. He, F. Zhao, X. Liang and Z. Li, “Effects of cations on the formation of ultrafiltration membrane fouling layers when filtering fulvic acid,” *Desalination*, vol. 352, pp. 174-180, 2014.
- [5] J. W. Mullin, *Crystallisation*, London: Butterworths, 1972.
- [6] R. F. Strickland-Constable, *Kinetics and Mechanism of Crystallization*, London and New York: Academic Press, 1968.
- [7] J. Nyvlt, O. Sohnel, M. Matuchova and M. Broul, *The Kinetics of Industrial Crystallization*, New York: Elsevier, 1985.
- [8] G. H. Nancollas, “Kinetics of Crystal Growth from solution,” *Journal of Crystal Growth*, vol. 3, no. 4, pp. 335-339, 1968.

- [9] D. H. Gerber, "The chemical manipulation of meta-stable brine supersaturated with gypsum: forcing precipitation by overriding the inhibitory effect of antiscalants on crystal formation," Stellenbosch University, Stellenbosch, 2011.
- [10] Z. Amjad and J. Hooley, "Influence of Polyelectrolytes on the Crystal Growth of Calcium Sulfate Dihydrate," *Journal of Colloid and Interface Science*, vol. 111, no. 2, pp. 496-503, 1986.
- [11] Z. Amjad, "Kinetics of crystal growth of calcium sulfate dihydrate: The influence of polymer composition, molecular weight, and solution pH," *Canadian Journal of Chemistry*, vol. 66, pp. 1529-1536, 1988.
- [12] S.-T. Liu and G. H. Nancollas, "The Kinetics of Crystal Growth of Calcium Sulfate Dihydrate," *Journal of Crystal Growth*, vol. 6, pp. 281-289, 1970.
- [13] S. T. Liu and G. H. Nancollas, "A Kinetic and Morphological Study of the Seeded Growth of Calcium Sulfate Dihydrate in the Presence of Additives," *Journal of Colloid and Interface Science*, vol. 52, no. 3, pp. 593-601, 1975.
- [14] J. D. Seader and E. J. Henley, *Separation Process Principles*, John Wiley & Sons. Inc., 2006.
- [15] C. J. Schram, R. J. Smyth, L. S. Taylor and S. P. Beaudoin, "Understanding Crystal Growth Kinetics in the Absence and Presence of a Polymer Using a Rotating Disk Apparatus," *Crystal Growth & Design*, vol. 16, pp. 2640-2645, 2016.
- [16] W. F. Klima and G. H. Nancollas, "The Growth of Gypsum," *AIChE Symposium Series*, vol. 83, no. 253, pp. 23-30, 1987.
- [17] B. R. Smith and F. Sweett, "The Crystallization of Calcium Sulfate Dihydrate," *Journal of Colloid and Interface Science*, vol. 37, no. 3, pp. 612-618, 1971.

Chapter 7: References

- [18] G. Nancollas, M. Reddy and F. Tsai, "Calcium sulfate dihydrate crystal growth in aqueous solution at elevated temperatures," *Journal of Crystal Growth*, vol. 20, pp. 125-134, 1973.
- [19] Z. Amjad, "Gypsum scale formation on heated metal surfaces: The Influence of polymer type and polymer stability on gypsum inhibition," *Desalination and Water Treatment*, vol. 51, pp. 4709-4718, 2013.
- [20] D. Zeng and W. Wang, "Solubility phenomena involving CaSO_4 in hydrometallurgical processes concerning heavy metals," *Pure Applied Chemistry*, vol. 83, no. 5, pp. 1045-1061, 2011.
- [21] W. H. Power, B. M. Fabuss and C. N. Satterfield, "Transient Solute Concentrations and Phase Changes of Calcium Sulfate in Aqueous Sodium Chloride," *Journal of Chemical and Engineering Data*, vol. 11, no. 2, pp. 149-154, 1966.
- [22] E. P. Partridge and A. H. White, "The solubility of calcium sulfate from 0 to 200 °C," *Journal of the American Chemical Society*, vol. 51, no. 2, pp. 360-370, 1929.
- [23] A. G. Ostroff and A. A. Metler, "Solubility of Calcium Sulfate Dihydrate in the System $\text{NaCl-MgCl}_2\text{-H}_2\text{O}$ from 28 to 70 °C," *Journal of Chemical and Engineering Data*, vol. 11, no. 3, pp. 346-350, 1966.
- [24] E. Bock, "On the Solubility of Anhydrous Calcium sulphate and of gypsum in concentrated solutions of sodium chloride at 25 °C, 30 °C, 40 °C, and 50 °C," *Canadian Journal of Chemistry*, vol. 39, pp. 1746-1751, 1961.
- [25] G. Innorta, E. Rabbi and L. Tomadin, "The gypsum-anhydrite equilibrium by solubility measurements," *Geochimica et Cosmochimica Acta*, vol. 44, no. 12, pp. 1931-1936, 1980.

- [26] W. H. Power, B. M. Fabuss and C. N. Satterfield, "Transient Solubilities in the Calcium Sulfate-Water System," *Journal of Chemical and Engineering Data*, vol. 9, no. 3, pp. 437-442, 1964.
- [27] W. L. Marshall and R. Slusher, "Thermodynamics of Calcium Sulfate Dihydrate in Aqueous Sodium Chloride Solutions, 0-110°C," *The Journal of Physical Chemistry*, vol. 70, no. 12, pp. 4015-4027, 1966.
- [28] K. K. Tanji, "Solubility of Gypsum in Aqueous Electrolytes as Affected by Ion Association and Ionic Strengths up to 0.15 M and at 25°C," *Environmental Science & Technology*, vol. 3, no. 7, pp. 656-661, 1969.
- [29] L. B. Yeatts and W. L. Marshall, "Solubility of Calcium Sulfate Dihydrate and Association Equilibria in Several Aqueous Mixed Electrolyte Salt Systems at 25°C," *Journal of Chemical and Engineering Data*, vol. 17, no. 2, pp. 163-168, 1972.
- [30] Z. Amjad, "Gypsum Scale Formation on Heat Exchanger Surfaces: The Influence of Natural and Synthetic Polyelectrolytes," *Tenside Surfactants Detergents*, vol. 41, no. 5, pp. 214-219, 2004.
- [31] J. W. Mullin and O. Sohnel, "Expressions of supersaturation in crystallization studies," *Chemical Engineering Science*, vol. 32, pp. 683-686, 1977.
- [32] G. K. Kirov, "Determination of the supersaturation in crystallization from solution of strong electrolytes," *Journal of Crystal Growth*, vol. 20, pp. 171-173, 1973.
- [33] S. Hamdona and O. Al Hadad, "Influence of additives on the precipitation of gypsum in sodium chloride solutions," *Desalination*, vol. 228, pp. 277-286, 2008.
- [34] O. Sohnel and J. Garside, "On Supersaturation Evaluation for solution growth," *Journal of Crystal Growth*, vol. 54, pp. 358-360, 1981.

Chapter 7: References

- [35] E. A. Abdel-Aal, M. M. Rashed and H. El-Shall, "Crystallization of calcium sulfate dihydrate at different supersaturation ratios and different free sulfate concentrations," *Crystal Research Technology*, vol. 39, no. 4, pp. 313-321, 2004.
- [36] A. Lancia, D. M. Musmarra and M. Prisciandaro, "Measuring Induction Period for Calcium Sulfate Dihydrate Precipitation," *AIChE Journal*, vol. 45, no. 2, pp. 390-397, 1999.
- [37] S. B. Ahmed, M. M. Tlili, M. Amami and M. B. Amor, "Gypsum Precipitation Kinetics and Solubility in the NaCl-MgCl₂-CaSO₄-H₂O System," *Industrial & Engineering Chemistry Research*, vol. 53, pp. 9554-9560, 2014.
- [38] G. J. Witkamp, J. P. Van Der Eerden and G. M. van Rosmalen, "Growth of Gypsum: I. Kinetics," *Journal of Crystal Growth*, vol. 102, no. 1-2, pp. 281-289, 1990.
- [39] W. P. Brandse and G. M. van Rosmalen, "The influence of sodium chloride on the crystallization rate of gypsum," *Journal of Inorganic and Nuclear Chemistry*, vol. 39, no. 11, pp. 2007-2010, 1977.
- [40] Z. Amjad, "Calcium Sulfate Dihydrate (Gypsum) Scale Formation on Heat Exchanger Surfaces: The Influence of Scale Inhibitors," *Journal of Colloid and Interface Science*, vol. 123, no. 2, pp. 523-536, 1988.
- [41] Z. Amjad, R. T. Landgraf and J. L. Penn, "Calcium sulfate dihydrate (gypsum) scale inhibition by PAA, PAPEMP, and PAA/PAPEMP blend," *International Journal of Corrosion and Scale Inhibition*, vol. 3, no. 1, pp. 35-47, 2014.
- [42] P. G. Klepetsanis, A. Kladi, T. Ostvold, C. G. Kontoyiannis, P. G. Koutsoukos, Z. Amjad and M. M. Reddy, "The inhibition of calcium carbonate formation in aqueous supersaturated solutions, Spontaneous precipitation and seeded crystal growth," in *Advances in Crystal Growth Inhibition Technologies*, New York, Springer US, 2002, pp. 123-137.

- [43] B. C. McCool, A. Rahardianto and Y. Cohen, "Antiscalant removal in accelerated desupersaturation of RO concentrate via chemically-enhanced seeded precipitation (CESP)," *Water Research*, vol. 46, no. 13, pp. 4261-4271, 2012.
- [44] A. Singer and P. Huang, "Effects of humic acid on the crystallization of aluminum hydroxides," *Clays and Clay Minerals*, vol. 38, no. 1, pp. 47-52, 1990.
- [45] H. Kodama and M. Schnitzer, "Effect of fulvic acid on the crystallization of aluminum hydroxides," *Geoderma*, vol. 24, no. 3, pp. 195-205, 1980.
- [46] H. Kodama and M. Schnitzer, "Effect of fulvic acid on the crystallization of Fe(III) oxides," *Geoderma*, vol. 19, no. 4, pp. 279-291, 1977.
- [47] Z. Amjad, "Seeded Growth of Calcium-containing scale forming minerals in the presence of inhibitors," *Corrosion/88*, vol. 421, pp. 1-11, 1988.
- [48] W. H. Leung and G. H. Nancollas, "A Kinetic study of the seeded growth of barium sulfate in the presence of additives," *Journal of Inorganic and Nuclear Chemistry*, vol. 40, no. 11, pp. 1871-1875, 1978.
- [49] M. Giuliatti, M. M. Seckler, S. Derenzo, M. I. Re and E. Cekinski, "Industrial crystallization and precipitation from solutions: state of the technique," *Brazilian Journal of Chemical Engineering*, vol. 18, no. 4, 2001.
- [50] T. N. Zwietering, "Suspending of solid particles in liquid by agitators," *Chemical Engineering Science*, vol. 8, no. 3, pp. 244-253, 1958.
- [51] Y. Wang, C. Combe and M. M. Clark, "The effects of pH and Calcium on the diffusion coefficient of humic acid," *Journal of Membrane Science*, vol. 183, pp. 49-60, 2001.

Chapter 7: References

- [52] S. Hong and M. Elimelech, "Chemical and physical aspects of natural organic matter (NOM) fouling of nanofiltration membranes," *Journal of Membrane Science*, vol. 159, pp. 159-181, 1997.
- [53] B. A. G. de Melo, F. L. Motta and M. H. A. Santan, "Humic acids: Structural properties and multiple functionalities for novel technological developments," *Materials Science and Engineering C*, vol. 62, pp. 967-974, 2016.
- [54] E. Thurman, R. L. Wershaw, R. Malcolm and D. Pinckney, "Molecular size of aquatic humic substances," *Organic Geochemistry*, vol. 4, no. 1, pp. 27-35, 1982.
- [55] V. Mema, "Identification of Extraction Methods for the Production of Humic Acids from Black Liquor," Stellenbosch University, Stellenbosch, 2006.
- [56] N. Kloster, M. Brigante, G. Zanini and M. Avena, "Aggregation Kinetics of Humic Acids in the Presence of Calcium Ions," *Colloids and Surfaces A: Physicochemical and Engineering Aspects*, vol. 427, pp. 76-82, 2013.
- [57] M. M. Reddy and A. R. Hoch, "Calcite Crystal Growth Rate Inhibition by Aquatic Humic Substances," in *Advances in Crystal Growth Inhibition Technologies*, New York, Springer US, 2002, pp. 107-121.
- [58] G. Naidu, S. Jeong and S. Vigneswaran, "Interaction of humic substances on fouling in membrane distillation for seawater desalination," *Chemical Engineering Journal*, vol. 262, pp. 946-957, 2015.
- [59] J. Na and Z. Yonggang, "The Effect of Humic Acid on Ultrafiltration Membrane Fouling," *Tenside Surfactants Detergents*, vol. 41, no. 5, pp. 214-219, 2004.
- [60] C. Tang, Z. He, F. Zhao, X. Liang and Z. Li, "Effects of cations on the formation of ultrafiltration membrane fouling layers when filtering fulvic acid," *Desalination*, vol. 352, pp. 174-180, 2014.

- [61] M. Brigante, G. Zanini and M. Avena, "Effect of pH, anions and cations on the dissolutions kinetics of humic acid particles," *Colloids and Surfaces A: Physicochemical and Engineering Aspects*, vol. 347, pp. 180-186, 2009.
- [62] M. Brigante, G. Zanini and M. Avena, "On the dissolution kinetics of humic acid particles; Effects of pH, temperature and Ca^{2+} concentration," *Colloids and Surfaces A: Physicochemical and Engineering Aspects*, vol. 294, pp. 64-70, 2007.
- [63] C. J. Milne, D. G. Kinniburgh, W. H. van Riemsdijk and E. Tipping, "Generic NICA-Donnan Model Parameters for Metal-Ion Binding by Humic Substances," *Environmental Science & Technology*, vol. 37, pp. 958-971, 2003.
- [64] I. Christl, C. J. Milne, D. G. Kinniburgh and R. Krezschmar, "Relating ion binding by fulvic and humic acids to chemical composition and molecular size. 2. Metal binding," *Environmental Science & Technology*, vol. 35, no. 12, pp. 2512-2517, 2001.
- [65] M. Oner, O. Dogan and G. Oner, "The influence of polyelectrolytes architecture on calcium sulfate dihydrate growth retardation," *Journal of Crystal growth*, vol. 187, pp. 427-437, 1998.
- [66] F. Alimi, H. Elfil and A. Gadri, "Kinetics of the precipitation of calcium sulfate dihydrate in a desalination unit," *Desalination*, vol. 157, pp. 9-16, 2003.
- [67] J. Shukla, V. P. Mohanda and A. Kumar, "Effect of pH on the solubility of $\text{CaSO}_4 \cdot 2\text{H}_2\text{O}$ in Aqueous NaCl Solutions and Physicochemical Solution Properties at 35°C ," *Journal of Chemical Engineering Data*, vol. 53, pp. 2797-2800, 2008.
- [68] Ghorab, Y. Hanaa, Abou el Fetou and H. Safaa , "Factors affecting the solubility of gypsum: II. Effect of sodium hydroxide under various conditions," *Journal of Chemical Technology and Biotechnology*, vol. 35, no. 1, pp. 36-40, 1985.

Chapter 7: References

- [69] M. Schnitzer, "Recent findings on the characterization of humic substances extracted from soils from widely differing climatic zones," *Soil Organic Matter Studies; Proceedings of a Symposium Bruanschweig*, p. 117, 1976.
- [70] "International Humic Substance Society," International Humic Substance Society, [Online]. Available: www.ihss.com. [Accessed 15 August 2016].
- [71] M. E. Tadros, J. Skalny and R. S. Kalyoncu, "Kinetics of Calcium Hydroxide Crystal Growth from Solution," *Journal of Colloid and Interface Science*, vol. 55, no. 1, p. 1976, 1976.
- [72] J. G. Hering and M. M. Morel, "Humic Acid Complexation of Calcium and Copper," *Environmental Science Technology*, vol. 22, no. 10, pp. 1234-1237, 1988.
- [73] A. Braghetta, F. A. DiGiano and W. P. Ball, "Nanofiltration of Natural Organic Matter: pH and Ionic Strength Effects," *Journal of Environmental Engineering*, vol. 123, pp. 628-641, 1997.
- [74] J. G. Hering and F. M. M. Morel, "Humic Acid Complexation of Calcium and Copper," *Environmental Science Technology*, vol. 22, no. 10, pp. 1234-1237, 1988.
- [75] Z. Jue and J. C. Giddings, "Determination of Molecular Weight Distributions of Fulvic and Humic Acids Using Flow Field-Flow Fractionation," *Environmental Science Technology*, vol. 21, pp. 289-295, 1987.
- [76] M. M. Clark and P. Lucas, "Diffusion and partitioning of humic acid in a porous ultrafiltration membrane," *Journal of Membrane Science*, vol. 143, pp. 13-25, 1998.
- [77] D. B. Babcock and P. C. Singer, "Chlorination and Coagulation of Humic and Fulvic acids," *Journal (American Water Works Association)*, vol. 71, no. 3, pp. 149-152, 1979.

Appendix A: DETAILED METHODOLOGY

In this Appendix a detailed description is given of the preparation of solutions, the calibration and cleaning of pH probes and the experimental procedure that was used to carry out the experimental work of this study.

A.1. Solution preparation

The following solutions were prepared for use in the experimental work:

- Sodium sulphate
- Calcium chloride
- Ethylenediaminetetracetic acid (EDTA)
- Diluted hydrochloric acid
- Humic acid Solution
- Fulvic acid Solution

A.1.1. Sodium sulphate

Anhydrous sodium sulphate salt was dried overnight in a vacuum oven at 60-80°C. From the oven the dried salt was placed in a desiccator to cool down to ambient temperature (depending on the season, ambient temperature ranged from 14-25°C). The desired amount of sodium sulphate was weighed on an analytical scale with an accuracy of ± 0.001 grams. The weighed salt was then dissolved in MilliQ water in a grade A 1000 ml beaker. Although sodium sulphate is very soluble in water, the reaction with water is endothermic and the addition of heat will assist the process. After all the salt had been dissolved in water, the solution was poured into a grade A volumetric flask and the flask was filled up to the required volume. The solution was then left overnight to ensure complete dissolution of the salt before use.

Appendix A: Detailed Methodology

A.1.2. Calcium chloride

Calcium chloride has an extremely hygroscopic nature, which makes it possible for the calcium chloride to absorb water. This can result in lower calcium concentration than originally calculated. The calcium salt was therefore carefully weighed as quickly as possible on an analytical scale with an accuracy of ± 0.001 g. The salt was then easily dissolved in MilliQ water using grade A glassware. From there the salt solution was poured into a volumetric flask, filled up to the desired volume and also left overnight for complete dissolution to take effect before use.

A.1.3. Ethylenediaminetetracetic acid (EDTA)

EDTA was used for the cleaning of the batch reactors due to its ability to bind with metal ions and form complexes, especially with calcium. A solution of 0.03 M EDTA was used for this cleaning purpose. EDTA, in the form of a white powder, was weighed off and added to distilled water. EDTA does not dissolve in cold water below a pH of 8. Approximately 10 ml of 50% sodium hydroxide solution was added to increase the pH. The solution was placed on a magnetic stirrer with hotplate to increase the temperature. The hotplate setting was set to 5 and the solution left to stir until all the EDTA had been dissolved. Three litres of 0.03 M EDTA solution was prepared at a time. About 500 ml of 0.03 M EDTA solution was then used to clean the batch reactors each time.

A.1.4. Hydrochloric acid

A solution of 0.1 M hydrochloric acid was prepared by adding 10 ml of 32% hydrochloric acid, obtained from Merck, to a 1 L grade A volumetric flask. The flask was then filled up with distilled water. This solution was then used for all dilutions and standard preparations.

A.1.5. Humic acid

Commercial humic acid, obtained from Sigma-Aldrich, was used as is with no further purification of the powder. The following humic acid stock solutions were prepared for use in the experimental work:

A.1. Solution preparation**Table A-1: Humic acid concentration make up.**

Working Concentration (mg/l)	Working Volume (ml)	Make up concentration (mg/l)	Make Up Volume (ml)
5	10	205	500
10	10	410	500
15	10	615	500

All solutions were prepared in MilliQ water. For each of the working concentrations, 10 ml of the corresponding stock solutions were added to the supersaturated working fluid for each experimental run.

A.1.6. Fulvic acid

Fulvic acid obtained from the International Humic Substance Society (IHSS) was used with no further purification of the powder. Due to the expensive nature of the chemical, a stock solution of 615 mg/l was prepared. A volume of 250 ml of the solution was prepared by dissolving ± 154 mg of fulvic acid in MilliQ water. Fulvic acid was weighed with an analytical scale to an accuracy of ± 0.001 g. A grade A 250 ml volumetric flask was then used to measure off the correct volume. The prepared solution was stored in a fridge at a temperature of $\pm 4^{\circ}\text{C}$. The following concentrations were prepared through dilution of the stock solution to a total volume of 12 ml.

Table A-2: Fulvic acid concentration utilised.

Working Concentration (mg/l)	Stock solution concentration (mg/l)	Stock solution volume (ml)	Total volume (ml)
1.0		0.8	12
2.5		2.0	12
5.0	615	4.0	12
10.0		8.0	12
15.0		12	12

Appendix A: Detailed Methodology

A.2. Experimental procedure

For the batch crystallisation process the following step by step procedure was followed to carry out the experimental work:

- 1) Switch on the air conditioner of the laboratory. The environmental temperature is controlled in this manner to ensure that the temperature of the heating bath can be accurately controlled. If the laboratory temperature becomes elevated, the temperature of the heating bath tends to overshoot and bringing it back down to the correct temperature can be difficult and time consuming.
- 2) Make sure that all the valves from the heating bath are open.
- 3) Ensure that all pipes from the heating bath to the reactor vessel are secure and tightly fit to ensure that no water spillage might occur and damage any electrical equipment.
- 4) Switch on all plugs of the electrical equipment.
- 5) Turn on the control unit of the heating bath and set it to the correct temperature.
- 6) Turn on the circulator and pump.
- 7) Turn over the reactor vessels and place them gently on the magnetic stirrer.
- 8) Make sure that the vessels are dry on the inside. If there should be any water droplets still on the inside of the reactor, carefully dry these away.
- 9) Place the magnetic stirrer bars gently in the vessels.
- 10) Measure off 200 ml of each of the solutions calcium chloride (Solution 1) and sodium sulphate (Solution 2) using 200 ml volumetric flasks. Fill the last bit of the volumetric flask to the line dropwise with a plastic pipette.
- 11) Place solution 2 inside the heating bath.
- 12) Carefully pour over solution 1 into the reactor. Hold the top of the volumetric flask close to the inside surface of the reactor vessel to minimise splashing.
- 13) Place the PVC lid on top of the reactor.
- 14) Turn on the magnetic stirrer at an rpm setting of 400.
- 15) Calibrate the pH probe (see section A.3 for the calibration procedure).
- 16) After the pH and temperature probe have been placed inside the reactor vessel, wait for the correct temperature to be reached. Let a minimum of 30 min pass to ensure that solution 2 have reached the correct temperature.

A.2. Experimental procedure

- 17) When the correct temperature has been reached, remove solution 2 from the heating bath and dry the outside of the volumetric flask to ensure that the working fluid is not contaminated by any water droplets.
- 18) Carefully pour solution 2 into the reactor vessel following the same procedure as in step 12.
- 19) Start the stopwatch and start the logging of the pH and temperature.
- 20) Wait for the pH reading to stabilise and take down the reading.
- 21) If no additive is required, move on to step 24. Add 10 ml of the correct organic solution to the supersaturated mixture.
- 22) Repeat step 20).
- 23) Adjust the pH to the desired level. To increase the pH, add 0.05 M NaOH with a micropipette until the correct reading is reached and add 0.05 M HCl to decrease the pH level. At least 3-4 minutes is given for the adjustment of the pH level. The volume of NaOH and HCl added to adjust the pH is taken as negligible.
- 24) At 5 min take the first sample with a 5 ml grade A glass pipette.
- 25) Inject the 5 ml sample into a syringe equipped with a 0.22 μm syringe filter.
- 26) Push the sample through the syringe filter into a grade A 100 ml volumetric flask to ensure that all crystal particles are removed from the sample.
- 27) Fill the 100 ml volumetric flask up to the line with 0.1 M HCl solution. This will result in a dilution of 20 times to ensure that the sample is out of the supersaturated state.
- 28) Mark the volumetric flask clearly with the sample number.
- 29) For experimental runs without seeding move on to step 30. Add seed crystals within 1 min after the first sample was taken at 5 min. Seed crystals are weighed off in a centrifugal tube. A volume of 3 ml MilliQ water is added to the crystals and the milky wet solution is added to the supersaturated solution. The tube is then rinsed with another 1 ml of MilliQ water, which is also added to the mixture in the reactor.
- 30) Sample at time intervals. For long induction periods, sampling was carried out every half hour to an hour before the onset of crystallisation. As soon as crystallisation was observed, sampling was carried out every 10 min for the first

Appendix A: Detailed Methodology

hour, every 20 min for the second hour, every 30 min for the third hour and every 30 min to an hour for the remainder of an experimental run, if required.

- 31) After sampling, the samples need to be poured over into 15 ml centrifugal tubes for analysis. Mark two centrifugal tubes with the correct sample number (i.e. Sample Name and Number-A & B). Fill the two tubes with the correct sample. Duplicate samples were kept in order to rerun analyses if it was required later on. All samples are stored in a closed cupboard at ambient temperature in the laboratory.
- 32) At the completion of the experimental run, turn off the control unit for the heating bath, as well as the pump and circulator.
- 33) Empty the reactor vessel of its contents.
- 34) Fill the reactor vessel with 0.03 M EDTA solution (see section A.1.3. for preparation) and rinse at 1000 rpms for a minimum of 30 min.
- 35) Empty the reactor of EDTA solution, fill it up with distilled water and rinse at 1000 rpms for a minimum of 10 min.
- 36) Empty the reactor of the water, turn the reactor over on a paper towel and leave it to dry overnight.
- 37) Turn off the magnetic stirrer and all electrical plugs as well as the air conditioner of the laboratory.
- 38) Clean all necessary glassware required for the next experimental run (see section A.3. for cleaning of equipment).

A.3. Cleaning of equipment

a) Volumetric flask for working fluid

The 200 ml volumetric flasks used for the transport of solution 1 and 2 to the reactor were washed thoroughly with soap water, rinsed twice with tap water and lastly rinsed with distilled water. Thereafter the two flasks were dried overnight in a vacuum oven at a temperature of 60-80°C.

b) Pipette for sampling

The sampling pipette used during the experiments was rinsed 3 to 4 times between each sample with MilliQ water. This was done to ensure that any crystals that might have stayed behind after sampling were cleaned from the pipette. Between experiments the pipette was washed thoroughly using the same procedure and left to dry overnight.

c) Reactor vessel

After the completion of each experimental run the reactor was washed with EDTA solution for a minimum of 30 minutes. The EDTA solution was then poured out and the reactor was rinsed further with distilled water for a minimum of 10 minutes and left to dry overnight. Refer to Appendix A for the preparation of EDTA solution.

d) Volumetric flasks for sampling and dilution

The 100 ml volumetric flasks used for sampling and dilution were thoroughly cleaned with soap water between experiments. The flasks were rinsed 2 to 3 times with tap water and lastly rinsed with distilled water before it was left to dry overnight. Before each experimental run the flasks were rinsed again with the dilution medium (0.1 M HCl).

Appendix A: Detailed Methodology

A.4. pH calibration

Before the start of each experimental run carried out during this study, the pH probes were calibrated with a 3-point calibration. The pH electrode was calibrated in the pH range between 4.00 and 10.00 using pH buffer solutions of 4.00, 7.00 and 10.00. pH is very temperature sensitive. Therefore, temperature compensation was automatically implemented by the meter according to the temperature that was measured by the temperature probe. Calibration was performed as close to the working temperature as possible. The following procedure was followed for the calibration of the pH probe:

- 1) Switch on the Hanna meter and select calibration.
- 2) Clear the previous calibration.
- 3) Select the first pH buffer for calibration.
- 4) Remove the reference fill cap of the pH probe as well as the protective cap. The reference fill cap is removed to improve response time and pH readings.
- 5) Rinse the pH and temperature probe with distilled water. Make sure that all crystals that may have formed from the storage solution and the electrolyte solution are washed away.
- 6) Gradually shake dry the pH probe. Do not wipe the pH probe with a cloth or any other material as this will result in electrostatic charge and could damage the electrode.
- 7) Gently put the pH probe and temperature probe in the first pH buffer solution.
- 8) As soon as the meter has beeped that the reading is stable, press accept on the meter.
- 9) If the second pH buffer is not selected automatically, select the second pH buffer for calibration.
- 10) Repeat steps 5 to 8.
- 11) Select the last pH buffer for calibration and repeat steps 5 to 8 again.
- 12) At the completion of calibration, rinse the pH and temperature probe thoroughly and carefully shake dry the pH electrode and wipe dry the temperature probe. The pH and temperature probe can now be inserted into the reactor for the recording of the pH and temperature.

A.5. ICP calibration

- 13) After the completion of an experimental run, rinse the pH and temperature probe thoroughly with distilled water.
- 14) Replace the reference fill cap and protective cap of the probe. Make sure that there is ample storage solution in the protective cap. The pH probe can either be stored in 3.5 M potassium chloride (KCl) or pH 4.00 buffer solution.

A.5. ICP calibration

For the calibration of the ICP the following standard solutions were prepared:

- 1 ppm
- 10 ppm
- 50 ppm
- 100 ppm
- 150 ppm
- 250 ppm

The solutions were prepared through a series dilution of a 1000 ppm Ca standard solution. For each analytical run a calibration was performed. Three quality control (QC) samples of 10 ppm were prepared for each analytical run. This is done to ensure accuracy, reliability and repeatability of the ICP.

A.6. Reactor modifications

A second reactor was used for the experiments and this resulted in some discrepancies, since the first reactor could not be duplicated to a 100% degree. The new reactor had a smoother inside surface, an inside diameter of 72 mm and a height of 130 mm. This resulted in an increased induction period with the new reactor under the same conditions as was used for the original reactor (Figure A.1). Due to its cleaner and smoother inside finish, crystallisation was inhibited longer in the new reactor. A smoother inside surface means that the inside surface has less roughness and imperfections, which means that there are less areas where particles could attach to create crystal growth 'areas'. This has an overall delaying effect on the crystallisation process.

Appendix A: Detailed Methodology

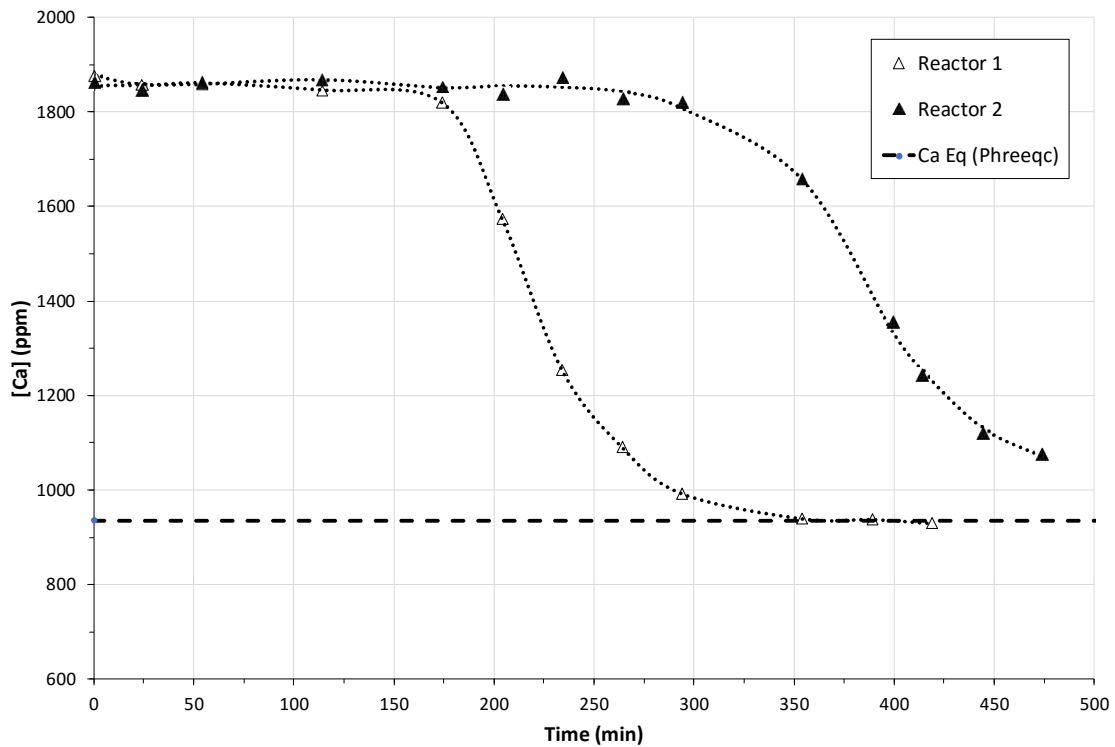


Figure A.1: Desupersaturation curves for the old reactor compared to the new reactor before treatment.

Due to the phenomenon described above, all reaction vessels were treated with hydrofluoric acid and baked overnight to ensure that they were clean and smooth on the inside. Furthermore, the decision was made to use a single reactor for a single supersaturation concentration for spontaneous crystallisation. The same was done as far as possible for experiments that were conducted in the presence of seed crystals. However, this effect was assumed to be negligible in the presence of seed crystals with constant agitation.

Figure A.2. presents the desupersaturation curves obtained for repeat runs in both reactors after treatment. It is clear that the results are much more comparable. Any deviations could be attributed to experimental and analytical error or slight differences in reactor size.

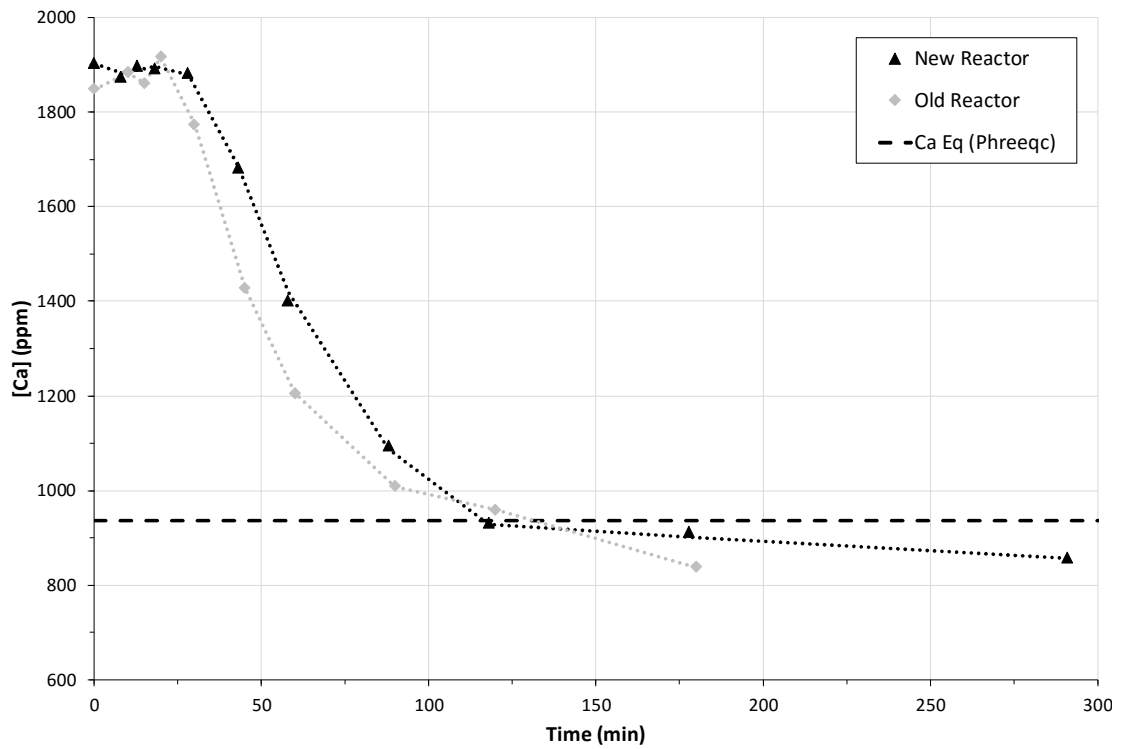
A.6. Reactor modifications

Figure A.2: Desupersaturation curves for the old reactor compared to the new reactor after treatment.

Appendix B: Experimental results

Appendix B: EXPERIMENTAL RESULTS

The experimental raw data of each relevant experiment carried out during this project is presented in this chapter. All experiments were carried out at a temperature of 25°C and a constant stirring rate of 400 rpm. All pH values quoted are the initial values recorded for each experiment. For the preliminary and baseline experiments, the stated pH value is the value that was recorded after the supersaturated solutions had been mixed completely. In experiments where pH adjustment was required, the value after adjustment was recorded before the first sample was taken.

All reported calcium concentrations are the absolute measured values (in ppm or mg/l), multiplied with the dilution factor (20x). The molar values are also reported and were used for generation of the kinetic data in this document. Molar values are calculated by dividing the absolute measured value by the molar mass of calcium (40.08 g/mol) and multiplying the answer with the dilution factor.

B.1. Preliminary results

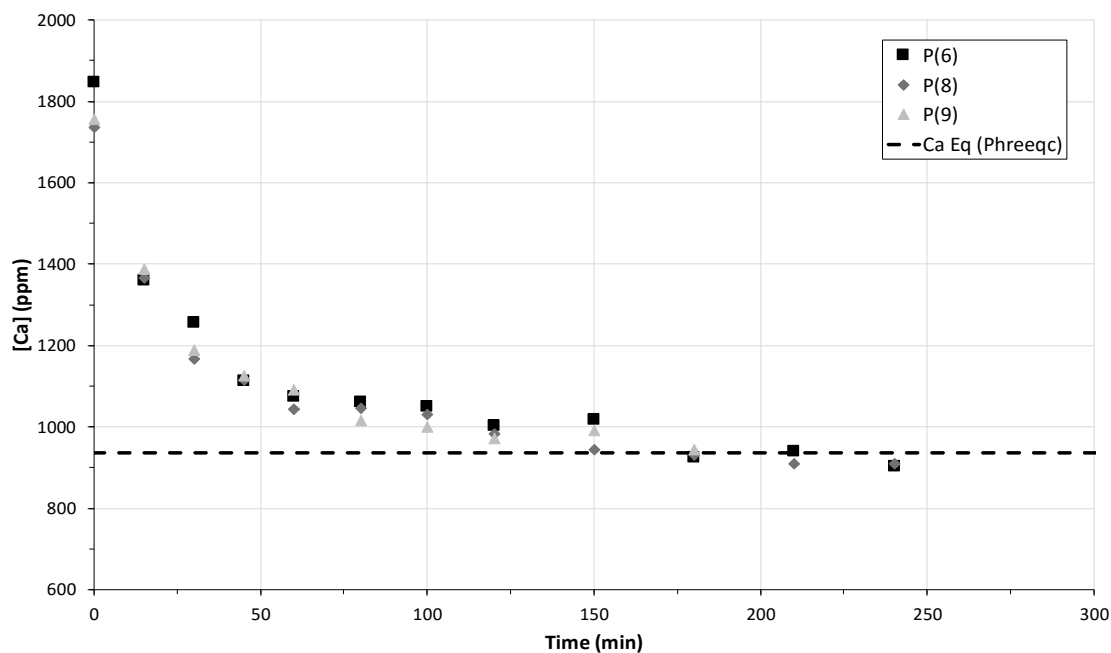


Figure B.1: Desupersaturation curves for preliminary runs P(6), P(8) and P(9) at 0.05 mol/l [Ca], 15 mg/l HA, 2000 mg/l Seed and Temperature of 25°C.

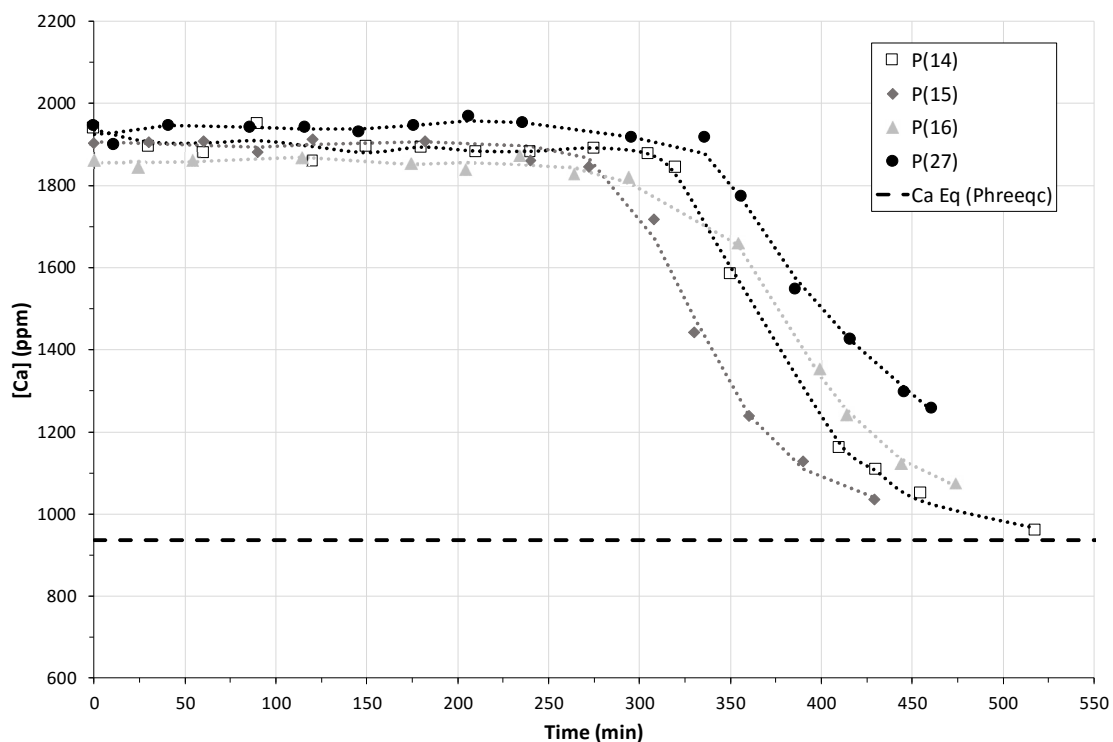
B.1. Preliminary results

Figure B.2: Desupersaturation curves for preliminary runs P(14), P(15), P(16) and P(27) at 0.05 mol/l [Ca], 15 mg/l HA and Temperature 25°C with no seeding.

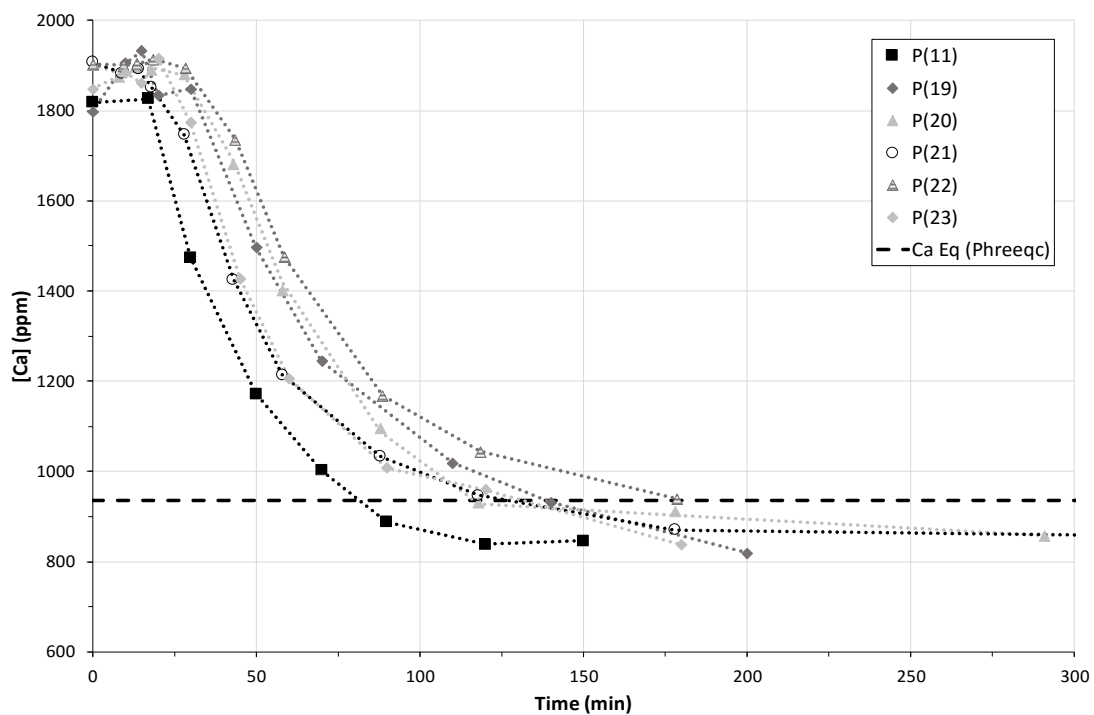


Figure B.3: Desupersaturation curves for preliminary runs P(11), P(19) – P(23). [Ca] = 0.05 mol/l and Temperature 25°C.

Appendix B: Experimental results**Table B.1: Preliminary experimental data for P(6) and P(8).**

Experimental Conditions					
Initial Concentration (mol/l) $\times 10^3$			Humic Acid (mg/l)		Seed Crystals (mg/l)
50			15		2000
P (6)			P (8)		
Time (min)	[Ca] (ppm)	[Ca] (mol/l) $\times 10^3$	Time (min)	[Ca] (ppm)	[Ca] (mol/l) $\times 10^3$
0	1846.000	46.058	0	1736.472	43.325
15	1360.000	33.932	15	1367.078	34.109
30	1256.000	31.337	30	1166.327	29.100
45	1114.000	27.794	45	1116.036	27.845
60	1074.000	26.796	60	1044.682	26.065
80	1062.000	26.497	80	1046.563	26.112
100	1050.000	26.198	100	1029.831	25.694
120	1001.920	24.998	120	982.968	24.525
150	1018.000	25.399	150	943.491	23.540
180	925.680	23.096	180	931.956	23.252
210	940.000	23.453	210	909.282	22.687
240	902.000	22.505	240	909.000	22.680

Table B.2: Preliminary experimental data for P(9) and P(28).

Experimental Conditions			
Initial Concentration (mol/l) $\times 10^3$		Humic Acid (mg/l)	Seed Crystals (mg/l)
50		15	2000
P (9)			
Time (min)	[Ca] (ppm)	[Ca] (mol/l) $\times 10^3$	
0	1755.338	43.796	
15	1388.851	34.652	
30	1189.385	29.675	
45	1125.495	28.081	
60	1091.162	27.225	
80	1014.608	25.315	
100	999.641	24.941	
120	973.169	24.281	
150	990.717	24.718	
180	944.593	23.568	

B.1. Preliminary results**Table B.3: Preliminary experimental data for P(11) and P(19).**

Experimental Conditions					
Initial Concentration (mol/l) $\times 10^3$		Humic Acid (mg/l)		Seed Crystals (mg/l)	
50		-		-	
P (11)			P(19)		
Time (min)	[Ca] (ppm)	[Ca] (mol/l) $\times 10^3$	Time (min)	[Ca] (ppm)	[Ca] (mol/l) $\times 10^3$
0	1818.000	45.359	0	1798.238	44.866
17	1826.000	45.559	10	1905.809	47.550
30	1474.000	36.776	15	1932.813	48.224
50	1172.000	29.242	20	1833.953	45.757
70	1002.000	25.000	30	1848.396	46.118
90	888.000	22.156	50	1496.723	37.343
120	838.000	20.908	70	1243.968	31.037
150	846.000	21.108	110	1018.569	25.413
			140	931.183	23.233
			200	819.295	20.441

Table B.4: Preliminary experimental data for P(20) and P(21).

Experimental Conditions					
Initial Concentration (mol/l) $\times 10^3$		Humic Acid (mg/l)		Seed Crystals (mg/l)	
50		-		-	
P (20)			P(21)		
Time (min)	[Ca] (ppm)	[Ca] (mol/l) $\times 10^3$	Time (min)	[Ca] (ppm)	[Ca] (mol/l) $\times 10^3$
0	1902.344	47.464	0	1907.192	47.585
8	1874.140	46.760	9	1883.180	46.986
13	1896.844	47.326	14	1891.963	47.205
18	1890.929	47.179	18	1850.819	46.178
28	1881.034	46.932	28	1746.043	43.564
43	1681.382	41.951	43	1425.536	35.567
58	1401.448	34.966	58	1214.385	30.299
88	1095.347	27.329	88	1033.484	25.786
118	931.514	23.241	118	946.459	23.614
178	911.482	22.742	178	870.144	21.710
291	857.394	21.392	378	852.436	21.268

Appendix B: Experimental results**Table B.5: Preliminary experimental data for P(22) and P(23).**

Experimental Conditions					
Initial Concentration (mol/l) $\times 10^3$		Humic Acid (mg/l)		Seed Crystals (mg/l)	
50		-		-	
P (22)			P(23)		
Time (min)	[Ca] (ppm)	[Ca] (mol/l) $\times 10^3$	Time (min)	[Ca] (ppm)	[Ca] (mol/l) $\times 10^3$
0	1902.161	47.459	0	1848.410	46.118
10	1900.632	47.421	10	1883.288	46.988
14	1903.059	47.482	15	1860.755	46.426
19	1913.966	47.754	20	1915.994	47.804
29	1893.813	47.251	30	1773.501	44.249
44	1735.414	43.299	45	1427.114	35.607
59	1475.624	36.817	60	1205.338	30.073
89	1167.487	29.129	90	1008.264	25.156
119	1043.789	26.043	120	959.504	23.940
179	938.661	23.420	180	837.783	20.903

Table B.6: Preliminary experimental data for P(13) and P(14).

Experimental Conditions					
Initial Concentration (mol/l) $\times 10^3$		Humic Acid (mg/l)		Seed Crystals (mg/l)	
50		15		-	
P (13)			P(14)		
Time (min)	[Ca] (ppm)	[Ca] (mol/l) $\times 10^3$	Time (min)	[Ca] (ppm)	[Ca] (mol/l) $\times 10^3$
0	1662.602	41.482	0	1939.915	48.401
30	1624.864	40.541	30	1895.582	47.295
60	1641.779	40.963	60	1878.922	46.879
90	1650.133	41.171	90	1949.399	48.638
120	1638.855	40.890	120	1859.963	46.406
150	1598.627	39.886	150	1893.944	47.254
180	1548.074	38.625	180	1891.868	47.202
195	1448.131	36.131	210	1881.494	46.943
210	1294.824	32.306	240	1881.203	46.936
225	1192.336	29.749	275	1889.587	47.145
240	1108.174	27.649	305	1877.634	46.847
270	1005.492	25.087	320	1843.655	45.999
300	938.372	23.412	350	1583.378	39.505
335	894.318	22.313	410	1162.025	28.993
			430	1108.359	27.654
			455	1051.280	26.230
			518	960.526	23.965

B.1. Preliminary results**Table B.7: Preliminary experimental data for P(15) and P(17).**

Experimental Conditions					
Initial Concentration (mol/l) $\times 10^3$			Humic Acid (mg/l)		Seed Crystals (mg/l)
50			15		-
P (15)			P(17)		
Time (min)	[Ca] (ppm)	[Ca] (mol/l) $\times 10^3$	Time (min)	[Ca] (ppm)	[Ca] (mol/l) $\times 10^3$
0	1902.766	47.474	0	1862.435	46.468
30	1906.688	47.572	24	1844.449	46.019
60	1907.247	47.586	54	1861.844	46.453
90	1881.653	46.947	114	1867.671	46.599
120	1912.009	47.705	174	1852.882	46.230
182	1908.672	47.622	204	1838.300	45.866
240	1860.347	46.416	234	1872.697	46.724
272	1845.699	46.050	264	1827.470	45.596
308	1717.927	42.862	294	1819.635	45.400
330	1442.072	35.980	354	1659.677	41.409
360	1239.952	30.937	399	1354.761	33.801
390	1128.628	28.159	414	1242.173	30.992
429	1035.977	25.848	444	1120.619	27.960
			474	1075.464	26.833

Table B.8: Preliminary experimental data for P(18) and P(27).

Experimental Conditions					
Initial Concentration (mol/l) $\times 10^3$			Humic Acid (mg/l)		Seed Crystals (mg/l)
50			15		-
P (18)			P(27)		
Time (min)	[Ca] (ppm)	[Ca] (mol/l) $\times 10^3$	Time (min)	[Ca] (ppm)	[Ca] (mol/l) $\times 10^3$
0	1876.461	46.818	0	1945.442	48.539
24	1857.106	46.335	11	1900.105	47.408
54	1860.656	46.424	41	1946.016	48.553
114	1845.810	46.053	86	1941.684	48.445
174	1819.476	45.396	116	1941.148	48.432
204	1574.655	39.288	146	1929.329	48.137
234	1254.346	31.296	176	1944.862	48.525
264	1090.695	27.213	206	1967.707	49.094
294	992.546	24.764	236	1953.149	48.731
354	939.493	23.440	296	1917.214	47.835
389	937.834	23.399	336	1915.803	47.799
419	929.815	23.199	356	1773.079	44.239
			386	1546.816	38.593
			416	1424.159	35.533
			446	1297.449	32.371
			461	1256.914	31.360

Appendix B: Experimental results**Table B.9: Preliminary experimental data for P(15) and P(17).**

Experimental Conditions					
Initial Concentration (mol/l) $\times 10^3$			Humic Acid (mg/l)		Seed Crystals (mg/l)
50			5		-
P (24)			P(26)		
Time (min)	[Ca] (ppm)	[Ca] (mol/l) $\times 10^3$	Time (min)	[Ca] (ppm)	[Ca] (mol/l) $\times 10^3$
0	1891.159	47.185	0	1965.805	49.047
13	1956.101	48.805	12	1803.790	45.005
23	1947.109	48.581	22	1906.302	47.562
33	1926.204	48.059	32	1930.261	48.160
43	1854.977	46.282	42	1950.452	48.664
58	1945.661	48.544	57	1939.894	48.401
78	1932.517	48.217	77	1914.728	47.773
98	1849.785	46.152	97	1914.777	47.774
118	1661.533	41.455	117	1919.396	47.889
148	1373.570	34.271	147	1813.770	45.254
178	1116.975	27.869	177	1139.803	28.438
238	1049.148	26.176	237	1143.774	28.537
			297	979.332	24.434

Table B.10: Preliminary experimental data for P(25).

Experimental Conditions			
Initial Concentration (mol/l) $\times 10^3$		Humic Acid (mg/l)	Seed Crystals (mg/l)
50		10	-
P (25)			
Time (min)	[Ca] (ppm)	[Ca] (mol/l) $\times 10^3$	
0	1925.794	48.049	
10	1930.319	48.162	
20	1892.447	47.217	
30	1859.943	46.406	
40	1888.688	47.123	
55	1892.065	47.207	
75	1909.078	47.632	
95	1930.579	48.168	
115	1934.787	48.273	
145	1946.399	48.563	
175	1873.273	46.738	
235	1901.467	47.442	
265	1749.945	43.661	
295	1549.055	38.649	
325	1367.480	34.119	
385	1212.331	30.248	

B.1. Preliminary results**Table B.11: Preliminary experimental data for P(31) and P(34).**

Experimental Conditions		
Initial Concentration (mol/l) $\times 10^3$	Humic Acid (mg/l)	Seed Crystals (mg/l)
50	15	-
P (31)		
Seed Crystals (mg/l):	50	
Time (min)	[Ca] (ppm)	[Ca] (mol/l) $\times 10^3$
0	1723.519	43.002
11	1737.612	43.354
26	1746.290	43.570
41	1741.874	43.460
56	1870.732	46.675
71	1819.045	45.385
101	1822.654	45.475
132	1510.836	37.696
157	1530.567	38.188
176	1379.651	34.422
207	1158.949	28.916
236	1128.988	28.168
296	991.142	24.729
357	920.736	22.972
416	911.385	22.739
476	900.075	22.457

Table B.12: Preliminary experimental data for P(28) and P(35).

Experimental Conditions					
Initial Concentration (mol/l) $\times 10^3$		Humic Acid (mg/l)		Seed Crystals (mg/l)	
50		15		200	
P (28)			P (35)		
Time (min)	[Ca] (ppm)	[Ca] (mol/l) $\times 10^3$	Time (min)	[Ca] (ppm)	[Ca] (mol/l) $\times 10^3$
0	1925.984	48.053	0	1723.066	42.991
12	1878.318	46.864	7	1647.295	41.100
21	1808.068	45.111	19	1642.045	40.969
31	1769.711	44.154	39	1539.367	38.407
41	1716.318	42.822	59	1433.546	35.767
51	1639.880	40.915	79	1266.396	31.597
71	1593.541	39.759	99	1179.921	29.439
86	1496.900	37.348	119	1101.422	27.481
101	1406.404	35.090	149	1014.968	25.324
116	1380.687	34.448	179	976.728	24.369
146	1321.146	32.963	239	922.914	23.027
176	1227.198	30.619	299	877.670	21.898
236	1149.368	28.677	419	847.022	21.133
299	1104.945	27.568	479	844.173	21.062
386	1085.822	27.091			

Appendix B: Experimental results**Table B.13: Preliminary experimental data for P(31) and P(34).**

Experimental Conditions		
Initial Concentration (mol/l) $\times 10^3$		Humic Acid (mg/l)
50		15
P (31)		
Seed Crystals (mg/l):		50
Time (min)	[Ca] (ppm)	[Ca] (mol/l) $\times 10^3$
0	1723.519	43.002
11	1737.612	43.354
26	1746.290	43.570
41	1741.874	43.460
56	1870.732	46.675
71	1819.045	45.385
101	1822.654	45.475
132	1510.836	37.696
157	1530.567	38.188
176	1379.651	34.422
207	1158.949	28.916
236	1128.988	28.168
296	991.142	24.729
357	920.736	22.972
416	911.385	22.739
476	900.075	22.457

Table B.14: Preliminary experimental data for P(32).

Experimental Conditions		
Initial Concentration (mol/l) $\times 10^3$		Humic Acid (mg/l)
50		15
P (32)		
Seed Crystals (mg/l):		500
Time (min)	[Ca] (ppm)	[Ca] (mol/l) $\times 10^3$
0	1674.283	41.774
11	1489.356	37.160
26	1353.726	33.776
41	1222.982	30.514
56	1181.660	29.483
76	1092.347	27.254
96	1071.247	26.728
116	1003.833	25.046
146	967.680	24.144
176	970.024	24.202
236	903.009	22.530
296	884.857	22.077
356	895.685	22.347
416	881.460	21.993

B.1. Preliminary results**Table B.15: Preliminary experimental data for P(31) and P(34).**

Experimental Conditions					
Initial Concentration (mol/l) $\times 10^3$			Humic Acid (mg/l)		
50			15		
P (30)			P(33)		
Seed Crystals (mg/l):		1000	Seed Crystals (mg/l):		1000
Time (min)	[Ca] (ppm)	[Ca] (mol/l) $\times 10^3$	Time (min)	[Ca] (ppm)	[Ca] (mol/l) $\times 10^3$
0	1988.144	49.604	0	1705.976	42.564
9	1769.826	44.157	5	1668.241	41.623
19	1534.417	38.284	15	1381.367	34.465
29	1431.851	35.725	30	1221.272	30.471
39	1361.853	33.978	45	1150.251	28.699
49	1220.553	30.453	60	1072.549	26.760
59	1243.464	31.025	80	1068.381	26.656
79	1089.770	27.190	100	1022.769	25.518
99	1158.339	28.901	120	984.003	24.551
125	1115.503	27.832	150	906.327	22.613
169	1079.820	26.942	180	943.372	23.537
199	1041.608	25.988	240	922.603	23.019
229	1014.696	25.317	300	885.767	22.100
369	886.387	22.115	360	822.558	20.523
			420	869.783	21.701

Table B.16: Preliminary experimental data for P(7).

Experimental Conditions		
Initial Concentration (mol/l) $\times 10^3$		Humic Acid (mg/l)
50		-
P (7)		
Seed Crystals (mg/l):		2000
Time (min)	[Ca] (ppm)	[Ca] (mol/l) $\times 10^3$
0	1635.325	40.802
10	1350.453	33.694
20	1195.527	29.829
30	1118.256	27.901
40	1062.535	26.510
50	1042.840	26.019
60	1027.655	25.640
80	988.204	24.656
100	957.847	23.898
120	931.757	23.247
150	912.526	22.768
180	894.160	22.309

*Appendix B: Experimental results***B.2. Baseline data****Table B.17: BL-SS2 experimental raw data.**

Experimental Conditions					
Initial Concentration (mol/l) $\times 10^3$		Humic Acid (mg/l)		Seed Crystals (mg/l)	
37.1		-		-	
BL-SS2_A			BL-SS2_B		
pH		5.887	pH		5.877
Time (min)	[Ca] (ppm)	[Ca] (mol/l) $\times 10^3$	Time (min)	[Ca] (ppm)	[Ca] (mol/l) $\times 10^3$
0	1387.754	34.625	0	1391.149	34.709
8	1386.498	34.593	28	1420.109	35.432
15	1408.661	35.146	58	1423.117	35.507
25	1383.222	34.512	78	1395.226	34.811
43	1372.380	34.241	88	1407.230	35.111
58	1371.104	34.209	98	1351.835	33.728
88	1296.987	32.360	118	1311.255	32.716
118	1190.883	29.713	140	1177.739	29.385
178	1050.324	26.206	158	1097.706	27.388
238	882.276	22.013	178	995.999	24.850
328	844.189	21.063	238	869.303	21.689
418	826.025	20.609	329	838.182	20.913
478	828.389	20.668	418	819.692	20.451
			478	824.742	20.577

B.2. Baseline data**Table B.18 BL-SS3 experimental raw data.**

Experimental Conditions					
Initial Concentration (mol/l) $\times 10^3$		Humic Acid (mg/l)		Seed Crystals (mg/l)	
37.1		-		-	
BL-SS3_A			BL-SS3_B		
pH		5.752	pH		5.724
Time (min)	[Ca] (ppm)	[Ca] (mol/l) $\times 10^3$	Time (min)	[Ca] (ppm)	[Ca] (mol/l) $\times 10^3$
0	1738.455	43.375	0	1684.158	42.020
8	1724.527	43.027	8	1675.961	42.267
18	1766.485	44.074	18	1678.214	41.872
26	1692.710	42.233	23	1685.114	41.562
33	1646.222	41.073	33	1527.716	38.117
48	1424.344	35.538	48	1312.100	32.737
71	1113.179	27.774	73	1092.661	27.262
98	1015.916	25.347	98	973.504	24.289
118	972.830	24.272	118	939.312	23.436
148	919.259	22.936	148	888.207	22.161
178	908.613	22.670	178	863.351	21.541
238	892.919	22.278	238	851.168	21.237
328	897.515	22.393	328	846.207	21.113
418	869.926	21.705	418	846.902	21.130
478	865.182	21.586	478	837.997	20.908
BL-SS3_C					
pH		7.128			
Time (min)	[Ca] (ppm)	[Ca] (mol/l) $\times 10^3$			
0	1730.734	43.182			
10	1728.196	43.119			
22	1718.759	42.883			
30	1675.833	41.812			
40	1461.277	36.459			
55	1276.856	31.858			
75	1112.220	27.750			
98	1008.013	25.150			
119	952.773	23.772			
145	910.384	22.714			
175	869.793	21.701			
209	859.501	21.445			
235	835.581	20.848			
295	842.236	21.014			

Appendix B: Experimental results**Table B.19: BL-SS4 experimental raw data.**

Experimental Conditions					
Initial Concentration (mol/l) $\times 10^3$		Humic Acid (mg/l)		Seed Crystals (mg/l)	
37.1		-		-	
BL-SS4_A			BL-SS4_B		
pH	5.833		pH	5.776	
Time (min)	[Ca] (ppm)	[Ca] (mol/l) $\times 10^3$	Time (min)	[Ca] (ppm)	[Ca] (mol/l) $\times 10^3$
0	2283.725	56.9792	0	2271.047	56.6629
8	2258.368	56.3465	5	2275.531	56.7747
15	2134.138	53.247	9	2169.972	54.141
25	1657.167	41.3465	18	1649.001	41.1427
43	1269.492	31.6739	28	1302.360	32.494
58	1129.508	28.1813	40	1100.272	27.4519
88	1015.060	25.3259	58	980.904	24.4737
118	942.517	23.5159	88	952.423	23.7631
178	940.308	23.4608	118	975.754	24.3452
238	939.255	23.4345	178	968.473	24.1635
328	931.697	23.2459	238	941.441	23.489
418	929.422	23.1892	328	933.487	23.2906
478	932.394	23.2633	418	895.603	22.3454
			478	912.995	22.7793

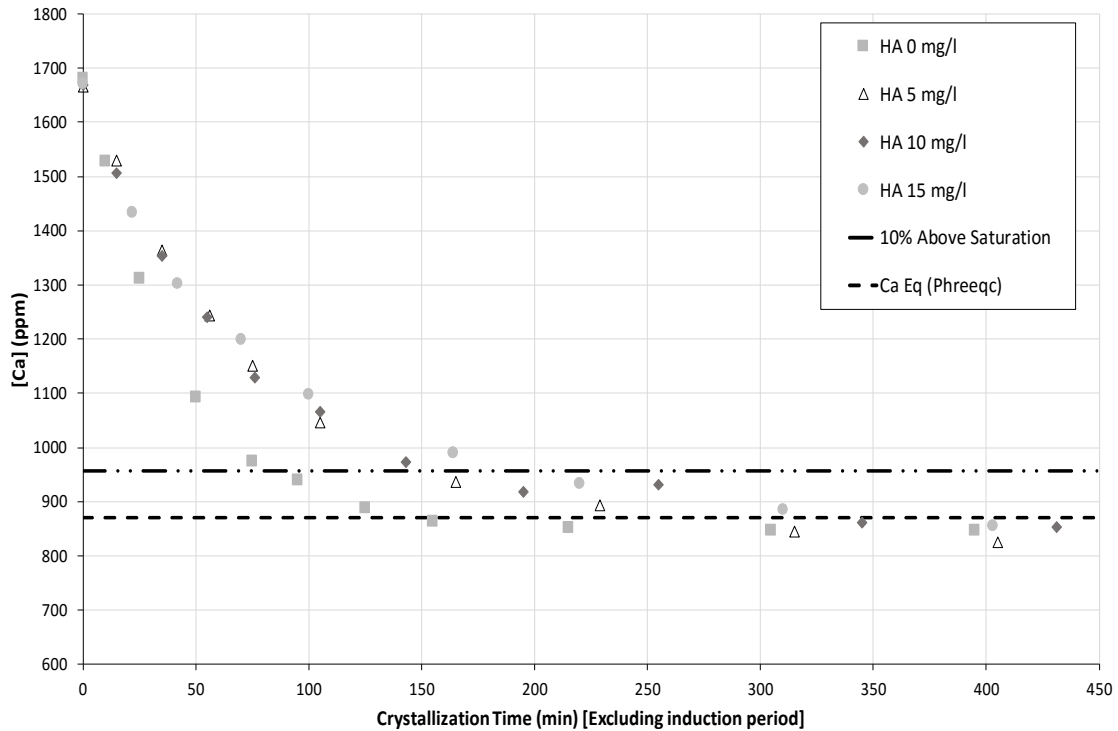
B.3. Humic acid unseeded experimental data

Figure B.4: Desupersaturation curves illustrating the effect of HA on the crystal growth curve at SS3, initial adjusted pH 4.5 and Temperature 25°C with no seeding.

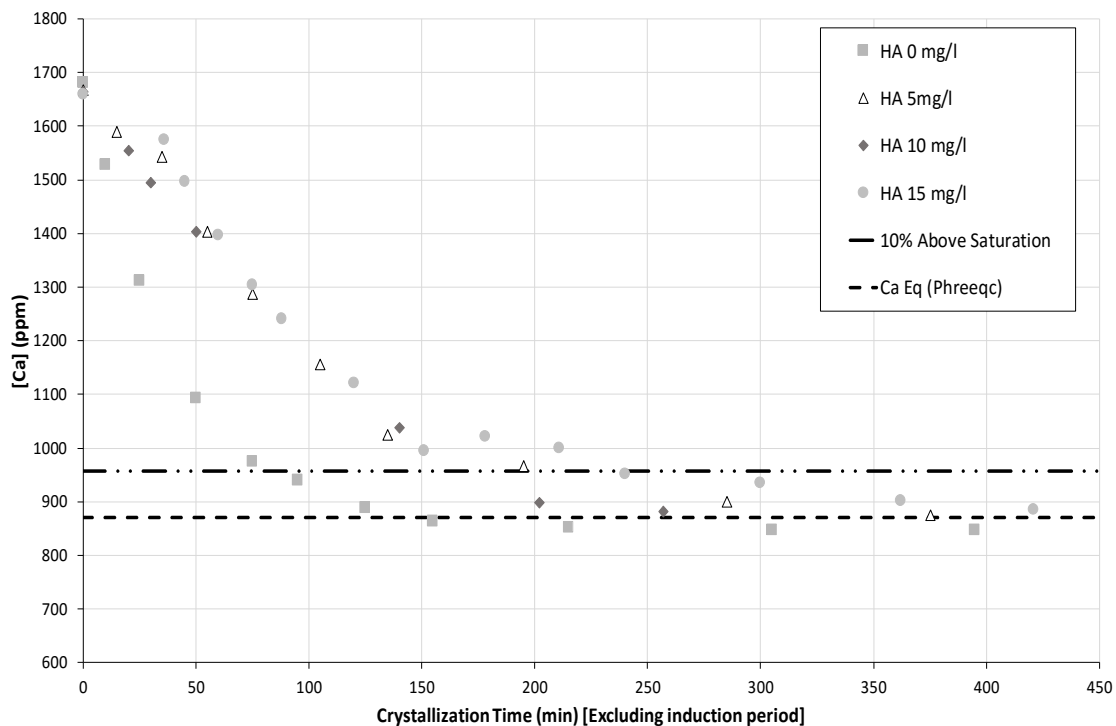
B.3. Humic acid unseeded experimental data

Figure B.5: Desupersaturation curves illustrating the effect of HA on the crystal growth curve at SS3, initial adjusted pH 9.5 and Temperature 25°C with no seeding.

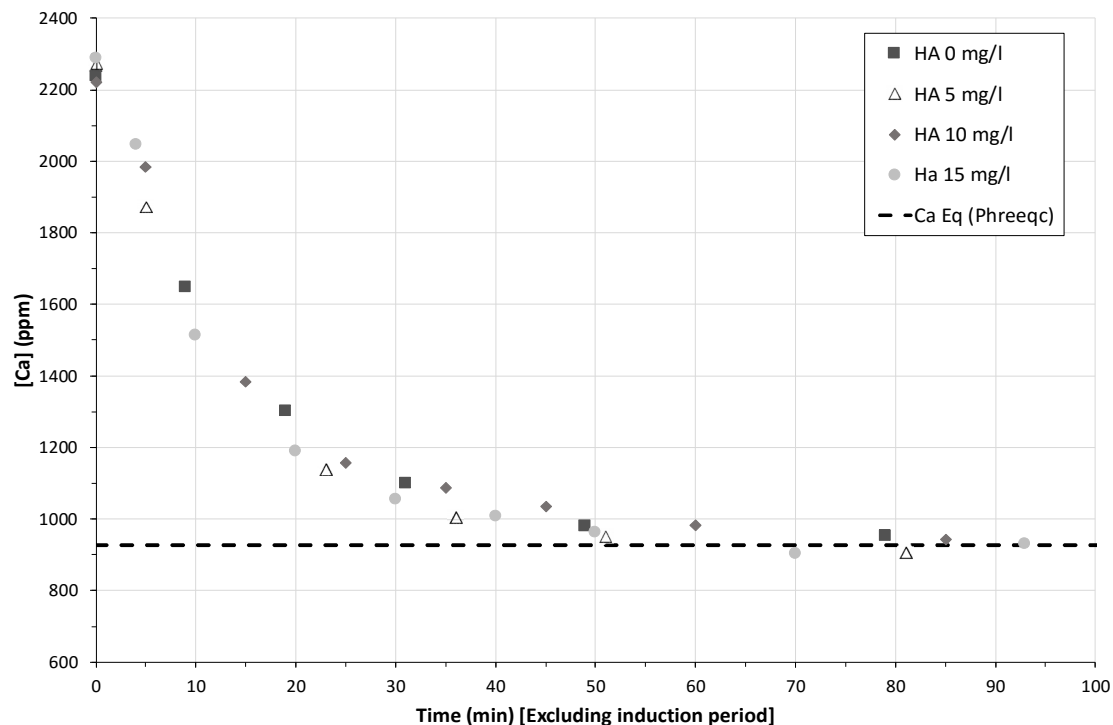


Figure B.6: Desupersaturation curves illustrating the effect of HA on the crystal growth curve at SS4, initial adjusted pH 4.5 and Temperature 25°C with no seeding.

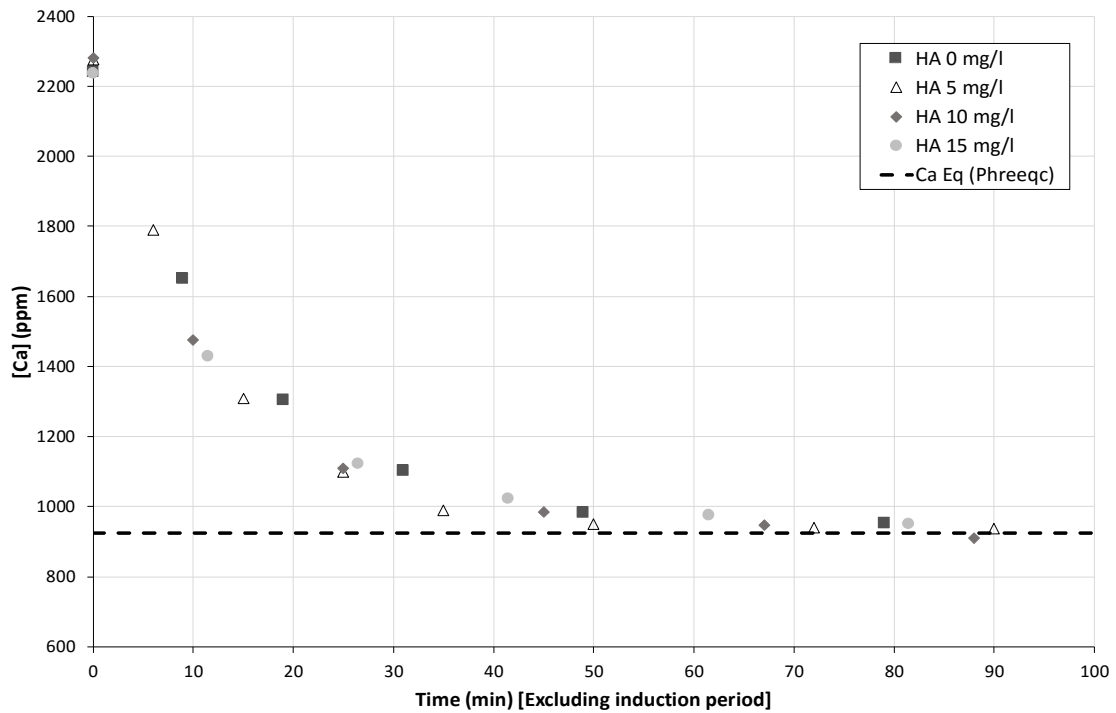
Appendix B: Experimental results

Figure B.7: Desupersaturation curves illustrating the effect of HA on the crystal growth curve at SS4, initial adjusted pH 7.0 and Temperature 25°C with no seeding.

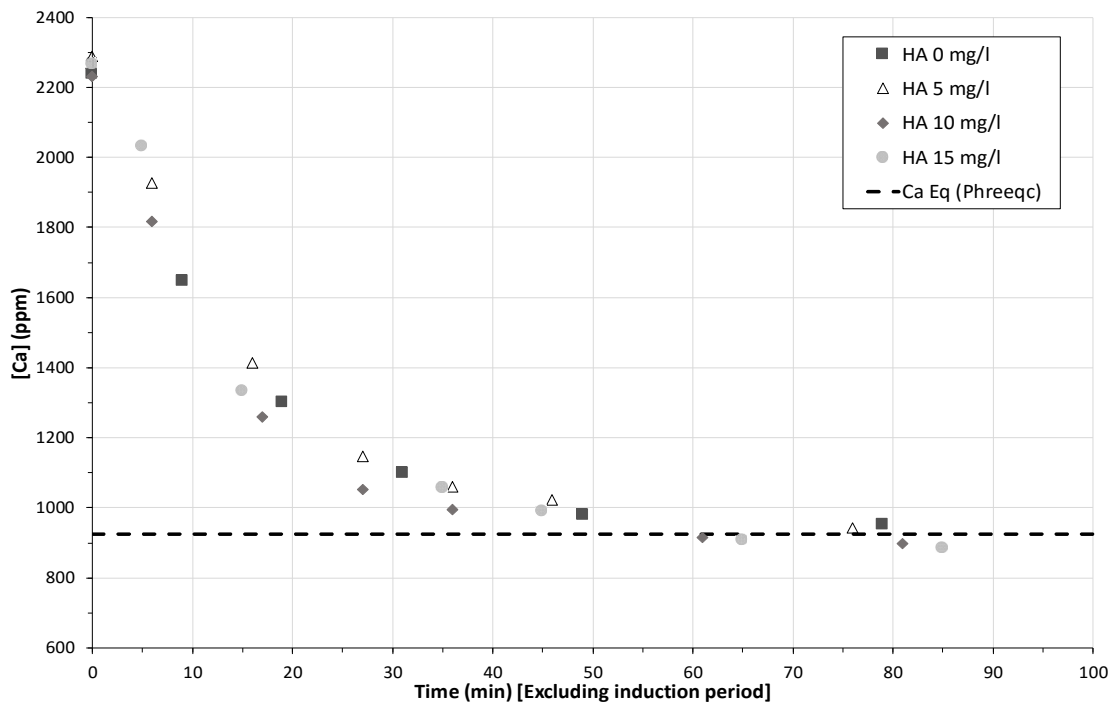


Figure B.8: Desupersaturation curves illustrating the effect of HA on the crystal growth curve at SS4, initial adjusted pH 9.5 and Temperature 25°C with no seeding.

B.3. Humic acid unseeded experimental data**Table B-20: HA-01 experimental raw data.**

Experimental Conditions		
Initial Concentration (mol/l) $\times 10^3$	Humic Acid (mg/l)	Seed Crystals (mg/l)
37.1	5	-
HA-01_A		
pH	4.542	
Time (min)	[Ca] (ppm)	[Ca] (mol/l) $\times 10^3$
0	1348.671	33.649
54	1354.771	33.802
115	1347.577	33.622
175	1348.259	33.639
236	1348.120	33.636
297	1355.462	33.819
357	1340.699	33.451

Table B-21: HA-02 experimental raw data.

Experimental Conditions		
Initial Concentration (mol/l) $\times 10^3$	Humic Acid (mg/l)	Seed Crystals (mg/l)
37.1	-	-
HA-02_A		
pH	7.048	
Time (min)	[Ca] (ppm)	[Ca] (mol/l) $\times 10^3$
0	1446.780	36.097
55	1436.839	35.849
115	1423.520	35.517
175	1395.842	34.826
237	1422.242	35.485
267	1468.464	36.638
355	1446.738	36.096
415	1443.678	36.020
445	1455.450	36.314
475	1432.816	35.749
535	1424.750	35.548
565	1409.972	35.179

Appendix B: Experimental results**Table B.22: HA-03 experimental raw data.**

Experimental Conditions		
Initial Concentration (mol/l) $\times 10^3$	Humic Acid (mg/l)	Seed Crystals (mg/l)
37.1	5	-
HA-03_A		
pH	9.495	
Time (min)	[Ca] (ppm)	[Ca] (mol/l) $\times 10^3$
0	1447.246	36.109
21	1431.228	35.709
46	1477.102	36.854
76	1472.525	36.740
106	1432.681	35.746
126	1396.172	34.835
166	1468.535	36.640
230	1452.175	36.232
330	1452.918	36.250
436	1439.205	35.908
526	1438.156	35.882

Table B.23: HA-04 experimental raw data.

Experimental Conditions							
Initial Concentration (mol/l) $\times 10^3$		Humic Acid (mg/l)		Seed Crystals (mg/l)			
41.9		5		-			
HA-04_A			HA-04_B				
pH		4.501		pH		4.515	
Time (min)	[Ca] (ppm)	[Ca] (mol/l) $\times 10^3$	Time (min)	[Ca] (ppm)	[Ca] (mol/l) $\times 10^3$		
0	1670.057	41.669	0	1683.832	42.048		
48	1681.850	41.848	25	1688.751	41.945		
55	1669.245	41.884	43	1660.515	41.828		
70	1643.896	40.904	51	1679.835	41.838		
85	1529.697	38.352	65	1676.717	41.752		
105	1363.521	34.073	81	1641.975	40.407		
126	1243.436	30.949	95	1502.479	37.959		
145	1150.172	28.721	117	1344.389	33.752		
175	1045.909	26.067	136	1239.760	30.887		
235	935.606	23.307	156	1150.763	28.628		
299	892.350	22.113	186	1053.042	26.152		
385	844.348	21.067	243	939.630	23.461		
475	824.973	20.449	304	914.612	22.618		
531	803.062	20.091	357	899.020	22.266		
			455	859.590			

B.3. Humic acid unseeded experimental data**Table B.24: HA-05 experimental raw data.**

Experimental Conditions					
Initial Concentration (mol/l) $\times 10^3$		Humic Acid (mg/l)		Seed Crystals (mg/l)	
37.1		5		-	
HA-05_A			HA-05_B		
pH 6.860			pH 7.130		
Time (min)	[Ca] (ppm)	[Ca] (mol/l) $\times 10^3$	Time (min)	[Ca] (ppm)	[Ca] (mol/l) $\times 10^3$
0	1677.673	41.858	0	1685.787	42.061
13	1688.104	42.118	54	1685.369	42.050
32	1677.434	41.852	69	1680.114	41.919
72	1686.181	42.070	84	1687.705	42.108
97	1686.145	42.069	100	1622.390	40.479
112	1674.519	41.779	114	1515.513	37.812
132	1544.656	38.539	134	1339.742	33.427
152	1412.329	35.238	174	1147.794	28.638
175	1256.318	31.345	205	1025.253	25.580
202	1162.537	29.005	234	957.385	23.887
232	1066.219	26.602	294	912.070	22.756
293	948.113	23.656	354	893.441	22.291
382	884.158	22.060	445	845.872	21.105
472	856.825	21.378	529	845.844	21.104
HA-05_C					
pH 7.061					
Time (min)	[Ca] (ppm)	[Ca] (mol/l) $\times 10^3$			
0	1715.790	42.809			
25	1710.946	42.688			
45	1712.223	42.720			
65	1700.588	42.430			
85	1702.089	42.467			
95	1708.363	42.624			
107	1700.217	42.421			
115	1708.991	42.639			
125	1651.339	41.201			
135	1493.621	37.266			
146	1298.784	32.405			
157	1183.583	29.531			
165	1126.068	28.096			
175	1079.688	26.938			
205	996.507	24.863			
235	950.187	23.707			
265	906.576	22.619			
296	880.868	21.978			
355	853.382	21.292			
397	853.923	21.305			

Appendix B: Experimental results**Table B.25: HA-06 experimental raw data.**

Experimental Conditions					
Initial Concentration (mol/l) $\times 10^3$		Humic Acid (mg/l)		Seed Crystals (mg/l)	
41.9		5		-	
HA-06_A			HA-06_B		
pH		9.506	pH		9.453
Time (min)	[Ca] (ppm)	[Ca] (mol/l) $\times 10^3$	Time (min)	[Ca] (ppm)	[Ca] (mol/l) $\times 10^3$
0	1676.335	41.825	0	1668.198	41.622
58	1681.814	41.961	55	1682.646	41.982
88	1678.783	41.886	85	1681.023	41.942
106	1752.839	43.734	110	1677.700	41.859
120	1663.292	41.499	137	1673.589	41.756
131	1634.413	40.779	145	1661.276	41.449
141	1565.267	39.054	160	1627.671	40.611
156	1371.003	34.207	175	1589.472	39.657
176	1315.311	32.817	195	1542.168	38.477
206	1128.011	28.144	215	1402.306	34.988
236	1026.270	25.606	235	1285.962	32.085
266	979.675	24.443	265	1155.351	28.826
326	925.081	23.081	295	1024.054	25.550
416	859.310	21.440	355	966.701	24.119
476	844.058	21.059	445	899.755	22.449
536	855.693	21.350	535	873.882	21.803

Table B.26: HA-07 experimental raw data.

Experimental Conditions					
Initial Concentration (mol/l) $\times 10^3$		Humic Acid (mg/l)		Seed Crystals (mg/l)	
56.6		5		-	
HA-07_A			HA-07_B		
pH		4.508	pH		4.536
Time (min)	[Ca] (ppm)	[Ca] (mol/l) $\times 10^3$	Time (min)	[Ca] (ppm)	[Ca] (mol/l) $\times 10^3$
0	2280.299	56.894	0	2275.996	56.786
5	2279.814	56.882	5	2272.160	56.691
12	1693.441	42.252	10	1873.286	46.739
22	1241.867	30.985	28	1137.254	28.375
32	1138.537	28.407	41	1006.120	25.103
42	1053.457	26.284	56	951.116	23.730
57	995.895	24.848	86	905.438	22.591
78	928.560	23.168	116	866.489	21.619
97	921.598	22.994	176	866.529	21.620
117	917.221	22.885	236	867.117	21.635
147	922.275	23.011	326	867.625	21.647
177	931.212	23.234	416	860.473	21.469
			476	864.412	21.567

B.3. Humic acid unseeded experimental data**Table B.27: HA-08 experimental raw data.**

Experimental Conditions					
Initial Concentration (mol/l) $\times 10^3$		Humic Acid (mg/l)		Seed Crystals (mg/l)	
56.6		5		-	
HA-08_A			HA-08_B		
pH 6.960			pH 7.198		
Time (min)	[Ca] (ppm)	[Ca] (mol/l) $\times 10^3$	Time (min)	[Ca] (ppm)	[Ca] (mol/l) $\times 10^3$
0	2276.405	56.797	0	2275.203	56.767
7	2275.109	56.764	8	2266.898	56.559
13	1788.211	44.616	15	1753.249	43.744
22	1308.028	32.635	30	1207.864	30.136
32	1099.413	27.430	45	1060.155	26.451
42	988.656	24.667	60	987.673	24.643
57	948.144	23.656	80	951.324	23.736
79	939.316	23.436	123	936.591	23.368
97	936.933	23.377	150	923.348	23.038
117	919.670	22.946	180	918.865	22.926
147	932.013	23.254	240	917.072	22.881
177	900.944	22.479	300	924.382	23.063

Table B.28: HA-09 experimental raw data.

Experimental Conditions			
Initial Concentration (mol/l) $\times 10^3$		Humic Acid (mg/l)	Seed Crystals (mg/l)
56.6		5	-
HA-09_A			
pH 9.470			
Time (min)	[Ca] (ppm)	[Ca] (mol/l) $\times 10^3$	
0	2299.915	57.383	
10	2280.346	56.895	
16	1927.079	48.081	
26	1414.139	35.283	
37	1147.253	28.624	
46	1061.344	26.481	
56	1023.181	25.528	
86	942.503	23.516	
116	932.432	23.264	
136	931.086	23.231	
206	930.627	23.219	
236	930.429	23.214	

Appendix B: Experimental results**Table B.29: HA-13 experimental raw data.**

Experimental Conditions					
Initial Concentration (mol/l) $\times 10^3$		Humic Acid (mg/l)		Seed Crystals (mg/l)	
41.9		10		-	
HA-13_A			HA-13_B		
pH		4.541	pH		4.512
Time (min)	[Ca] (ppm)	[Ca] (mol/l) $\times 10^3$	Time (min)	[Ca] (ppm)	[Ca] (mol/l) $\times 10^3$
0	1688.151	42.120	0	1672.235	41.722
55	1687.587	42.105	55	1667.985	41.616
98	1665.686	41.559	81	1668.590	41.631
115	1536.621	38.339	100	1664.863	41.538
135	1413.009	35.255	115	1506.350	37.584
155	1296.566	32.349	135	1352.818	33.753
175	1195.366	29.825	155	1239.905	30.936
205	1100.577	27.459	176	1129.437	28.180
235	1042.515	26.011	205	1065.917	26.595
295	947.308	23.635	243	972.982	24.276
355	916.178	22.859	295	917.235	22.885
415	880.158	21.960	355	930.305	23.211
477	864.843	21.578	445	861.388	21.492
			531	853.007	21.283

Table B.30: HA-14 experimental raw data.

Experimental Conditions					
Initial Concentration (mol/l) $\times 10^3$		Humic Acid (mg/l)		Seed Crystals (mg/l)	
41.9		10		-	
HA-14_A			HA-14_B		
pH		7.177	pH		7.228
Time (min)	[Ca] (ppm)	[Ca] (mol/l) $\times 10^3$	Time (min)	[Ca] (ppm)	[Ca] (mol/l) $\times 10^3$
0	1668.921	41.640	0	1664.398	41.527
55	1689.217	42.146	54	1676.294	41.824
111	1660.002	41.417	84	1672.058	41.718
130	1680.093	41.918	114	1667.711	41.610
145	1655.654	41.309	144	1669.198	41.647
165	1494.241	37.281	159	1658.606	41.382
186	1330.486	33.196	174	1661.756	41.461
206	1246.201	31.093	194	1664.168	41.521
237	1100.641	27.461	215	1452.673	36.244
266	1037.306	25.881	234	1365.247	34.063
295	981.984	24.501	259	1182.363	29.500
355	917.475	22.891	296	1078.870	26.918
448	871.615	21.747	354	969.743	24.195
533	870.312	21.714	444	880.861	21.978
			534	842.084	21.010

B.3. Humic acid unseeded experimental data**Table B.31: HA-15 experimental raw data.**

Experimental Conditions					
Initial Concentration (mol/l) $\times 10^3$		Humic Acid (mg/l)		Seed Crystals (mg/l)	
41.9		10		-	
HA-15_A			HA-15_B		
pH		9.422	pH		9.493
Time (min)	[Ca] (ppm)	[Ca] (mol/l) $\times 10^3$	Time (min)	[Ca] (ppm)	[Ca] (mol/l) $\times 10^3$
0	1696.401	42.325	0	1673.865	41.763
47	1668.469	41.628	54	1666.617	41.582
107	1658.606	41.382	99	1669.185	41.646
172	1655.471	41.304	134	1670.304	41.674
197	1668.893	41.639	176	1666.020	41.567
222	1632.399	40.729	206	1668.889	41.639
237	1644.096	41.020	222	1665.897	41.564
252	1552.804	38.743	234	1668.566	41.631
267	1339.789	33.428	254	1668.872	41.639
282	1200.029	29.941	274	1623.544	40.508
322	1020.014	25.449	294	1553.754	38.766
352	974.043	24.302	304	1494.007	37.276
417	907.431	22.640	324	1402.207	34.985
472	876.756	21.875	414	1037.360	25.882
			476	898.121	22.408
			531	880.671	21.973

Table B.32: HA-16 experimental raw data.

Experimental Conditions					
Initial Concentration (mol/l) $\times 10^3$		Humic Acid (mg/l)		Seed Crystals (mg/l)	
56.6		10		-	
HA-16_A			HA-16_B		
pH		4.508	pH		4.523
Time (min)	[Ca] (ppm)	[Ca] (mol/l) $\times 10^3$	Time (min)	[Ca] (ppm)	[Ca] (mol/l) $\times 10^3$
0	2222.317	55.447	0	2230.001	55.639
7	2220.102	55.392	6	2247.982	56.087
12	1984.212	49.506	9	2216.662	55.306
22	1384.880	34.553	19	1476.368	36.836
32	1157.002	28.867	29	1161.952	28.991
42	1086.578	27.110	44	1022.540	25.512
52	1034.736	25.817	68	942.594	23.518
67	981.906	24.499	89	898.133	22.409
92	942.669	23.520	99	930.501	23.216
117	926.218	23.109	119	930.872	23.225
147	919.105	22.932	156	918.964	22.928
178	922.974	23.028	179	919.385	22.939
			241	910.123	22.708

Appendix B: Experimental results**Table B.33: HA-17 experimental raw data.**

Experimental Conditions					
Initial Concentration (mol/l) $\times 10^3$		Humic Acid (mg/l)		Seed Crystals (mg/l)	
56.6		10		-	
HA-17_A			HA-17_B		
pH		7.275	pH		7.103
Time (min)	[Ca] (ppm)	[Ca] (mol/l) $\times 10^3$	Time (min)	[Ca] (ppm)	[Ca] (mol/l) $\times 10^3$
0	2295.631	57.276	0	2269.118	56.615
5	2282.909	56.959	7	2290.289	57.143
10	2256.708	56.305	12	2268.596	56.602
20	1474.945	36.800	22	1429.783	35.673
35	1107.744	27.638	37	1069.455	26.683
55	984.234	24.557	57	952.708	23.770
77	945.257	23.584	80	896.259	22.362
98	908.769	22.674	102	863.224	21.538
115	905.361	22.589	117	922.036	23.005
145	917.548	22.893	150	920.651	22.970
175	913.858	22.801	175	919.156	22.933
236	923.255	23.035	237	919.507	22.942
299	921.964	23.003			

Table B.34: HA-18 experimental raw data.

Experimental Conditions					
Initial Concentration (mol/l) $\times 10^3$		Humic Acid (mg/l)		Seed Crystals (mg/l)	
56.6		10		-	
HA-18_A			HA-18_B		
pH		9.505	pH		9.485
Time (min)	[Ca] (ppm)	[Ca] (mol/l) $\times 10^3$	Time (min)	[Ca] (ppm)	[Ca] (mol/l) $\times 10^3$
0	2249.277	56.120	0	2290.468	57.147
7	2242.548	55.952	12	2289.197	57.116
16	2206.678	55.057	16	2289.552	57.125
22	1819.090	45.386	22	1773.764	44.256
33	1261.179	31.467	35	1199.807	29.935
43	1053.580	26.287	42	1130.043	28.195
52	996.100	24.853	57	987.545	24.639
77	917.362	22.888	84	939.585	23.443
97	899.321	22.438	98	912.862	22.776
117	948.774	23.672	117	909.684	22.697
147	942.366	23.512	147	931.373	23.238
197	923.748	23.048	197	918.022	22.905
254	888.653	22.172	241	925.947	23.102

B.3. Humic acid unseeded experimental data**Table B.35: HA-22 experimental raw data.**

Experimental Conditions		
Initial Concentration (mol/l) $\times 10^3$	Humic Acid (mg/l)	Seed Crystals (mg/l)
41.9	15	-
HA-22_B		
pH		4.512
Time (min)	[Ca] (ppm)	[Ca] (mol/l) $\times 10^3$
0	1676.678	41.833
56	1685.272	42.048
86	1682.166	41.970
100	1687.775	42.110
115	1682.422	41.977
135	1605.160	40.049
157	1432.759	35.747
177	1301.368	32.469
205	1198.533	29.904
235	1096.857	27.367
299	990.079	24.703
355	932.252	23.260
445	884.756	22.075
538	854.055	21.309

Table B.36: HA-23 experimental raw data.

Experimental Conditions		
Initial Concentration (mol/l) $\times 10^3$	Humic Acid (mg/l)	Seed Crystals (mg/l)
41.9	15	-
HA-23_A		HA-23_B
pH		6.978
7.245		
Time (min)	[Ca] (ppm)	[Ca] (mol/l) $\times 10^3$
0	1666.499	41.579
53	1642.834	40.989
113	1682.636	41.982
153	1686.410	42.076
188	1711.457	42.701
238	1694.822	42.286
253	1686.069	42.068
273	1676.314	41.824
293	1550.666	38.689
313	1431.497	35.716
343	1236.638	30.854
383	1104.183	27.549
413	1074.388	26.806
473	999.027	24.926
533	934.694	23.321
591	927.099	23.131
Time (min)	[Ca] (ppm)	[Ca] (mol/l) $\times 10^3$
0	1673.300	41.749
55	1672.349	41.725
115	1686.985	42.090
175	1690.990	42.190
207	1675.748	41.810
225	1674.178	41.771
240	1678.011	41.867
255	1686.427	42.077
275	1683.259	41.997
295	1651.666	41.209
325	1450.523	36.191
356	1288.054	32.137
445	1021.350	25.483
548	941.664	23.495
595	922.263	23.011
		41.749

Appendix B: Experimental results**Table B.37: HA-24 experimental raw data.**

Experimental Conditions					
Initial Concentration (mol/l) $\times 10^3$		Humic Acid (mg/l)		Seed Crystals (mg/l)	
41.9		15		-	
HA-24_A			HA-24_B		
pH		9.507	pH		9.541
Time (min)	[Ca] (ppm)	[Ca] (mol/l) $\times 10^3$	Time (min)	[Ca] (ppm)	[Ca] (mol/l) $\times 10^3$
0	1660.416	41.428	0	1677.087	41.843
52	1643.696	41.010	55	1688.706	42.133
112	1651.847	41.214	115	1663.029	41.493
173	1652.348	41.226	175	1655.08	41.294
215	1644.683	41.035	236	1652.519	41.231
277	1611.000	40.195	266	1636.346	40.827
292	1658.151	41.371	295	1644.261	41.024
318	1684.419	42.026	331	1573.311	39.254
333	1661.983	41.467	340	1495.734	37.319
352	1658.465	41.379	355	1396.613	34.846
375	1662.110	41.470	370	1303.142	32.514
393	1642.083	40.970	383	1240.503	30.951
414	1654.158	41.271	415	1120.185	27.949
442	1591.383	39.705	446	994.091	24.803
472	1506.688	37.592	473	1020.504	25.462
512	1351.771	33.727	506	999.991	24.950
532	1198.313	29.898	535	951.216	23.733
592	1029.860	25.695	595	935.266	23.335
648	925.654	23.095	657	900.589	22.470
			716	884.812	22.076
			744	864.741	21.575

B.3. Humic acid unseeded experimental data**Table B.38: HA-25 experimental raw data.**

Experimental Conditions					
Initial Concentration (mol/l) $\times 10^3$		Humic Acid (mg/l)		Seed Crystals (mg/l)	
56.6		15		-	
HA-25_A			HA-25_B		
pH 4.533			pH 4.512		
Time (min)	[Ca] (ppm)	[Ca] (mol/l) $\times 10^3$	Time (min)	[Ca] (ppm)	[Ca] (mol/l) $\times 10^3$
0	2245.756	56.032	0	2287.063	57.062
6	2254.692	56.255	7	2288.914	57.109
17	1498.937	37.399	11	2048.007	51.098
35	1087.403	27.131	17	1514.187	37.779
55	1014.153	25.303	27	1188.598	29.656
85	951.513	23.740	37	1055.544	26.336
118	961.010	23.977	47	1008.516	25.163
177	945.523	23.591	57	961.812	23.997
235	947.024	23.628	77	904.052	22.556
325	912.743	22.773	100	931.451	23.240
415	895.750	22.349	119	932.666	23.270
477	915.273	22.836	147	912.210	22.760
			177	928.638	23.170
HA-25_C					
pH 4.476					
Time (min)	[Ca] (ppm)	[Ca] (mol/l) $\times 10^3$			
0	2266.251	56.543			
7	2201.800	54.935			
13	1886.489	47.068			
23	1273.266	31.768			
35	1043.840	26.044			
47	976.603	24.366			
56	925.138	23.082			
76	927.518	23.142			
98	896.945	22.379			
116	911.082	22.732			
147	908.364	22.664			

Appendix B: Experimental results**Table B.39: HA-26 experimental raw data.**

Experimental Conditions					
Initial Concentration (mol/l) $\times 10^3$		Humic Acid (mg/l)		Seed Crystals (mg/l)	
56.6		-		-	
HA-26_A			HA-26_B		
pH		7.076	pH		7.045
Time (min)	[Ca] (ppm)	[Ca] (mol/l) $\times 10^3$	Time (min)	[Ca] (ppm)	[Ca] (mol/l) $\times 10^3$
0	2260.576	56.402	0	2276.957	56.810
10	2247.989	56.088	7	2280.350	56.895
14	2193.699	54.733	17	2285.125	57.014
25	1426.194	35.584	27	1493.527	37.264
40	1119.723	27.937	42	1063.564	26.536
55	1021.403	25.484	59	960.421	23.963
75	973.378	24.286	84	932.038	23.254
95	948.896	23.675	104	910.404	22.715
115	922.174	23.008	117	904.830	22.576
145	914.064	22.806	149	876.362	21.865
179	929.303	23.186	178	912.372	22.764
235	917.853	23.154	207	917.699	22.897
295	910.664	22.721			
361	910.379	22.998			

B.3. Humic acid unseeded experimental data**Table B.40: HA-27 experimental raw data.**

Experimental Conditions					
Initial Concentration (mol/l) $\times 10^3$		Humic Acid (mg/l)		Seed Crystals (mg/l)	
56.6		15		-	
HA-27_A			HA-27_B		
pH 9.519			pH 9.306		
Time (min)	[Ca] (ppm)	[Ca] (mol/l) $\times 10^3$	Time (min)	[Ca] (ppm)	[Ca] (mol/l) $\times 10^3$
0	2266.905	56.559	0	2294.387	57.245
26	2260.469	56.399	8	2246.391	56.048
32	1740.303	43.421	19	2266.519	56.550
42	1238.182	30.893	39	2273.894	56.734
53	1058.445	26.408	47	2176.114	54.294
67	958.875	23.924	55	1812.749	45.228
87	944.953	23.577	74	1281.258	31.968
108	924.094	23.056	99	1084.589	27.061
127	927.583	23.143	121	1029.679	25.691
150	923.078	23.031	149	964.448	24.063
177	922.916	23.027	179	932.421	23.264
207	918.435	22.915	241	910.129	22.708
			299	919.747	22.948
			389	919.413	22.939
			479	925.415	22.665
			539	865.602	21.785
HA-27_C					
pH 9.508					
Time (min)	[Ca] (ppm)	[Ca] (mol/l) $\times 10^3$			
0	2269.385	56.621			
7	2266.951	56.561			
17	2260.720	56.405			
32	2268.701	56.604			
37	2031.569	50.688			
47	1335.206	33.314			
67	1057.580	26.387			
77	990.823	24.721			
97	908.667	22.671			
117	886.187	22.110			
149	907.844	22.651			
175	871.311	21.739			

Appendix B: Experimental results

B.4. Humic acid seeded experimental data

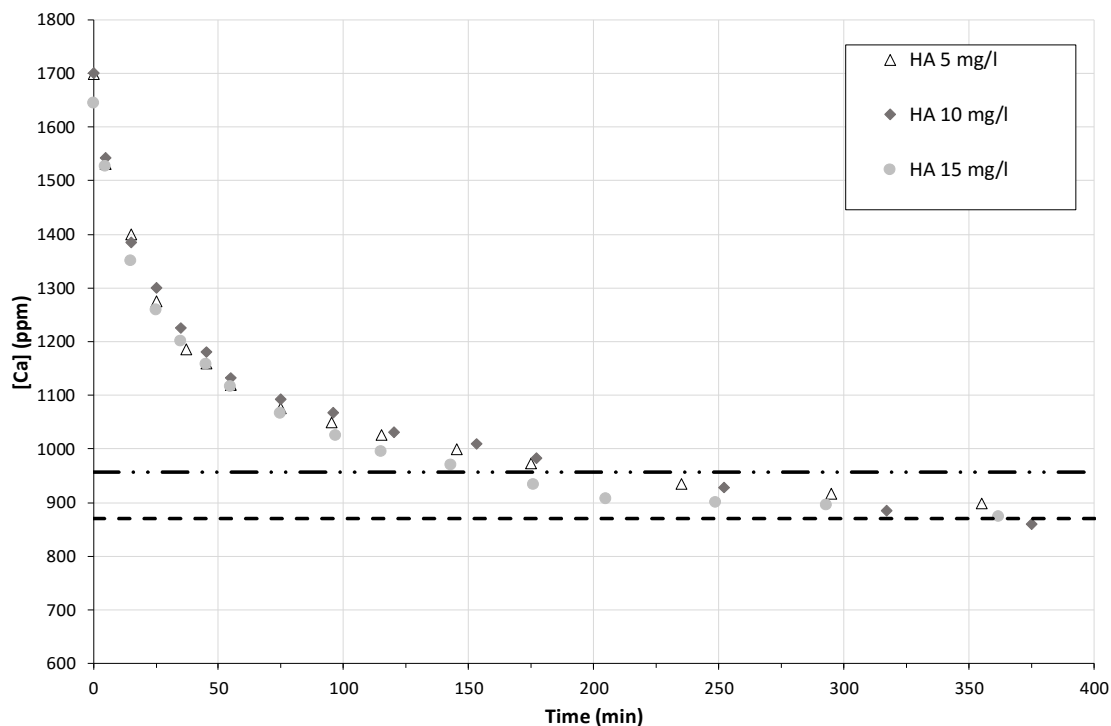


Figure B.9: Desupersaturation curves illustrating the effect of HA.
 $[Ca] = 0.0419 \text{ mol/l}$; Seed 1000 mg/l; pH 7.00 and Temperature 25°C.

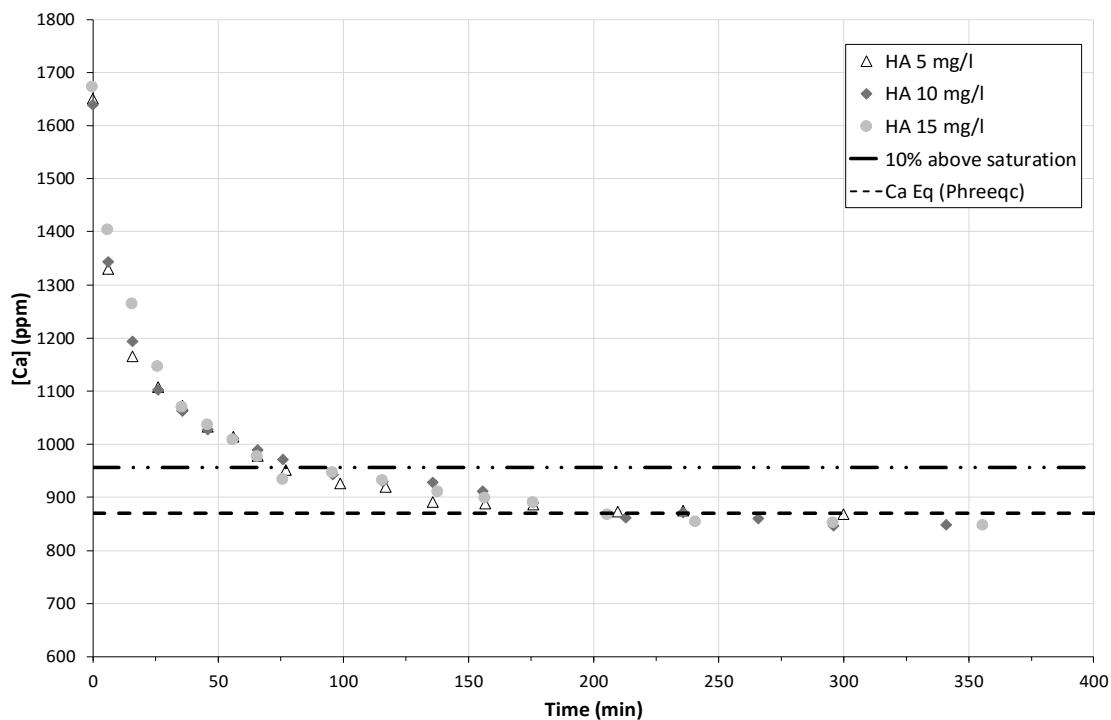


Figure B.10: Desupersaturation curves illustrating the effect of HA.
 $[Ca] = 0.0419 \text{ mol/l}$; Seed 2000 mg/l; pH 7.00 and Temperature 25°C.

B.4. Humic acid seeded experimental data**Table B.41: HS-01 experimental raw data.**

Experimental Conditions		
Initial Concentration (mol/l) $\times 10^3$	Humic Acid (mg/l)	Seed Crystals (mg/l)
41.9	10	1000
HS-01_A		
pH	4.501	
Time (min)	[Ca] (ppm)	[Ca] (mol/l) $\times 10^3$
0	1707.163	42.594
5	1545.341	38.556
15	1419.804	35.424
25	1321.133	32.962
35	1227.637	30.630
45	1199.729	29.933
55	1162.284	28.999
75	1121.641	27.985
95	1075.425	26.832
120	1019.563	25.438
145	1012.860	25.271
177	992.826	24.771
205	955.131	23.831
235	956.456	23.864
302	869.587	21.696
355	887.304	22.138

Table B.42: HS-02 experimental raw data.

Experimental Conditions		
Initial Concentration (mol/l) $\times 10^3$	Humic Acid (mg/l)	Seed Crystals (mg/l)
41.9	10	1000
HS-02_A		
pH	5.465	
Time (min)	[Ca] (ppm)	[Ca] (mol/l) $\times 10^3$
0	1723.627	43.005
6	1492.075	37.227
16	1335.537	33.322
28	1250.255	31.194
36	1215.396	30.324
46	1158.961	28.916
56	1131.653	28.235
80	1088.915	27.169
96	1076.616	26.862
116	1031.657	25.740
147	993.965	24.800
176	970.116	24.204
214	959.074	23.929
240	948.058	23.654
296	922.982	23.028
358	923.027	23.030
416	875.328	21.840

Appendix B: Experimental results**Table B.43: HS-03 experimental raw data.**

Experimental Conditions					
Initial Concentration (mol/l) $\times 10^3$		Humic Acid (mg/l)		Seed Crystals (mg/l)	
41.9		10		1000	
HS-03_A			PS-03_A		
pH 7.148			pH 7.090		
Time (min)	[Ca] (ppm)	[Ca] (mol/l) $\times 10^3$	Time (min)	[Ca] (ppm)	[Ca] (mol/l) $\times 10^3$
0	1694.179	42.270	0	1700.463	42.427
5	1589.266	39.652	5	1541.583	38.463
15	1390.996	34.705	15	1384.125	34.534
26	1298.287	32.392	25	1300.174	32.439
35	1238.926	30.911	35	1225.227	30.570
45	1174.443	29.302	45	1180.617	29.457
55	1130.783	28.213	55	1132.374	28.253
75	1081.196	26.976	75	1092.476	27.257
102	1046.646	26.114	96	1067.441	26.633
115	1010.344	25.208	120	1030.456	25.710
145	986.506	24.613	153	1009.496	25.187
175	953.280	23.784	177	982.951	24.525
205	955.596	23.842	252	928.282	23.161
235	923.165	23.033	317	884.445	22.067
302	912.904	22.777	375	858.935	21.431
350	924.124	23.057			
419	863.568	21.546			
480	841.644	20.999			

Table B.44: HS-04 experimental raw data.

Experimental Conditions			
Initial Concentration (mol/l) $\times 10^3$		Humic Acid (mg/l)	Seed Crystals (mg/l)
41.9		10	1000
HS-04_A			
pH 8.070			
Time (min)	[Ca] (ppm)	[Ca] (mol/l) $\times 10^3$	
0	1692.522	42.229	
5	1608.183	40.124	
15	1423.667	35.521	
25	1328.824	33.154	
35	1241.452	30.974	
45	1186.847	29.612	
55	1122.813	28.014	
75	1107.187	27.624	
103	1049.954	26.196	
150	1012.687	25.267	
192	982.958	24.525	
205	966.252	24.108	
237	943.521	23.541	
300	929.542	23.192	
355	904.740	22.573	
415	836.347	20.867	

B.4. Humic acid seeded experimental data**Table B.45: HS-05 experimental raw data.**

Experimental Conditions		
Initial Concentration (mol/l) $\times 10^3$	Humic Acid (mg/l)	Seed Crystals (mg/l)
41.9	10	1000
HS-05_A		
pH	9.554	
Time (min)	[Ca] (ppm)	[Ca] (mol/l) $\times 10^3$
0	1704.166	42.519
5	1530.929	38.197
15	1408.537	35.143
25	1285.623	32.076
35	1238.753	30.907
45	1193.290	29.773
55	1139.899	28.441
75	1084.321	27.054
95	1049.898	26.195
115	1020.726	25.467
145	994.489	24.813
175	968.974	24.176
205	946.942	23.626
295	918.031	22.905
365	882.321	22.014
415	863.280	21.539
499	860.178	21.462

Table B.46: HS-06 experimental raw data.

Experimental Conditions		
Initial Concentration (mol/l) $\times 10^3$	Humic Acid (mg/l)	Seed Crystals (mg/l)
41.9	10	1000
HS-06_A		
pH	4.494	
Time (min)	[Ca] (ppm)	[Ca] (mol/l) $\times 10^3$
0	1761.153	43.941
5	1665.108	41.545
15	1616.384	40.329
25	1552.092	38.725
35	1483.089	37.003
45	1446.354	36.087
55	1396.093	34.833
65	1364.859	34.053
75	1279.668	31.928
96	1205.603	30.080
130	1108.096	27.647
145	1074.985	26.821
205	1015.229	25.330
235	972.719	24.269
295	939.930	23.451
353	904.399	22.565
415	878.467	21.918
475	863.660	21.548

Appendix B: Experimental results**Table B.47: HS-07 experimental raw data.**

Experimental Conditions					
Initial Concentration (mol/l) $\times 10^3$		Humic Acid (mg/l)		Seed Crystals (mg/l)	
41.9		10		1000	
HS-07_A			HS-07_B		
pH 9.516			pH 9.459		
Time (min)	[Ca] (ppm)	[Ca] (mol/l) $\times 10^3$	Time (min)	[Ca] (ppm)	[Ca] (mol/l) $\times 10^3$
0	1684.974	42.040	0	1697.356	42.349
5	1688.256	42.122	5	1673.728	41.760
15	1671.709	41.709	15	1674.168	41.771
25	1685.806	42.061	25	1671.784	41.711
35	1658.768	41.386	35	1622.292	40.476
46	1571.194	39.201	45	1591.946	39.719
55	1517.476	37.861	55	1576.882	39.343
73	1422.927	35.502	65	1519.944	37.923
95	1333.557	33.272	86	1426.209	35.584
119	1236.533	30.852	100	1345.703	33.575
136	1193.200	29.770	115	1306.013	32.585
174	1077.110	26.874	148	1214.164	30.294
206	1039.686	25.940	184	1116.801	27.864
243	986.921	24.624	207	1064.003	26.547
295	924.163	23.058	241	1013.392	25.284
385	882.879	22.028	295	963.491	24.039
415	860.819	21.478	355	921.845	23.000
475	859.925	21.455	415	912.319	22.762

Table B.48: HS-08 experimental raw data.

Experimental Conditions					
Initial Concentration (mol/l) $\times 10^3$		Humic Acid (mg/l)		Seed Crystals (mg/l)	
41.9		10		1000	
HS-08_A			HS-08_B		
pH 7.173			pH 6.984		
Time (min)	[Ca] (ppm)	[Ca] (mol/l) $\times 10^3$	Time (min)	[Ca] (ppm)	[Ca] (mol/l) $\times 10^3$
0	1685.546	42.055	0	1642.207	40.97322
5	1684.791	42.036	5	1652.797	41.23745
15	1608.730	40.138	16	1641.150	40.94686
25	1553.037	38.748	26	1609.467	40.15635
37	1466.150	36.581	35	1552.119	38.72551
49	1390.192	34.685	45	1464.940	36.5504
55	1362.323	33.990	60	1387.932	34.62903
65	1333.365	33.268	75	1326.440	33.0948
75	1284.802	32.056	97	1250.810	31.20783
95	1221.793	30.484	117	1182.718	29.50893
115	1137.291	28.376	145	1113.280	27.77643
145	1061.703	26.490	175	1062.821	26.51748
175	1022.951	25.523	206	1044.243	26.05395
206	982.603	24.516	235	996.479	24.86225
244	955.853	23.849	292	940.014	23.45344
299	901.313	22.488	362	889.555	22.19449
355	862.301	21.514	413	876.831	21.87702
416	865.466	21.593	452	853.858	21.30384

B.4. Humic acid seeded experimental data**Table B.49: HS-09 experimental raw data.**

Experimental Conditions					
Initial Concentration (mol/l) $\times 10^3$		Humic Acid (mg/l)		Seed Crystals (mg/l)	
41.9		15		200	
HS-09_A			HS-09_B		
pH		7.130	pH		7.038
Time (min)	[Ca] (ppm)	[Ca] (mol/l) $\times 10^3$	Time (min)	[Ca] (ppm)	[Ca] (mol/l) $\times 10^3$
0	1742.427	43.474	0	1736.207	43.319
5	1677.099	41.844	5	1672.114	41.719
15	1668.225	41.622	15	1663.681	41.509
25	1673.841	41.762	25	1663.390	41.502
35	1662.388	41.477	35	1661.526	41.455
45	1668.353	41.626	45	1651.095	41.195
55	1611.158	40.199	55	1652.565	41.232
85	1499.386	37.410	77	1572.198	39.226
95	1470.988	36.701	95	1492.581	37.240
117	1392.645	34.747	117	1408.974	35.154
146	1300.199	32.440	145	1332.532	33.247
173	1242.556	31.002	178	1227.724	30.632
209	1174.697	29.309	207	1166.030	29.093
235	1120.189	27.949	235	1138.489	28.405
295	1059.571	26.436	295	1042.489	26.010
352	1008.833	25.170	355	985.157	24.580
405	959.705	23.945	412	904.657	22.571
475	956.093	23.855	469	871.566	21.746

Table B.50: HS-10 experimental raw data.

Experimental Conditions		
Initial Concentration (mol/l) $\times 10^3$	Humic Acid (mg/l)	Seed Crystals (mg/l)
41.9	15	1000
HS-10_A		
pH		7.040
Time (min)	[Ca] (ppm)	[Ca] (mol/l) $\times 10^3$
0	1643.132	40.996
5	1526.278	38.081
15	1349.007	33.658
25	1258.473	31.399
35	1199.293	29.922
45	1156.157	28.846
55	1114.640	27.810
75	1065.524	26.585
97	1023.456	25.535
115	993.285	24.783
143	969.212	24.182
176	932.720	23.271
205	905.326	22.588
249	899.183	22.435
293	894.355	22.314
362	872.159	21.760
415	866.075	21.609

Appendix B: Experimental results**Table B.51: HS-11 experimental raw data.**

Experimental Conditions		
Initial Concentration (mol/l) $\times 10^3$	Humic Acid (mg/l)	Seed Crystals (mg/l)
41.9	5	1000
HS-11_A		
pH	7.177	
Time (min)	[Ca] (ppm)	[Ca] (mol/l) $\times 10^3$
0	1698.195	42.370
5	1530.829	38.194
15	1399.954	34.929
25	1274.251	31.793
37	1185.645	29.582
45	1158.943	28.916
55	1118.173	27.899
75	1075.391	26.831
95	1049.587	26.187
115	1025.666	25.590
145	999.626	24.941
175	971.685	24.244
235	934.270	23.310
295	915.562	22.843
355	897.528	22.393

Table B.52: HS-12 experimental raw data.

Experimental Conditions					
Initial Concentration (mol/l) $\times 10^3$		Humic Acid (mg/l)		Seed Crystals (mg/l)	
41.9		5		200	
HS-12_A			HS-12_B		
pH 7.086			pH 7.042		
Time (min)	[Ca] (ppm)	[Ca] (mol/l) $\times 10^3$	Time (min)	[Ca] (ppm)	[Ca] (mol/l) $\times 10^3$
0	1674.139	41.770	0	1650.494	41.180
5	1632.862	40.740	6	1583.216	39.501
15	1563.957	39.021	16	1541.034	38.449
25	1495.453	37.312	26	1479.508	36.914
35	1440.971	35.952	36	1406.917	35.103
47	1363.317	34.015	46	1369.809	34.177
55	1323.775	33.028	56	1330.407	33.194
75	1227.239	30.620	76	1250.486	31.200
96	1157.350	28.876	96	1159.040	28.918
115	1108.557	27.659	114	1125.601	28.084
143	1044.497	26.060	161	1036.550	25.862
188	985.549	24.590	176	1002.807	25.020
207	975.819	24.347	206	988.073	24.653
239	937.399	23.388	236	960.221	23.958
299	888.852	22.177	267	911.971	22.754
356	887.820	22.151	299	899.644	22.446
			356	879.048	21.932
			419	864.813	21.577

B.4. Humic acid seeded experimental data**Table B.53: HS-14 experimental raw data.**

Experimental Conditions		
Initial Concentration (mol/l) $\times 10^3$	Humic Acid (mg/l)	Seed Crystals (mg/l)
41.9	5	200
HS-14_A		
pH	7.170	
Time (min)	[Ca] (ppm)	[Ca] (mol/l) $\times 10^3$
0	1649.508	41.155
6	1329.058	33.160
16	1165.531	29.080
26	1106.401	27.605
36	1071.571	26.736
46	1031.607	25.739
56	1014.237	25.305
66	977.471	24.388
77	951.299	23.735
99	925.090	23.081
117	919.118	22.932
136	890.668	22.222
157	887.957	22.155
176	885.417	22.091
210	872.248	21.763
236	874.486	21.819
300	867.908	21.654

Table B.54: HS-15 experimental raw data.

Experimental Conditions		
Initial Concentration (mol/l) $\times 10^3$	Humic Acid (mg/l)	Seed Crystals (mg/l)
41.9	15	2000
HS-15_A		
pH	6.832	
Time (min)	[Ca] (ppm)	[Ca] (mol/l) $\times 10^3$
0	1638.410	40.878
6	1342.459	33.494
16	1192.950	29.764
26	1101.254	27.476
36	1062.089	26.499
46	1026.759	25.618
56	1009.781	25.194
66	988.615	24.666
76	969.731	24.195
96	941.773	23.497
116	928.146	23.157
136	927.741	23.147
156	909.821	22.700
176	888.568	22.170
213	860.941	21.481
236	871.490	21.744
266	859.811	21.452
296	846.613	21.123
341	847.433	21.144

Appendix B: Experimental results**Table B.55: HS-16 experimental raw data.**

Experimental Conditions		
Initial Concentration (mol/l) $\times 10^3$	Humic Acid (mg/l)	Seed Crystals (mg/l)
41.9	10	2000
HS-16_A		
pH	7.097	
Time (min)	[Ca] (ppm)	[Ca] (mol/l) $\times 10^3$
0	1670.983	41.691
6	1402.471	34.992
16	1262.722	31.505
26	1144.124	28.546
36	1069.179	26.676
46	1035.868	25.845
56	1007.620	25.140
66	974.940	24.325
76	931.423	23.239
96	945.148	23.582
116	931.336	23.237
138	909.529	22.693
157	897.846	22.401
176	888.233	22.162
206	866.004	21.607
241	852.263	21.264
296	850.227	21.213
356	845.928	21.106

B.5. Fulvic acid experimental data**Table B.56: FA-01 experimental raw data.**

Experimental Conditions		
Initial Concentration (mol/l) $\times 10^3$	Fulvic Acid (mg/l)	Seed Crystals (mg/l)
41.9	15.0	-
FA-01_A		
pH	6.965	
Time (min)	[Ca] (ppm)	[Ca] (mol/l) $\times 10^3$
6	1674.238	41.772
15	1683.517	42.004
30	1669.942	41.665
60	1685.270	42.048
90	1674.236	41.772
120	1676.281	41.823
180	1685.361	42.050
240	1689.759	42.160
305	1646.546	41.081
330	1668.925	41.640
420	1654.058	41.269
495	1668.243	41.623
540	1687.833	42.112

B.5. Fulvic acid experimental data**Table B.57: FA-02 experimental raw data.**

Experimental Conditions		
Initial Concentration (mol/l) $\times 10^3$	Fulvic Acid (mg/l)	Seed Crystals (mg/l)
41.9	5.0	-
FA-02_A		
pH	7.094	
Time (min)	[Ca] (ppm)	[Ca] (mol/l) $\times 10^3$
0	1671.747	41.710
25	1672.033	41.717
57	1682.506	41.979
85	1670.675	41.684
116	1684.321	42.024
175	1666.711	41.585
215	1622.634	40.485
250	1675.900	41.814
265	1673.400	41.752
326	1686.609	42.081
360	1668.640	41.633
445	1660.252	41.423
506	1673.407	41.752

Table B.58: FA-03 experimental raw data.

Experimental Conditions		
Initial Concentration (mol/l) $\times 10^3$	Fulvic Acid (mg/l)	Seed Crystals (mg/l)
41.9	5.0	-
FA-03_A		
pH	4.518	
Time (min)	[Ca] (ppm)	[Ca] (mol/l) $\times 10^3$
0	1687.807	42.111
55	1672.165	41.721
115	1682.928	41.989
175	1681.543	41.955
235	1669.070	41.643
297	1678.925	41.889
315	1673.750	41.760
336	1676.630	41.832
355	1495.448	37.312
377	1322.749	33.003
396	1188.513	29.654
415	1083.158	27.025
445	1043.407	26.033
475	1004.454	25.061
505	962.606	24.017
535	891.823	22.251

Appendix B: Experimental results**Table B.59: FA-04 experimental raw data.**

Experimental Conditions		
Initial Concentration (mol/l) $\times 10^3$	Fulvic Acid (mg/l)	Seed Crystals (mg/l)
41.9	2.5	-
FA-04_A		
pH	4.509	
Time (min)	[Ca] (ppm)	[Ca] (mol/l) $\times 10^3$
0	1665.827	41.563
25	1668.355	41.626
57	1671.276	41.698
112	1667.679	41.609
135	1669.409	41.652
145	1662.577	41.481
159	1548.593	38.638
169	1434.280	35.785
177	1360.400	33.942
198	1197.261	29.872
216	1109.371	27.679
236	1044.494	26.060
269	960.364	23.961
296	914.849	22.826
342	869.780	21.701
404	868.258	21.663

Table B.60: FA-05 experimental raw data.

Experimental Conditions					
Initial Concentration (mol/l) $\times 10^3$		Fulvic Acid (mg/l)		Seed Crystals (mg/l)	
41.9		2.5		-	
FA-05_A			FA-05_B		
pH 7.022			pH 7.173		
Time (min)	[Ca] (ppm)	[Ca] (mol/l) $\times 10^3$	Time (min)	[Ca] (ppm)	[Ca] (mol/l) $\times 10^3$
0	1680.245	41.922	0	1682.229	41.972
55	1692.150	42.219	55	1689.917	42.164
116	1690.067	42.167	146	1693.215	42.246
175	1690.422	42.176	235	1693.094	42.243
247	1685.172	42.045	326	1676.682	41.833
296	1688.105	42.118	376	1690.221	42.171
355	1692.894	42.238	415	1688.211	42.121
427	1689.686	42.158	449	1676.148	41.820
475	1686.518	42.079	478	1695.475	42.302
505	1682.649	41.982	507	1538.381	38.383
538	1687.309	42.099	526	1476.245	36.832
565	1687.351	42.100	545	1369.777	34.176
595	1570.525	39.185	565	1244.350	31.047
621	1413.168	35.259	586	1136.998	28.368
655	1219.300	30.422	605	1089.892	27.193
685	1097.480	27.382	625	1025.183	25.578
713	987.086	24.628	656	999.235	24.931
			688	942.630	23.519
			726	913.912	22.802
			775	873.479	21.793

B.5. Fulvic acid experimental data**Table B.61: FA-06 experimental raw data.**

Experimental Conditions		
Initial Concentration (mol/l) $\times 10^3$	Fulvic Acid (mg/l)	Seed Crystals (mg/l)
41.9	1.0	-
FA-06_A		
pH	7.038	
Time (min)	[Ca] (ppm)	[Ca] (mol/l) $\times 10^3$
0	1676.886	41.838
25	1683.628	42.007
55	1684.466	42.028
105	1677.386	41.851
135	1701.812	42.460
155	1669.737	41.660
175	1674.488	41.779
185	1671.330	41.700
196	1533.912	38.271
205	1422.152	35.483
215	1324.524	33.047
225	1244.803	31.058
236	1180.116	29.444
255	1078.310	26.904
296	977.399	24.386
325	933.274	23.285
355	901.817	22.500
415	861.286	21.489

Table B.62: FA-07 experimental raw data.

Experimental Conditions		
Initial Concentration (mol/l) $\times 10^3$	Fulvic Acid (mg/l)	Seed Crystals (mg/l)
41.9	1.0	-
FA-07_A		
pH	4.519	
Time (min)	[Ca] (ppm)	[Ca] (mol/l) $\times 10^3$
0	1670.733	41.685
15	1667.304	41.599
35	1673.295	41.749
47	1677.042	41.842
55	1666.011	41.567
66	1672.051	41.718
75	1578.108	39.374
85	1431.319	35.712
95	1330.394	33.193
105	1228.927	30.662
115	1145.519	28.581
149	1012.142	25.253
158	968.659	24.168
175	929.740	23.197
206	874.311	21.814
235	866.220	21.612
265	865.989	21.607
297	861.494	21.494
357	850.965	21.232

Appendix B: Experimental results**Table B.63: FA-08 experimental raw data.**

Experimental Conditions		
Initial Concentration (mol/l) $\times 10^3$	Fulvic Acid (mg/l)	Seed Crystals (mg/l)
41.9	1.0	-
FA-08_A		
pH	9.516	
Time (min)	[Ca] (ppm)	[Ca] (mol/l) $\times 10^3$
0	1688.400	42.126
56	1684.074	42.018
85	1673.997	41.766
116	1685.795	42.061
180	1686.819	42.086
205	1693.913	42.263
235	1688.513	42.129
265	1685.991	42.066
297	1695.160	42.294
330	1660.836	41.438
342	1673.254	41.748
355	1675.079	41.793
385	1660.004	41.417
400	1679.695	41.99
418	1531.944	38.222
441	1336.823	33.354
455	1221.601	30.479
477	1070.092	26.699
510	985.022	24.576
535	939.359	23.437
595	855.272	21.339

B.6. Fulvic acid seeded experimental runs**B.6. Fulvic acid seeded experimental runs****Table B.64: FS-01 experimental raw data.**

Experimental Conditions		
Initial Concentration (mol/l) $\times 10^3$	Fulvic Acid (mg/l)	Seed Crystals (mg/l)
41.9	10	200
FS-01_A		
pH	7.204	
Time (min)	[Ca] (ppm)	[Ca] (mol/l) $\times 10^3$
0	1671.987	41.716
5	1667.628	41.607
15	1662.784	41.487
25	1660.569	41.431
35	1655.472	41.304
48	1666.883	41.589
55	1657.598	41.357
75	1662.989	41.492
95	1664.131	41.520
115	1674.278	41.773
135	1670.781	41.686
155	1662.318	41.475
175	1661.798	41.462
208	1661.830	41.463
237	1663.568	41.506
265	1664.902	41.539
295	1675.116	41.794
357	1678.427	41.877
416	1656.972	41.342
485	1656.860	41.339

Table B.65: FS-02 experimental raw data.

Experimental Conditions		
Initial Concentration (mol/l) $\times 10^3$	Fulvic Acid (mg/l)	Seed Crystals (mg/l)
41.9	5	200
FS-02_A		
pH	7.194	
Time (min)	[Ca] (ppm)	[Ca] (mol/l) $\times 10^3$
0	1653.510	41.255
6	1651.409	41.203
27	1636.288	40.826
48	1604.473	40.032
66	1581.482	39.458
86	1569.263	39.153
106	1552.389	38.732
126	1547.678	38.615
146	1515.355	37.808
166	1498.948	37.399
186	1440.509	35.941
233	1348.772	33.652
266	1256.472	31.349
296	1197.498	29.878
327	1131.679	28.235
361	1040.382	25.958
416	939.783	23.448
476	908.879	22.677
536	863.497	21.544

Appendix B: Experimental results**Table B.66: FS-03 experimental raw data.**

Experimental Conditions		
Initial Concentration (mol/l) $\times 10^3$	Fulvic Acid (mg/l)	Seed Crystals (mg/l)
41.9	5	1000
FS-03_A		
pH	7.083	
Time (min)	[Ca] (ppm)	[Ca] (mol/l) $\times 10^3$
0	1663.439	41.50297
6	1591.505	39.70821
16	1537.676	38.36517
26	1450.914	36.20045
36	1370.344	34.19021
46	1265.001	31.56191
56	1219.933	30.43744
76	1122.972	28.01826
96	1092.575	27.25985
116	1058.879	26.41913
136	1020.852	25.47037
158	994.261	24.80692
176	989.333	24.68397
207	953.265	23.78406
241	953.345	23.78605
266	935.972	23.3526
296	929.959	23.20257
357	903.018	22.5304
416	888.932	22.17894
476	879.704	21.9487
536	876.111	21.85905

Table B.67: FS-04 experimental raw data.

Experimental Conditions		
Initial Concentration (mol/l) $\times 10^3$	Fulvic Acid (mg/l)	Seed Crystals (mg/l)
41.9	5	2000
FS-04_A		
pH	6.700	
Time (min)	[Ca] (ppm)	[Ca] (mol/l) $\times 10^3$
0	1674.304	41.774
6	1567.027	39.097
16	1321.230	32.965
26	1194.038	29.791
36	1105.448	27.581
46	1070.493	26.709
56	1032.077	25.750
66	1010.621	25.215
96	968.991	24.176
117	952.389	23.762
136	925.738	23.097
156	904.941	22.578
176	889.630	22.196
209	877.099	21.884
237	870.224	21.712
266	864.534	21.570
298	860.466	21.469
359	848.808	21.178
423	839.268	20.940

B.6. Fulvic acid seeded experimental runs**Table B.68: FS-05 experimental raw data.**

Experimental Conditions		
Initial Concentration (mol/l) $\times 10^3$	Fulvic Acid (mg/l)	Seed Crystals (mg/l)
41.9	10	2000
FS-05_A		
pH	6.909	
Time (min)	[Ca] (ppm)	[Ca] (mol/l) $\times 10^3$
0	1675.847	41.813
6	1599.236	39.901
21	1464.525	36.540
36	1340.941	33.457
51	1273.934	31.785
66	1221.847	30.485
86	1182.917	29.514
96	1153.763	28.786
116	1115.445	27.830
138	1082.541	27.010
157	1057.619	26.388
176	1039.128	25.926
206	1018.243	25.405
236	990.603	24.716
267	973.470	24.288
296	962.797	24.022
326	930.672	23.220
356	908.773	22.674
416	901.259	22.486

*Appendix B: Experimental results***B.7. pH control****Table B.69: PH-01 experimental raw data..**

Experimental Conditions					
Initial Concentration (mol/l) $\times 10^3$		Humic Acid (mg/l)		Seed Crystals (mg/l)	
41.9		10		-	
PH-01_A			PH-01_B		
pH ~ 9.500			pH ~ 9.500		
Time (min)	[Ca] (ppm)	[Ca] (mol/l) $\times 10^3$	Time (min)	[Ca] (ppm)	[Ca] (mol/l) $\times 10^3$
0	1686.537	42.079	0	1679.361	41.90
55	1682.905	41.989	55	1666.971	41.591
117	1678.938	41.890	115	1677.965	41.865
175	1680.637	41.932	176	1688.320	42.124
201	1668.351	41.626	205	1679.090	41.893
215	1681.342	41.950	233	1677.802	41.861
239	1667.543	41.605	266	1632.635	40.734
255	1675.577	41.806	295	1412.442	35.241
276	1627.693	40.611	328	1339.202	33.413
295	1587.728	39.614	355	1216.998	30.364
325	1516.111	37.827	390	1145.008	28.568
350	1446.506	36.090	415	1112.395	27.754
381	1321.232	32.965	446	1055.339	26.331
395	1301.564	32.474	475	1059.350	26.431
415	1265.480	31.574	535	988.401	24.661
445	1183.587	29.531	595	952.194	23.757
475	1117.439	27.880			
PH-01_C					
pH ~ 9.500					
Time (min)	[Ca] (ppm)	[Ca] (mol/l) $\times 10^3$			
0	1608.947	40.143			
51	1754.838	43.783			
115	1762.791	43.982			
175	1744.892	43.535			
205	1721.902	42.962			
216	1736.573	43.328			
238	1698.584	42.380			
265	1682.653	41.982			
295	1532.923	38.247			
324	1458.988	36.402			
352	1301.478	32.472			
387	1236.950	30.862			
415	1159.407	28.927			
445	1138.868	28.415			
472	1146.014	28.593			
531	1054.550	26.311			
601	1025.079	25.576			
638	1012.812	25.270			

Table B.70: PH-02 experimental raw data.

Experimental Conditions		
Initial Concentration (mol/l) $\times 10^3$	Fulvic Acid (mg/l)	Seed Crystals (mg/l)
41.9	5	2000
PH-02_A		
pH		
Time (min)	[Ca] (ppm)	[Ca] (mol/l) $\times 10^3$
0	1674.892	41.789
8	1495.783	37.320
15	1392.350	34.739
27	1293.017	32.261
42	1207.326	30.123
45	1185.153	29.570
55	1139.009	28.418
75	1129.070	28.170
95	1086.472	27.108
115	1059.649	26.438
145	1014.757	25.318
175	969.989	24.201
205	971.527	24.240
235	974.917	24.324
295	941.545	23.492
355	936.673	23.370
415	947.929	23.651

Table B.71: PH-03 experimental raw data.

Experimental Conditions					
Initial Concentration (mol/l) $\times 10^3$		Fulvic Acid (mg/l)		Seed Crystals (mg/l)	
41.9		10		2000	
PH-03_A			PH-03_B		
pH 9.500			pH 9.500		
Time (min)	[Ca] (ppm)	[Ca] (mol/l) $\times 10^3$	Time (min)	[Ca] (ppm)	[Ca] (mol/l) $\times 10^3$
0	1677.976	41.866	0	1664.114	41.520
5	1667.964	41.616	5	1657.517	41.355
20	1662.013	41.467	25	1615.024	40.295
35	1631.212	40.699	41	1591.001	39.696
45	1604.230	40.026	56	1572.931	39.245
55	1567.334	39.105	76	1451.857	36.224
65	1548.745	38.641	95	1392.768	34.750
75	1465.974	36.576	115	1349.641	33.674
95	1420.662	35.446	145	1249.085	31.165
115	1351.208	33.713	175	1174.784	29.311
142	1281.180	31.966	207	1113.143	27.773
175	1212.559	30.253	239	1064.676	26.564
207	1139.943	28.442	269	1037.527	25.886
235	1108.387	27.654	297	1004.481	25.062
265	1075.877	26.843	355	970.000	24.202
298	992.577	24.765	415	928.641	23.170
355	933.989	23.303	478	936.686	23.370
418	928.608	23.169	535	913.882	22.801
478	888.013	22.156	562	900.510	22.468
540	890.882	22.228			

Appendix C: PHREEQC® output data

Appendix C: PHREEQC® OUTPUT DATA

-----Solution composition-----

Elements	Molality	Moles
Ca	1.565e-02	1.565e-02
S(6)	1.565e-02	1.565e-02

-----Description of solution-----

pH = 7.000
 pe = 4.000
 Specific Conductance (uS/cm, 25 oC) = 2161
 Density (g/cm3) = 0.99920 (Millero)
 Activity of water = 1.000
 Ionic strength = 4.181e-02
 Mass of water (kg) = 1.000e+00
 Total alkalinity (eq/kg) = -4.735e-08
 Total carbon (mol/kg) = 0.000e+00
 Total CO2 (mol/kg) = 0.000e+00
 Temperature (deg C) = 25.000
 Electrical balance (eq) = 4.735e-08
 Percenterror, 100*(Cat-|An|)/(|Cat+|An|) = 0.00
 Iterations = 5
 Total H = 1.110124e+02
 Total O = 5.556882e+01

-----Distribution of species-----

Species	Molality	Log Activity	Log Molality	Log Activity	Gamma
OH-	1.215e-07	1.001e-07	-6.915	-7.000	-0.084
H+	1.161e-07	1.000e-07	-6.935	-7.000	-0.065
H2O	5.551e+01	9.996e-01	1.744	-0.000	0.000
Ca	1.565e-02				
Ca+2	1.045e-02	5.179e-03	-1.981	-2.286	-0.305
CaSO4	5.197e-03	5.247e-03	-2.284	-2.280	0.004
CaOH+	1.033e-08	8.591e-09	-7.986	-8.066	-0.080
CaHSO4+	3.696e-09	3.074e-09	-8.432	-8.512	-0.080
H(0)	1.402e-25				
H2	7.012e-26	7.079e-26	-25.154	-25.150	0.004
O(0)	0.000e+00				
O2	0.000e+00	0.000e+00	-42.085	-42.080	0.004
S(6)	1.565e-02				
SO4-2	1.045e-02	5.078e-03	-1.981	-2.294	-0.314
CaSO4	5.197e-03	5.247e-03	-2.284	-2.280	0.004
HSO4-	5.937e-08	4.937e-08	-7.226	-7.307	-0.080
CaHSO4+	3.696e-09	3.074e-09	-8.432	-8.512	-0.080

-----Saturation indices-----

Phase	SI	log IAP	log KT
Anhydrite	-0.22	-4.58	-4.36 CaSO4
Gypsum	0.00	-4.58	-4.58 CaSO4:2H2O
H2(g)	-22.00	-25.15	-3.15 H2
H2O(g)	-1.51	-0.00	1.51 H2O
O2(g)	-39.19	-42.08	-2.89 O2

Figure C.1: PHREEQC® output data for saturation of gypsum.

B.7. pH control

```

-----Solution composition-----
Elements Molality Moles
Ca      3.749e-02 3.749e-02
Cl      7.498e-02 7.498e-02
Na      7.499e-02 7.499e-02
S(6)    3.749e-02 3.749e-02

-----Description of solution-----
pH = 7.000
pe = 4.000
Specific Conductance (uS/cm, 25 oC) = 12038
Density(g/cm3) = 1.00520(Millero)
Activity of water = 0.996
Ionic strength = 1.726e-01
Mass of water(kg) = 1.000e+00
Total alkalinity (eq/kg) = -6.511e-08
Total carbon (mol/kg) = 0.000e+00
Total CO2 (mol/kg) = 0.000e+00
Temperature (deg C) = 25.000
Electrical balance (eq) = 2.379e-06
Percenterror, 100*(Cat-|An|)/(Cat+|An|) = 0.00
iterations = 6
Total H = 1.110124e+02
Total O = 5.565620e+01

-----Distribution of species-----
Species      Log Molality Log Activity Log Molality Log Activity Gamma
OH-          1.387e-07 9.975e-08 -6.858 -7.001 -0.143
H+           1.244e-07 1.000e-07 -6.905 -7.000 -0.095
H2O          5.551e+01 9.964e-01 1.744 -0.002 0.000
Ca           3.749e-02
Ca+2         2.570e-02 8.613e-03 -1.590 -2.065 -0.475
CaSO4        1.179e-02 1.227e-02 -1.928 -1.911 0.017
CaOH+        1.891e-08 1.424e-08 -7.723 -7.846 -0.123
CaHSO4+      9.546e-09 7.190e-09 -8.020 -8.143 -0.123
Cl           7.498e-02
Cl-          7.498e-02 5.424e-02 -1.125 -1.266 -0.141
H(0)         1.361e-25
H2           6.804e-26 7.079e-26 -25.167 -25.150 0.017
Na           7.499e-02
Na+          7.240e-02 5.442e-02 -1.140 -1.264 -0.124
NaSO4-       2.586e-03 1.948e-03 -2.587 -2.710 -0.123
NaOH         3.443e-09 3.583e-09 -8.463 -8.446 0.017
O(0)         0.000e+00
O2           0.000e+00 0.000e+00 -42.100 -42.083 0.017
S(6)         3.749e-02
SO4-2        2.311e-02 7.141e-03 -1.636 -2.146 -0.510
CaSO4        1.179e-02 1.227e-02 -1.928 -1.911 0.017
NaSO4-       2.586e-03 1.948e-03 -2.587 -2.710 -0.123
HSO4-        9.218e-08 6.943e-08 -7.035 -7.158 -0.123
CaHSO4+      9.546e-09 7.190e-09 -8.020 -8.143 -0.123

-----Saturation indices-----
Phase      SI log IAP log KT
Anhydrite  0.15 -4.21 -4.36 CaSO4
Gypsum     0.37 -4.21 -4.58 CaSO4:2H2O
H2(g)      -22.00 -25.15 -3.15 H2
H2O(g)     -1.51 -0.00 1.51 H2O
Halite     -4.11 -2.53 1.58 NaCl
O2(g)      -39.19 -42.08 -2.89 O2

```

Figure C.2: PHREEQC[®] output data for supersaturation ratio 2 (SS2) of gypsum.

Appendix C: PHREEQC® output data

```

-----Solution composition-----
Elements Molality Moles
Ca      4.751e-02 4.751e-02
Cl      9.502e-02 9.502e-02
Na      9.503e-02 9.503e-02
S(6)    4.752e-02 4.752e-02

-----Description of solution-----
pH = 7.000
pe = 4.000
Specific Conductance (uS/cm, 25 oC) = 14846
Density (g/cm3) = 1.00734 (Millero)
Activity of water = 0.995
Ionic strength = 2.158e-01
Mass of water (kg) = 1.000e+00
Total alkalinity (eq/kg) = -7.536e-08
Total carbon (mol/kg) = 0.000e+00
Total CO2 (mol/kg) = 0.000e+00
Temperature (deg C) = 25.000
Electrical balance (eq) = 3.008e-06
Percenterror, 100*(Cat-|An|)/(|Cat+|An|) = 0.00
Iterations = 6
Total H = 1.110124e+02
Total O = 5.569629e+01

-----Distribution of species-----
Species      Molality      Log Activity      Log Molality      Log Activity Gamma
OH-          1.422e-07     9.966e-08         -6.847          -7.001          -0.154
H+           1.258e-07     1.000e-07         -6.900          -7.000          -0.100
H2O          5.551e+01     9.955e-01         1.744           -0.002          0.000
Ca           4.751e-02
Ca+2         3.203e-02     1.010e-02         -1.494          -1.996          -0.501
CaSO4        1.548e-02     1.627e-02         -1.810          -1.789          0.022
CaOH+        2.243e-08     1.668e-08         -7.649          -7.778          -0.129
CaHSO4+      1.282e-08     9.531e-09         -7.892          -8.021          -0.129
Cl           9.502e-02
Cl-          9.502e-02     6.711e-02         -1.022          -1.173          -0.151
H(0)         1.347e-25
H2           6.736e-26     7.079e-26         -25.172         -25.150          0.022
Na           9.503e-02
Na+          9.135e-02     6.760e-02         -1.039          -1.170          -0.131
NaSO4-       3.678e-03     2.736e-03         -2.434          -2.563          -0.129
NaOH         4.231e-09     4.446e-09         -8.374          -8.352          0.022
O(0)         0.000e+00
O2           0.000e+00     0.000e+00         -42.106         -42.084          0.022
S(6)        4.752e-02
SO4-2        2.836e-02     8.074e-03         -1.547          -2.093          -0.546
CaSO4        1.548e-02     1.627e-02         -1.810          -1.789          0.022
NaSO4-       3.678e-03     2.736e-03         -2.434          -2.563          -0.129
HSO4-        1.056e-07     7.850e-08         -6.977          -7.105          -0.129
CaHSO4+      1.282e-08     9.531e-09         -7.892          -8.021          -0.129

-----Saturation indices-----
Phase      SI      log IAP      log KT
Anhydrite  0.27   -4.09        -4.36 CaSO4
Gypsum     0.49   -4.09        -4.58 CaSO4:2H2O
H2(g)      -22.00 -25.15        -3.15 H2
H2O(g)     -1.51  -0.00         1.51 H2O
Halite     -3.93  -2.34         1.58 NaCl
O2(g)     -39.19 -42.08        -2.89 O2

```

Figure C.3: PHREEQC® output data for supersaturation ratio 3 (SS3) of gypsum.

```

-----Solution composition-----
Elements Molality Moles
Ca      6.361e-02 6.361e-02
Cl      1.272e-01 1.272e-01
Na      1.272e-01 1.272e-01
S(6)   6.361e-02 6.361e-02

-----Description of solution-----
pH = 7.000
pe = 4.000
Specific Conductance (uS/cm, 25 oC) = 19230
Density (g/cm3) = 1.01076 (Millero)
Activity of water = 0.994
Ionic strength = 2.841e-01
Mass of water (kg) = 1.000e+00
Total alkalinity (eq/kg) = -8.971e-08
Total carbon (mol/kg) = 0.000e+00
Total CO2 (mol/kg) = 0.000e+00
Temperature (deg C) = 25.000
Electrical balance (eq) = 4.015e-06
Percenterror, 100*(Cat-|An|)/(Cat+|An|) = 0.00
Iterations = 6
Total H = 1.110124e+02
Total O = 5.576066e+01

-----Distribution of species-----
Species      Molality      Log      Log      Log
              Activity      Molality Activity Gamma
OH-          1.466e-07 9.950e-08 -6.834 -7.002 -0.168
H+           1.275e-07 1.000e-07 -6.895 -7.000 -0.105
H2O          5.551e+01 9.940e-01 1.744 -0.003 0.000
Ca           6.361e-02
Ca+2         4.204e-02 1.234e-02 -1.376 -1.909 -0.532
CaSO4        2.156e-02 2.302e-02 -1.666 -1.638 0.028
CaOH+        2.770e-08 2.036e-08 -7.558 -7.691 -0.134
CaHSO4+      1.835e-08 1.349e-08 -7.736 -7.870 -0.134
Cl           1.272e-01
Cl-          1.272e-01 8.718e-02 -0.895 -1.060 -0.164
H(0)         1.326e-25
H2           6.631e-26 7.079e-26 -25.178 -25.150 0.028
Na           1.272e-01
Na+          1.216e-01 8.841e-02 -0.915 -1.054 -0.138
NaSO4-       5.635e-03 4.142e-03 -2.249 -2.383 -0.134
NaOH         5.438e-09 5.806e-09 -8.265 -8.236 0.028
O(0)         0.000e+00
O2           0.000e+00 0.000e+00 -42.114 -42.085 0.028
S(6)        6.361e-02
SO4-2        3.641e-02 9.348e-03 -1.439 -2.029 -0.591
CaSO4        2.156e-02 2.302e-02 -1.666 -1.638 0.028
NaSO4-       5.635e-03 4.142e-03 -2.249 -2.383 -0.134
HSO4-        1.236e-07 9.089e-08 -6.908 -7.041 -0.134
CaHSO4+      1.835e-08 1.349e-08 -7.736 -7.870 -0.134

-----Saturation indices-----
Phase      SI      log IAP  log KT
Anhydrite  0.42 -3.94 -4.36 CaSO4
Gypsum     0.64 -3.94 -4.58 CaSO4:2H2O
H2(g)     -22.00 -25.15 -3.15 H2
H2O(g)    -1.51 -0.00 1.51 H2O
Halite    -3.70 -2.11 1.58 NaCl
O2(g)    -39.19 -42.09 -2.89 O2

```

Figure C.4: PHREEQC® output data for supersaturation ratio 4 (SS4) of gypsum.

Appendix D: Error analysis and deviations

Appendix D: ERROR ANALYSIS AND DEVIATIONS

Table D.1: Deviations for initial concentration at a supersaturation level of 3 (SS3).

Initial concentrations	SE	Standard deviation	RSD	%difference from calculated value
0.04157	8.862E-05	1.253E-04	0.30%	11.45%
0.04172	3.855E-05	5.452E-05	0.13%	11.15%
0.04196	4.735E-05	6.697E-05	0.16%	10.63%
0.04172	3.559E-05	5.034E-05	0.12%	11.13%
0.04260	2.743E-04	3.879E-04	0.93%	9.27%
0.04195	4.356E-05	6.160E-05	0.15%	10.66%
0.04160	7.820E-05	1.106E-04	0.26%	11.39%
0.04193	3.676E-05	5.198E-05	0.12%	10.70%
0.04163	6.960E-05	9.842E-05	0.24%	11.34%
0.04169	4.878E-05	6.899E-05	0.16%	11.21%
0.04159	8.410E-05	1.189E-04	0.28%	11.42%
0.04143	1.384E-04	1.957E-04	0.47%	11.75%
0.04152	1.070E-04	1.513E-04	0.36%	11.56%
0.04166	5.642E-05	7.979E-05	0.19%	11.26%
0.04194	4.033E-05	5.704E-05	0.14%	10.67%
0.04185	8.673E-06	1.226E-05	0.03%	10.87%
0.04124	2.072E-04	2.930E-04	0.70%	12.17%
0.04141	1.476E-04	2.087E-04	0.50%	11.81%
0.04177	1.911E-05	2.703E-05	0.06%	11.03%
0.04167	5.517E-05	7.803E-05	0.19%	11.25%
0.04186	1.362E-05	1.927E-05	0.05%	10.84%
0.04160	7.752E-05	1.096E-04	0.26%	11.38%
0.04211	1.006E-04	1.423E-04	0.34%	10.31%
0.04210	9.646E-05	1.364E-04	0.33%	10.34%
0.04170	4.391E-05	6.210E-05	0.15%	11.18%
0.04169	4.618E-05	6.531E-05	0.16%	11.20%
0.04194	3.983E-05	5.633E-05	0.13%	10.68%
0.04259	2.722E-04	3.849E-04	0.92%	9.28%
0.04300	4.174E-04	5.903E-04	1.41%	8.40%
0.04227	1.576E-04	2.229E-04	0.53%	9.97%
0.04243	2.131E-04	3.013E-04	0.72%	9.63%
0.04223	1.430E-04	2.023E-04	0.48%	10.06%
0.04252	2.457E-04	3.475E-04	0.83%	9.44%
0.04394	7.484E-04	1.058E-03	2.53%	6.41%
0.04186	1.407E-05	1.989E-05	0.05%	10.83%

Table D.1: Continued.

Initial concentrations	SE	Standard deviation	RSD	%difference from calculated value
0.04190	2.603E-05	3.681E-05	0.09%	10.76%
0.04205	7.816E-05	1.105E-04	0.26%	10.45%
0.04105	2.728E-04	3.858E-04	0.92%	12.56%
0.04197	5.070E-05	7.170E-05	0.17%	10.61%
0.04170	4.232E-05	5.984E-05	0.14%	11.17%
0.04100	2.926E-04	4.139E-04	0.99%	12.68%
0.04237	1.931E-04	2.730E-04	0.65%	9.75%
0.04177	1.914E-05	2.706E-05	0.06%	11.03%
0.04118	2.277E-04	3.220E-04	0.77%	12.29%
0.04116	2.364E-04	3.343E-04	0.80%	12.34%
0.04088	3.343E-04	4.728E-04	1.13%	12.93%
0.04169	4.697E-05	6.642E-05	0.16%	11.20%
0.04154	1.011E-04	1.430E-04	0.34%	11.53%
0.04123	2.104E-04	2.975E-04	0.71%	12.19%
0.04150	1.135E-04	1.605E-04	0.38%	11.60%
0.04177	1.768E-05	2.500E-05	0.06%	11.02%
0.04181	4.067E-06	5.752E-06	0.01%	10.94%
0.04182	1.254E-04	1.774E-04	0.42%	10.92%

Table D.2: Deviation for initial concentration at a supersaturation level of 4 (SS4).

Initial concentrations	SE	Standard deviation	RSD	%difference from calculated value
0.05689	1.452E-04	2.053E-04	0.36%	12.17%
0.05674	9.244E-05	1.307E-04	0.23%	12.48%
0.05678	1.072E-04	1.517E-04	0.27%	12.40%
0.05666	6.573E-05	9.296E-05	0.16%	12.65%
0.05714	2.340E-04	3.310E-04	0.59%	11.63%
0.05542	3.739E-04	5.288E-04	0.94%	15.29%
0.05568	2.827E-04	3.998E-04	0.71%	14.74%
0.05685	1.307E-04	1.848E-04	0.33%	12.25%
0.05679	1.094E-04	1.547E-04	0.27%	12.38%
0.05571	2.714E-04	3.838E-04	0.68%	14.68%
0.05713	2.306E-04	3.261E-04	0.58%	11.65%
0.05614	1.180E-04	1.668E-04	0.30%	13.75%
0.05709	2.151E-04	3.043E-04	0.54%	11.75%
0.05574	2.609E-04	3.689E-04	0.65%	14.61%
0.05574	2.603E-04	3.682E-04	0.65%	14.61%
0.05691	1.518E-04	2.147E-04	0.38%	12.13%
0.05648	7.735E-07	1.094E-06	0.00%	13.04%
0.05664	5.909E-05	8.357E-05	0.15%	12.69%
0.05655	2.506E-05	3.543E-05	0.06%	12.89%
0.05648	1.650E-04	2.333E-04	0.41%	13.04%

*Appendix D: Error analysis and deviations***Table D.3: Analysis of stock solution concentrations and reported deviations**

Sample Nr	Experimental Results(ppm)	Starting Concentration theoretical (ppm)	Starting concentration (mol/l)	Working Concentration (ppm)	Working concentration (mol/l)	%difference from calculated concentration
<i>Calcium</i>						
1	87.348	3493.907	0.08717	1704.345	0.04252	9.43%
4	86.894	3475.755	0.08672	1695.490	0.04230	9.90%
7	81.239	3412.027	0.08513	1664.404	0.04153	11.55%
11	64.989	3411.921	0.08513	1664.352	0.04153	11.55%
12	70.600	3530.022	0.08807	1721.962	0.04296	8.49%
13	87.101	3484.043	0.08693	1699.533	0.04240	9.68%
14	82.297	3456.454	0.08624	1686.075	0.04207	10.40%
15	86.046	3441.842	0.08587	1678.947	0.04189	10.78%
16	85.255	3410.201	0.08508	1663.513	0.04150	11.60%
STD			0.00099		0.00048	
RSD			0.01151		0.01151	
SE			0.00033		0.00016	
<i>Sodium</i>						
17	105.227	4209.099	0.09154	2053.219	0.04465	4.89%
18	84.764	4238.177	0.09217	2067.403	0.04496	4.23%
20	90.212	3788.922	0.08240	1848.255	0.04020	14.38%
21	80.216	4211.347	0.09159	2054.316	0.04468	4.84%
23	99.204	4166.583	0.09062	2032.479	0.04420	5.85%
24	106.476	4259.021	0.09263	2077.571	0.04518	3.76%
25	107.088	4283.510	0.09316	2089.517	0.04544	3.21%
STD			0.00343		0.00167	
RSD			0.03783		0.03783	
SE			0.00114		0.00056	

Table D.4: Overall analysis of sample errors and dilution errors.

Sample Number	Sample Weight (g)		Dilution Weight(g)	Volume Sample (ml)	Volume Dilution (ml)	Weight Dilution	Volume Dilution	%Error
S00	4.95	1.00%	94.91	4.96	95.35	20.24	20.21	1.18%
S01	5.00	0.00%	95.13	5.01	95.26	20.03	20.00	0.13%
S02	5.01	0.20%	94.53	5.02	94.95	19.93	19.90	0.37%
S03	5.00	0.00%	94.28	5.01	95.12	20.00	19.97	0.01%
S04	4.97	0.60%	94.6	4.98	95.13	20.11	20.09	0.57%
S05	4.97	0.60%	94.62	4.98	95.03	20.09	20.06	0.47%
S06	4.96	0.80%	94.26	4.97	94.39	20.00	19.97	0.02%
S07	5.00	0.00%	94.25	5.01	95.01	19.98	19.95	0.12%
S08	5.00	0.00%	94.2	5.01	95.25	20.02	19.99	0.12%
S09	4.92	1.60%	94.29	4.93	94.99	20.28	20.25	1.40%
S10	5.00	0.00%	95.07	5.01	95.82	20.14	20.11	0.69%
S11	4.93	1.40%	94.43	4.94	95.38	20.32	20.29	1.60%
S12	4.88	2.40%	94.71	4.89	95.16	20.47	20.44	2.37%
S13	4.93	1.40%	94.49	4.94	94.96	20.24	20.21	1.18%
S14	4.90	2.00%	94.4	4.91	95.25	20.41	20.38	2.06%
S15	4.89	2.20%	94.86	4.90	95.12	20.43	20.40	2.13%
S16	4.80	4.00%	94.68	4.81	95.20	20.81	20.78	4.03%
S17	4.91	1.80%	94.41	4.92	95.41	20.41	20.38	2.03%
Average		1.11%						1.14%
STD	0.054		0.277	0.055	0.275	0.222	0.222	
RSD	1.10%		0.29%	1.10%	0.29%	1.10%	1.10%	
SE	0.013		0.065	0.013	0.065	0.052	0.052	

*Appendix D: Error analysis and deviations***Table D.5: STD and RSD values for growth rate constants for baseline experiments.**

Experiment Name	k'	SSE	STD	RSD
$C_a = 41.9 \times 10^3 \text{ mol/l}$				
BL-SS2_A	2.1458	3.540E-05	0.001280	5.25%
BL-SS2_B	2.2046	3.593E-05	0.001254	5.15%
BL-SS3_A	2.1022	3.371E-05	0.001212	4.28%
BL-SS3_B	2.3323	2.382E-05	0.001129	4.08%
BL-SS4_A	3.0992	1.401E-05	0.000854	2.96%
BL-SS4_B	4.0940	2.764E-05	0.001233	4.20%
Average:		2.840E-05	0.001160	4.32%

Table D.6: STD and RSD values for growth rate constants for humic acid experiments.

Experiment Name	k'	SSE	STD	RSD
<i>Ca = 41.9 × 10³ mol/l</i>				
HA-04_A	1.2159	1.982E-05	0.000921	3.31%
HA-04_B	1.2645	1.278E-05	0.000734	2.68%
HA-05_A	0.9566	2.601E-05	0.001023	3.62%
HA-05_B	1.4071	1.508E-05	0.000901	3.24%
HA-05_C	1.6767	4.486E-05	0.001245	4.16%
HA-06_A	1.3375	1.405E-05	0.000786	2.77%
HA-06_B	0.7340	4.738E-05	0.001399	4.74%
HA-13_A	0.9769	1.842E-05	0.000852	3.00%
HA-13_B	1.2532	1.322E-05	0.000764	2.72%
HA-14_A	1.1509	1.568E-05	0.000871	3.09%
HA-14_B	1.1732	1.601E-05	0.000846	3.09%
HA-15_A	1.5049	2.478E-05	0.001088	3.77%
HA-15_B	0.7653	3.338E-05	0.001433	4.86%
HA-22_B	1.1643	5.837E-06	0.000534	1.95%
HA-23_A	0.8660	1.588E-05	0.000821	2.78%
HA-23_B	0.9600	1.171E-05	0.000894	3.25%
HA-24_A	0.5115	5.424E-05	0.001685	5.54%
HA-24_B	0.7080	7.488E-05	0.001474	5.09%
	Average:	2.578E-05	0.001015	3.54%
<i>Ca = 56.60 × 10³ mol/l</i>				
HA-07_A	4.7056	2.905E-05	0.001204	4.05%
HA-07_B	4.5430	4.587E-05	0.001855	5.96%
HA-08_A	4.8709	4.711E-05	0.001596	5.26%
HA-08_B	4.2099	3.133E-05	0.001389	4.62%
HA-09_A	3.6077	5.900E-05	0.001709	5.43%
HA-16_A	3.7767	6.683E-05	0.001580	5.00%
HA-16_B	5.7730	1.547E-05	0.001065	3.73%
HA-17_A	5.7313	1.417E-05	0.001046	3.72%
HA-17_B	6.4608	1.256E-05	0.001071	3.79%
HA-18_A	4.4810	4.861E-05	0.001805	5.62%
HA-18_B	4.6373	2.780E-05	0.001405	4.39%
HA-25_A	4.8576	1.424E-05	0.001055	3.68%
HA-25_B	4.2145	7.619E-05	0.001897	5.85%
HA-25_C	4.4973	8.476E-05	0.002194	7.09%
HA-26_A	5.6453	1.077E-05	0.000831	3.01%
HA-26_B	6.0449	2.543E-05	0.001409	5.02%
HA-27_A	5.3457	4.029E-05	0.001545	5.18%
HA-27_B	1.6224	1.425E-04	0.002628	7.90%
HA-27_C	3.7118	8.834E-05	0.002238	7.01%
	Average:	4.633E-05	0.001554	5.07%
	Overall Average:	3.633E-05	0.001292	4.32%

Appendix D: Error analysis and deviations**Table D.7: STD and RSD values for growth rate constants for fulvic acid experiments**

Experiment Name	k'	SSE	STD	RSD
FA-03_A	1.3527	1.941E-05	0.000859	3.08%
FA-04_A	1.3527	2.851E-05	0.001057	3.64%
FA-05_A	0.7055	3.171E-05	0.001302	4.21%
FA-05_B	0.7833	5.658E-05	0.001413	4.87%
FA-06_A	1.5872	2.076E-05	0.000863	3.08%
FA-07_A	1.8062	3.827E-05	0.001189	4.23%
FA-08_A	1.3149	2.727E-05	0.001208	4.17%
Average:		3.179E-05	0.001127	3.90%

Table D.8: STD and RSD values for growth rate constants for seeded experiments of humic acid

Experiment Name	k'	SSE	STD	RSD
HS-01_A	1.7006	2.993E-06	0.000237	0.86%
HS-02_A	2.0203	4.898E-06	0.000290	0.97%
HS-03_A	1.8514	1.884E-06	0.000201	0.73%
HS-03_B	1.8327	1.399E-06	0.000185	0.65%
HS-04_A	1.6788	2.577E-06	0.000222	0.78%
HS-05_A	1.8773	2.911E-06	0.000220	0.80%
HS-06_A	0.7373	3.102E-05	0.000811	2.67%
HS-07_A	0.8342	2.355E-05	0.000846	3.05%
HS-07_B	0.5539	4.531E-05	0.001087	3.60%
HS-08_A	0.7920	3.120E-05	0.000903	3.12%
HS-08_B	0.7578	2.608E-05	0.000816	2.80%
HS-09_A	0.4882	1.452E-05	0.000625	2.12%
HS-09_B	0.5599	3.689E-05	0.000972	3.48%
HS-10_A	2.1209	2.573E-06	0.000221	0.86%
HS-11_A	2.0154	1.652E-06	0.000186	0.68%
HS-12_A	0.8806	3.212E-05	0.000892	3.10%
HS-12_B	0.8651	3.260E-05	0.000807	2.79%
HS-14_A	5.0839	3.575E-06	0.000320	1.27%
HS-15_A	4.7294	1.324E-06	0.000169	0.66%
HS-16_A	4.1785	5.207E-06	0.000321	1.29%
Average:		1.521E-05	0.0005166	1.81%

Table D.9: STD and RSD values for growth rate constants for seeded experiments of fulvic acid.

Experiment Name	k'	SSE	STD	RSD
FS-03_A	1.214	2.004E-05	0.000685	2.24%
FS-04_A	3.116	1.471E-05	0.000539	1.96%
FS-05_A	1.027	1.594E-06	0.000187	0.61%
Average:		1.212E-05	0.000470	1.61%

Appendix E: ANALYSIS REPORTS

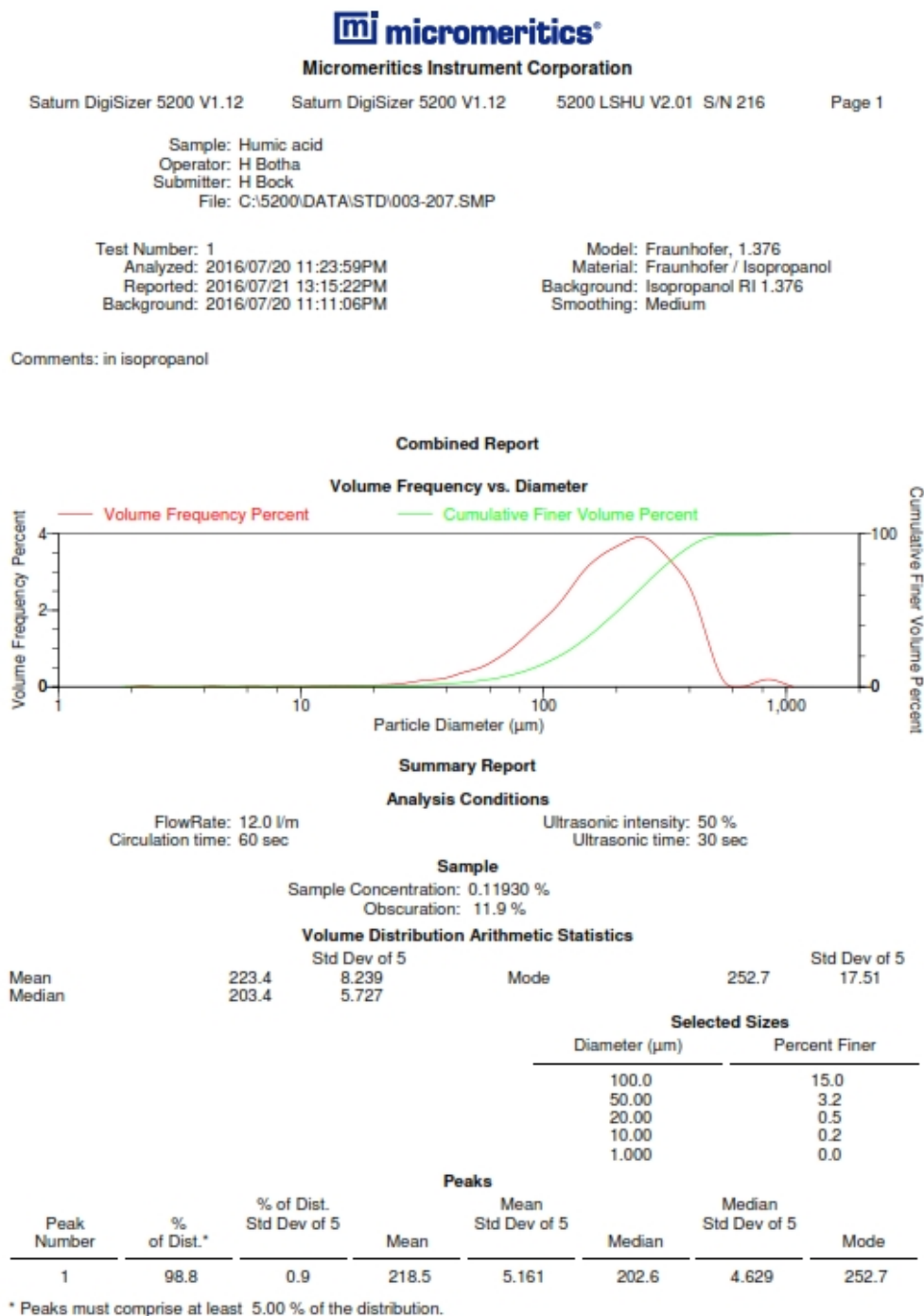


Figure E.1: Particle size analysis report for Sigma Aldrich Humic Acid.

Appendix E: Analysis reports

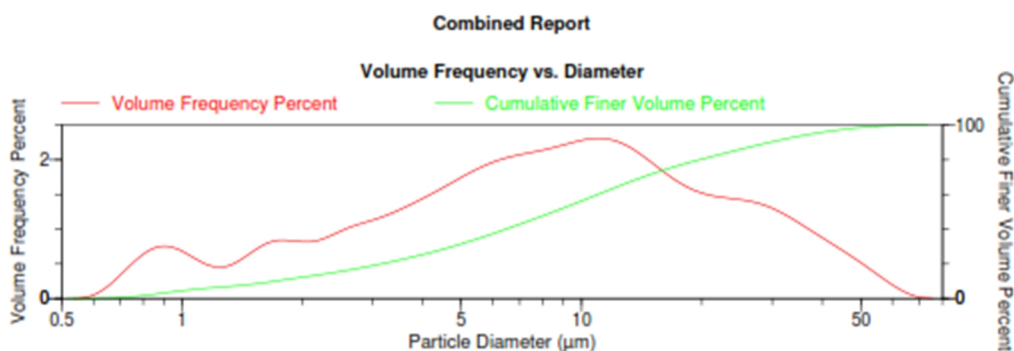
micromeritics®
Micromeritics Instrument Corporation

Saturn DigiSizer 5200 V1.12 Saturn DigiSizer 5200 V1.12 5200 LSHU V2.01 S/N 216 Page 1

Sample: Calcium sulphate di-hydrate
 Operator: H Botha
 Submitter: H Bock
 File: C:\5200\DATA\STD\003-210.SMP

Test Number: 3 Model: (1.530, 0.1000000), 1.376
 Analyzed: 2016/08/16 15:36:09PM Material: Gypsum / Isopropanol
 Reported: 2016/08/17 11:12:00PM Background: Isopropanol RI 1.376
 Background: 2016/08/16 15:15:28PM Smoothing: Medium

Comments: in isopropanol



Summary Report

Analysis Conditions

FlowRate: 12.0 l/m Ultrasonic intensity: 60 %
 Circulation time: 60 sec Ultrasonic time: 60 sec

Sample

Sample Concentration: 0.00627 %
 Obscuration: 18.3 %

Volume Distribution Arithmetic Statistics

	Mean	Std Dev of 3	Mode	Std Dev of 3
Mean	12.35	0.277	11.29	0.000
Median	8.511	0.448		

Selected Sizes

Diameter (µm)	Percent Finer
100.0	100.0
50.00	98.6
20.00	80.4
10.00	56.2
1.000	4.4

Peaks

Peak Number	% of Dist.*	% of Dist. Std Dev of 3	Mean	Mean Std Dev of 3	Median	Median Std Dev of 3	Mode
1	6.9	0.1	0.940	0.005	0.923	0.006	0.897
2	5.8	0.3	1.687	0.003	1.687	0.004	1.789
3	87.3	0.4	13.95	0.262	10.02	0.390	11.29

* Peaks must comprise at least 5.00 % of the distribution.

Figure E.2: Particle size analysis report for Calcium sulphate dihydrate used as seed crystals.



3Flex 4.00

3Flex Version 4.00
Serial # 103 Unit 1 Port 3

Page 1 of 35

Sample: CaSO₄.2H₂O
 Operator: H Botha, Dept Process Eng, US
 Submitter: H Bock
 File: C:\3Flex\data\000-376.SMP

Started: 2016/08/31 08:53:02	Analysis adsorptive: N ₂
Completed: 2016/09/01 08:39:13	Analysis bath temp.: 77.303 K
Report time: 2016/09/07 11:49:28	Thermal correction: Yes
Sample mass: 1.1313 g	Warm free space: 15.7335 cm ³ Measured
Cold free space: 55.7688 cm ³	Equilibration interval: 15 s
Low pressure dose: 1.5000 cm ³ /g STP	Sample density: 1.000 g/cm ³
Automatic degas: No	

Summary Report**Surface Area**Single point surface area at $p/p^* = 0.239244398$: 15.2373 m²/gBET Surface Area: 15.3378 m²/gt-Plot Micropore Area: 0.4506 m²/gt-Plot external surface area: 14.8872 m²/gBJH Adsorption cumulative surface area of pores
between 10.000 Å and 4 000.000 Å width: 16.9468 m²/gBJH Desorption cumulative surface area of pores
between 17.000 Å and 3 000.000 Å width: 14.5609 m²/g**Pore Volume**Single point adsorption total pore volume of pores
less than 3 402.061 Å width at $p/p^* = 0.994348278$: 0.043505 cm³/gSingle point desorption total pore volume of pores
less than 3 402.061 Å width at $p/p^* = 0.994348278$: 0.043505 cm³/gt-Plot micropore volume: 0.000245 cm³/gBJH Adsorption cumulative volume of pores
between 10.000 Å and 4 000.000 Å width: 0.042589 cm³/gBJH Desorption cumulative volume of pores
between 17.000 Å and 3 000.000 Å width: 0.042320 cm³/g**Pore Size**

Adsorption average pore diameter (4V/A by BET): 113.458 Å

Desorption average pore diameter (4V/A by BET): 113.458 Å

BJH Adsorption average pore width (4V/A): 100.524 Å

BJH Desorption average pore width (4V/A): 116.257 Å

DFT Pore Size

Total Volume in Pores	<=	2 166.32 Å	:	0.04151 cm ³ /g
Area in Pores	>	2 166.32 Å	:	0.145 m ² /g
Total Area in Pores	>=	3.93 Å	:	14.559 m ² /g

Horvath-KawazoeMaximum pore volume at $p/p^* = 0.053561755$: 0.005116 cm³/g

Figure E.3: BET analysis report for Calcium sulphate dihydrate used as seed crystals.

Appendix F: Sample calculations

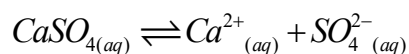
Appendix F: SAMPLE CALCULATIONS

F.1. Supersaturation concentration

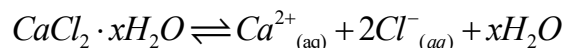
The supersaturation were calculated using equation 3.1 and 3.2. The saturation concentration of calcium sulphate was determined to be 627.25 mg/l by PHREEQC[®]. That is equivalent to 0.01565 mol/l. Thus, using equation 3.1 for a supersaturation ratio of 3, for example, the concentration will be calculated as:

$$\begin{aligned} [Ca^{2+}]_i &= S \times [Ca^{2+}]_s \\ &= 3 \times 0.01565 \\ &= 0.04695 \text{ mol/l} \end{aligned}$$

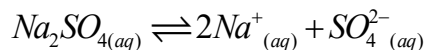
The relationship of calcium sulphate is given as



It can be seen that $[Ca^{2+}] = [SO_4^{2-}] = 0.04695 \text{ mol/l}$. From the following relationship, 1 mole $Ca^{2+} = 1 \text{ mole } CaCl_2$



The supersaturation concentration of $CaCl_2$ required would be 0.04695 mol/l. For the relationship of sodium sulphate, the same hold true. 1 mole $SO_4^{2-} = 1 \text{ mole } Na_2SO_4 = 0.04695 \text{ mol/l}$.



The relationship for Cl^- and Na^+ is 2:1 to Ca^{2+} . Thus $[Cl^-] = [Na^+] = 2 \times [Ca^{2+}] = 2 \times 0.04695 \text{ mol/l} = 0.9390 \text{ mol/l}$. In order to compensate for an extra 10 ml for the working fluid, the concentration of the stock solutions had to be adjusted. This is done for addition of the HS and seed crystals. For SS3, the concentration was calculated to be:

F.2. Concentration error with pH adjustment

$$\begin{aligned}
 C_1V_1 &= C_2V_2 \\
 C_1 &= \frac{C_2V_2}{V_1} \\
 C_1 &= \frac{0.04695 \times 410}{200} \\
 &= 0.09625 \text{ mol/l}
 \end{aligned}$$

Note that the above concentration is theoretical and that the actual concentration was determined through ICP analysis.

The dilution factor required from the stock solution for the working fluid was then:

$$\text{Dilution Factor} = \frac{0.09625}{0.04695} = 2.05$$

F.2. Concentration error with pH adjustment

Depending on the pH level required per experimental run a volume of buffer needs to be added to the working fluid to adjust the pH. A maximum amount of 1 ml is added to adjust the pH. The calculation of concentration is as follows:

$$\begin{aligned}
 C_1V_1 &= C_2V_2 \\
 C_2 &= \frac{C_1V_1}{V_2}
 \end{aligned}$$

Thus, for a concentration of $C_1 = 1881.756 \text{ mg/l}$ and a volume of $V_1 = 410 \text{ ml}$ and $V_2 = 411 \text{ ml}$, C_2 will yield:

$$\begin{aligned}
 C_2 &= \frac{1881.756 \times 410}{411} \\
 &= 1877.178 \text{ mg/l}
 \end{aligned}$$

The error is then calculated as:

$$\begin{aligned}
 \% \text{Error} &= \left(\frac{1881.756 - 1877.178}{1881.756} \right) \times 100\% \\
 &= 0.243\%
 \end{aligned}$$

Appendix F: Sample calculations**F.3. Standard deviations, relative standard deviations and standard error**

Standard deviation was calculated as follow:

$$\sigma_D = \sqrt{\frac{1}{N} \sum_{i=1}^N (x_i - \bar{x})^2} \quad (\text{F-1})$$

where σ_D is the standard deviation; x_i is the individual value in the dataset; \bar{x} is the mean of the data and N is the total number of data points in the set. All deviations were calculated through weighing a number of samples with an accuracy of ± 0.01 grams and using the density of water at 25°C to convert to volume. The deviations for a sample in set of 17 points for example were then calculated:

$$\begin{aligned} \sigma_D &= \sqrt{\frac{1}{17} \sum_{i=1}^N (x_i - 4.96)^2} \\ &= 0.055 \text{ ml} \end{aligned}$$

The relative standard deviation was calculated as follow and is presented as a percentage:

$$\begin{aligned} \%RSD &= \frac{\sigma_D}{\bar{x}} \times 100\% \\ &= \frac{0.055}{4.96} \times 100\% \\ &= 1.11\% \end{aligned} \quad (\text{F-2})$$

The standard error of the mean was calculated as follow:

$$\sigma_M = \frac{0.055}{\sqrt{17}} = 0.013 \text{ ml} \quad (\text{F-3})$$

Thus, the STD, RSD and SE for a sample was 0.055 ml, 1.11% and 0.013 ml respectively.